

UNCLASSIFIED

---

AD 296 938

*Reproduced  
by the*

ARMED SERVICES TECHNICAL INFORMATION AGENCY  
ARLINGTON HALL STATION  
ARLINGTON 12, VIRGINIA



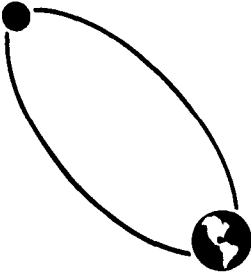
---

UNCLASSIFIED

**Best  
Available  
Copy**

NOTICE: When government or other drawings, specifications or other data are used for any purpose other than in connection with a definitely related government procurement operation, the U. S. Government thereby incurs no responsibility, nor any obligation whatsoever; and the fact that the Government may have formulated, furnished, or in any way supplied the said drawings, specifications, or other data is not to be regarded by implication or otherwise as in any manner licensing the holder or any other person or corporation, or conveying any rights or permission to manufacture, use or sell any patented invention that may in any way be related thereto.

63-2-4



## FINAL REPORT

### FIELD STUDY OF VARIATION IN CHARACTERISTICS OF SEISMIC NOISE AND SIGNALS WITH GEOLOGIC AND GEOGRAPHIC ENVIRONMENT

PROJECT NO. VT/078

REPORT NO. VT/078-28

PREPARED FOR

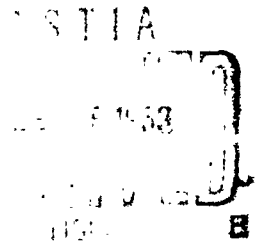
United States Air Force Technical Applications Center

WASHINGTON 25, D. C.

Under Contract AF 33(600)-42048

296 938

15 JANUARY 1963 VOL. I





FINAL REPORT  
FIELD STUDY OF VARIATION IN CHARACTERISTICS  
OF SEISMIC NOISE AND SIGNALS WITH  
GEOLOGIC AND GEOGRAPHIC ENVIRONMENT

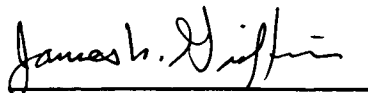
PROJECT NO. VT/078      REPORT NO. VT/078-28

Prepared for  
UNITED STATES AIR FORCE TECHNICAL APPLICATIONS CENTER  
Washington 25, D.C.

Under Contract AF33(600)-42048

15 January 1963 Vol. I

Prepared by:



J. N. Griffin  
Project Engineer

Approved by:



F. B. Coker  
Division Manager

UNITED EARTH SCIENCES  
Division of  
UNITED ELECTRODYNAMICS, INC.

AFTAC Project No.:

VT/078

Project Title: FIELD STUDY OF VARIATION IN CHARACTERISTICS OF  
SEISMIC NOISE AND SIGNALS WITH GEOLOGIC AND  
GEOGRAPHIC ENVIRONMENT

ARPA Order No.:

104-60

ARPA Code No.:

8100

Contractor:

United Earth Sciences, Division of  
United ElectroDynamics, Inc.

Date of Contract:

2 September 1960

Amount of Contract:

\$746,541

Contract Number:


AF33(600)-42048

Contract Expiration Date:

31 December 1962

Project Engineer:

James N. Griffin  
Telephone: 836-3882  
Alexandria, Virginia




## ABSTRACT

A two-year study was conducted to determine relationships among seismic noise, teleseismic signals, and various geologic and geographic recording environments.

Variation in seismic noise and signal with geologic-geographic recording environment was measured in California, the Pacific Northwest and in the Appalachian Mountains - Atlantic coastal plain areas, between March 1961 and September 1962. ~~In each area, a profile of 8 to 10 stations was selected along a line perpendicular to regional structural trends.~~ One centrally located station remained fixed, recording simultaneously with another roving station which consecutively recorded in locations of varying geologic and topographic environment.

At both stations signal and noise was recorded on film and magnetic tape by tripartite arrays of 4 short-period and 1 long-period vertical seismometers. Noise data gathered was processed by power spectrum analysis to define the noise amplitude spectrum at each recording station. Some cross-spectrum analysis was done on Pacific Northwest data in order to study noise source directions, coherency and phase velocities.

Variations in noise and teleseismic signals were then correlated with variations in geologic-geographic recording environment, and ~~the~~ following conclusions were drawn:

- 
- 1) Relative signal-to-noise ratio depends strongly on ocean distance for stations less than 500 kilometers (300 miles) inland. Signal-to-noise ratios were highest at stations farthest inland, and decreased rapidly as station locations closer to the ocean were occupied.
  - 2) Relative signal strength in California coastal marine sediments and inland Tertiary sediments was usually several times as high as on massive granite.
  - 3) Noise amplitude at a specified frequency is determined largely by ocean distance and wind speed, at stations less than 500 kilometers from the ocean. Noise amplitude increases exponentially between periods of 0.4 and 5.0 seconds. Determination of average noise amplitude for each period band included correction for temporary changes in regional noise level.
  - 4) On both the California and Appalachian profiles, there was relatively pronounced cross-correlation among changes in geology, topography, ocean distance and average noise level,

so that their separate relationships to average noise level were difficult to determine. However, it was found that average noise amplitude at each station could be mathematically described, usually within a factor of three, by a function of noise frequency and shoreline distance. After adjustment for assumed influence on noise level of variations in lithology and structure, average noise level could usually be described within a factor of two. A single function described the amplitude spectrum of average noise at every station of a profile, for periods between 0.4 and 5.0 seconds and distances less than about 500 kilometers from the coastline. Constants of the function changed somewhat, but not its form, between profiles.

- 5) Noise sources in the general direction of the nearest ocean were frequently indicated in source direction studies. About 40% of noise above 1 second period observed in a two-month source direction study at two Pacific Northwest stations came from a  $60^{\circ}$  sector in the direction of the ocean, with phase velocity of about 4 km/sec. Another 30% came from ambiguous or inconsistent directions, showed abnormal apparent phase velocity, and was possibly from simultaneous multiple sources. The remaining 30% was not analyzed because of its low amplitude or inconsistency. Isolated samples taken from all three profiles showed .5 second noise coming from the general direction of the ocean.
- 6) Best signal-to-noise ratios at locations less than about 300 kilometers from the ocean might be provided by a linear array designed to cancel ocean noise; at more than 300 kilometers from the ocean, cancellation of noise from random directions might be more important. This is suggested by the persistent relationship between the ocean and noise source directions in detailed studies in the Pacific Northwest and in spot-checks of California and Appalachian recordings, and by the rapid increase in average noise level as the ocean is approached.
- 7) Evidence from California stations indicates that teleseisms are recorded more strongly in Cenozoic sedimentary provinces than in granitic provinces. It is recommended that existing data be studied to show whether this is true in other areas, and specifically to show whether teleseisms are recorded more strongly in inland sedimentary provinces than in granitic provinces.

## TABLE OF CONTENTS

	<u>Page</u>
Introduction	1
1. Results of Investigations	1-1
1.1 Seismic Noise and Signal Characteristics in Relation to Geologic, Geographic and Temporal Environment	1-1
1.1.1 Noise Amplitude Variation with Environment	1-1
1.1.1.0 Categories of Noise Amplitude Variations	1-1
1.1.1.1 Variation with Regional Geology, Geography and Topography	1-3
1.1.1.2 Variation with Local Geology and Topography	1-10
1.1.1.3 Variation with Time	1-11
1.1.1.4 Distinctive Characteristics of Noise Amplitude and Velocity Spectra	1-12
1.1.1.4.1 Filter Studies	1-12
1.1.2 Noise Source Directions and Phase Velocities	1-13
1.1.2.1 Dominant Noise Source Direction	1-13
1.1.2.2 Seismic Noise Velocity	1-14
1.1.2.3 Noise Coherency	1-15
1.1.3 Relative Signal Strength Variations with Environment	1-15
1.1.3.1 Signal Strength Variations with Regional Geologic Environment	1-16
1.1.3.2 Signal Strength Variation with Local Seismometer Environment	1-18
1.1.3.3 Effect of Background Noise on Signal Strength Measurements	1-19
1.1.4 Variation of Signal-to-Noise Ratio with Environment	1-21

## TABLE OF CONTENTS (Continued)

	<u>Page</u>
2. Areas Surveyed	2-1
2.1 The California Profile	2-1
2.1.1 General Description	2-1
2.1.2 Selection of Locations for Signal and Noise Recording	2-2
2.2 The Pacific Northwest Profile	2-4
2.2.1 General Description	2-4
2.2.2 Selection of Locations for Signal and Noise Recording	2-4
2.3 The Appalachian Profile	2-7
2.3.1 General Description	2-7
2.3.2 Selection of Locations for Signal and Noise Recording	2-8
3. Field Operations	3-1
3.1 Field Instruments and Equipment	3-1
3.1.1 Short Period Instrumentation	3-1
3.1.1.1 Seismometers	3-1
3.1.1.2 Short Period Amplifiers	3-1
3.1.1.3 Tape Recording System	3-2
3.1.1.4 Film Recording System	3-3
3.1.1.5 Calibration and Timing	3-3
3.1.2 Long-Period Instrumentation	3-4
3.1.2.1 Seismometers	3-4
3.1.2.2 Long-Period Amplifier Filter Recording System	3-5
3.1.3 Weather Recording Instruments	3-5
3.1.4 Support Equipment	3-6
3.1.4.1 Diesel Generators	3-6

## TABLE OF CONTENTS (Continued)

	<u>Page</u>
3.1.4.2 Vehicles and Trailers	3-6
3.1.4.3 Signal Cables	3-6
3.1.4.4 Lightning Arrestors	3-6
3.1.4.5 Seismometer Vault Liners	3-7
3.2 Field Measurements	3-8
3.2.1 Noise and Signal Recording Routine	3-8
3.2.1.1 Seismometer Array Configuration	3-8
3.2.1.2 Recording Channel Assignments	3-8
3.2.1.3 Daily Recording Routine	3-9
3.2.2 Calibrations and Tests	3-9
3.2.2.1 Monthly Detailed Calibration	3-10
3.2.2.2 Daily Calibrations	3-11
3.2.2.3 Calibration of Weather Recording Equipment	3-11
3.2.2.4 Absolute Calibration of the Long Period Seismometer	3-12
4. Data Reduction and Analysis	4-1
4.1 Noise Analysis Methods	4-1
4.1.1 Power Spectrum Analysis of Seismic Noise	4-1
4.1.1.1 General Descriptions of Power and Cross-Power Density Spectra	4-1
4.1.1.2 Wave Analyzer Systems	4-4
4.1.1.2.1 Tape and Loop Transports	4-4
4.1.1.2.2 Power Spectrum Analyzer	4-4
4.1.1.2.3 Cross-Spectrum Analyzer	4-5
4.1.1.3 Instrument Constants and Sample Selection	4-6

## TABLE OF CONTENTS (Continued)

	<u>Page</u>
4.1.1.4 Calibration of Power Spectra	4-7
4.1.2 Noise Amplitude Measurements from Power Spectra	4-8
4.1.2.1 Comparison of PSD-determined Noise Amplitudes with Trace-determined Noise Amplitudes	4-8
4.1.2.2 Ground Motion Amplitude Computations from Analog PSD's	4-9
4.1.3 Noise Source Direction, Phase Velocity and Coherency Determinations	4-10
4.1.3.1 Phase Shift Measurements	4-10
4.1.3.2 Noise Source Direction Determination	4-11
4.1.3.3 Determination of Apparent Phase Velocity	4-12
4.1.3.4 Phase Coherency Measurements	4-13
4.2 Signal Strength Determinations	4-13
4.2.1 Measurements	4-13
4.2.2 Corrections	4-14
4.2.3 Investigation of "Scatter" in Signal Ratios	4-14
4.3 Correlation of Seismic Signal and Noise with Geologic, Geographic and Time Variables	4-15
4.3.1 Methods Used in Correlating Noise Level with Environment	4-15
4.3.1.1 Correction for Time Variations in Noise Level before Correlation	4-16
4.3.1.2 Correlation by Multiple Regression	4-17
4.3.1.3 Selection and Definition of Environmental Variables	4-19
4.3.1.4 Method of Evaluating Results of the Correlation Program	4-20
4.3.2 Signal Strength Correlation	4-21
5. Conclusions and Recommendations	5-1



# List of Figures

Figure No.		Follows Page No.
	California Profile	2
	Pacific Northwest Profile	2
	Appalachian Profile	2
1.1.1.1.1	Relative Noise Amplitudes at each Seismometer Position of California and Pacific Northwest Stations for 1.25 - 1.50 Second Period Band	1-2
1.1.1.1.3	Long-Term Average Noise Amplitudes for 9 Frequency Bands at California Stations	1-3
1.1.1.1.4	Long-Term Average Noise Amplitudes for 9 Frequency Bands at Pacific Northwest Stations	1-3
1.1.1.1.5	Long-Term Average Noise Amplitudes for 9 Frequency Bands at Appalachian Stations	1-3
1.1.1.1.6	Approximation of Long-Term Average Noise Amplitude Spectra at each Recording Station by a Function of Coastline Distance and Noise Frequency	1-5
1.1.1.1.7	Frequency-Dependent Noise Amplitude Residuals at each Recording Station after Removal of Variations with Coastline Distance of Values of the Spectrum-Approximating Function $Y(f,x)$	1-6
1.1.1.6.8	Cumulative Distributions of California Noise Amplitudes for 1.25 - 1.50 Sec. Period	1-7
1.1.1.1.8	Observed vs Predicted Noise Amplitude: Observed Long-term Average Noise Amplitudes and Corresponding Values Predicted by Distance-Frequency Function $Y(f,x)$	1-9
1.1.1.1.9	Observed vs Predicted Noise Amplitudes: Observed Long-Term Average Noise Am- plitudes and Corresponding Values Predicted by Distance-Frequency Function $Y(f,x)$ after Adjustment for Estimated Effects of Differences in Geologic Environments Between recording Stations	1-9
	Correlation Statistics from Studies of Noise Amplitude Variations in the 2.2 cps and .73 cps Bands	1-10

List of Figures (Continued)

Figure No.		Follows Page No.
1.1.1.4.1.1	Master Station California Profile	1-11
1.1.1.4.1.2	Master Station Pacific NW Profile	1-11
1.1.1.4.1.3	Master Station Appalachian Profile	1-11
1.1.1.4.2.1	Seasonal Variation in Noise Level for 3 Period Bands California Profile	1-11
1.1.1.4.2.2	Seasonal Variation in Noise Level for 3 Period Bands Pacific NW Profile	1-11
1.1.1.4.2.3	Seasonal Variation in Noise Level for 3 Period Bands Appalachian Profile	1-11
1.1.1.6.4.3	Mabton SS 61-355-15:00:00z Wind Speed 7.5 Knots	1-11
1.1.1.6.4.4	Mabton Wind Speed 7.5 Knots PSD SS 355 1500 00-320 Channel No. 2	1-11
1.1.1.6.4.5	Toppenish Ridge MS 61-341-20:00:00z Wind Speed 2.5 knots	1-11
1.1.1.6.4.6	Toppenish Ridge Wind Speed 2.5 Knots PSD SS 341 2000 00-320 Channel No. 2	1-11
1.1.1.3.1	Effect of Wind on Placement of Seismometers at Panamint SS 61-180- 14:16Z	1-11
1.1.1.6.1	Typical Amplitude Spectrum of Long and Short Period Seismic Noise	1-12
1.1.1.6.2	Typical Amplitude Spectrum of Long and Short Period Seismic Noise	1-12
1.1.1.6.3	Typical Amplitude Spectrum of Long and Short Period Seismic Noise	1-12
1.1.1.6.3.6	Paterson SS PSD SS 62 011 0500-0503:20 Channel No. 5	1-12
1.1.1.6.3.7	Paterson SS PSD SS 62 011 0301-0303 Channel No. 5	1-12
1.1.1.6.3.8	Paterson Slave Station Seismometer #5	1-12
1.1.1.6.3.1	Spectrum of High and Low Frequency Seismic Background Noise on Channel 3 before Teleseism at 1411	1-12
1.1.1.6.3.2	Spectrum of Teleseism at 1411 in Low Frequency Background Noise of Channel 4	1-12
1.1.1.6.3.3.	Spectrum of Low Frequency Seismic Background Noise on Channel 4 before Teleseism at 1411	1-12
1.1.1.6.3.4	Spectrum of Teleseism at 1411 in High and Low Frequency Background Noise of Channel 3.	1-12
1.1.1.6.3.5	Mendota SS 62-094 1411 GMT	1-12
1.1.1.6.3.9	Spectrum of Strong Teleseism at 0517	1-12
1.1.1.6.3.10	Paterson Slave Station Seismometer #5	1-12
1.1.1.6.4.8	Toppenish Ridge MS 61-349-16:33:00z Train Noise	1-12
1.1.1.6.4.9	Toppenish Ridge Train Noise PSD	1-12

# List of Figures (Continued)

Figure No.		Follows Page No.
1.1.2.1a	Paterson Station Pacific Northwest Source Directions and Phase Ve- locities for Seismic Noise Below 1 cps from Cross-Spectrum Studies at Toppenish and Paterson	1-13
1.1.2.1b	Paterson Station Probable Pacific Northwest Source Directions and Phase Velocity for 1.0 - 2.0 cps Noise based on Cross-Spectrum Studies at Paterson Station	1-13
1.1.2.2	Dominant Noise Source Directions in the Pacific Northwest	1-13
1.1.2.3	Dominant Noise Source Directions in the Pacific Northwest	1-13
1.1.2.4	Indeterminate Noise in the Pacific Northwest	1-13
1.1.2.10	Toppenish Ridge Source Azimuth vs Noise Frequency	1-13
1.1.2.11	Paterson Source Azimuth vs Noise Frequency	1-13
1.1.1.6.4.10	Paterson SS 62-030-10:00:00z Dam Noise	1-14
1.1.1.6.4.11	1.5 - 2.0 CPS Noise Apparently from McNary Dam area of Columbia River	1-14
1.1.2.15	Average Phase Velocity at Toppenish Ridge	1-14
1.1.2.16	Noise Coherency Values between Peripheral Seismometers of 1/2 and 1 mile Radius Arrays	1-15
1.1.2.17	Change in Coherency of Seismic Noise with Increasing Seismometer Separation	1-15
1.1.3.3.1	Relative Teleseismic Signal Strengths at different slave station Locations	1-17
1.1.3.2.1	Gravity Values	1-17
1.1.3.2.1	Relation of Bouguer Gravity Anomaly to Relative Signal Strength at Califor- nia and Pacific Northwest Stations	1-17
1.1.3.1	Relative Strength of Reception of Teleseismic Signals at Each Seismo- meter position of California and Pacific Northwest Stations	1-17
	Correlation Statistics from Studies of Local Signal Strength and S/N Ratio Variations Partial Correlation Coefficients	1-17

List of Figures (Continued)

Figure No.		Follows Page No.
1.1.3.3.3a	Seismic Background Noise in Signal Strength Measurements	1-19
1.1.3.3.3b	Effect of Seismic Noise on Signal Strength Ratios	1-20
1.1.3.4	Epicenters and First Motion Periods of Teleseisms Studied on VT/078	1-20
1.1.4.1	Average Signal-to-Noise Ratios at each seismometer position	1-21
2.1.1	California Geomorphology	2-2
2.1.2	Surface Geology California Profile	2-2
2.1.3	Tectonics California Profile	2-2
2.1.4	Diagrammatic Cross Section of Califor- nia Profile from Pismo Beach, Califor- nia to Death Valley, California	2-2
2.1.5	Bouguer Gravity Map California Profile	2-2
2.2.1	Pacific Northwest Geomorphology	2-5
2.2.2	Surface Geology Pacific Northwest Profile	2-5
2.2.3	Tectonics Pacific Northwest Profile	2-5
2.2.4	Diagrammatic Cross Section of Pacific Northwest Profile from Grays Harbor, Washington to Idaho Border	2-5
2.2.5	Bouguer Gravity Map Pacific Northwest	2-5
2.3.1	Appalachian Geomorphology	2-8
2.3.2	Surface Geology Appalachian Profile	2-8
2.3.3	Tectonic Appalachian Profile	2-8
2.3.4	Diagrammatic Cross Section of Appalachian Profile from Birch River, West Virginia to Bodie Island, North Carolina	2-8
2.3.5	Bouguer Gravity Map Appalachian Profile	2-8
3.1.0	Block Diagram of Field Recording Equipment	3-1
3.1.1	Master Station Instrument Van, Pickup, and Generator	3-1
3.1.2	General View of the Field Recording System	3-1
3.1.3	J-M Short Period Seismometer With and without case	3-1
3.1.2.2.1	Response to Constant Velocity Drive of Long and Short Period Recording Systems	3-1

### List of Figures (Continued)

Figure No.		Follows Page No.
3.1.4	Front View of Short Period Solid State Amplifiers	3-1
	Rear View of Short Period Amplifiers	3-1
3.1.1.2.1a	System Noise for Amplifier with Trans- former Input - PSD	3-2
3.1.1.2.1b	System Noise for Amplifier with Trans- former Input - PSD	3-2
3.1.5	Tape Recording System, Master and Slave Station	3-2
3.1.6	Front View of Calibration Panel	3-3
3.1.7	Long-Period Seismometer Oven with Cover Removed, Showing Aluminum Inner Shell, Heater Wires and Thermostat	3-4
	Press-Ewing Long-Period Seismometer Without Case	3-4
3.1.8	7.5 Kilowatt Diesel Powered Generator Used to Supply 110 Volt AC Power to Recording Station	3-6
3.1.9	Inside and Outside Views of Lightning Arresters Installed at Each Seismo- meter Position	3-6
	Central Lightning Arrester Installed at Instrument Trailer	3-6
3.1.10	Short-Period Vault Liners with Covers Motor Generator in Background	3-6
3.1.11	Slave Station Instrument Trailer	3-6
3.2.2.0	Digging Pit for the Long-Period Seismo- meter	3-7
	Short-Period Seismometer Vault Liner in Place. Liner is covered with metal lid for burial after installation of seismometer. Long-Period vault in background	3-7
3.1.12	Exploded View, Johnson Matheson Seismo- meter, Model 6480	3-7
3.2.1	Array Configuration	3-8
3.2.2	VT/078 System Response Calibration	3-11
3.2.2.4.1	Long-Period and Short-Period Response to the same Drive (LP and SP seismo- meters located side-by-side) PSD	3-12
3.2.2.5	Magnification of Long-Period System @ 0 db (on 20x viewing screen)	3-12
3.2.2.6	Magnification of Slave Station Short-Period System (to 20x viewing screen) 0 db	3-12
3.2.2.7	Magnification of Master Station Short-Period System (to 20x viewing screen) 0 db	3-12

List of Figures (Continued)

Figure No.		Follows Page No.
4.1.1	Steps in Data Analysis	4-1
4.1.2	Data Analysis Station Block Diagram	4-4
4.1.3	Data Analysis Center Equipment Tape Transport, FM Discriminators, Loop Transport, Band-Pass Filters, and Wave Analyser System, from Left to Right	4-4
4.1.4	Generation of Cross Spectrum Analogs	4-5
4.1.5	Determination of Noise Source Direction from Cross Spectra	4-10
4.1.6	Determination of Maximum Phase Shifts to be expected around an array of known dimensions, for plane surface waves of 4 km/sec phase velocity	4-10
4.1.8	Average Phase Velocity of Seismic Noise	4-10
4.1.9	Illustration of How Cross Spectrum Plots Show Noise Coherency	4-13

## INTRODUCTION

Project VT/078 was initiated for the purpose of recording seismic noise and signals under a variety of geologic and geographic conditions, and correlating the resulting data to determine how the characteristics of noise and signals varied with the physical environment of the recording site. The basic knowledge yielded by the study would then be available for practical application to a number of problems, including the design and selection of sites for seismographic stations with optimum conditions of signal-to-noise ratio.

The specific objectives of the two phases of the project were as follows:

### Phase I: Construction of Mobile Seismograph Stations

- a. To select, procure and assemble a set of field equipment for a master and a slave seismographic station, each of which would record broad band earth noise and signal characteristics on magnetic tape.
- b. To select, procure and assemble a set of data analysis equipment for routine processing of field tapes from the master and slave stations, such analysis to include power spectral density of recorded noise and filtering for optimization of signal-to-noise ratio of earthquake signals.

### Phase II: Field Operations and Data Analysis

- a. To select suitable areas for regional and local noise studies.
- b. To set up the master and slave recording stations and field data reduction offices for at least three selected areas, and to conduct a field measurement program along a profile line for each area, recording short and long period noise, under various geologic and topographic conditions.
- c. To conduct routine data analysis of the recorded seismic waves, determining their power spectral density and coherency, and to correlate the results with the various geological and topographic conditions as well as with time variables, including wind velocity, from the aspect of seismometer array design.

Work on the project began in September, 1960, and the assembly and testing of equipment was completed by March, 1961, when field

operations were begun on a profile across the state of California. On completion of recording in California in November, 1961, recording continued on a second profile in the Pacific Northwest, and then on a third profile across the Appalachian Mountains. The locations of recording stations on these profiles are shown on the maps following this Introduction. Field recording was completed in September, 1962. Although analysis of data began soon after the start of field recording, final conclusions were drawn only after data from all three profiles had been analyzed.

The final report on Project VT/078 is organized to give three categories of information. The first part of the report describes the results of the investigations of the characteristics of seismic noise and signal in relation to geologic and topographic environment. Following this section are general descriptions of the major geologic-geographic features of the areas surveyed, of the equipment and methods used in the field recording program, and of the data analysis methods employed. The last section consists of a group of appendices, including detailed descriptions of recording positions, tabulations and graphs of observed noise amplitude, source direction, coherency and velocity, calibration statistics, and typical noise samples from each recording station.



## SUPPLEMENTARY NOTES

### Page 1-15 Section 1.1.2.3 Noise Coherency.

Coherency has a maximum value of 1.0, by definition. Coherency values calculated and plotted in Figure 1.1.2.16 are sometimes greater than 1.0 because of cumulative error in calibrating, measuring and calculating cross-spectrum values from which coherency was determined.

### Page 1-15 Section 1.1.3 Relative Signal Strength Variations.

In determining regional variations in average teleseismic signal strength among slave seismometers (relative to a master station reference seismometer), magnification corrections were made for every teleseism, but these were used only to check for long-term gain changes between the master station reference channel and slave station channel #2. However, in determining local signal strength variations within each slave array, gain corrections were used for each seismometer. Magnification corrections included corrections for differences between master and slave recording channels in attenuator settings, seismometer motor constants, voltage gain of recording systems, and frequency response.

All signal strength ratios were calculated both with and without magnification corrections; the average ratio at each slave station did not change significantly with application of magnification corrections (other than attenuator corrections). Relative magnification between slave and master seismometers remained essentially constant, as well as could be determined from daily calibration data see (Appendix 6.9). First motion period of each teleseism was nearly the same at the slave as at the master station; the difference could seldom be determined accurately enough to provide a sound basis for frequency response corrections. For these reasons it was decided that signal strength variations between slave stations could be determined

just as accurately by correcting only for attenuator settings as by using complete magnification corrections. Data in Figure 1.1.3.3.1 is corrected only for attenuator settings.

Page 1-18 Section 1.1.3.2 Signal Strength Variation with Local Environment.

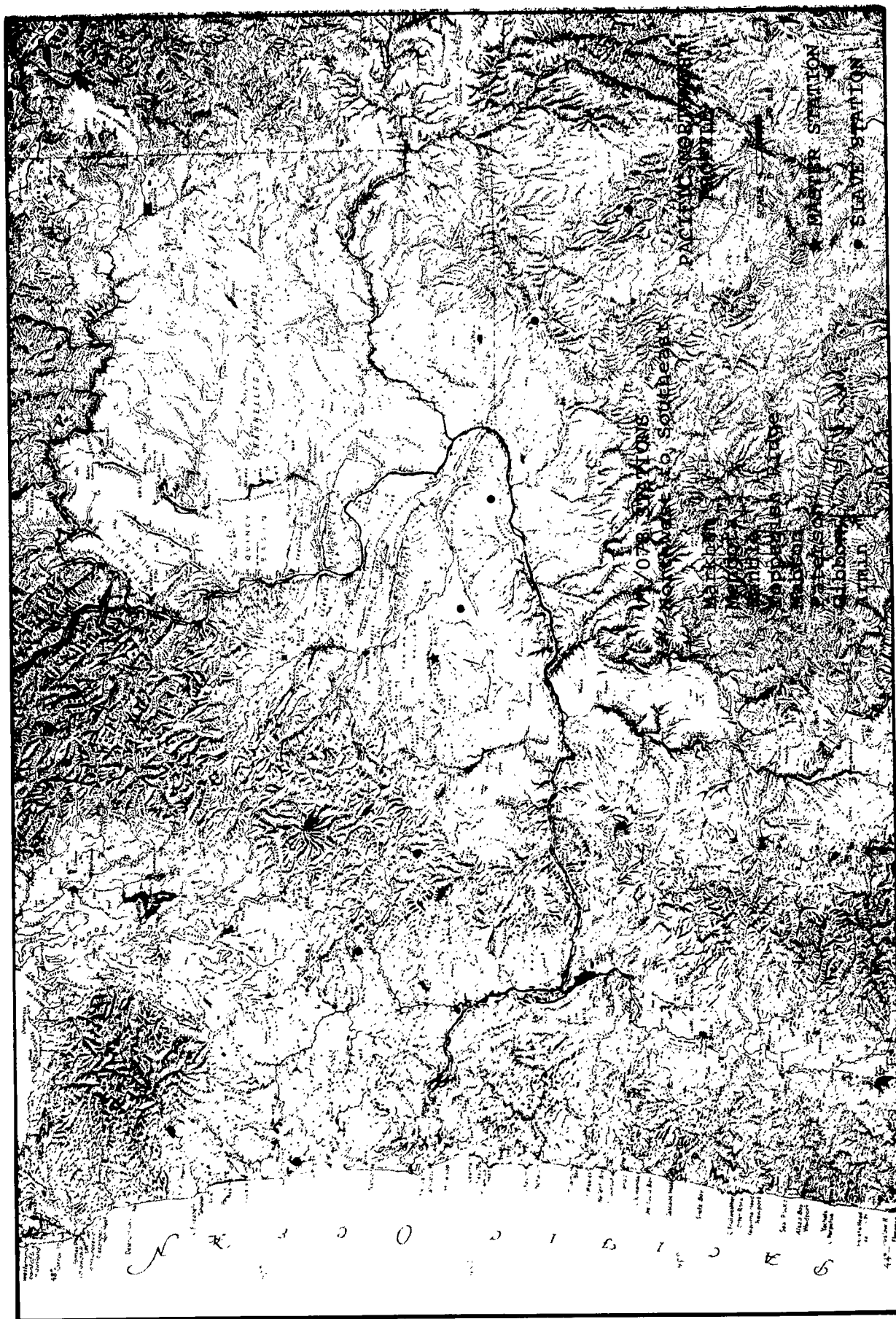
Fewer "hardrock" positions are shown in Figure 1.1.3.1 than in Figure 1.1.1.1.1 (of Section 1.1.1.1) because only the seismometer positions are shown in Figure 1.1.3.1 for which signal strength measurements were made. At some seismometer positions teleseism measurements were not made because they corresponded to channels on film recordings where first motion was consistently off the film or not clearly visible. In Figure 1.1.1.1.1, however, all seismometer positions actually occupied are shown, since noise measurements were made on all channels. At Huasna station in Figure 1.1.3.1, teleseisms were recorded and measured for the "hardrock" seismometer positions #71 and #74. Positions #72 and #78 were also hardrock positions, but signal strength ratios for these positions do not appear in Figure 1.1.3.1, since teleseisms recorded there were not measured.

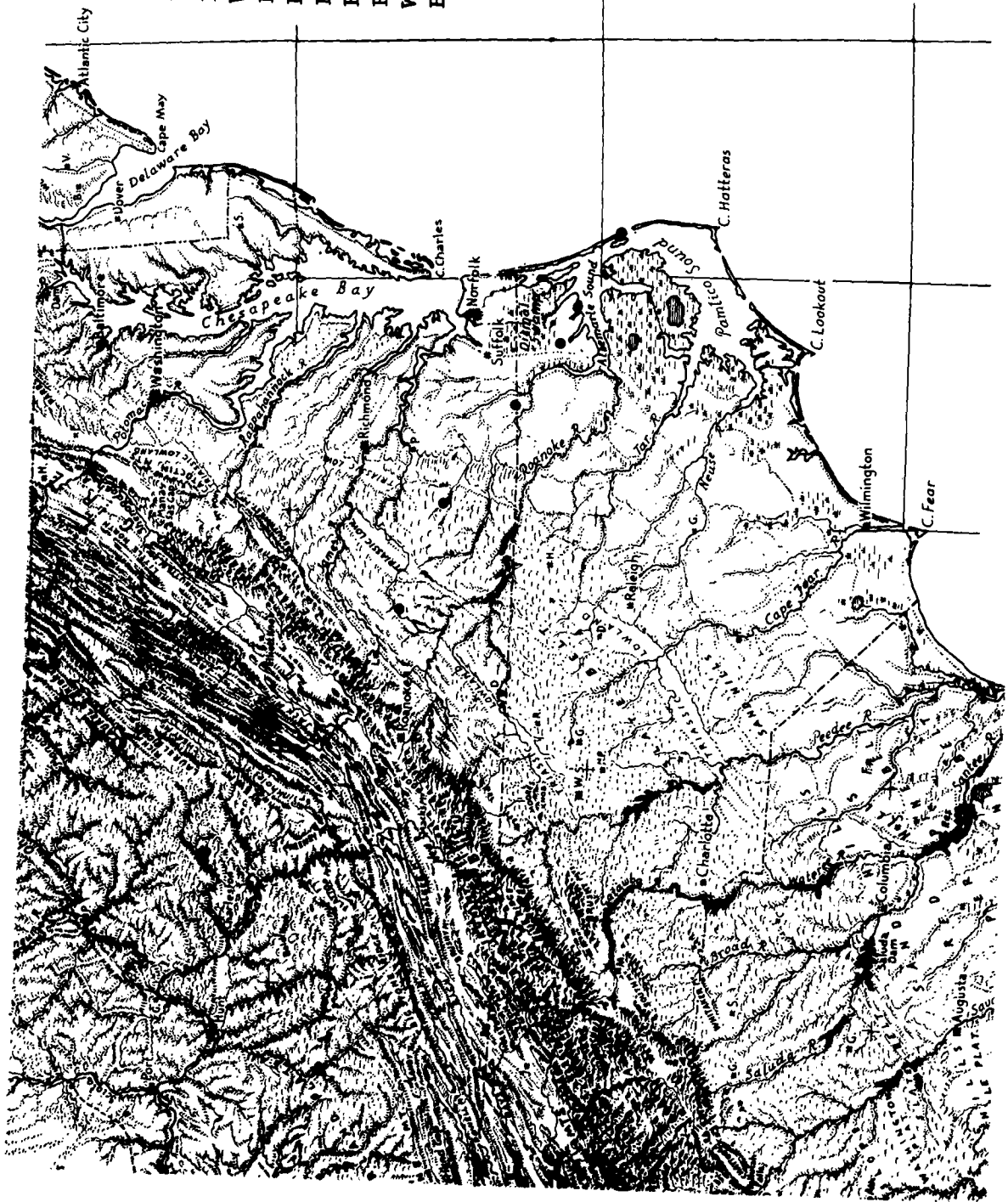
Plots of average signal strength ratios (Figure 1.1.3.1) and average signal-to-noise ratios (Figure 1.1.4.1) for each seismometer position are deceptively simple because they do not show the wide range through which signal strength data scatters. Average deviation from one seismometer of a slave array is usually larger than the difference between averages within the array, and each position was occupied too briefly to define clearly an average signal strength value for that position. For this reason the local variations in Figure 1.1.3.1 and 1.1.4.1 are of questionable significance, other than to show that regional variations are larger than local variations.

Page 3-2 Section 3.1.1.2 Short-period Amplifiers.

Magnification curves for short-period systems with modified amplifiers are shown preceeding page 3-13.







# VT/078 STATIONS Northwest to Southeast

- Birch River
- Warm Springs★
- Buena Vista
- Farmville
- Rawlings
- Franklin
- Belvidere
- Weeksville
- Bodie Island

## APPALACHIAN PROFILE

SCALE 0 50 mi.

- ★ Master Station
- Slave Station

## 1. Results of Investigations

### 1.1 Seismic Noise and Signal Characteristics in Relation to Geologic, Geographic and Temporal Environment

#### 1.1.1 Noise Amplitude Variation with Environment

The seismic noise amplitudes discussed in this report are relative values with respect to a single arbitrarily defined calibration standard. Amplitude values of ground motion for each frequency band are derived from mean seismometer voltage through a wave analyzer filter of 1 cps band-width, relative to the seismometer voltage known to be generated by sinusoidal ground motion of a known amplitude and frequency. Although these values reflect true relative differences in average noise amplitudes across the seismic noise spectrum and among the locations surveyed, their magnitudes will not necessarily be the same as those for seismic noise measurements based on some other calibration standard.

##### 1.1.1.0 Categories of Noise Amplitude Variations

Observed ground motion amplitude variations fell into two categories:

1) Frequency-dependent differences in noise amplitude nearly independent of time or physical environment. Both ground motion amplitude and velocity always increased rapidly with period up to 5 seconds, and the frequency-dependent amplitude change from 0.4 to 5.0 seconds accounted for much of the total observed amplitude variation across the noise spectrum. This has been known for many years (lc)\*. Between about 7 and 10 seconds, noise amplitude decreased with period. The total range of variation in all observed long-term-average ground motion amplitudes between 0.4 and 5.0 seconds period was 50,000 to 1. Within this total, frequency-dependent amplitude changed through about 500 to 1 for most recording stations.

2) Change in noise amplitude with change in recording environment, affecting many or all frequencies. These amplitude variations are of two distinct types:

- a) Relative differences between noise amplitudes at different recording locations, due only to constant differences in geologic-geographic characteristics of the areas. Identification of variation of this type was of major interest in this study. Constant differences in long-term averages for different locations ranged through 50 to 1 in long-period bands and 100 to 1 in bands of shortest period, and were mostly determined by the distance from the ocean, although long-term average wind speed at each station probably influenced average amplitudes.

---

\*(lc) Romney, C.F. (1952) Symposium on Microseisms Page 66. (See References)

- b) Time-dependent changes in noise amplitude related to changes in local wind speed, passage of tropical storms, and similar factors. Time-dependent average ground motion amplitudes varied 20 to 1 or more across almost the entire short-period spectrum in extreme cases, when blizzards and high winds swept across exposed stations in the Pacific Northwest.

The time-dependent variations in noise level tended to obscure relative differences in noise level between different geographic locations. Estimates of long-term differences were based on relatively few samples of noise from each location, when it is considered that their average values depended to a large extent on the dates of the samples because of the strong influence of temporary variations. To eliminate, or at least to reduce the effect of these temporary variations so that long-term noise level differences among locations occupied only briefly could be estimated, fixed reference seismometers monitored the time variations in noise level at slave stations. Average noise amplitude at each peripheral slave seismometer (which was moved to different locations during the period of station recording) was normalized to the simultaneously recorded amplitude at the central slave seismometer (which remained fixed during the period of station recording). This amplitude, in turn, was normalized to the corresponding amplitude recorded at the master station, where the seismometers remained fixed during the entire period of recording on the profile. When correlation in time variations was good among all seismometers, this procedure, in effect, extended the recording time at each slave seismometer from the actual period of a week or two at one location to several months. Long-term differences in noise amplitude among all seismometer positions, were thus estimated by short-term averages from which temporary fluctuations had been removed. These normalized amplitudes were used to study the effect on noise level of geology and other environmental variables.

Long-term average noise levels at each seismometer position of the California and Pacific Northwest profiles, computed in the above fashion, are shown in Figure 1.1.1.1.1. Each seismometer position occupied on each profile was identified by the specific number indicated at the bottom of the figure. Stations are identified and described in Section 2 and the seismometer positions for each assigned number are described in Section 6. For the most part, differences in average noise level between seismometer positions within an array were small compared to the differences between stations.



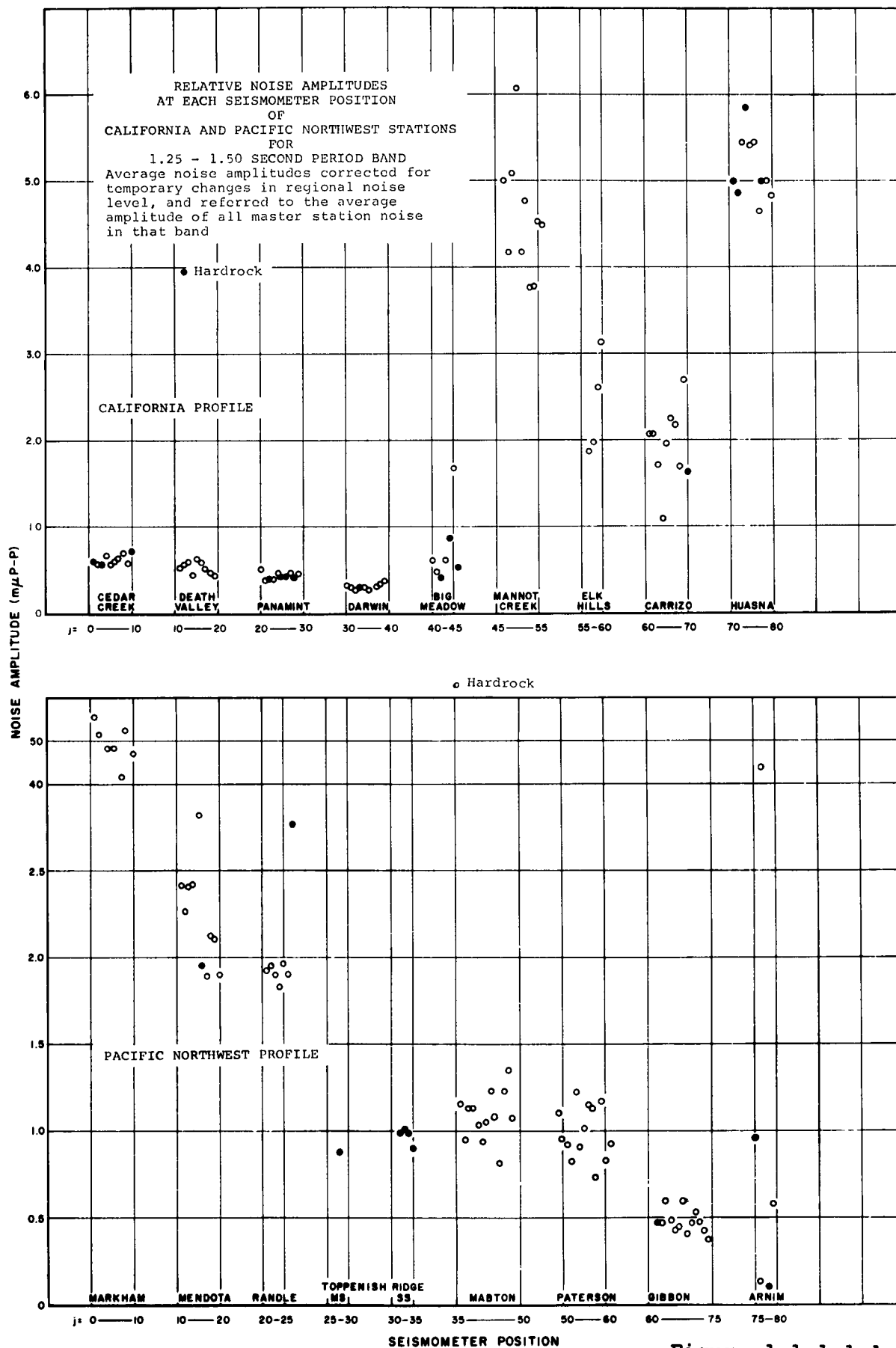


Figure 1.1.1.1.1

#### 1.1.1.1 Variation with Regional Geology, Geography and Topography

Regional environment as used here refers to the large-scale physical features common to the vicinity of a seismograph station. These include distinctions between mountainous regions and lowlands or valleys, characteristics of the geologic province occupied, distance from the ocean, and similar features defined in Section 6.4.

Of all the differences in regional environment of the slave stations occupied, the one most consistently related to differences in long-term average noise level was the distance of the recording location from the ocean. All stations on all three profiles were within 550 kilometers of the ocean. Noise level in every band from 0.4 to 5 seconds period was distributed about an approximately exponential decrease in amplitude as distance from the ocean increased (Figures 1.1.1.1.3 - 1.1.1.1.5). At many stations the deviations from the general trend could be approximately related to lithologic and structural environment of the recording station. Some deviations, especially at higher frequencies, could be related to cultural noise, but for others there was no obvious explanation. Noise levels at the inland-most station of two profiles were all higher than indicated by the trend, and appeared to be higher on the California profile, although this was not clear.

Noise amplitude decrease with increasing ocean distance was as high as 100 to 1, over a distance of 500 km. In order to emphasize noise level variations due to environmental factors other than ocean distance, an attempt was made to fit a function describing the observed distance-dependent noise levels for each short-period frequency band. It was found that logarithms of amplitude and distance formed nearly linear trends for all stations and all frequency bands, if the logs of distance from the nearest coastline were plotted against the logs of average noise amplitude in each frequency band (Figures 1.1.1.1.3 - 1.1.1.1.5). At inland stations the nearest coastline was that of the ocean itself, while at stations near an ocean the nearest coastline was often along a bay or sound. The use of this distance does not imply that seismic noise recorded at inland stations was generated at the nearest coastline. Selection of coastline distance as a parameter was based merely on the observation that it showed an approximately log-linear relation to amplitude, and thus provided a relatively manageable way to estimate for each frequency band how much of the observed amplitude variation between stations might be related to ocean distance and how much was probably due to other factors. Previous studies by Dinger (2c)\*,

---

\*(2c) Dinger, J. E. 1952 Symposium on Microseisms, page 87.

1000

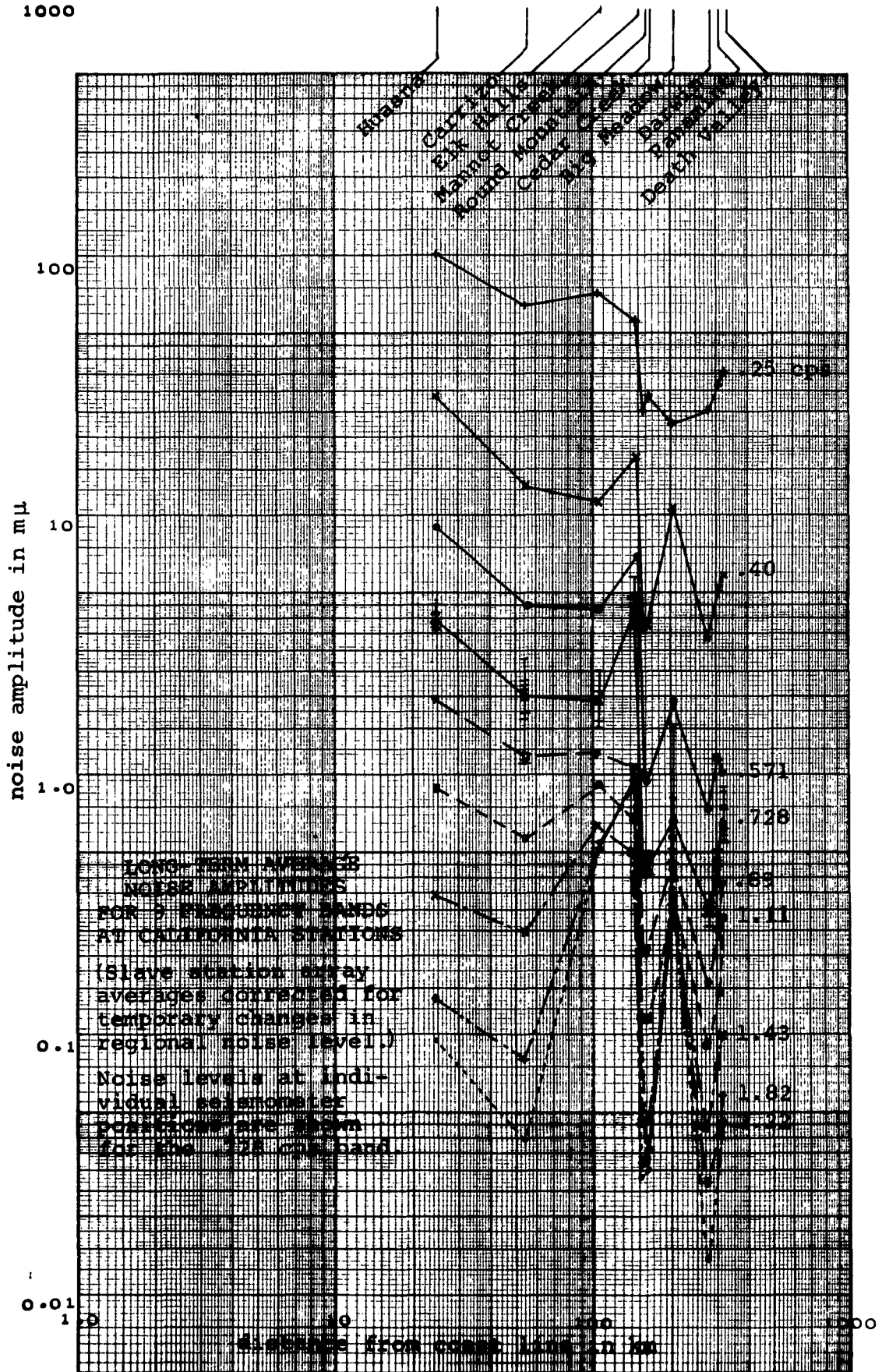


Figure 1.1.1.1.3

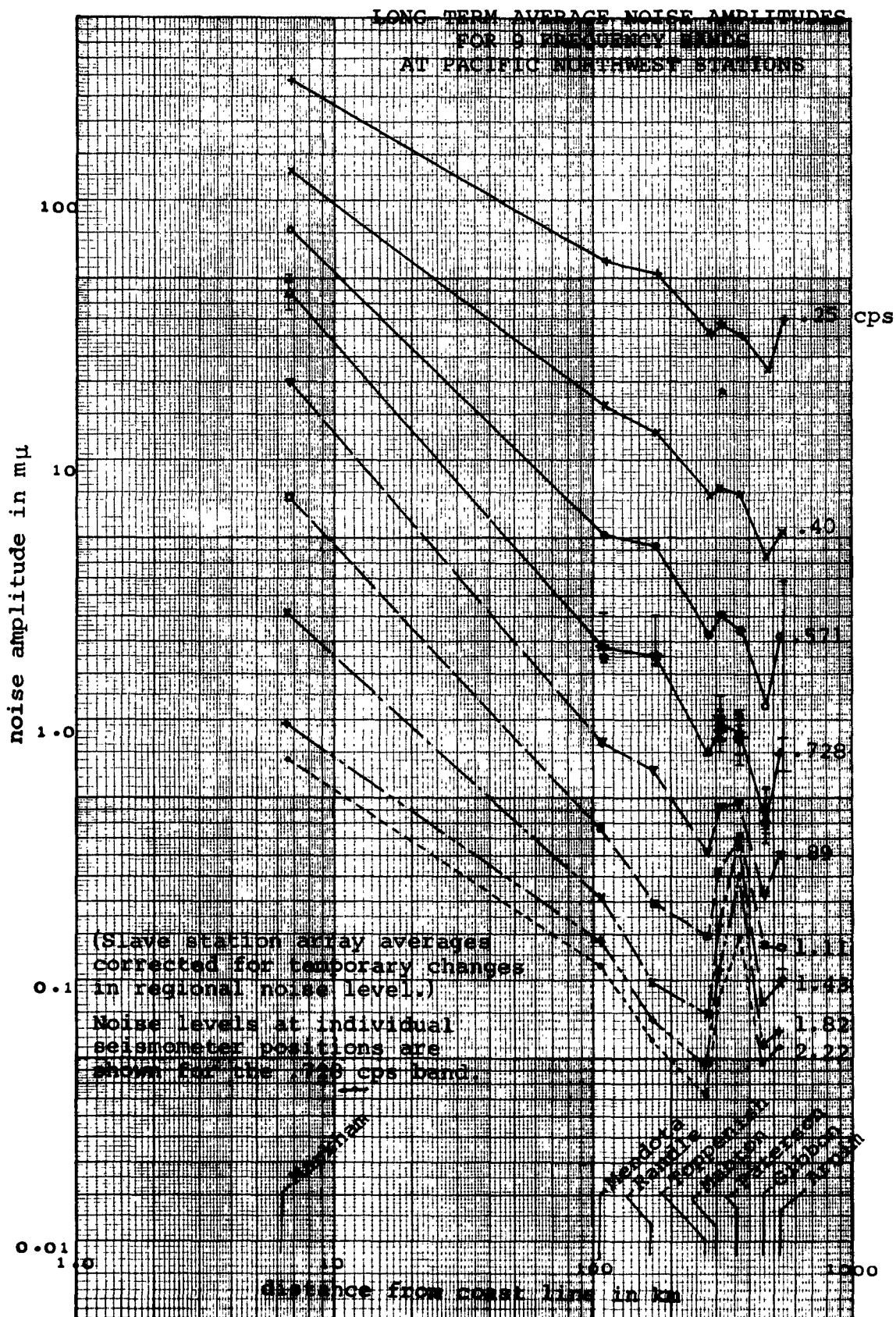
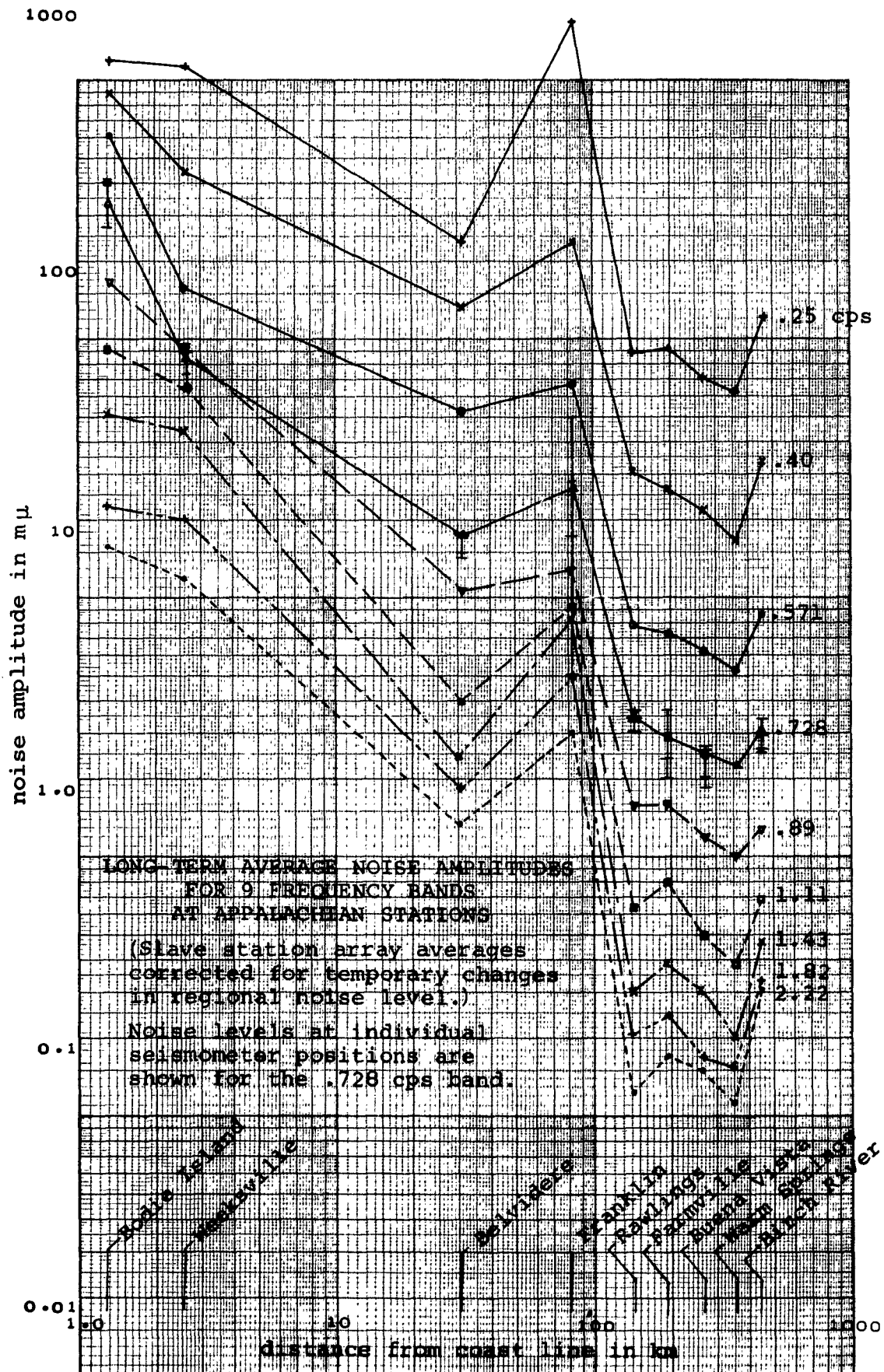


Figure 1.1.1.1.4



**Figure 1.1.1.1.5**

indicate that most ocean-related noise of periods longer than one second is probably generated at the continental shelf, not at coastlines.

The rate of decrease of amplitude with ocean distance appeared to be a fairly smooth function of frequency for stations of all three profiles. Attenuation of amplitude with distance was lowest at longest periods, most pronounced at periods between 0.7 and 1.0 seconds and decreased again for periods less than about 0.7 seconds. This apparent decrease in rate of attenuation at very short periods might have been caused by increasing contribution to long-term average noise level by locally generated wind noise. Another consideration is that the power spectrum plots (from which amplitudes were determined) were usually very small in this range, so error in measurement of power spectrum levels was relatively large.

The very large differences in noise amplitude due to differences in ocean distance tended to mask noise level differences due to other environmental characteristics of each profile, such as station geology and topography. The influence of these other types of variables was also difficult to identify for another reason, which was that there tended to be a progressive change in geologic environment with increasing distance from the coast, rather than random distribution of geologic characteristics along the profile (See Section 2). All three profiles were oriented perpendicularly to the regional trends of geographic and structural features, and two of the three began in Tertiary sediments at the coast and ended in granite or indurated Paleozoic sediments inland (Figures 2.1.1 - 2.3.5). On the Appalachian and California profiles, topographic variation also became more pronounced as distance inland increased. This relatively high degree of correlation between noise amplitude, ocean distance and geologic-topographic environment made it important that a way be found to separate the effect of ocean distance from that of geology and topography. The approximate log-linearity of noise amplitude and coastline distance suggested a method.

It was found that amplitudes on the average linear trends of Figures 1.1.1.1.3 - 1.1.1.1.5 could be closely approximated on all three profiles and for all frequency bands by a function  $Y(f,x)$  of noise frequency ( $f$ ) in cps and distance to nearest coastline ( $x$ ) in kilometers.  $Y(f,x)$  in millimicrons p-p is given by the expression

$$Y(f,x) = Y_0(f) \left[ \frac{x}{x_0} \right]^{k(f)}$$

where  $\ln Y_0(f) = a e^{-\beta (\ln f/\gamma)^2} - \ln 50$

and  $k(f) = a e^{-b (\ln f/c)^2}$

and where  $x_0$ ,  $\alpha$ ,  $\beta$ ,  $\gamma$ ,  $a$ ,  $b$ , and  $c$  are the constants given below:

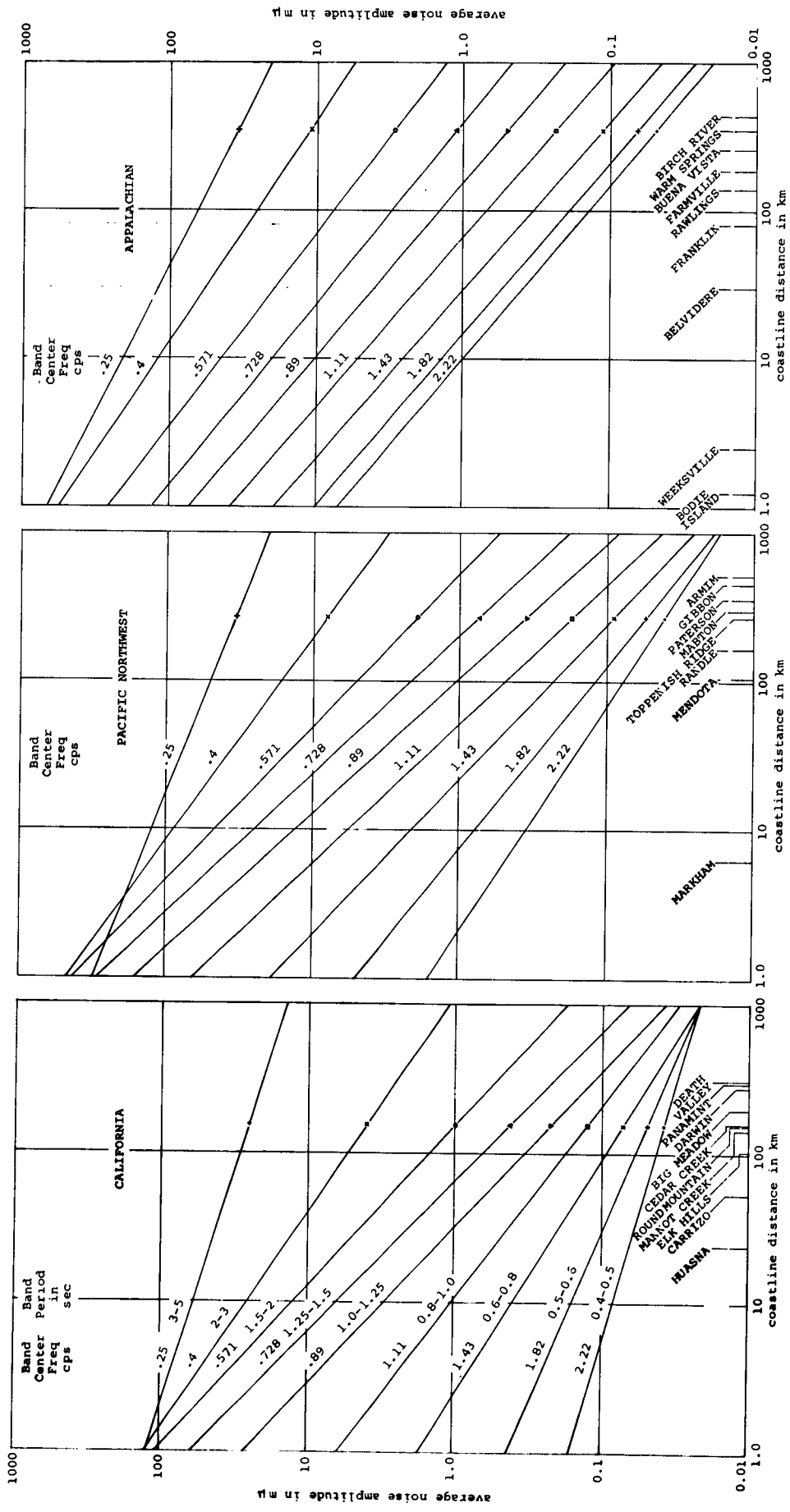
Profile	$x_0$	$\alpha$	$\beta$	$\gamma$	$a$	$b$	$c$
California	154 km	9.00	.275	.10	-.990	1.00	.73
Pacific Northwest	270km	7.85	.365	.17	-1.094	.620	.90
Appalachian	350km	7.61	.382	.20	-.878	.169	1.40

This function (for each profile) is plotted in Figure 1.1.1.1.6. The function  $Y_0(f)$  closely approximates the long-term average noise amplitude spectrum at the master station of each profile, which is located  $x_0$  kilometers from the nearest coastline and whose amplitude values are indicated by symbols over the master station locations of Round Mountain, Toppenish, and Warm Springs. The function  $k(f)$  describes the rate of change of noise amplitude with coastline distance in a narrow band of frequencies about  $f$  cps. The function  $Y(f,x)$  is thus an approximate description of what the master station noise amplitude spectrum would have been had the station been located at other than  $x_0$  kilometers inland, but with no change in geologic-topographic environment.

The function  $Y(f,x)$  was used to estimate how the amplitude spectrum at each slave station would have differed from that of the master station had noise level not been influenced by ocean distance. Observed slave station noise amplitudes at each frequency were divided by the corresponding values of  $Y(f,x)$  and the ratios were multiplied by  $Y_0(f)$ , giving an estimate of the slave station noise amplitude spectra with the effect of ocean distance removed. The deviations in these amplitudes thus reflected the influence on noise level of random variations in geology and topography more strongly than did the unmodified spectra.

The slope function  $k(f)$  is partly determined by geologic-topographic environment because of the correlation between ocean distance and the geologic-topographic environment, especially on the California and Appalachian profiles. Its use as a pure attenuation factor in estimating and removing distance-dependent variation in noise level, therefore, very likely also removed some of the geology-dependent differences between stations, the very differences being sought. This factor largely confounded the effort to define possible influence on noise level of the thinning of the thick wedge of Cenozoic sediments in the Atlantic Coastal Plain.





### APPROXIMATION OF LONG-TERM AVERAGE NOISE AMPLITUDE SPECTRA AT EACH RECORDING STATION BY A FUNCTION OF COASTLINE DISTANCE AND NOISE FREQUENCY

Long-term average noise amplitudes  $Y(f)$  mμ, in frequency bands centered at  $(f)$  cps, at stations  $(x)$  km from the nearest coastline, approximated by the function

$$Y(f,x) = \Phi_1(f) \cdot [a,x]^{\Phi_2(f)}$$

Where  $\Phi_1(f)$ ,  $\Phi_2(f)$  and  $a_1$  are known.

Figure 1.1.1.1.6



Noise amplitudes for 9 bands between 0.4 and 5.0 seconds period, corrected for ocean distance effect, are shown for all stations of each profile in Figure 1.1.1.1.7. These are essentially residuals of data from Figures 1.1.1.1.3 - 1.1.1.1.5 with the log-linear trends removed. The major geologic and topographic features of each profile are summarized in diagrammatic cross-section below each graph. (The master stations for each profile are not identified in this figure. The California master station at Round Mountain is the first station to the right of Mannot Creek, the Pacific Northwest master station at Toppenish Ridge is the first station to the right of Randle, and the Appalachian master station at Warm Springs is the first station to the left of Birch River). The function  $Y_0(f)$  describing the master station

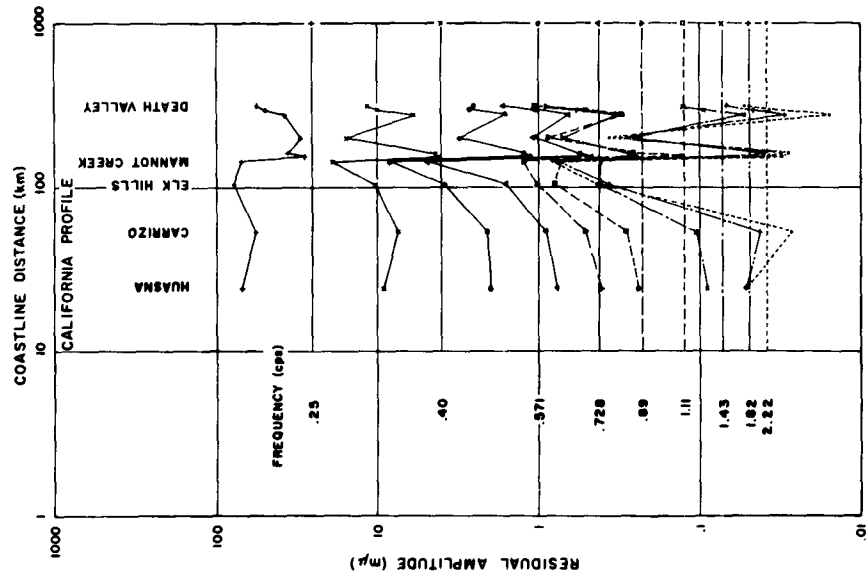
noise amplitude in each frequency band is shown as a horizontal line at the amplitude appropriate to the indicated frequency band. Slave station amplitudes for that band, corrected for variation with distance, are plotted as "residuals" about  $Y_0(f)$ .

Residual amplitudes appear to be of three types: those randomly distributed along each profile, whose magnitude is dependent on frequency, those consistently high or low for a few consecutive slave stations, and those which show approximately uniform change along the whole profile.

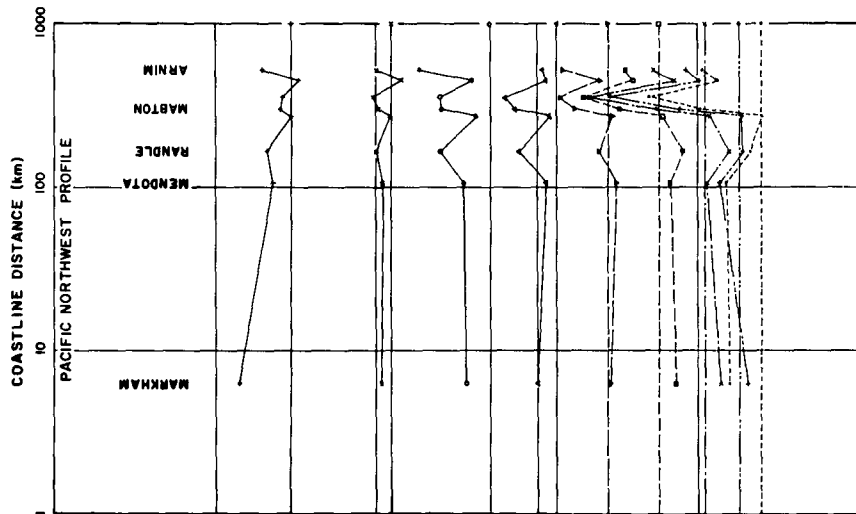
1) Residuals of the first type are the largest and for the most part can be directly related to unusual recording environment at specific slave stations. At Mannot Creek in California and Franklin in Virginia (see Figure 1.1.1.1.6 for station locations and Figure 1.1.1.1.7 for residuals), noise amplitudes across the whole spectrum were very high. Each station was located on a wedge of seaward-dipping Tertiary marine sediments, near the vertex of the wedge, where sediments were less than 1500 meters thick. Both were at the inland limit of major Cenozoic sedimentary provinces (See Figures 2.1.4 and 2.3.4). The high noise level at Franklin may have been due to swampy terrain in the Franklin area. The ground at Mannot Creek was typically dry and solid at the surface. Residual noise amplitude for shorter periods was more pronounced at Mannot Creek than at Franklin. Possibly the source of Mannot Creek noise was cultural, from nearby oilfields and cities, or possibly noise amplitude increased with thinning of the sedimentary wedge. Theoretical studies of Love wave amplitudes by De Noyer (3c)\* indicate a possible increase in Love wave amplitude with decrease in thickness of the propagating layer, and studies by

---

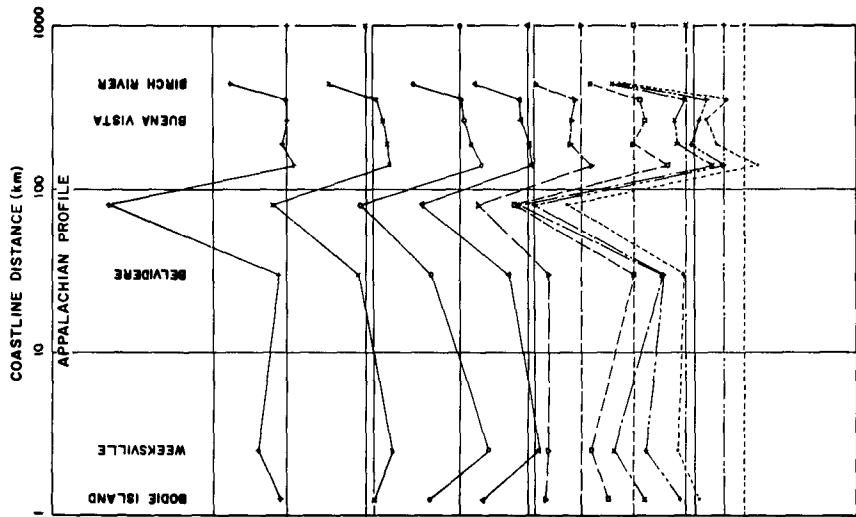
\* (3c) De Noyer, J. Bulletin of the Seismological Society of America Vol. 51, #2, April 1961, pages 227 - 235.



Diagrammatic Cross Section of California Profile



Diagrammatic Cross Section of Pacific Northwest Profile



Diagrammatic Cross Section of Appalachian Profile

# FREQUENCY-DEPENDENT NOISE AMPLITUDE RESIDUALS AT EACH RECORDING STATION AFTER REMOVAL OF VARIATIONS WITH COASTLINE DISTANCE OF VALUES OF THE SPECTRUM-APPROXIMATING FUNCTION $Y(f, x)$

Removal of estimated effect of proximity to ocean emphasizes noise-level variations with geologic environment

Figure 1.1.1.1.7

Gutenberg, Donn and others indicate that the change in crustal thickness at continental boundaries constitutes a barrier to any wave for which the crust acts as a wave guide. Dissipation of energy in the form of large-amplitude motion at such barriers might explain some of the large amplitudes observed. The large amplitudes at Mannot Creek cannot be explained away entirely as due to cultural noise because the amplitudes near 1.4 seconds period show very nearly log-normal distribution (Figure 1.1.1.6.8), not favoring any specific amplitude. Such distribution seems unlikely for cultural noise from oilfields where activity remains constant.

Noise level at Elk Hills station on the other side of the valley from Mannot Creek also showed high noise level at short periods. However, this was high-level noise distributed raggedly in frequency between 0.1 and 1.0 second period and was very likely caused by nearby oilfield activity. In contrast, Mannot Creek noise was dominant at 0.5 and 1.5 seconds period (See Figures 6.7.1.3 and 6.7.1.4 in the Appendices).

Other stations showed large unsystematic deviations in residual amplitude which could be explained more easily. Big Meadow station on the California profile was located in a swampy, peat-filled basin in the mountains. The extremely high noise level there was probably due to standing waves generated in the jelly-like fill during frequent storms. (This effect was probably influential to some extent at Franklin, also). The Big Meadow station was abandoned after brief occupancy because of dangerous lightning storms. Paterson station in the Pacific Northwest showed high-level noise below 1 second period, very probably due to cultural noise from the McNary Dam area (See Section 1.1.2). The inland-most station of the Pacific Northwest and Appalachian profiles showed residuals; the residual at Armin is probably due to a nearby river; the residual at Birch River has not been explained. Deviations at coastal stations are probably due to the inability to correct completely for the temporary and extreme variations in noise level, so that the long-term averages for these stations are inexact.

2) Residuals of the second type, those with consistently high values for a few consecutive stations, were found mainly at slave stations in Tertiary sediments of the California and Appalachian profiles. The Mannot Creek and Franklin stations both appear to mark a point of offset in the trend line for stations on either side. Stations on the seaward side of the offset were in Tertiary sediments in both cases, while stations on the inland side were in Paleozoic sediments or granite.

3) Residuals which showed continuous change along the entire profile (such as along the 0.5 cps band for the Appalachian profile) indicate

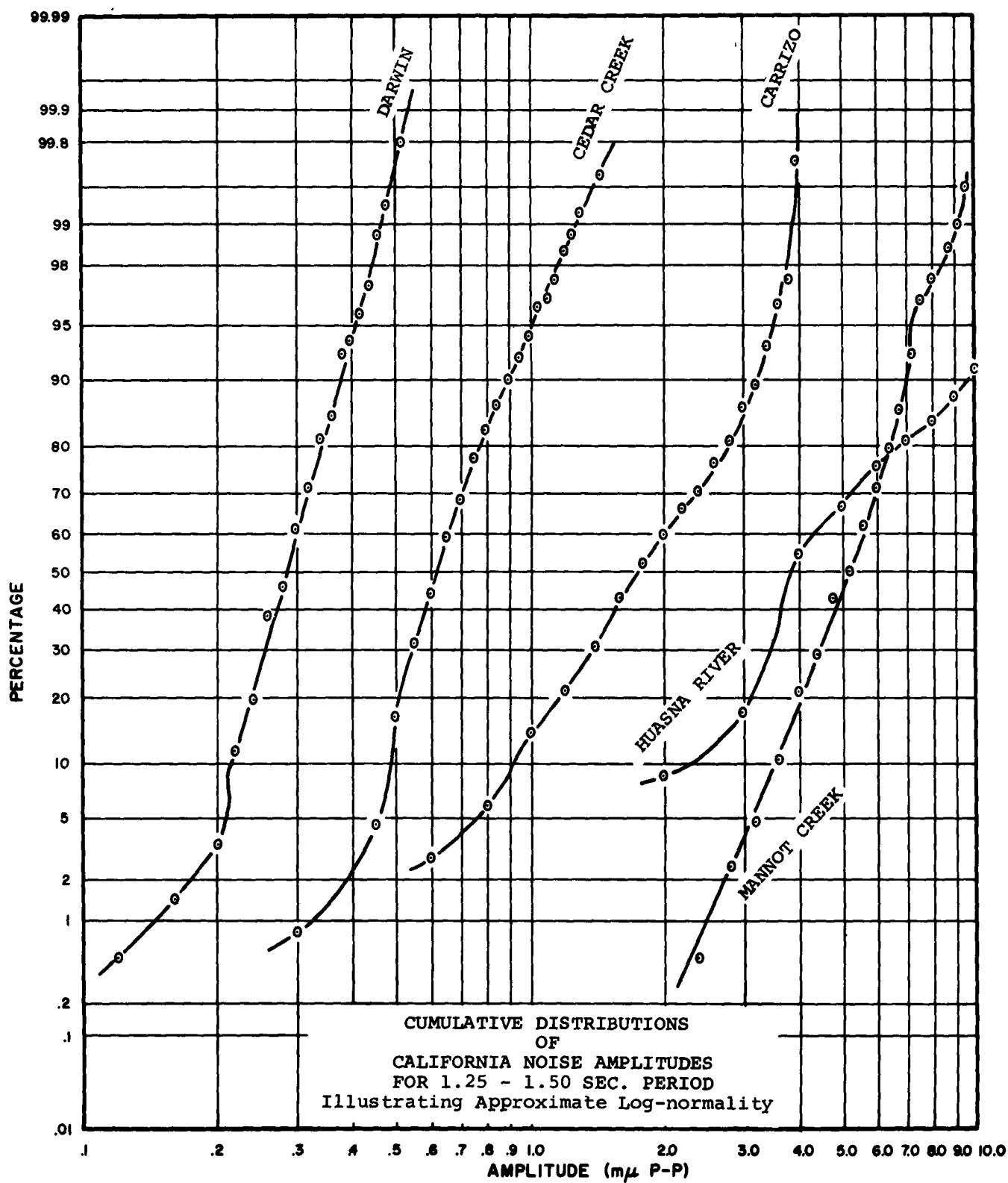


Fig. 1.1.1.6.8

deviations of the smooth slope function  $k(f)$  from observed slopes. Constants of  $Y(f,x)$  were determined to give the best fit at low frequencies, but to fit other frequencies as well as possible while maintaining a function of the same form for all three profiles.

Deviations of observed noise amplitudes from the corresponding values of  $Y(f,x)$  at each station appear to be functions of frequency, especially for high-frequency noise. At lower frequencies, however, multiplication of  $Y(f,x)$  by some constant determined for each station will practically eliminate deviations across the whole low-frequency spectrum. If it is assumed that these correction factors are determined by the regional lithology of each slave station, their magnitudes must be equal for all stations in the same lithologic province. This is equivalent to an assumption that a predetermined lithologic contrast will cause a predictable change in noise level, without need for consideration of transmission coefficients across the contrast. On the other hand, if it is assumed that a change in noise level between two lithologic provinces is due to the nature of the energy transmission coefficient across their contact, then noise source direction and geologic structure must be considered as much or more than lithology alone.

Neither assumption can really be tested with the data available here, because noise level, regional structural and lithologic contrasts all tend to change progressively with increasing distance inland on both the California and Appalachian profiles. Residuals in the Pacific Northwest are relatively small, as are both lithologic and structural contrasts. The only indication in this study that contrasts in residual noise levels might be more related to structural than to lithologic contrasts is in data from Mannot Creek and Franklin, where high noise levels might also be explained by the local surface features mentioned earlier. The cause of change in noise level could be interpreted more clearly if recording stations had been spaced more closely across zones of geologic contrast.

Because of the high degree of dependence among contrasts in structure, lithology, ocean distance, and noise level, the residuals of type 2 can be arbitrarily assigned to lithology alone for determination of correction factors. A constant correction factor for each lithologic province was assigned to values of  $Y(f,x)$  at each station and this procedure removed much of the originally observed residual values. A correction factor considering structure was included for Mannot Creek and Franklin, and one for unusual conditions of local surface lithology (peat bog at Big Meadow and swampy ground at Franklin, when appropriate. These factors, listed below, were intended to adjust observed residuals at each station to hypothetical residuals for a station recording on massive granite. No corrections were applied to Pacific Northwest

stations, because of relative uniformity of lithology, obscurity of structural features, and uniformity of noise level residuals along the profile.

#### Correction Factors

	<u>Regional Lithology</u>			<u>Struc- ture</u>	<u>Local Lithology</u>	
	<u>granite</u>	<u>Paleozoic sediments</u>	<u>Tertiary sediments</u>		<u>Bog (Deep Mud)</u>	<u>Swampland (Packed Sand)</u>
Recording Environment:				Wedge		
California	1	1	2	2.5	3	-
Appalachian	1	1.4	2.1	2	-	1.4

The function  $Y(f,x)$  was multiplied by as many of these factors as were appropriate at each slave station of a profile, and divided by as many as were appropriate to the master station for that profile. This adjusted  $Y(f,x)$  at each slave station for assumed influence of lithologic and structural variations between master and slave stations.

Figures 1.1.1.1.8 and 1.1.1.1.9 are graphs showing the correlation between observed long-term average noise amplitudes and those calculated by adjusted and unadjusted values of  $Y(f,x)$ . The correlations of Figure 1.1.1.1.8 are against the function of noise frequency and ocean distance alone, while those of Figure 1.1.1.1.9 are against values of  $Y(f,x)$  after adjustment for lithologic and structural variations between recording stations. To facilitate their presentation the figures are labelled as "predicted vs. observed" amplitudes. The use of the word "predicted" is not intended to imply that long-term average noise amplitudes are determined by the specific variables used in the function describing these amplitudes. The choice of variables was based on the observation that noise amplitude could be described in terms of these variables, and does not invalidate use of any other set of variables which might also be correlated with long-term average noise amplitudes. For example, wind speed increases are known to be correlated with noise amplitude increases, so that differences in long-term average values of wind speed among recording stations is probably involved in noise level data being considered here. Long-term average wind speed can be considered a geographical environmental constant, and its change is often approximately proportional to ocean distance, for stations not very far inland. Short-term fluctuations in wind speed are often large, but changes in long-term average wind speed values with increasing distance from the ocean are small in most cases, and have not been considered here.

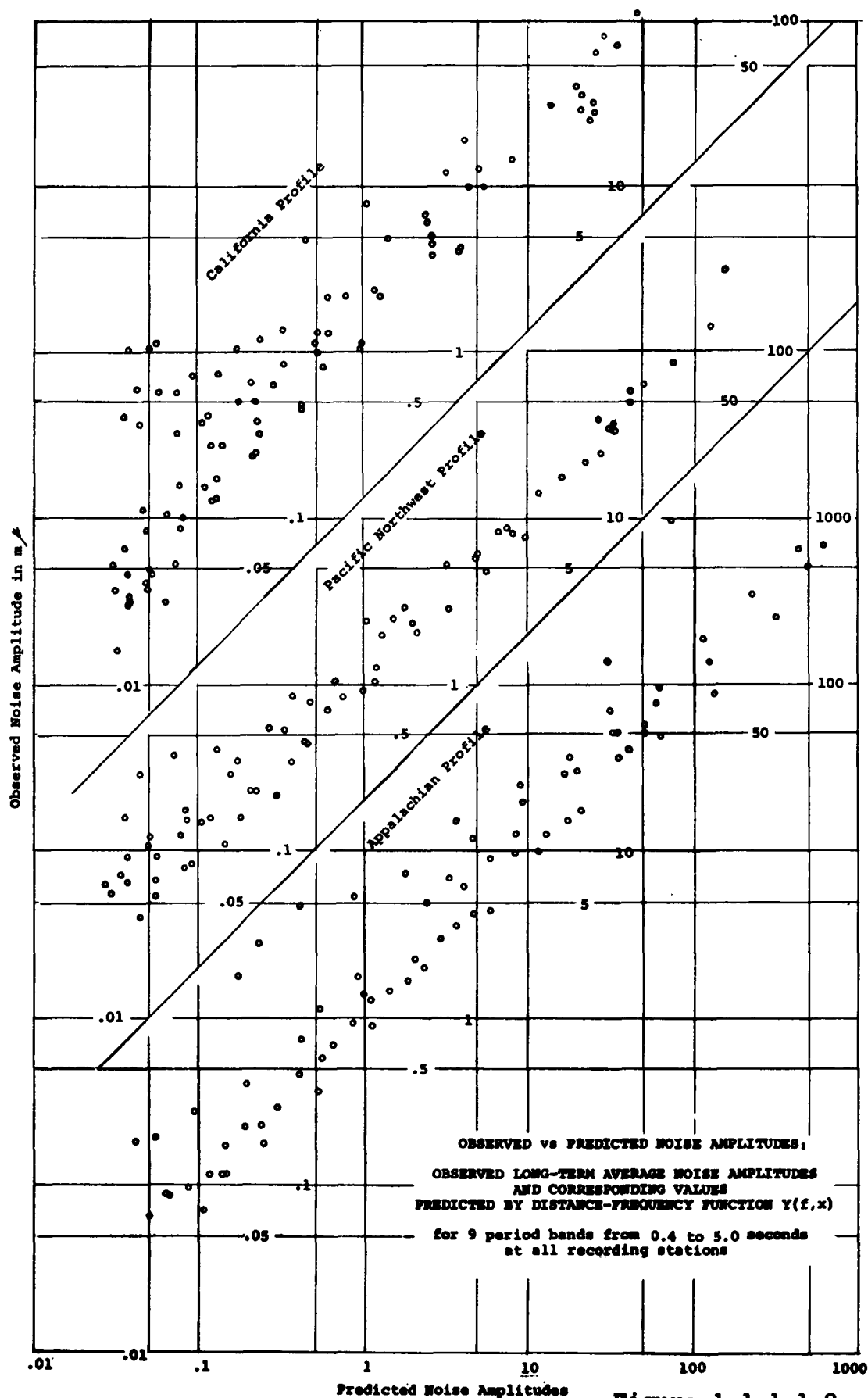


Figure 1.1.1.1.8

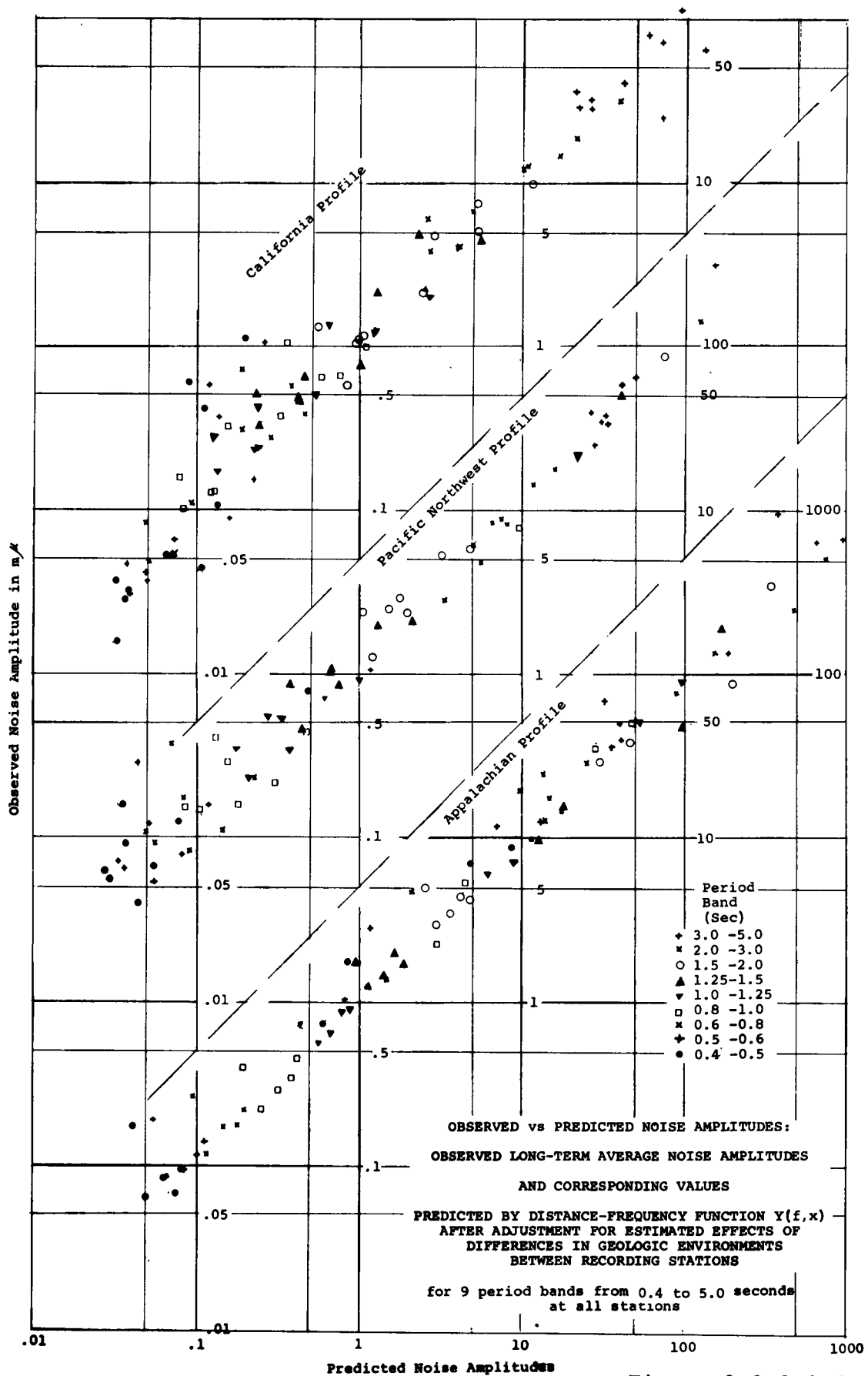


Figure 1.1.1.1.9



#### 1.1.1.2. Variation with Local Geology and Topography

Local variations in geology and topography are defined here as variations of the kind observed over the mile or two separating seismometers of a single array. They could not be clearly related to noise level except for relatively high frequencies.

Normalized noise levels at each seismometer position of an array (to that for the fixed central seismometer) controlled the relatively large time-dependent changes in noise level and permitted reliable estimation of noise level differences due to variations in local geology and topography. Local variations in response to seismic noise were small compared to noise level differences between recording stations, except when seismometers were located on swampy ground. Average noise levels for a single noise band at each seismometer position of the California and Pacific Northwest profiles are shown in Figure 1.1.1.1.1. Variation in noise amplitude among seismometer positions was about 20% of the average noise level over the whole array.

Relative changes in noise level with relative changes in geology and topography within seismometer arrays for noise in the 2.2 and 7.3 cps bands was tested by means of a multiple regression program, described in section 4.3. The results are listed in the following table, in which the program for 6 December was a test in the 2.2 cps band and all other were tests in the 0.73 cps band.

The principal earth variables tested against noise level were alluvial thickness, relative solidity, density and porosity of the rock type in which each seismometer was planted, and general type of topography around the seismometer. Noise levels in the band tested in the multiple regression program showed only a suggested noise level increase with alluvial thickness and perhaps with rock density. Inspection of film recordings of seismic noise often showed substantial differences in noise level between seismometers directly on hardrock and those on loose sediment but these differences were largely limited to frequencies above 2 cps. Such large contrasts in recording environment were too infrequent in the data available to show up well in the correlation program.

## 2.2 cps and .73 cps Bands

- (1) Sample includes noise levels at easimeters indicated for all stations of profile except Big Meadow, Elk Mills.
- (2) Sample includes all California easimeter positions except Big Meadow, Elk Mills.
- (3) Sample includes all easimeter positions at Death Valley Penamint, Mannett Creek and Carrizo Stations.

(1) Sample includes noise levels at all stations of profile except Big Meadow, Elk Mills.

(2) Sample includes all California seismometer stations except Big Meadow, Elk Mills.

(2) Sample includes all California salamander positions except any reserves, six miles.

### 1.1.1.3 Variation with Time

This section presents briefly some of the time-dependent noise amplitude variations observed, which included daily and seasonal variations and wind-derived noise. As wind-generated noise is being studied in a separate project, it will not be discussed in detail here.

Average daily variations in noise amplitudes for the three master stations are shown in Figures 1.1.1.4.1.1 through 1.1.1.4.1.3. These figures show the means and standard deviations of all noise in three frequency bands sampled at the hours of the day indicated on the figures. At the California master station the noise level in all three bands remained fairly constant throughout the day, with only a suggestion that minimum means and deviations occurred at 1700 GMT. The hour of minimal noise level is not easy to define on any of the graphs but appeared to be during the early morning hours, at least at the California and Pacific Northwest master stations. The sudden break in trend of Appalachian profile data at 2400 is probably a reflection of the sampling distribution which defined the curve, since Appalachian data were less densely sampled than those of the other two profiles.

The seasonal variations shown in Figures 1.1.1.4.2.1 through 1.1.1.4.2.3 are based on average noise amplitude means and deviations in consecutive 10-day periods at the three master stations, and show that minimum noise levels occurred in summer months. The Pacific Northwest maximum in early March was probably due to a high coincidence of windy samples.

High wind speeds in the Pacific Northwest were very closely correlated with high-amplitude noise across much of the short-period spectrum, but was most noticeable above 1 cps. Recent studies\* indicate that 60 to 90% of short-term and daily variation in noise level can be expressed as an exponential function of wind speed above about 9 miles per hour. Examples of records and spectra of short-period noise during low and moderate wind are shown in Figures 1.1.1.6.4.3 through 1.1.1.6.4.6.

The effect on wind noise of sheltering a seismometer inside a mine shaft is shown in Figure 1.1.1.3.1, which consists of records of two earthquakes during moderate and low wind. Noise on hardrock inside the mine shaft during moderate wind outside is very similar to noise on alluvium just outside the mine shaft during low wind.

---

\*Bradford, J. (1962) Weather-Seismic Noise Correlation Study, Progress Report #12, Prepared for Geophysical Research Directorate, United States Air Force (Contract AF19(628)-230).

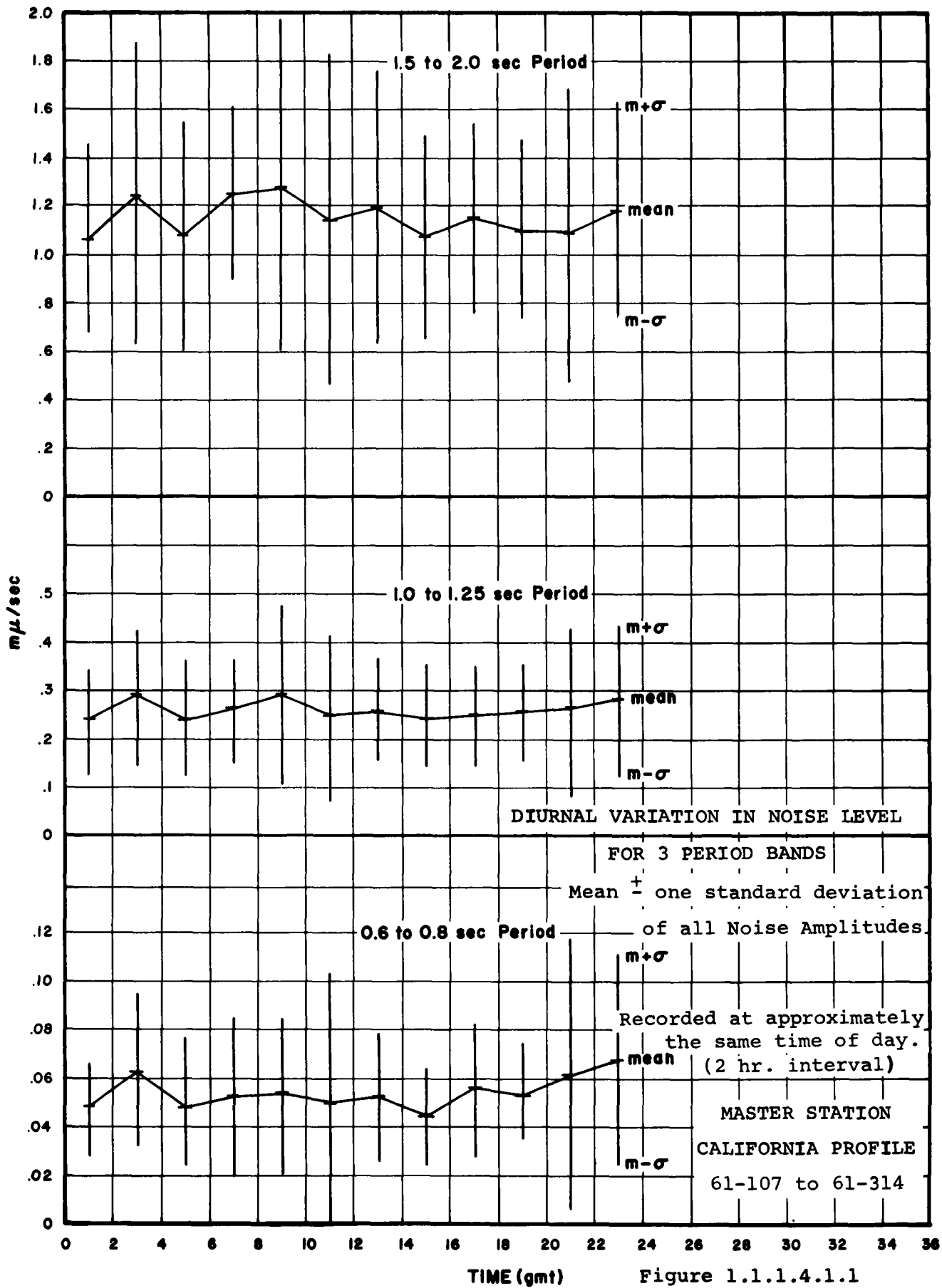
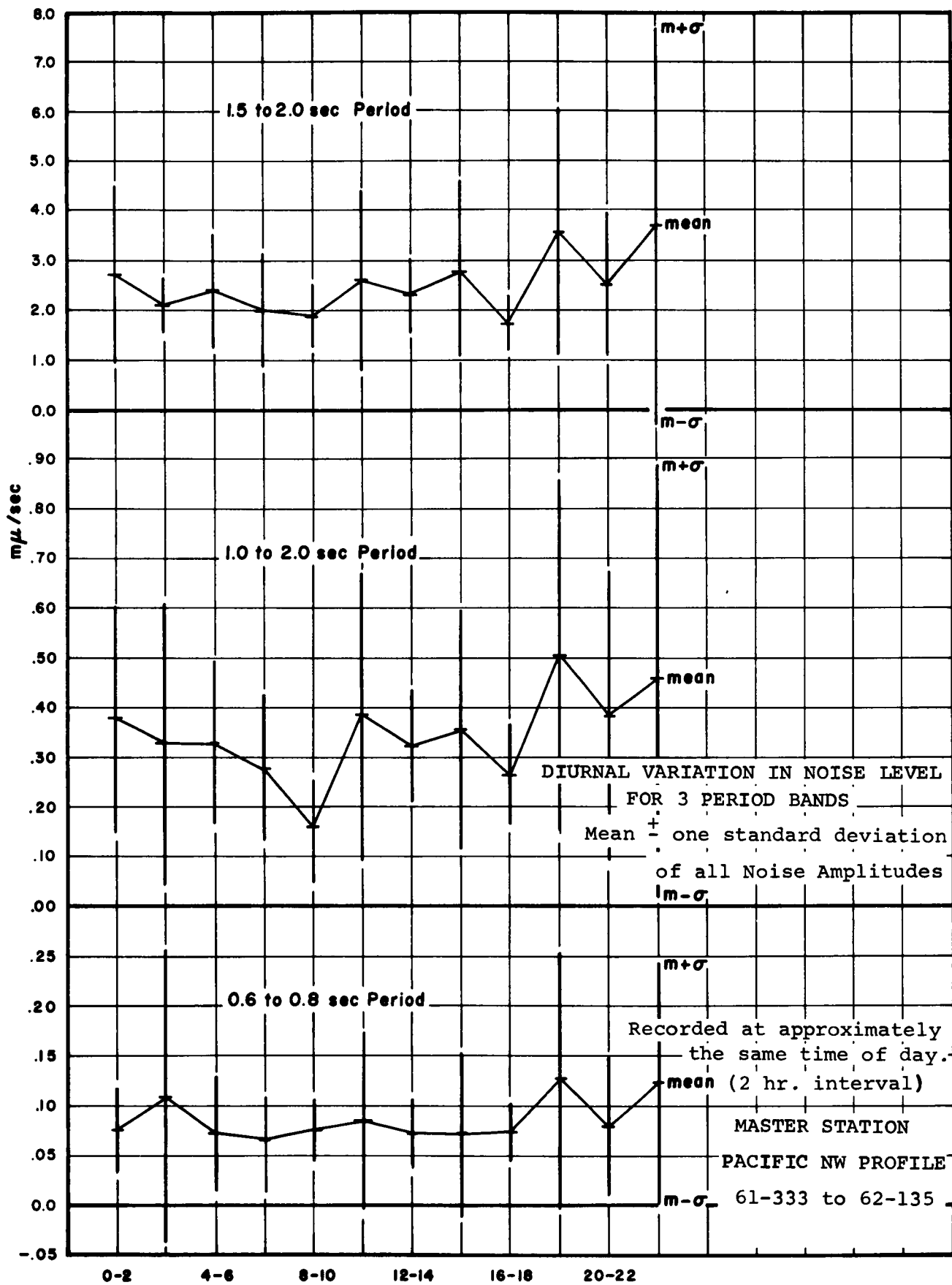


Figure 1.1.1.4.1.1



TIME (gmt) Figure 1.1.1.4.1.2

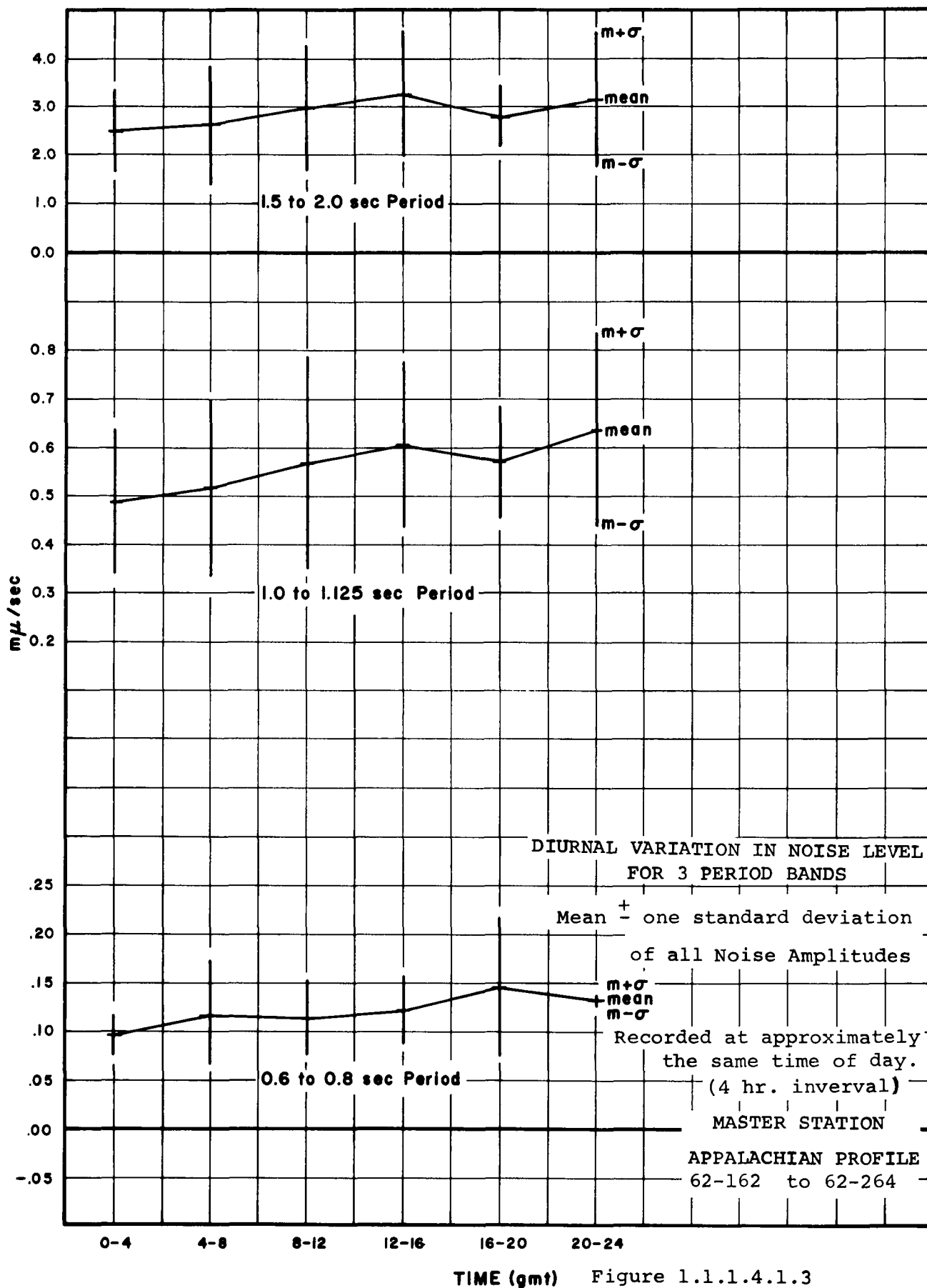


Figure 1.1.1.4.1.3

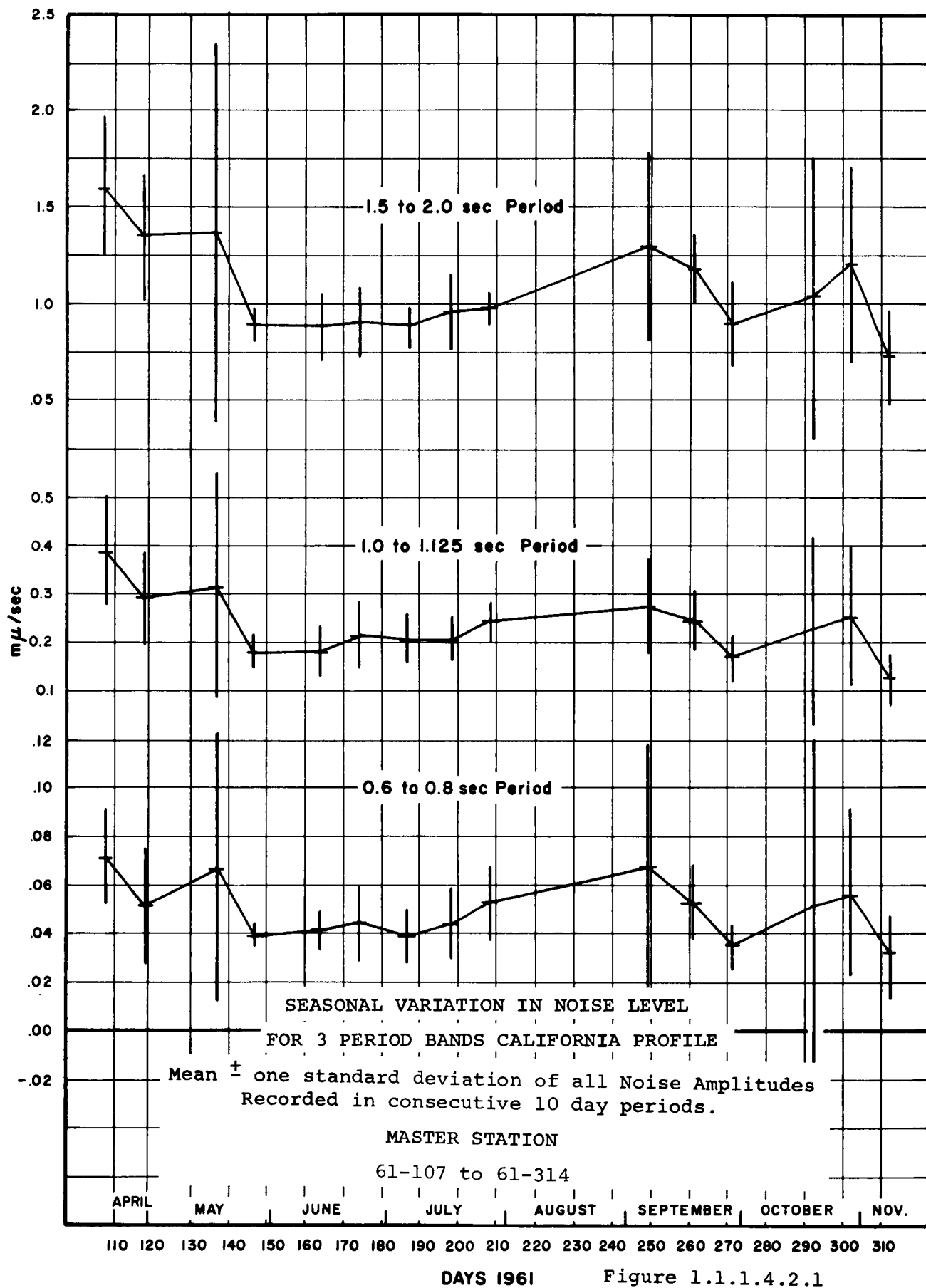


Figure 1.1.1.4.2.1

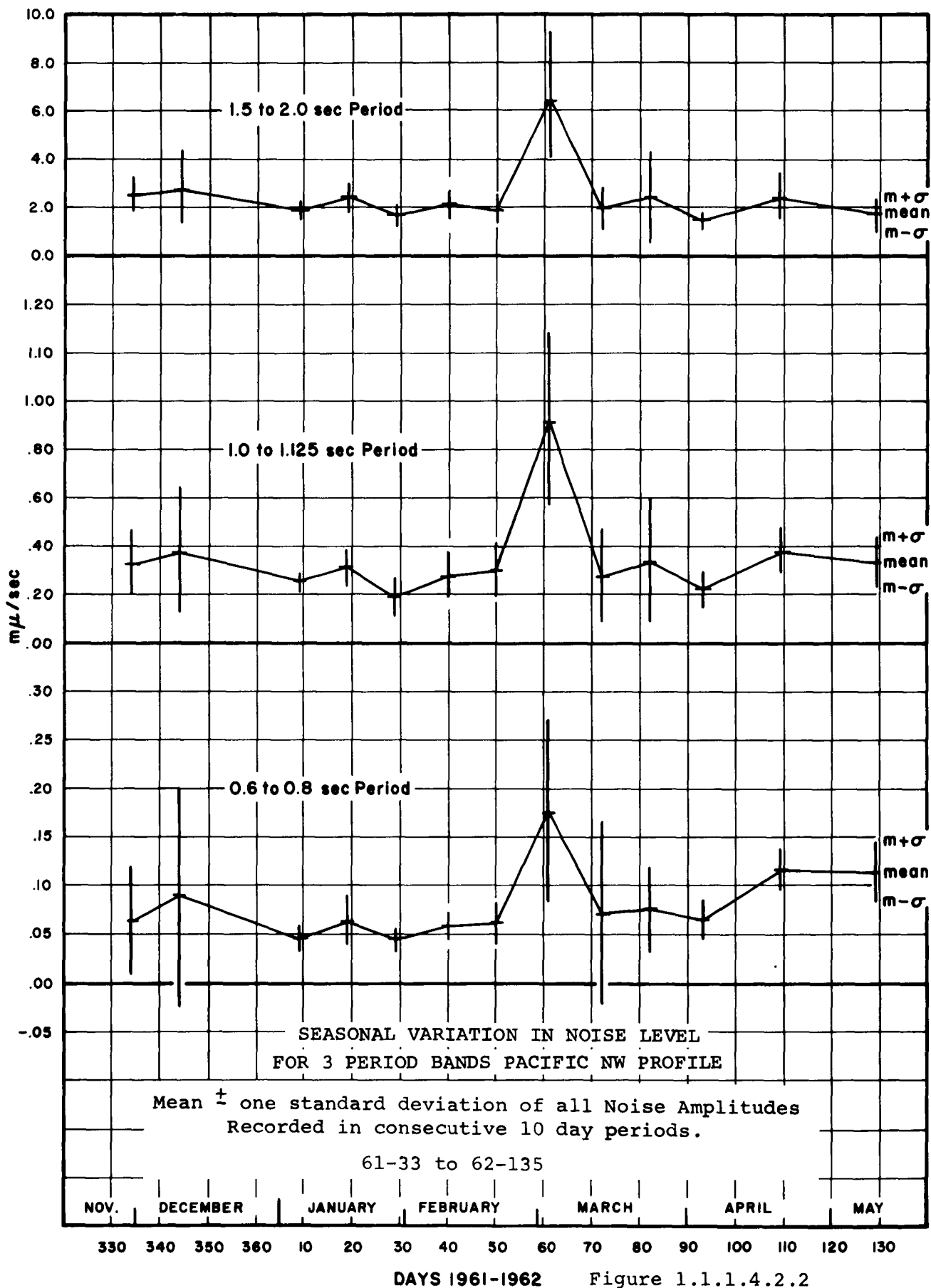


Figure 1.1.1.4.2.2



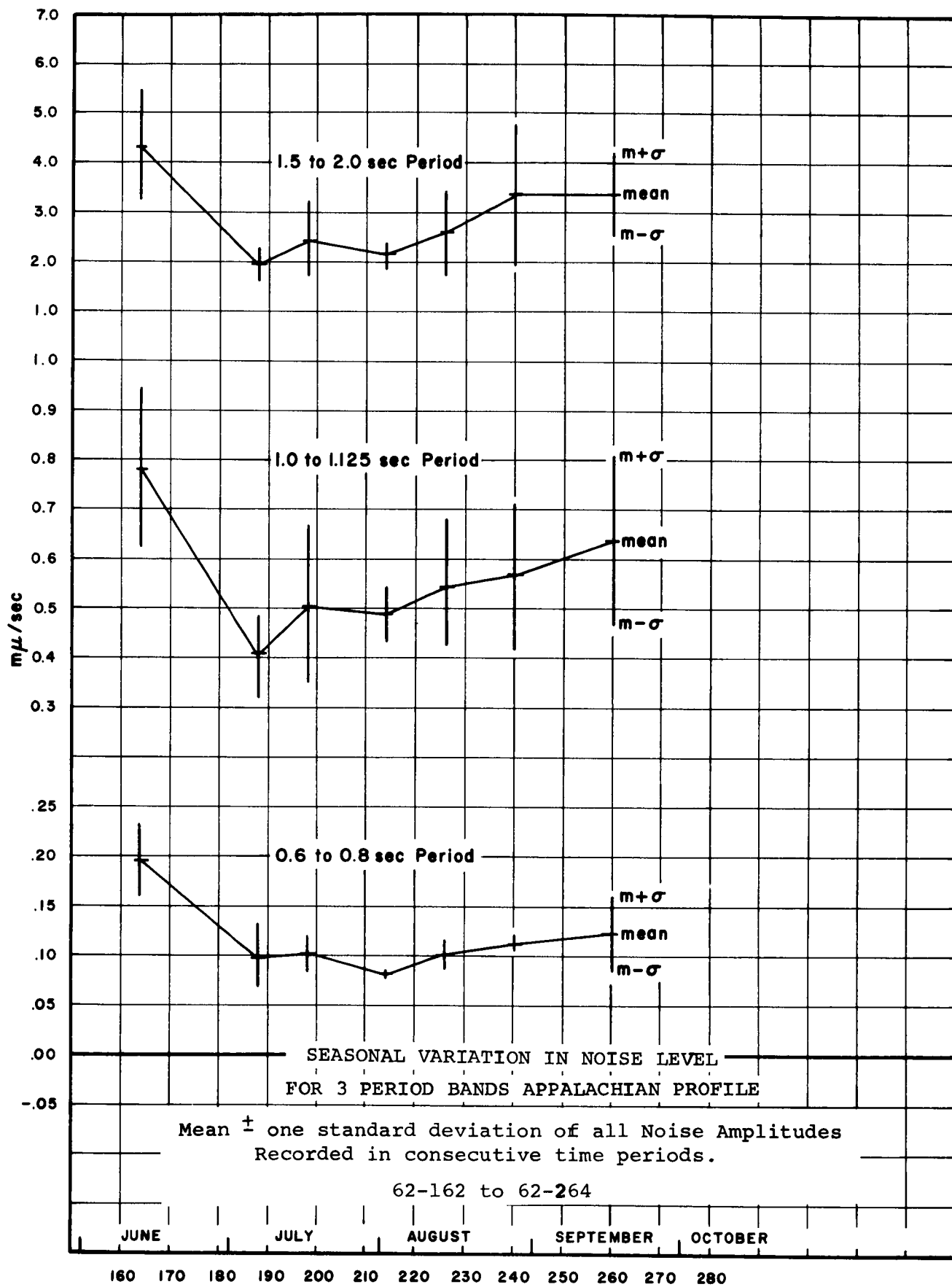
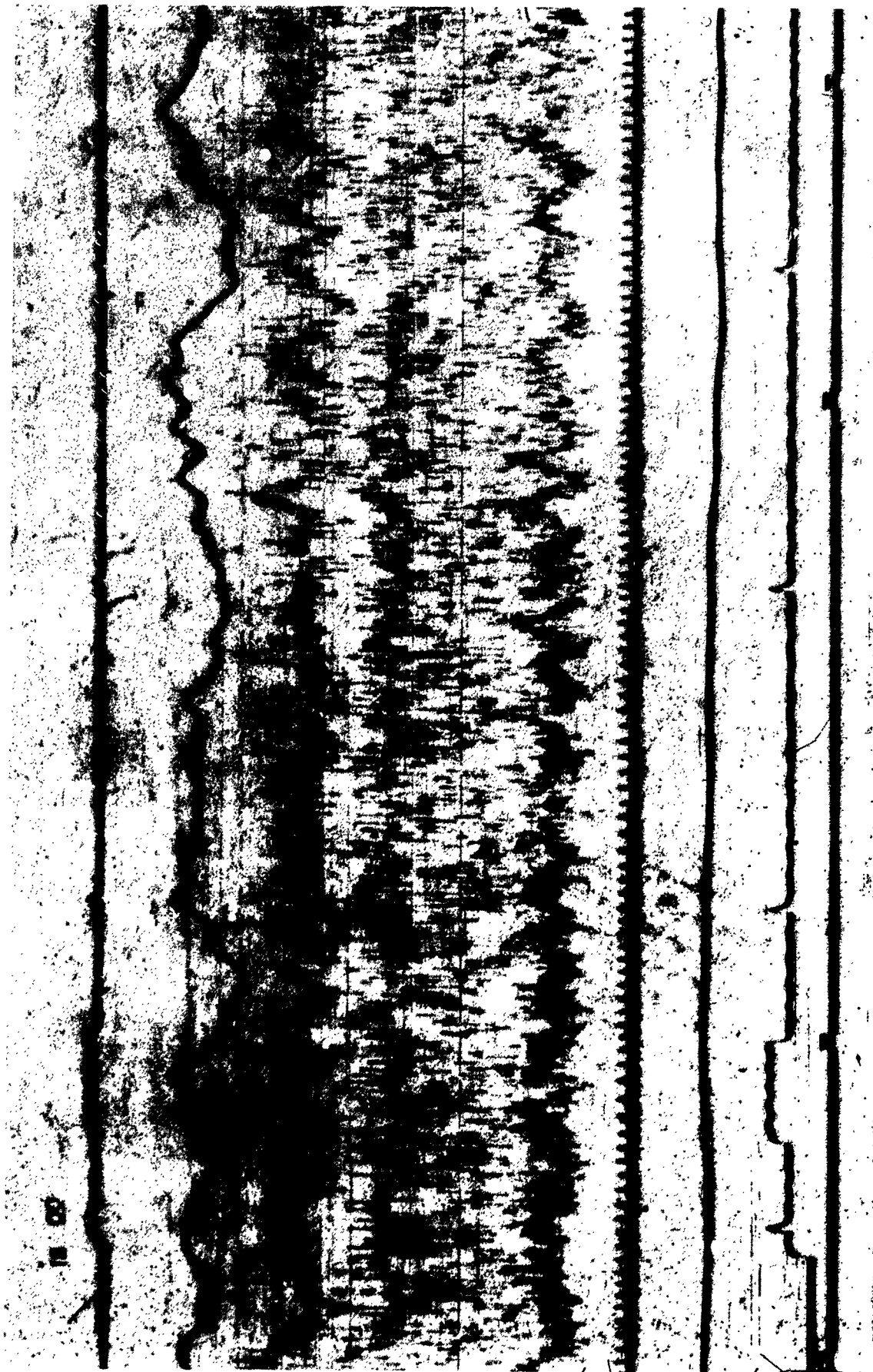


Figure 1.1.1.4.2.3



MABTON  
SS 61-355-15:00:00Z  
Wind Speed 7.5 knots  
Figure 1.1.1.6.4.3

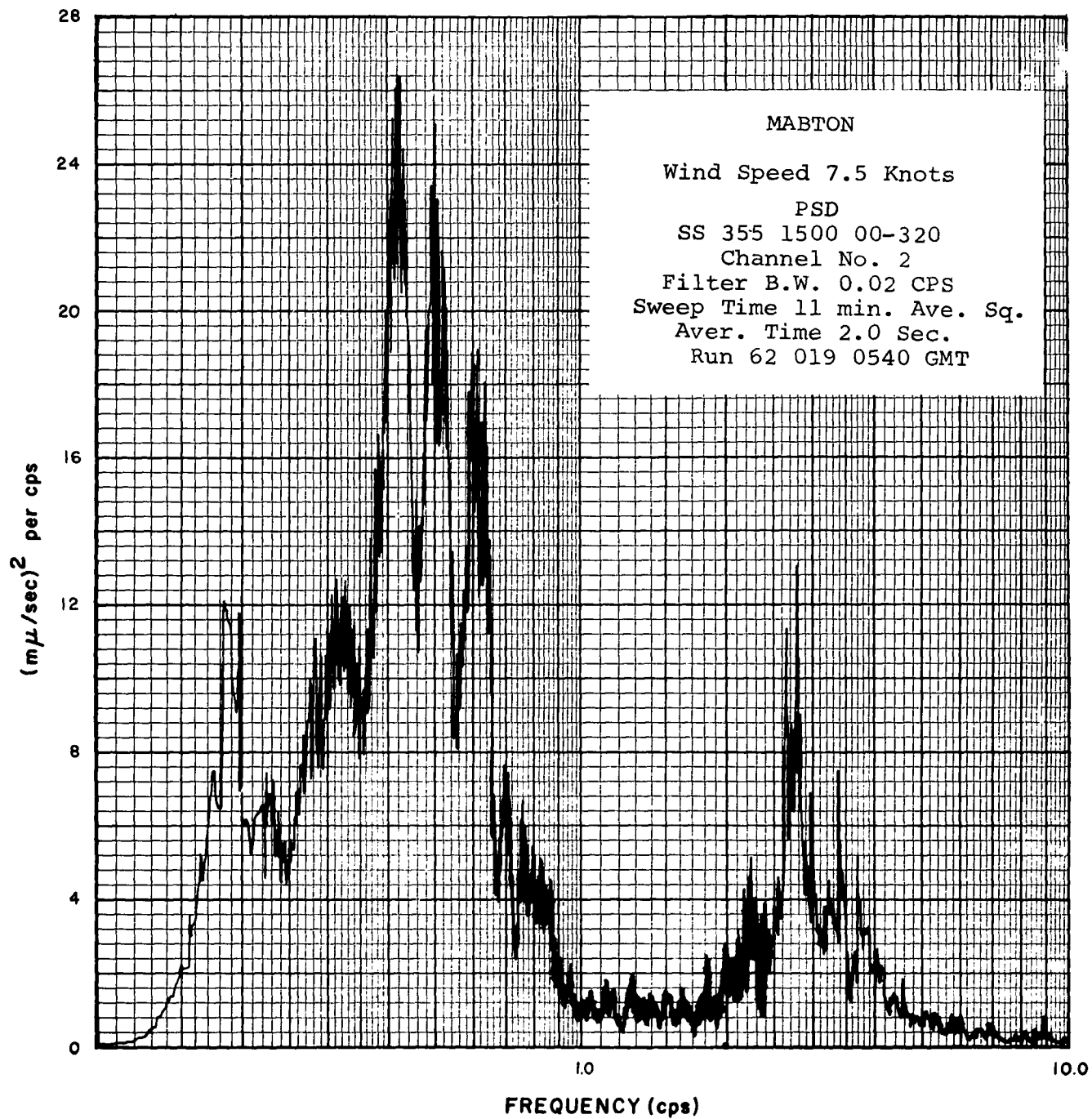
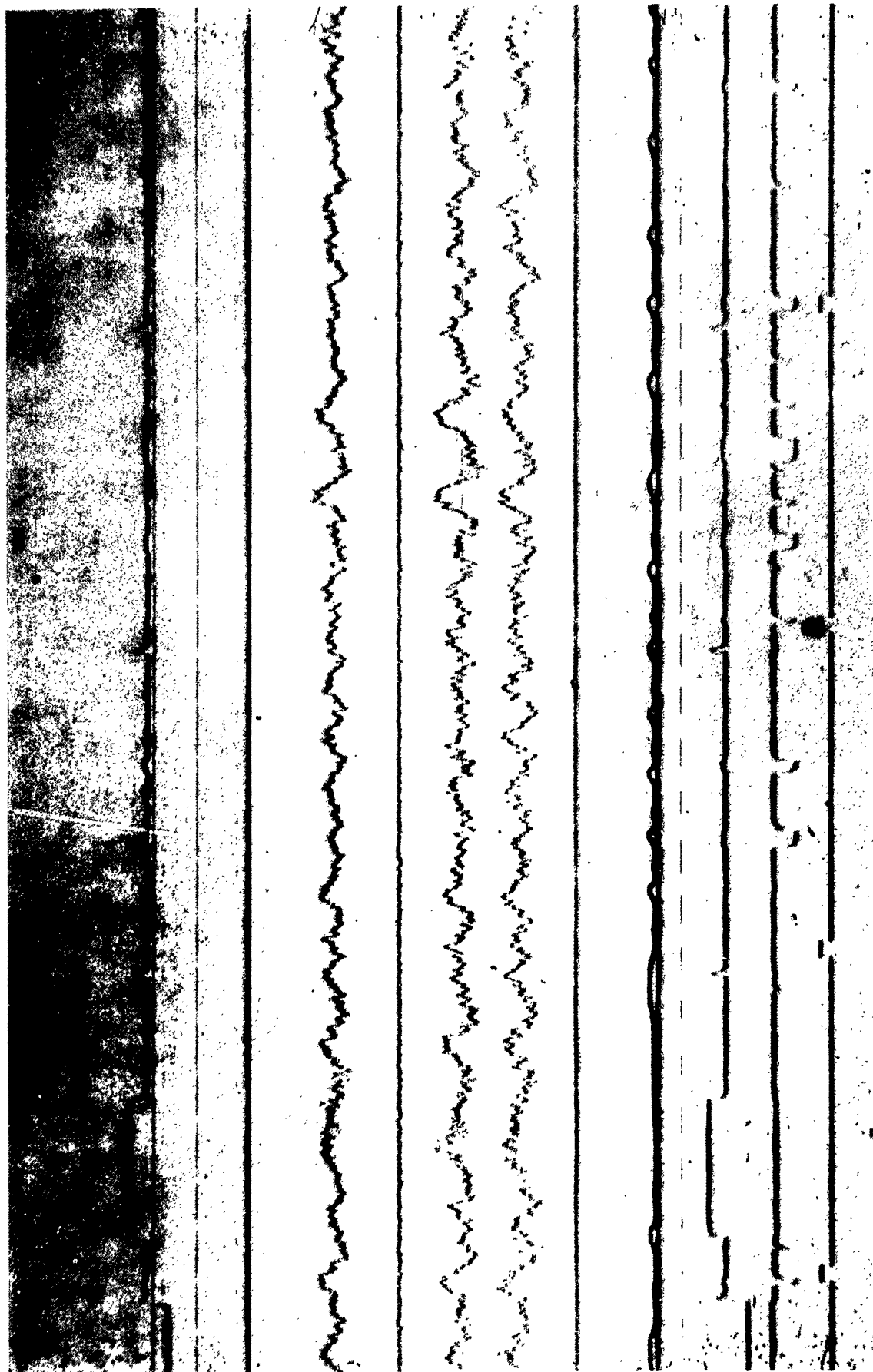


Figure 1.1.1.6.4.4



TOPPENISH RIDGE  
MS 61-341-20:00:00Z  
Wind Speed 2.5 knots

Figure 1.1.1.6.4.5

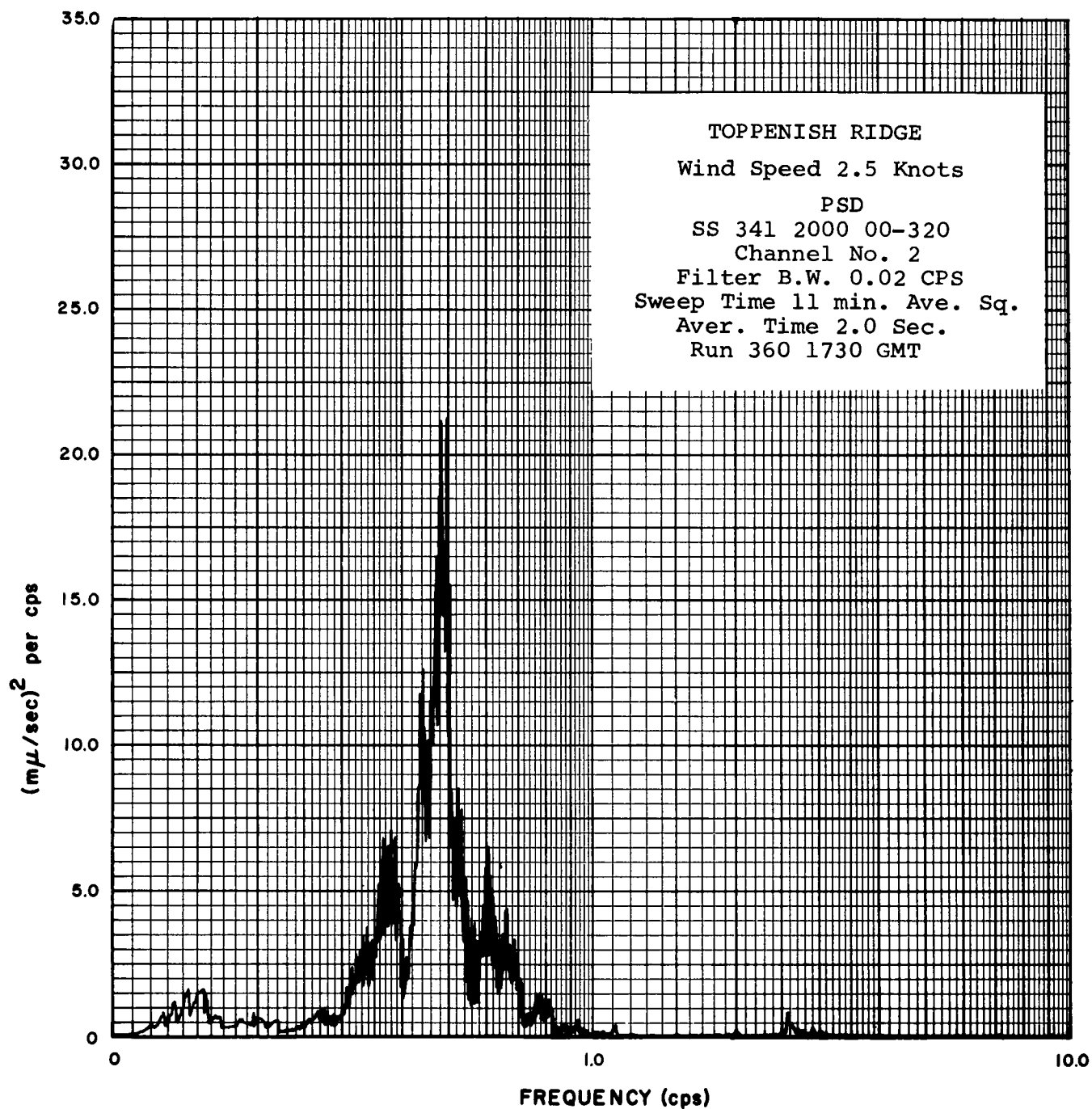
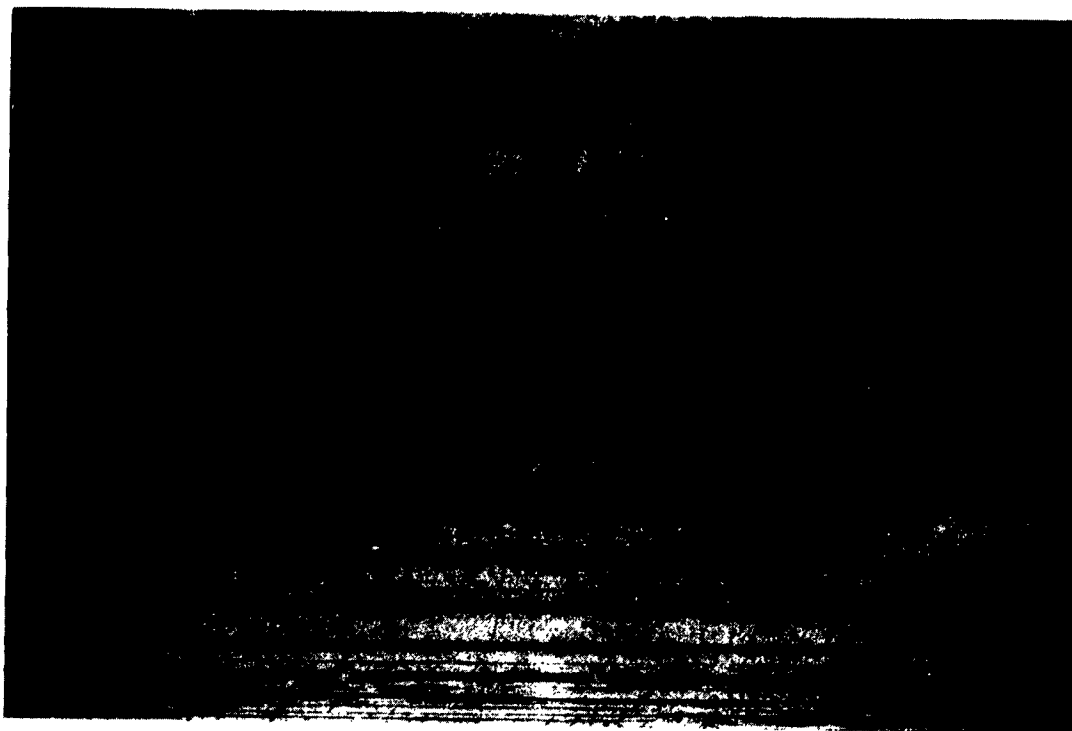


Figure 1.1.1.6.4.6



EFFECT OF WIND ON PLACEMENT OF SEISMOMETERS AT PANAMINT

SS 61-180-14:16Z

Seismometers # 1,2,4,5 on alluvium.  
Seismometer # 3 in mine.

SS 61-181-07:48Z

Seismometers on alluvium.

Figure 1.1.1.3.1

#### 1.1.1.4 Distinctive Characteristics of Noise Amplitude and Velocity Spectra

The typical master station amplitude spectra of Figures 1.1.1.6.1 through 1.1.1.6.3 are representative illustrations of the main features of amplitude spectra measured at all stations. Amplitude rises sharply with period to a maximum between 5 and 7 seconds, then decreases for periods between 7 and about 15 seconds. The increase in amplitude for periods beyond 20 seconds is questionable and might be caused by long-period seismometer response to temperature and barometric pressure variations in addition to seismic noise.

##### 1.1.1.4.1 Filter Studies

General features of ground motion velocity spectra were shown by power spectral density plots of noise samples, such as Figure 1.1.1.6.3.6. In this example, a "window" occurs in the spectrum, where low-level noise in the 1 cps band is flanked by high-level noise at frequencies above and below 1 cps. A teleseism which occurred almost in the center of this window (Figure 1.1.1.6.3.7) was reproduced through various degrees of bandpass filtering around the 1 cps band (Figure 1.1.1.6.3.8). The top trace is essentially an unfiltered recording of the teleseism, while the next three traces show the results of various degrees of bandpass filtering. The teleseism is made more clearly visible but is severely distorted by phase shift in sharp (24 db/octave) filtering. Figures 1.1.1.6.3.1 through 1.1.1.6.3.10 are spectra and filtered traces of several other teleseisms in background noise of various types, Figure 1.1.1.6.3.5 especially showing a teleseism almost totally lost in background noise before filtering. Amplitude measurements on filtered teleseisms are unreliable because of phase distortion, but bandpass filtering assists rapid visual monitoring in many cases.

Sometimes noise was restricted to a very narrow band and might be entirely removed by band rejection filtering, such as the nearly sinusoidal noise of about 3 cps frequency shown in Figures 1.1.1.6.4.8 and 1.1.1.6.4.9. In the Pacific Northwest this noise is apparently associated with the passage of railroad trains.

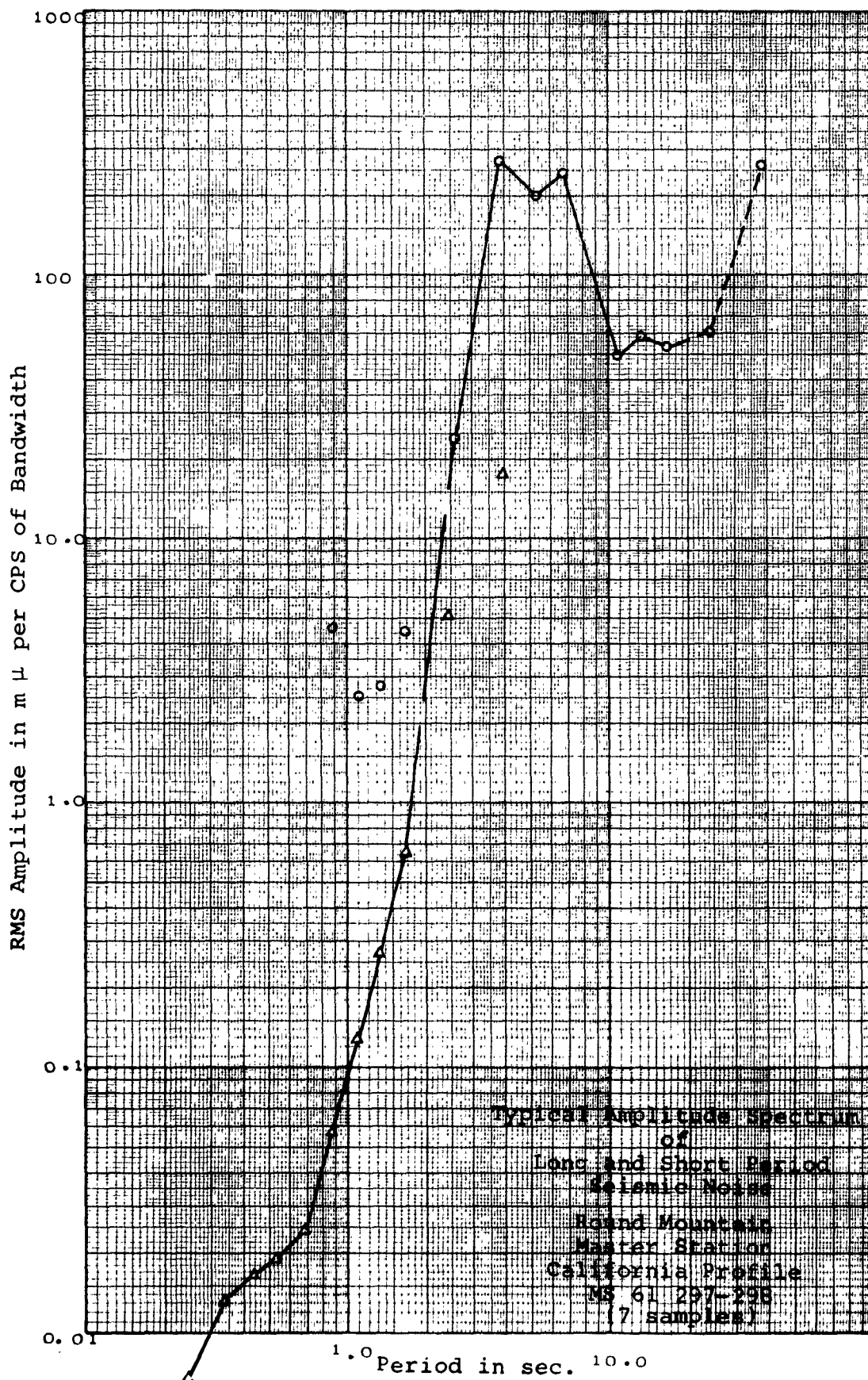


Figure 1.1.1.6.1



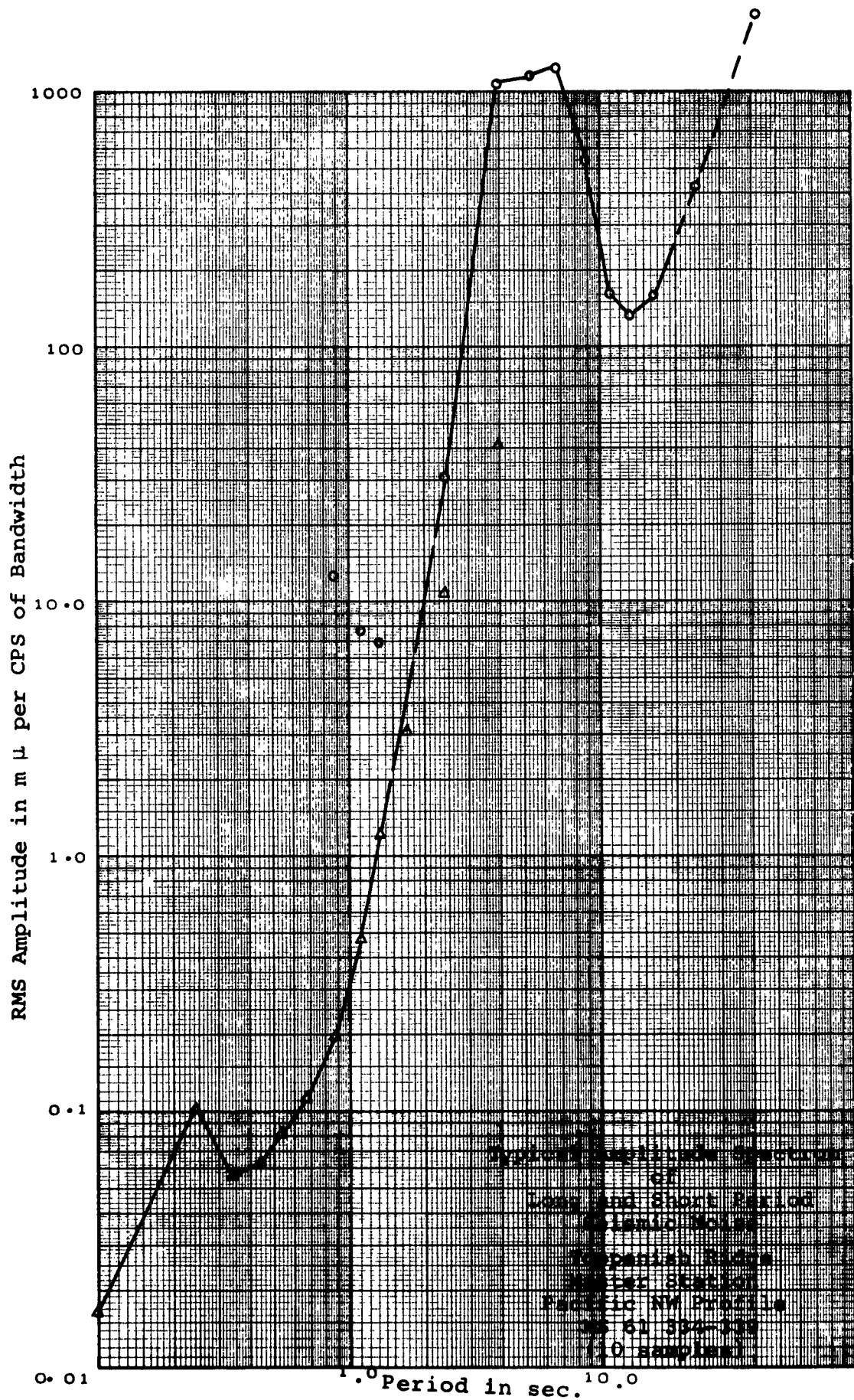


Figure 1.1.1.6.2

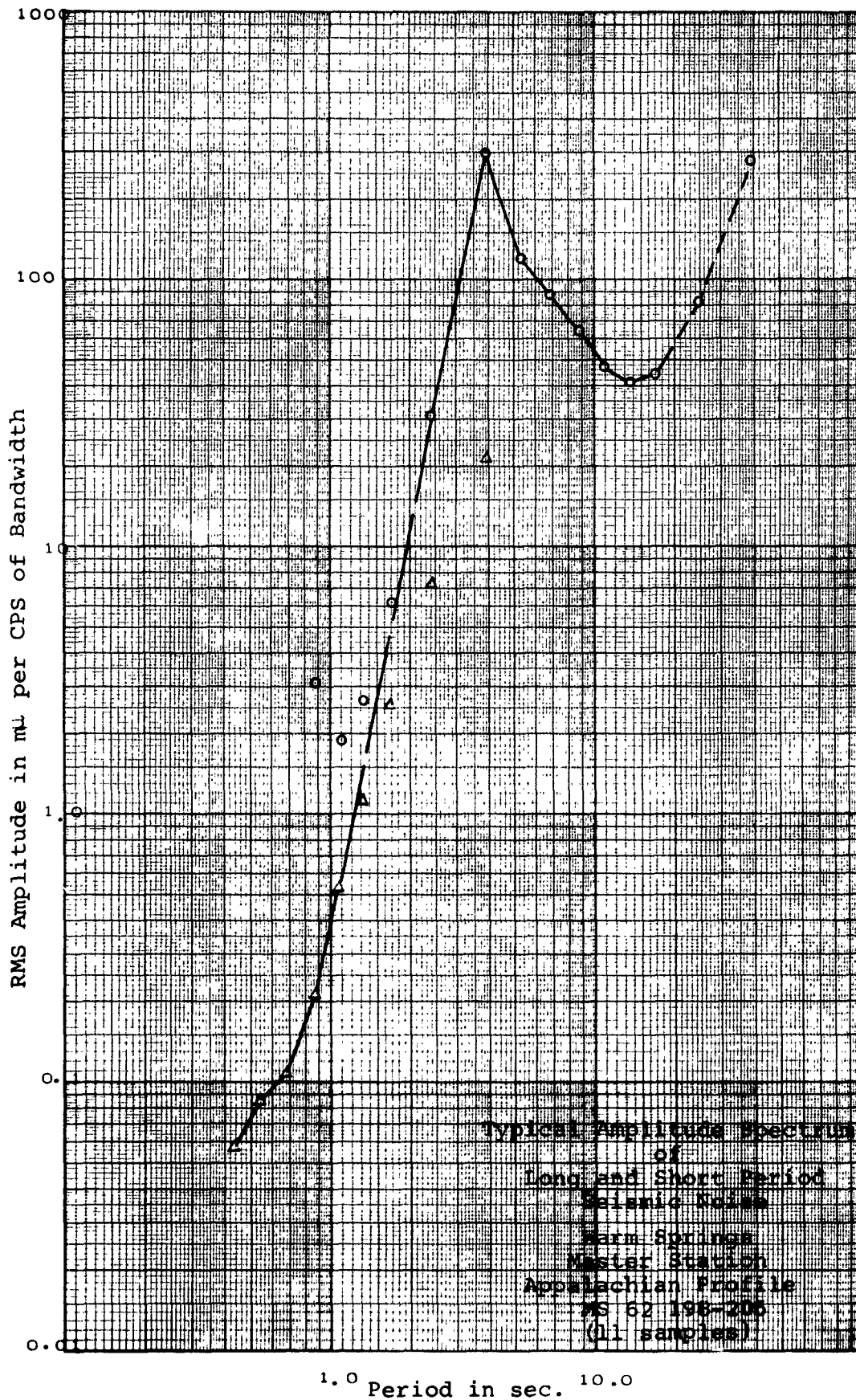


Figure 1.1.1.6.3

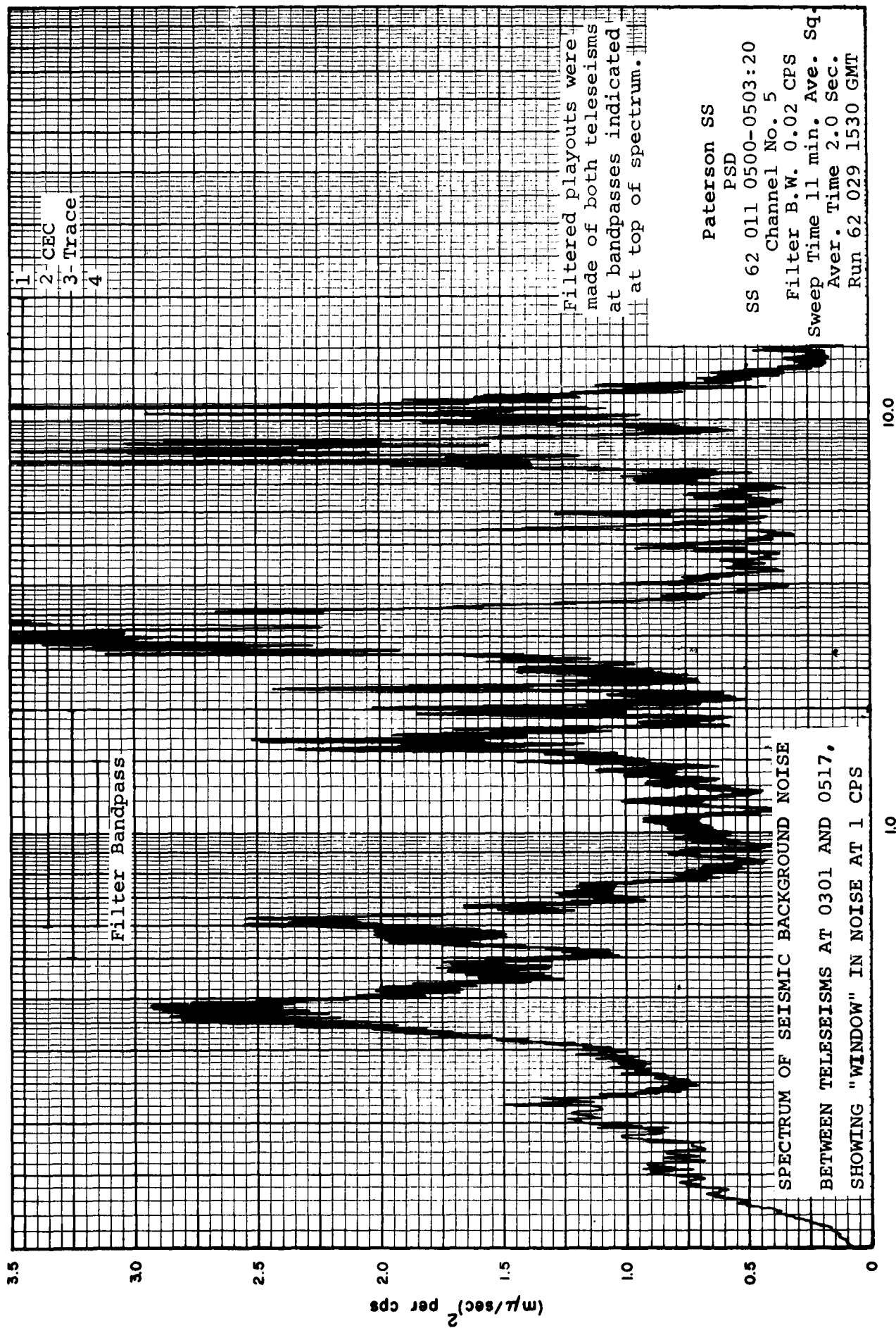


Fig. 1.1.1.6.3.6

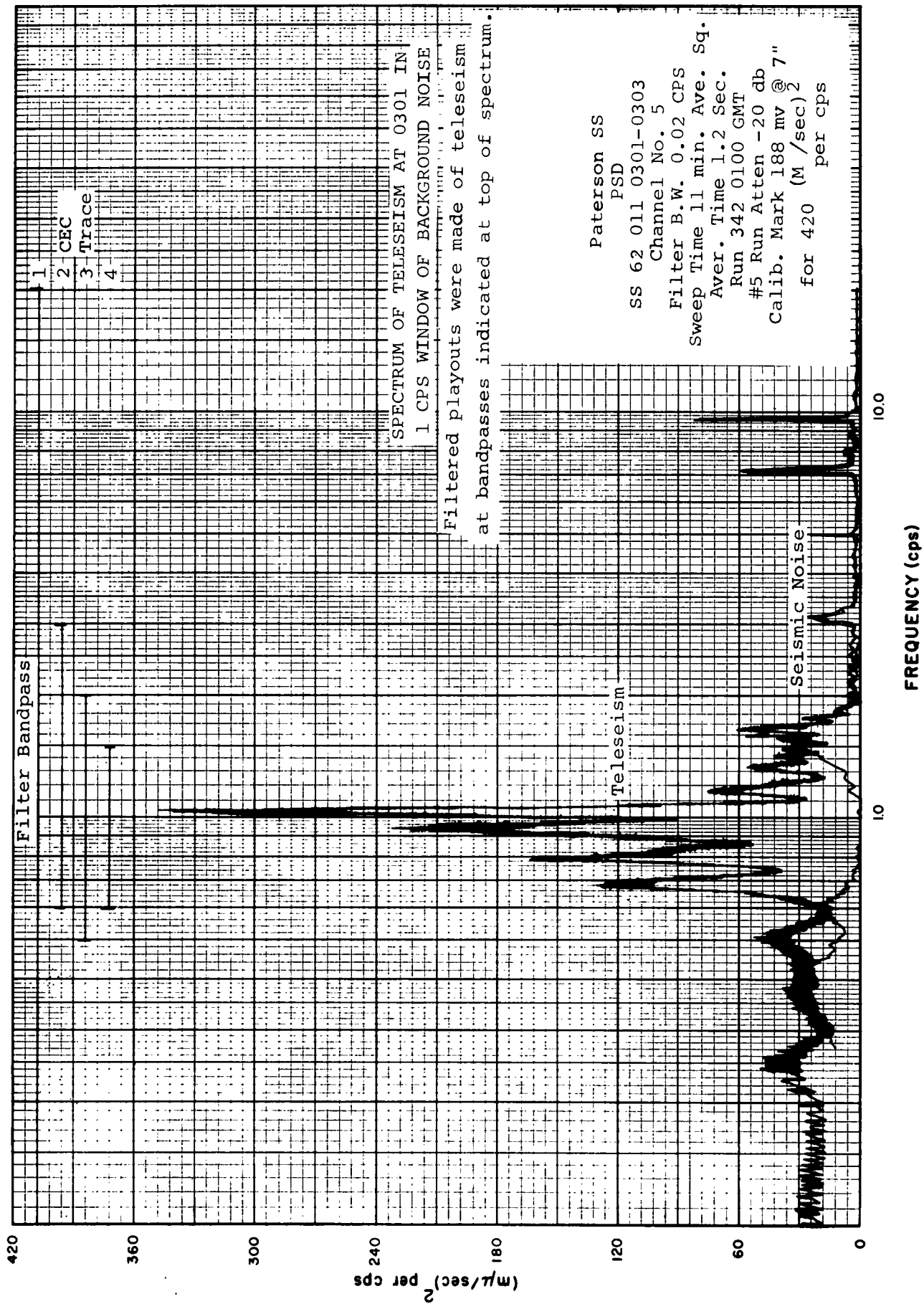
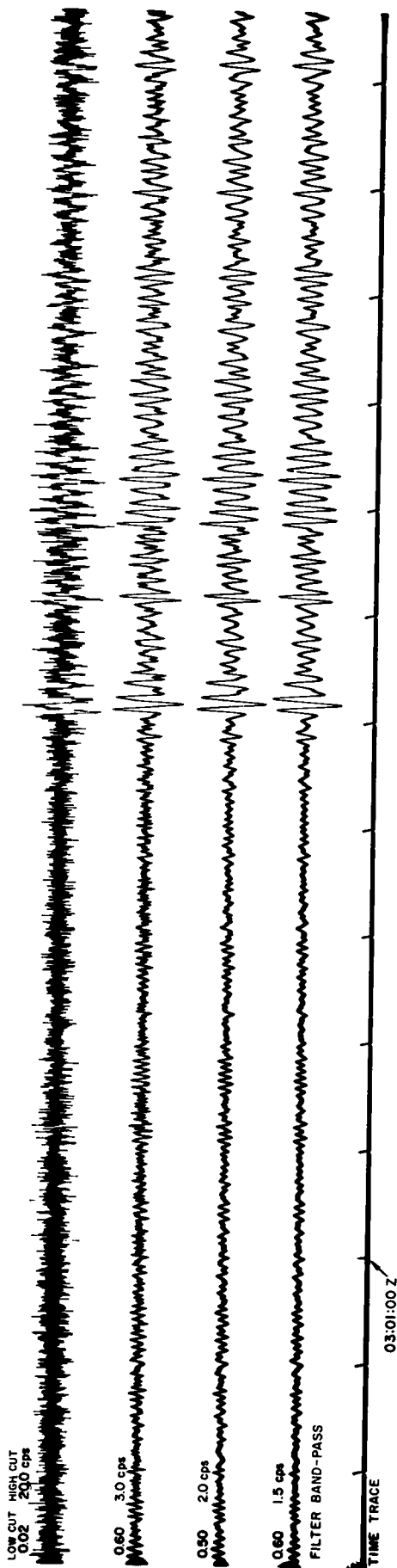


Figure 1.1.1.6.3.7



TELESEISM 0301 RECORDED THROUGH NATURAL 1 CPS "WINDOW" IN NOISE SPECTRUM SHOWING  
REDUCTION OF NOISE  
by  
VARIOUS DEGRESS OF BANDPASS FILTERING.

PATERSON SLAVE STATION  
Seismometer # 5

SS 010-1930 011-1845

Figure 1.1.1.6.3.8

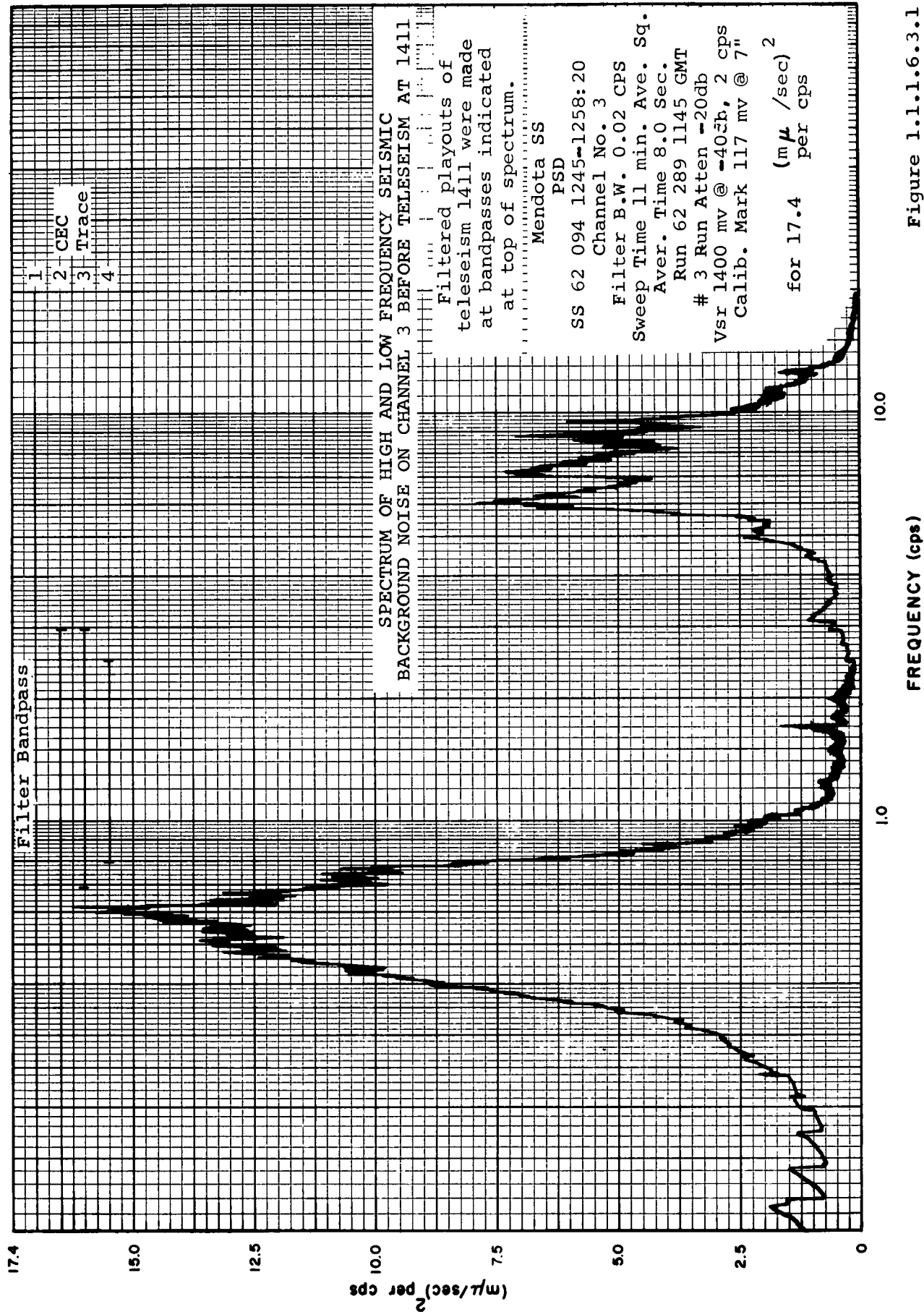


Figure 1.1.1.6.3.1



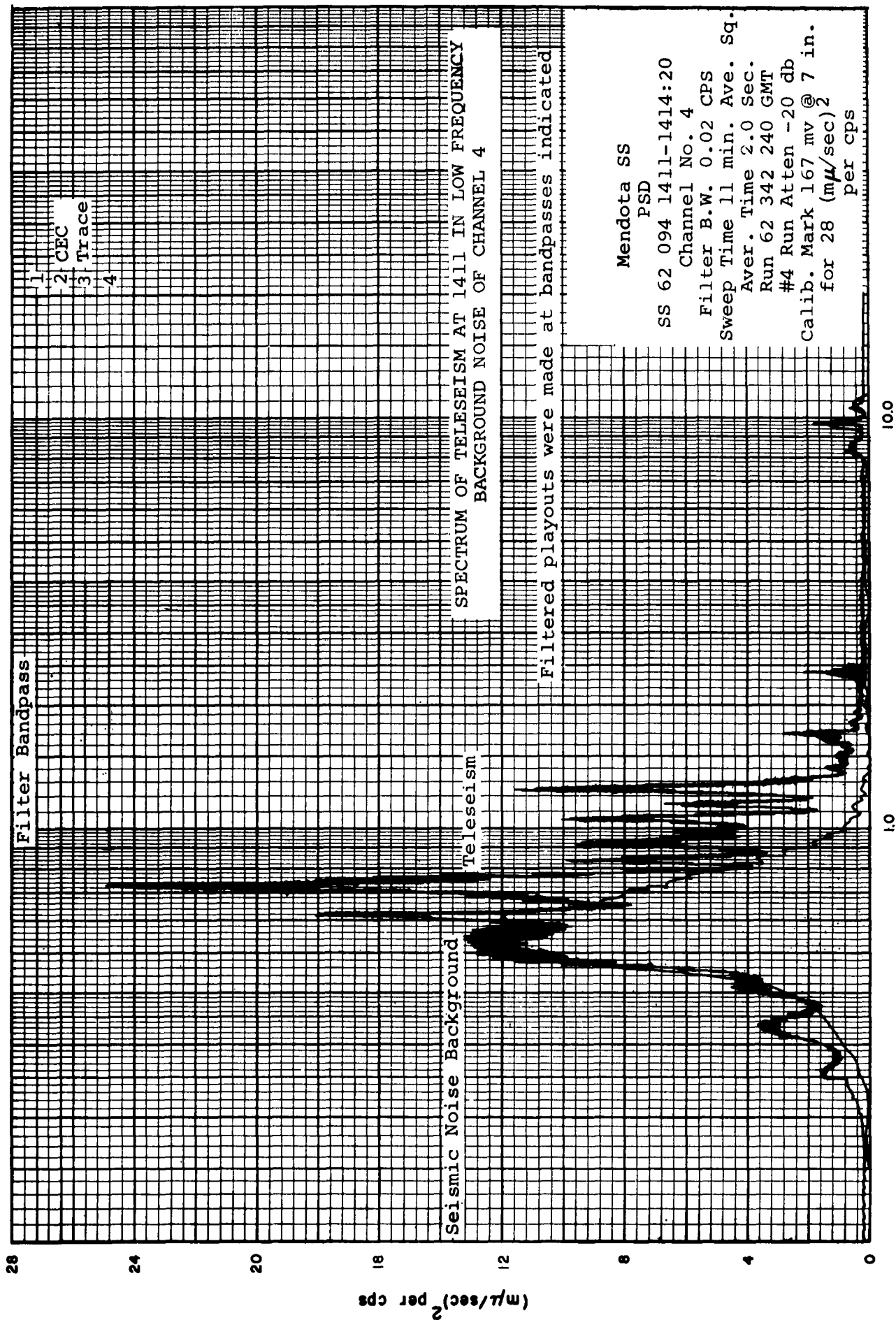


Fig. 1.1.1.6.3.2

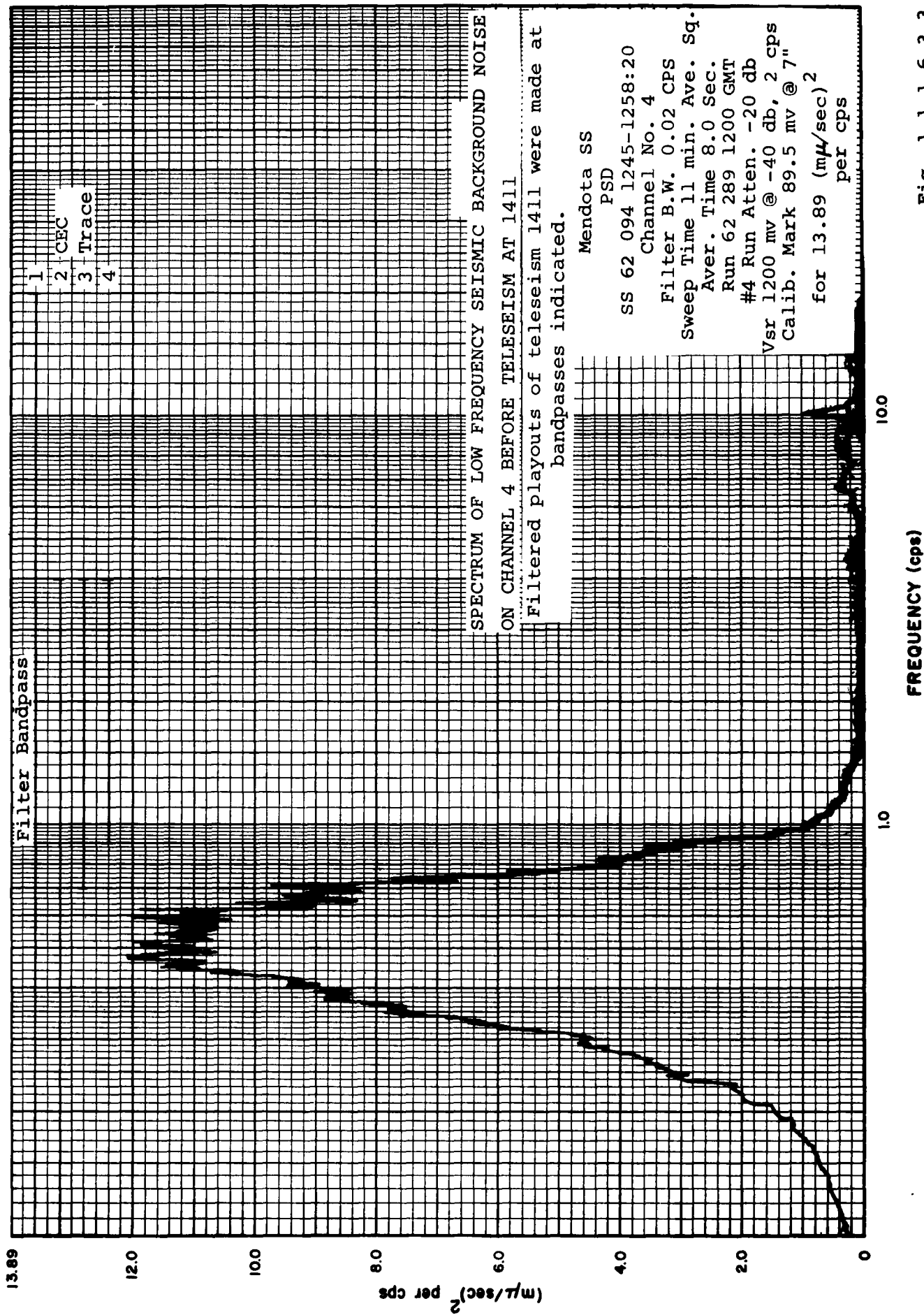


Fig. 1.1.1.6.3.3



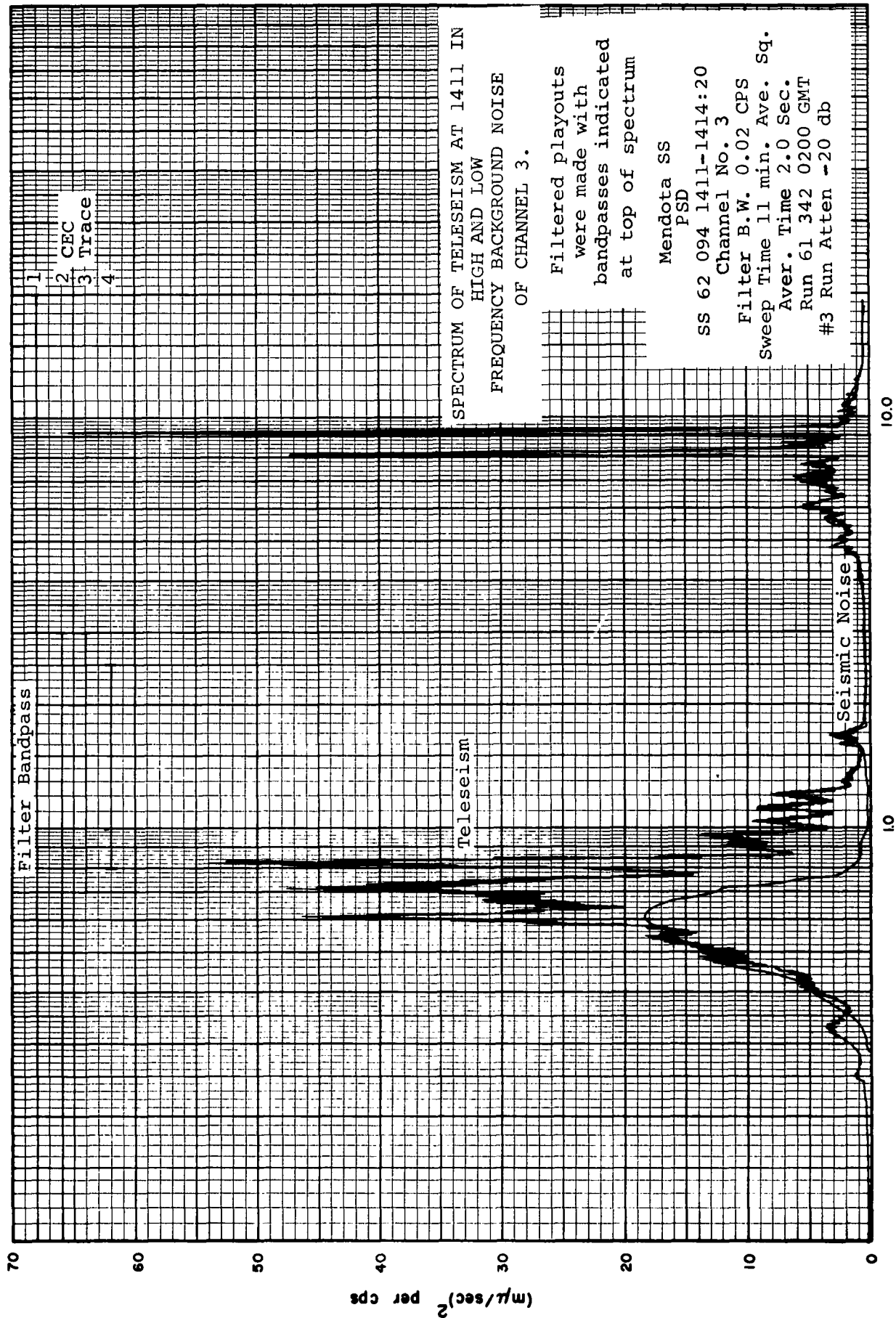
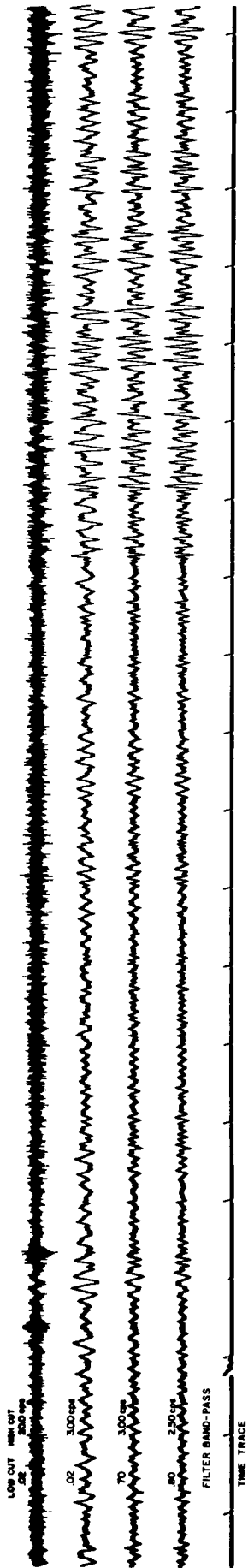
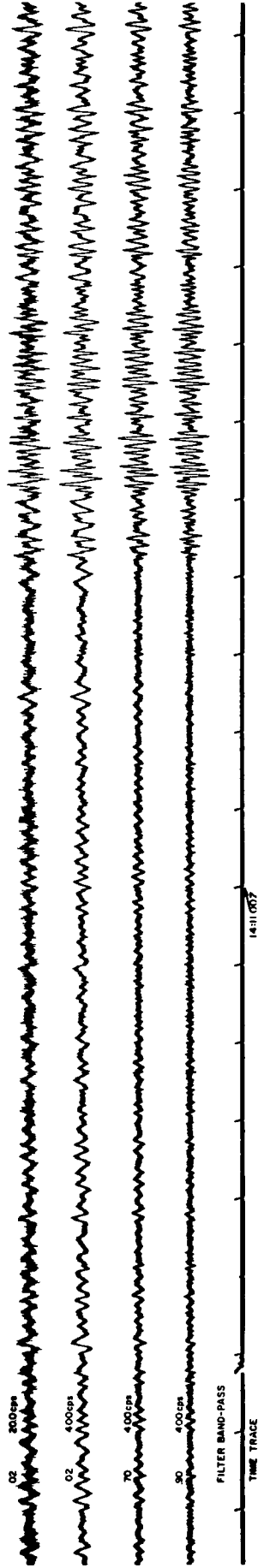


Fig. 1.1.1.6.3.4



1411 recorded on Seismometer No. 3 through natural 1 -4 cps  
"window" in noise spectrum showing reduction of low-frequency  
noise by various degrees of bandpass filtering.



Teleseism recorded at Seismometer No. 4 where dominant noise  
is low-frequency, showing reduction of low-frequency noise by  
various degrees of high-pass filtering.

MENDOTA

SS 62-094 1411 GMT

Figure 1.1.1.6.3.5

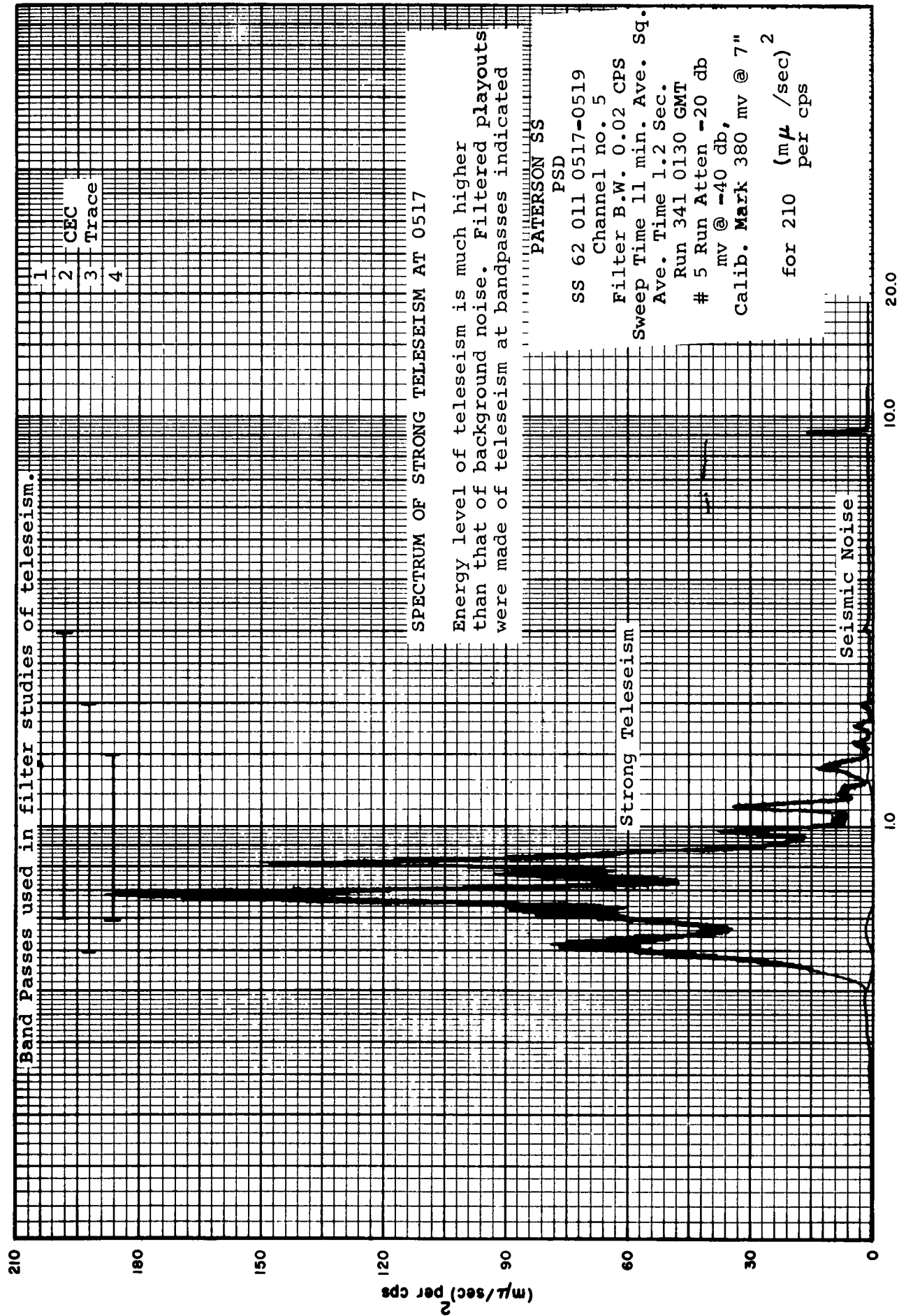
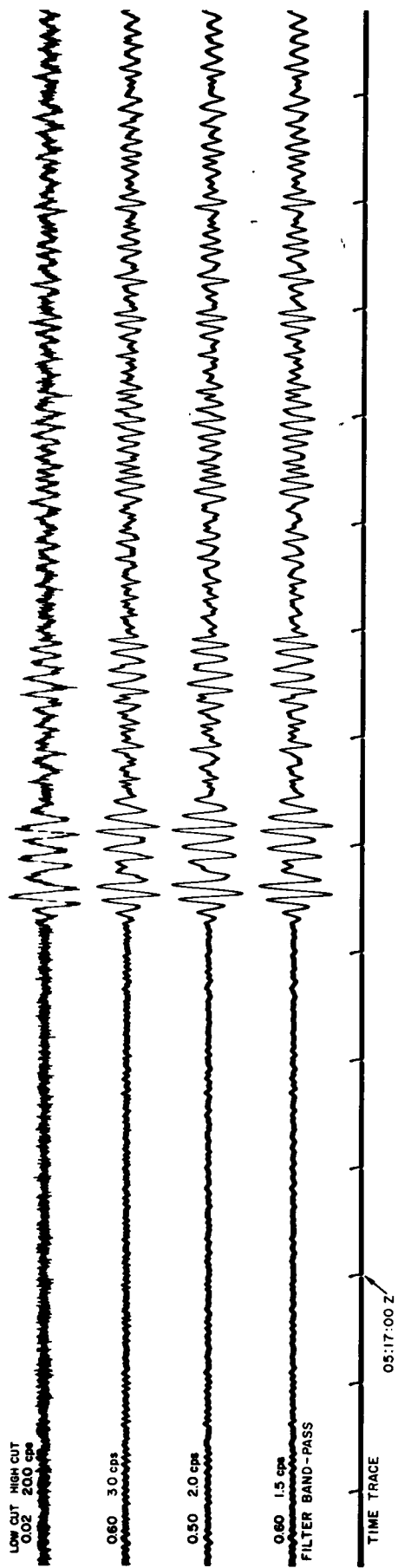


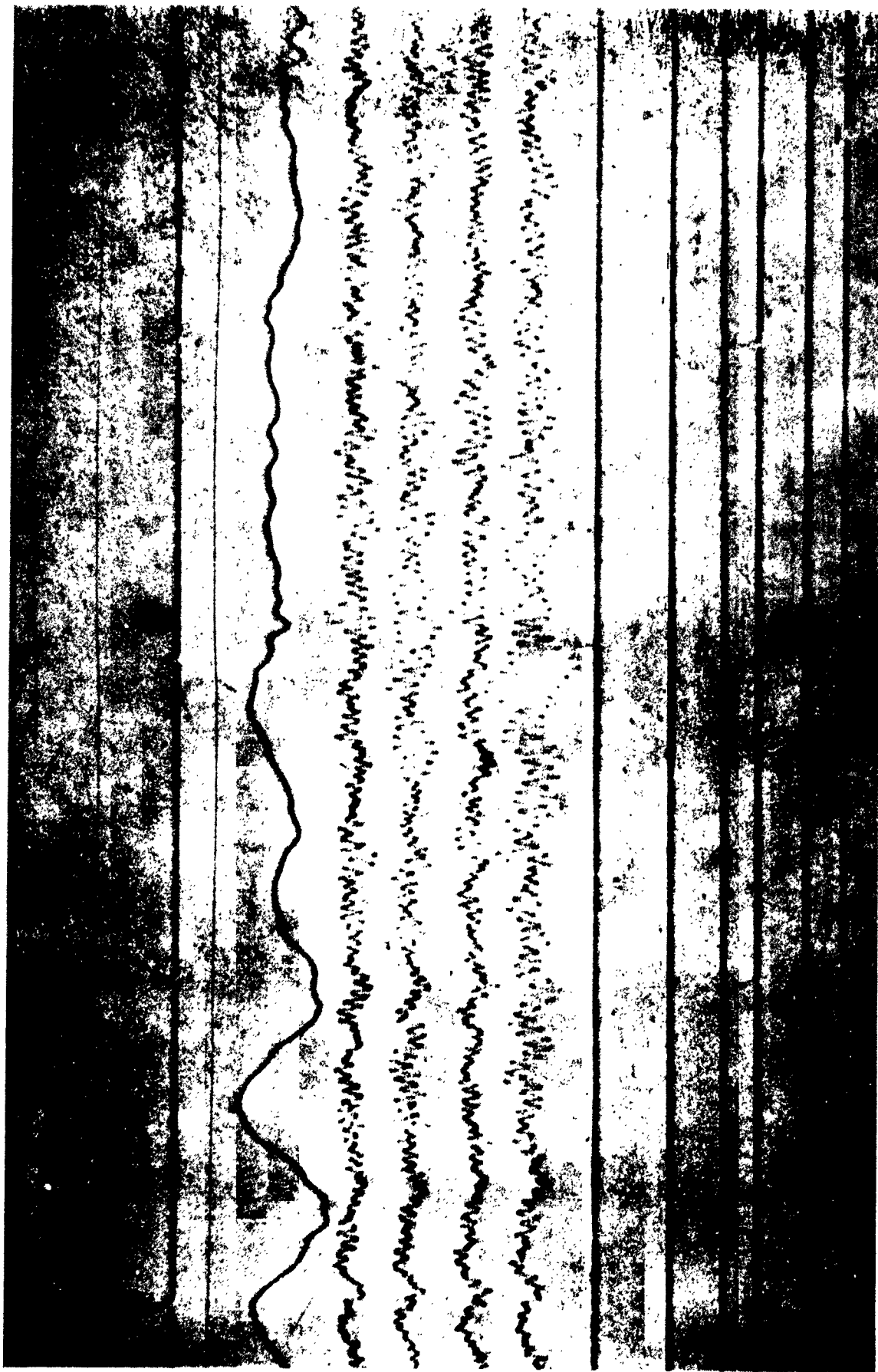
Figure 1.1.1.6.3.9



TELESEISM 0517 RECORDED THROUGH NATURAL 1 CPS "WINDOW" IN NOISE SPECTRUM SHOWING  
REDUCTION OF NOISE  
by  
VARIOUS DEGREES OF BANDPASS FILTERING.

PATERSON SLAVE STATION  
Seismometer # 5

Figure 1.1.1.6.3.10



TOPPENISH RIDGE  
MS 61-349-16:33:00z  
Train Noise

Figure 1.1.1.6.4.8

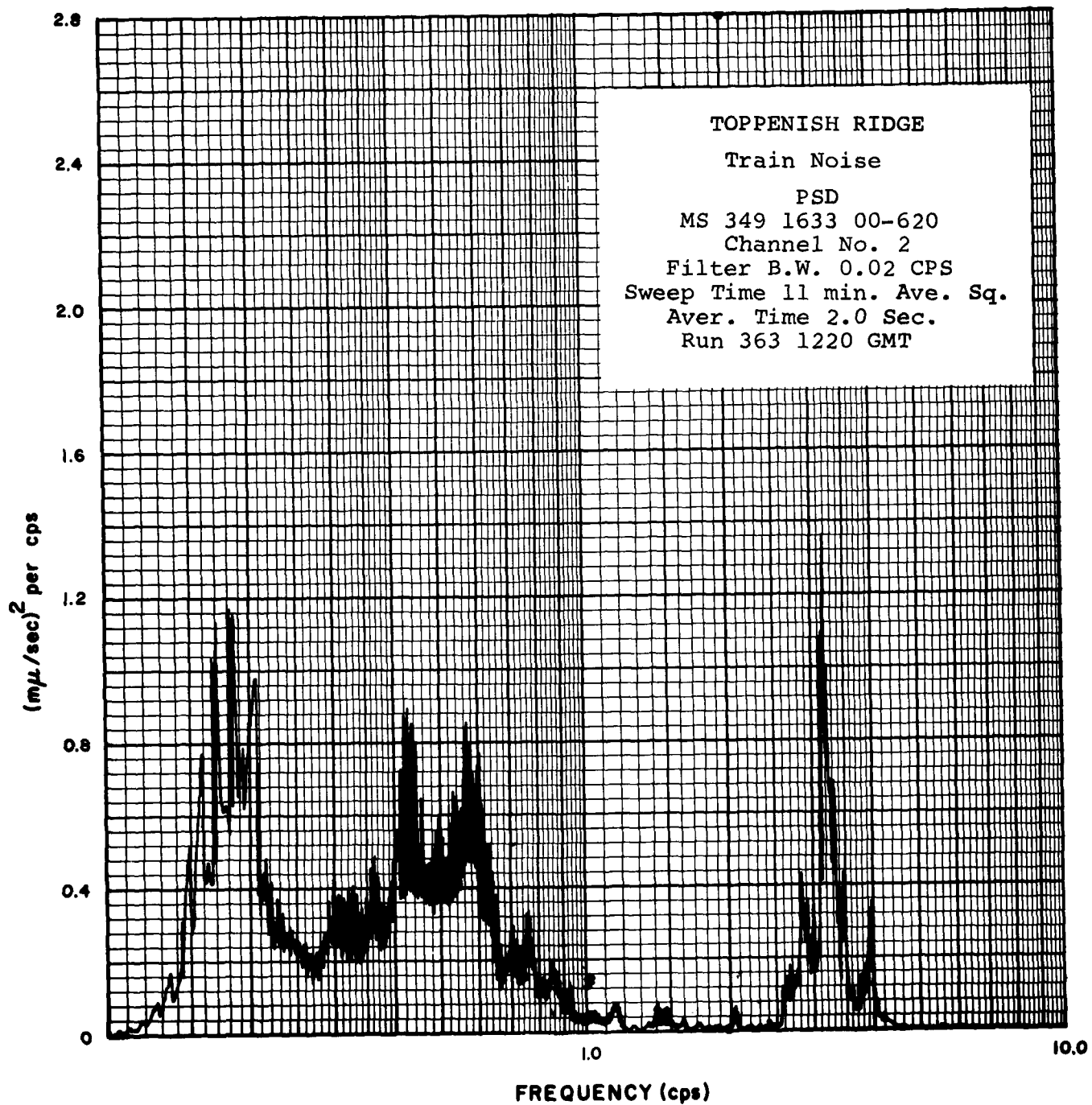


Figure 1.1.1.6.4.9

### 1.1.2 Noise Source Directions and Phase Velocities

Cross-spectrum analysis of seismic noise recordings at the Pacific Northwest stations of Toppenish Ridge and Paterson provided data for most of the conclusions on noise source direction and phase velocity summarized in Figures 1.1.2.1a and b. Some cross-spectra were also analyzed from recordings at Mabton (between Toppenish Ridge and Paterson) and Markham (on the coast).

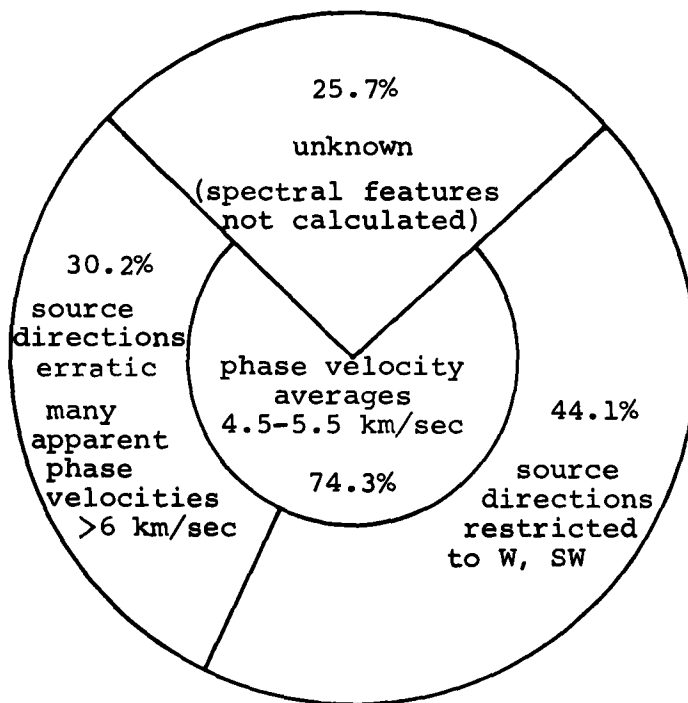
Figures 1.1.2.1 through 1.1.2.4 summarize behavior of noise from Toppenish Ridge and Paterson, based on cross-spectra representing about 0.2% of the microseismic activity at these stations during January 1962. These data include about 70% of all the noise between 0.2 and 1.0 cps in each spectrum, and about 35% of the noise between 1.0 and 2.0 cps. Data unaccounted for represent noise whose spectral features were not calculated because of inconsistencies or low amplitude.

Reliability of source directions and phase velocities determined from cross-spectral data depends on the assumption that all the noise analyzed is from surface waves of phase velocity between about 2.5 and 5.0 km/sec. (See Section 4.1.3). This assumption makes possible determination of phase shifts (and consequently apparent source directions) for noise of less than 1 cps recorded from arrays of less than 1 mile radius. For noise above 1 cps recorded on arrays of 1 mile radius, phase shifts cannot be determined uniquely without knowledge of phase velocities.

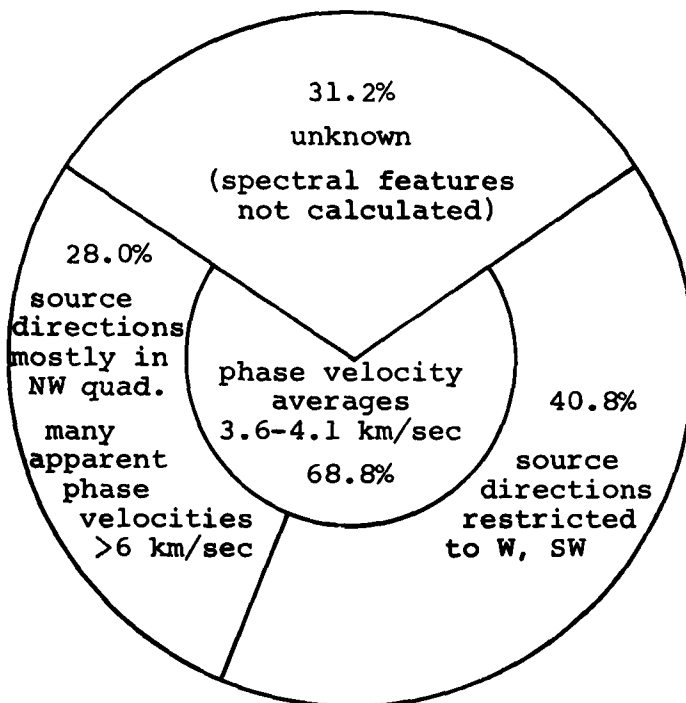
Source direction and velocity data from cross-spectra were verified by inspection of film recordings of noise samples from several stations. Very rudimentary checks of source direction and phase velocity were made on all three profiles by measuring average differences in arrival time of 0.5 cps wave trains at each seismometer of the array.

#### 1.1.2.1 Dominant Noise Source Direction

Cross-spectral analyses consistently showed that the most common noise source direction for frequencies below 2 cps was the direction of the nearest coastline, plus or minus about 30°. This direction was also noted for 0.5 cps noise on film recordings. Phase shifts on film from the California stations of Round Mountain, Death Valley, Panamint and Huasna indicate a source direction of 0.5 cps noise in the southwest quadrant, the direction of the ocean. At Warm Springs on the Appalachian profile, film recordings indicate source direction to the east for noise of this frequency, again the direction of the ocean. Ocean direction is apparently the main noise source direction at inland stations remote from cultural or river-related noise. (This observation applies only to stations less than 350 km inland, since cross-spectra were not made for sites further inland.)



TOPPENISH RIDGE STATION

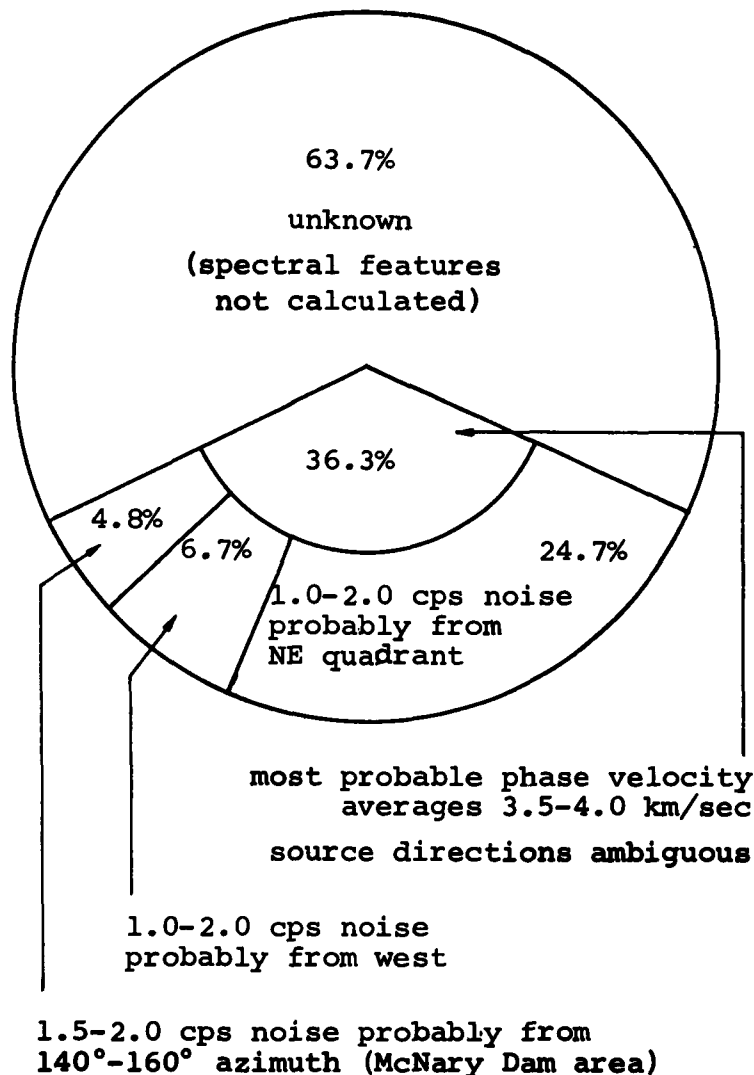


PATERSON STATION

PACIFIC NORTHWEST SOURCE DIRECTIONS AND PHASE VELOCITIES  
 FOR SEISMIC NOISE BELOW 1 cps  
 FROM CROSS-SPECTRUM STUDIES AT TOPPENISH AND PATERSON  
 Based on an approximately 0.2% sample of  
 total 0.2-1.0 cps noise in a 90 day period

Fig. 1.1.2.1a

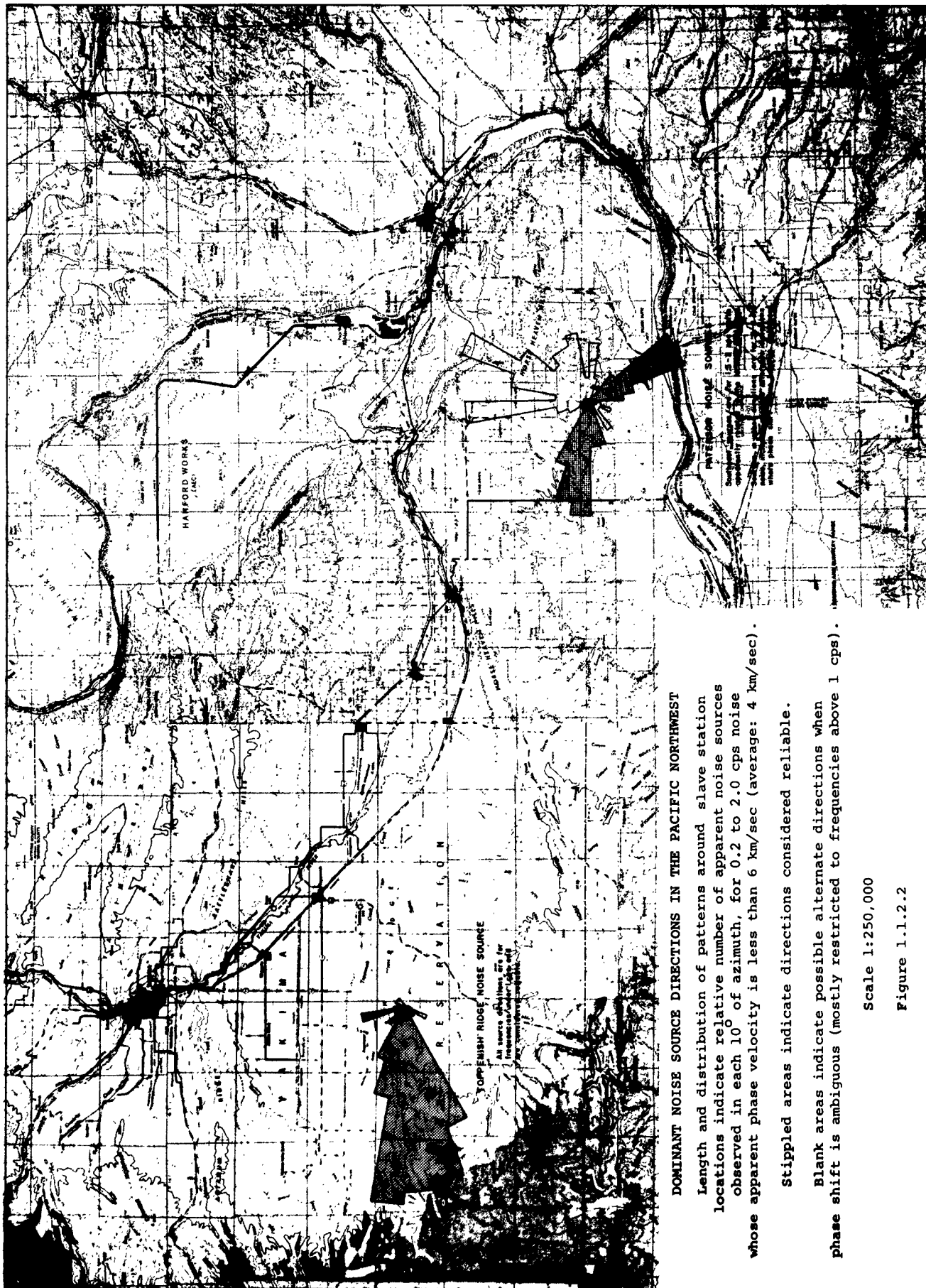


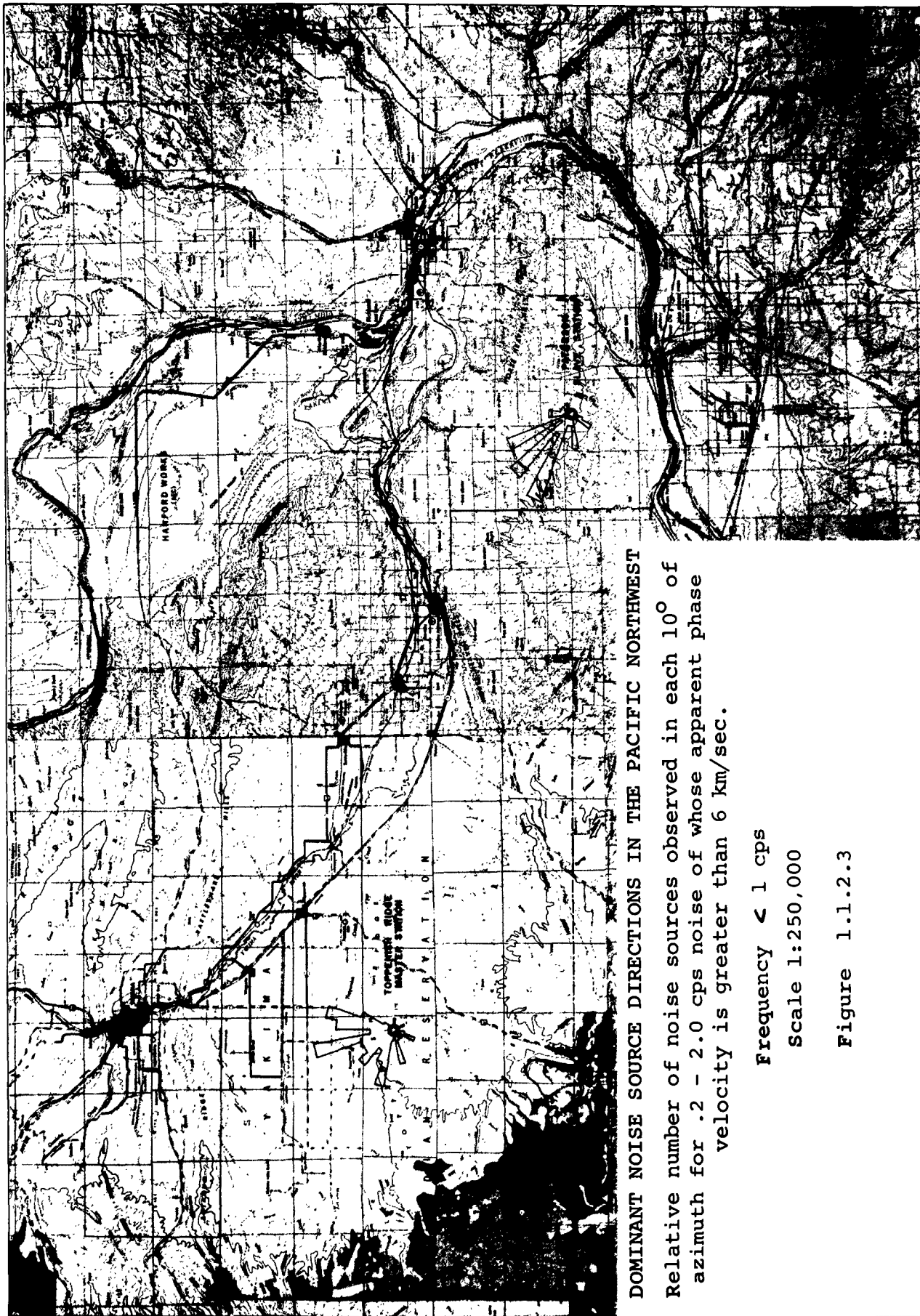


#### PATERSON STATION

PROBABLE PACIFIC NORTHWEST SOURCE DIRECTIONS & PHASE VELOCITY  
FOR 1.0-2.0 cps NOISE  
BASED ON CROSS-SPECTRUM STUDIES AT PATERSON STATION  
Directions and velocities shown are  
most probable of several possibilities

Fig. 1.1.2.1b





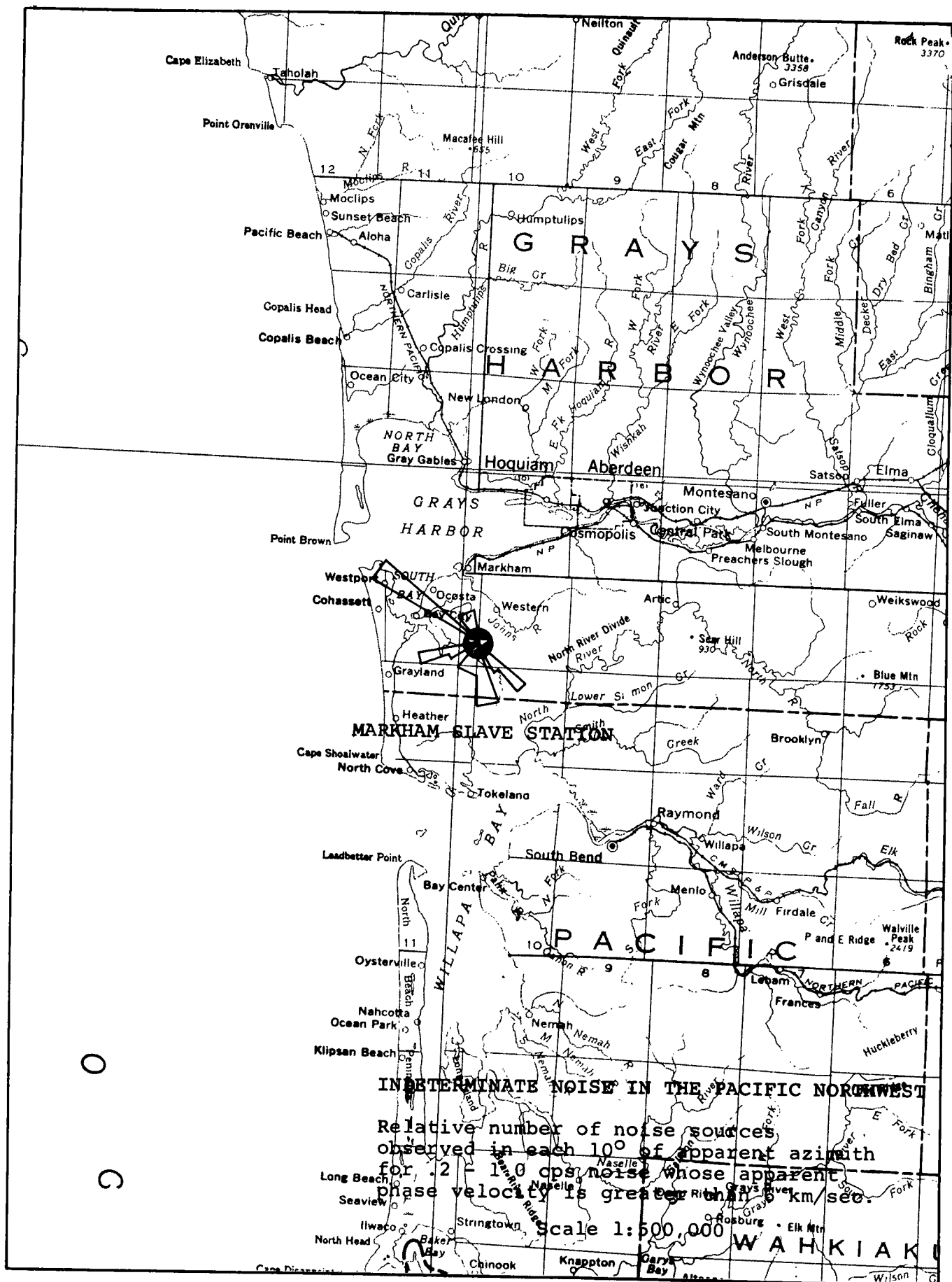
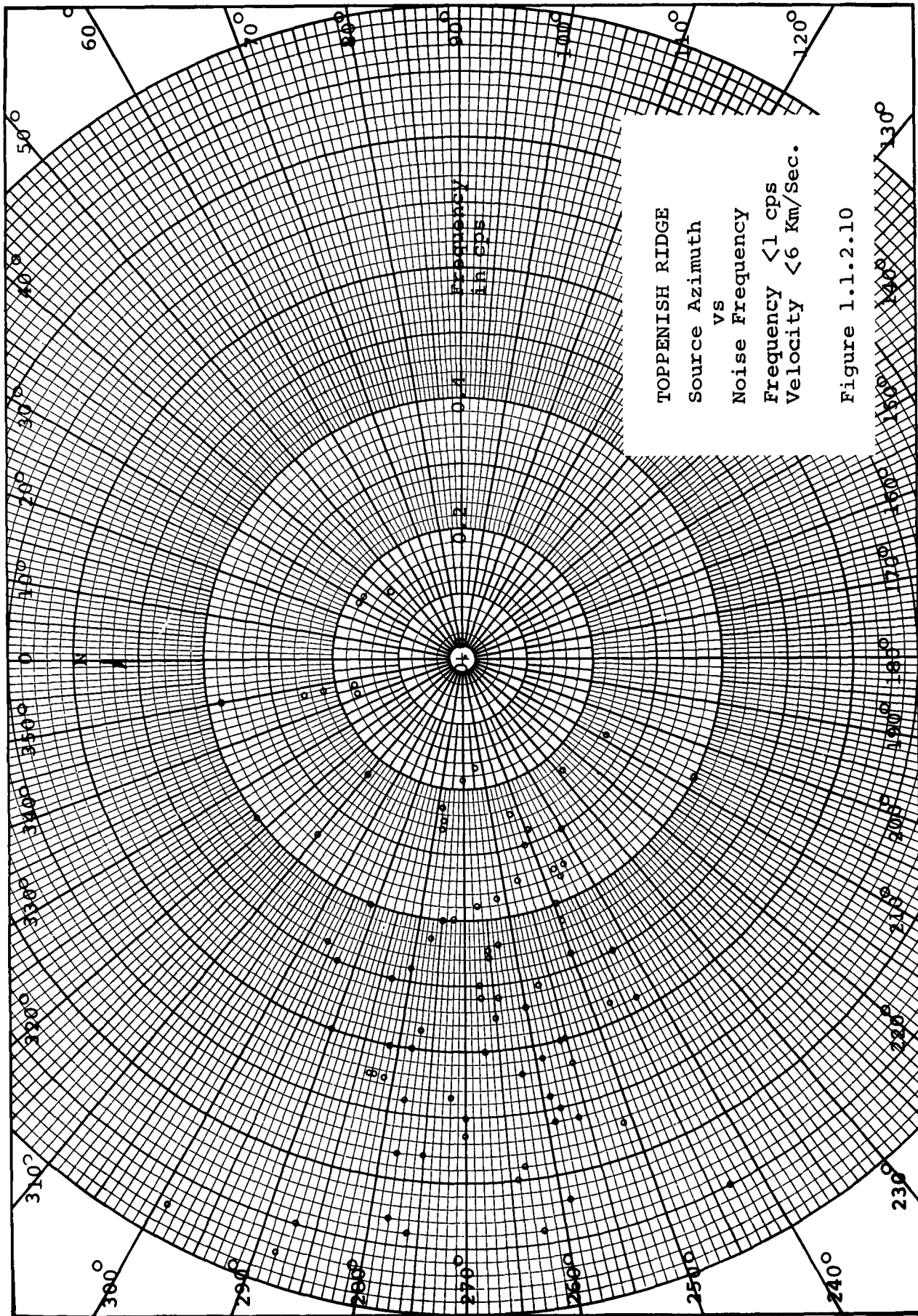
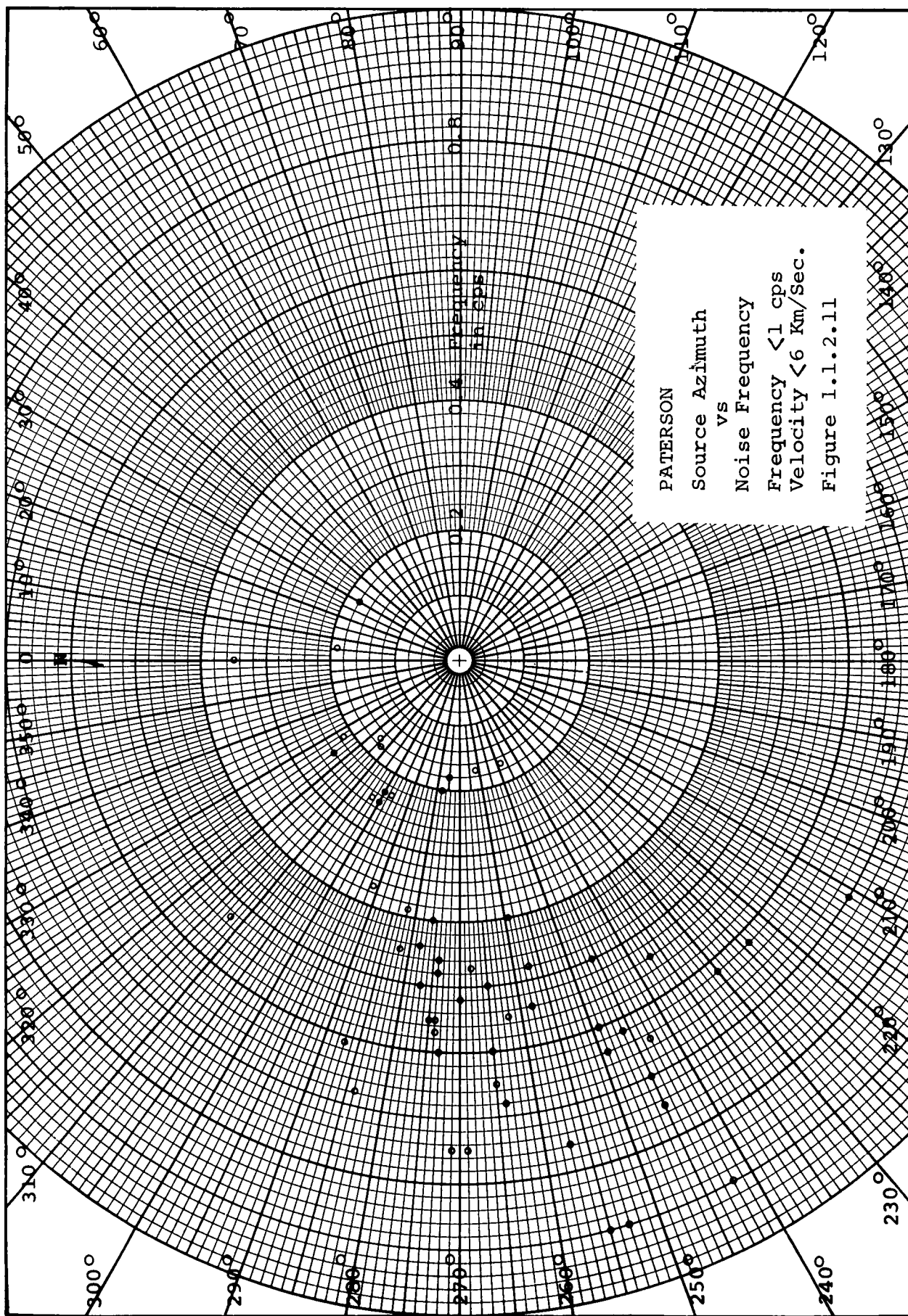


Figure 1.1.2.4







The amplitude of cultural noise related to cities, railroads and possibly dams is significant for probably about 50 km. For example, at Paterson, 1.5 to 2 cps noise of high level apparently came from  $140^{\circ}$  -  $160^{\circ}$  azimuth and was probably related to activity at McNary Dam, 15 km away. This same noise was not recorded at Toppenish Ridge, 100 km from McNary Dam, and probably not at Mabton, 75 km from the dam. The peculiar behavior of amplitude of this noise supports associating it with the dam. Continuous playouts of 24-hour recordings of this noise showed that on three consecutive days its amplitude doubled rather abruptly every night, remained constant for several hours, then abruptly halved until the next night. This change might have been associated with nightly opening of spillways at McNary Dam or with sudden increase in volume of flow below the dam. A sample of this noise is shown in Figures 1.1.1.6.4.10 and .11.

At both Paterson and Toppenish Ridge about 30% of the noise spectrum below 2 cps was difficult to interpret because the source directions were spread widely and erratically, and many apparent phase velocities were higher than expected for plane surface waves. It is assumed that the difficulties were the result of complex interference patterns of mixtures of cultural noise from nearby cities, wind noise and river noise.

Study of cross-spectra alone will not distinguish between the source direction of a single coherent plane wave and an apparent source direction resulting from interference of noise from several simultaneous fixed sources. However, the average phase velocity of 4 or 5 km/sec indicated by maximum observed phase shifts (See Section 4.1) is a reasonable value for fairly simple plane waves, which suggests noise source directions more restricted than random.

#### 1.1.2.2 Seismic Noise Velocity

Cross-spectral studies indicate that the average velocity of seismic noise for all frequencies below 2 cps is probably between 4 and 5 km/sec in the Pacific Northwest. Examination of phase shifts on film recordings shows this same general velocity for 0.5 cps noise at stations on all three profiles.

Plots of phase shift against frequency (Figure 1.1.2.15) show average minimum velocity of 4 to 5 km/sec, but many anomalously small phase shifts suggest that some apparent velocities might be due either to interference patterns from multiple surface-noise sources, or to possible mixing of some teleseism signal with the noise being samples.

Velocities for frequencies above 1 cps recorded on 1 mile radius arrays cannot be uniquely determined from cross-spectra alone. When maximum phase shift can conceivably be close to or larger than  $180^{\circ}$ ,



PATERSON  
SS 62-030-10:00:00z  
Dam Noise

Figure 1.1.1.6.4.10



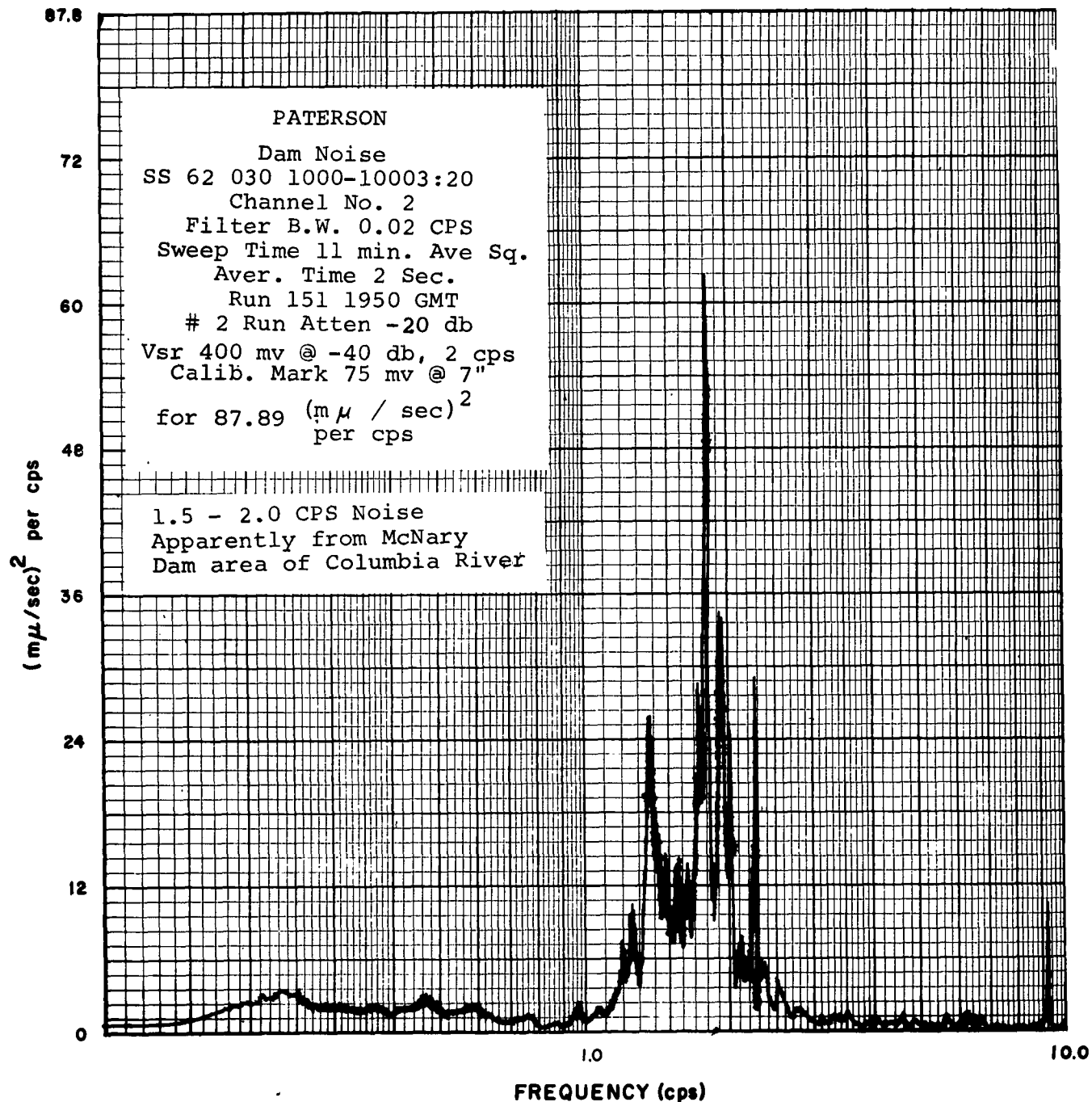
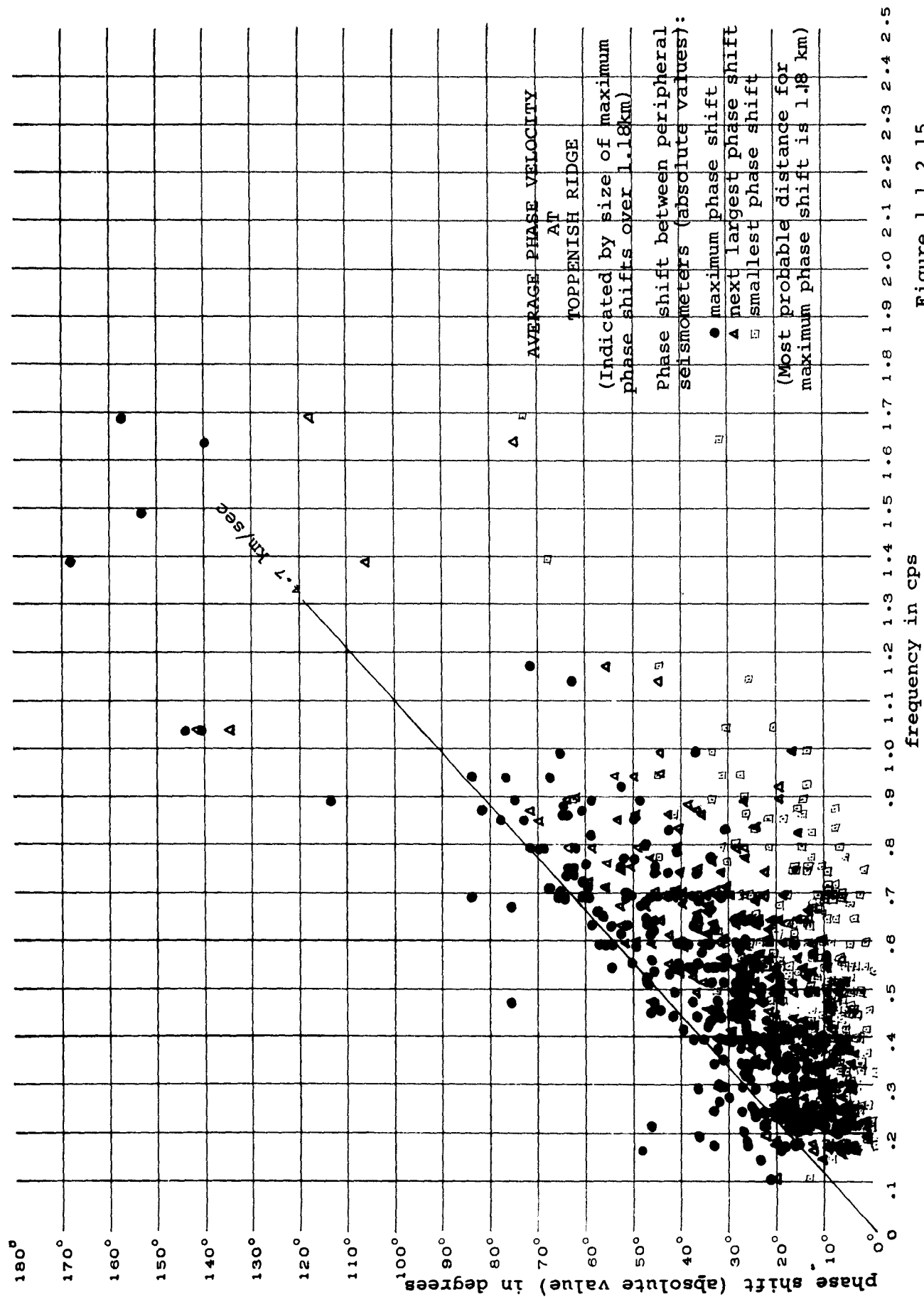


Figure 1.1.1.6.4.11



cross-spectral data can be interpreted in more than one way, with choice between the two or more possibilities made difficult by random error in calibration and calculation.

### 1.1.2.3 Noise Coherency

Phase coherency between outputs of two seismometers x and y for a specified frequency and over a specified sample length, is defined by the relation

$$\sqrt{\frac{Co_{xy}^2 + Quad_{xy}^2}{(PSD_x)(PSD_y)}} \text{ which}$$

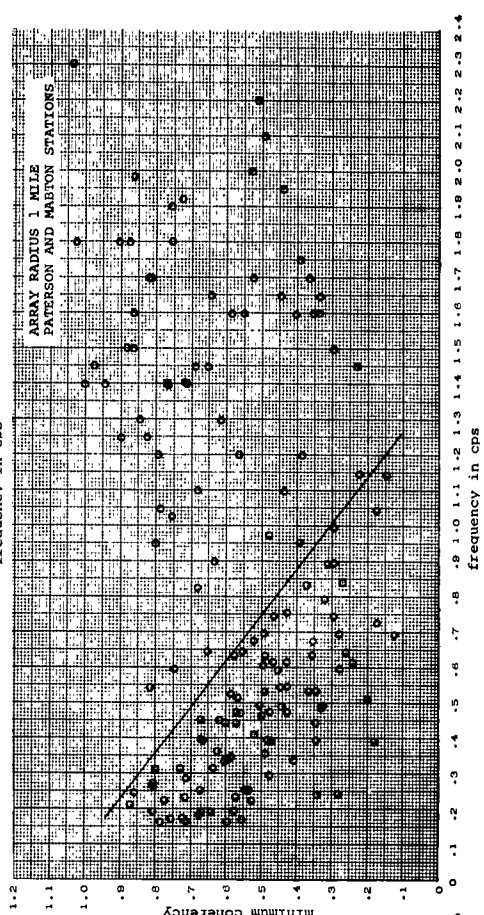
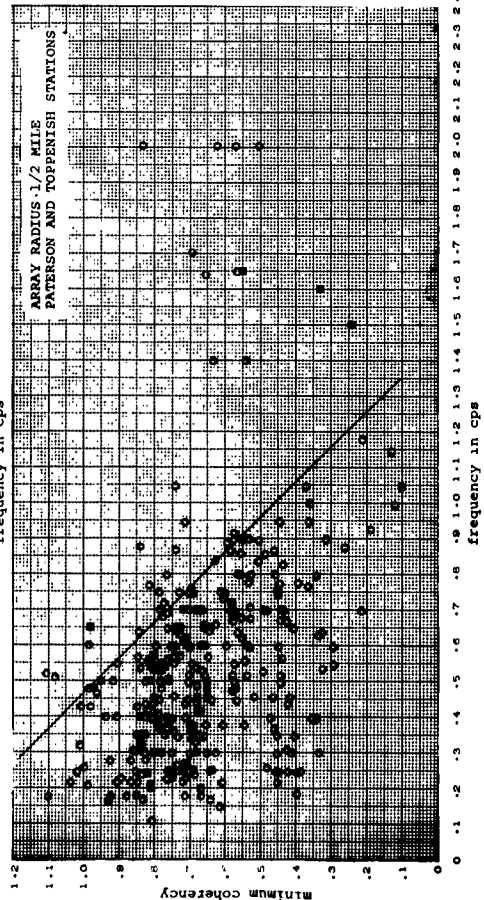
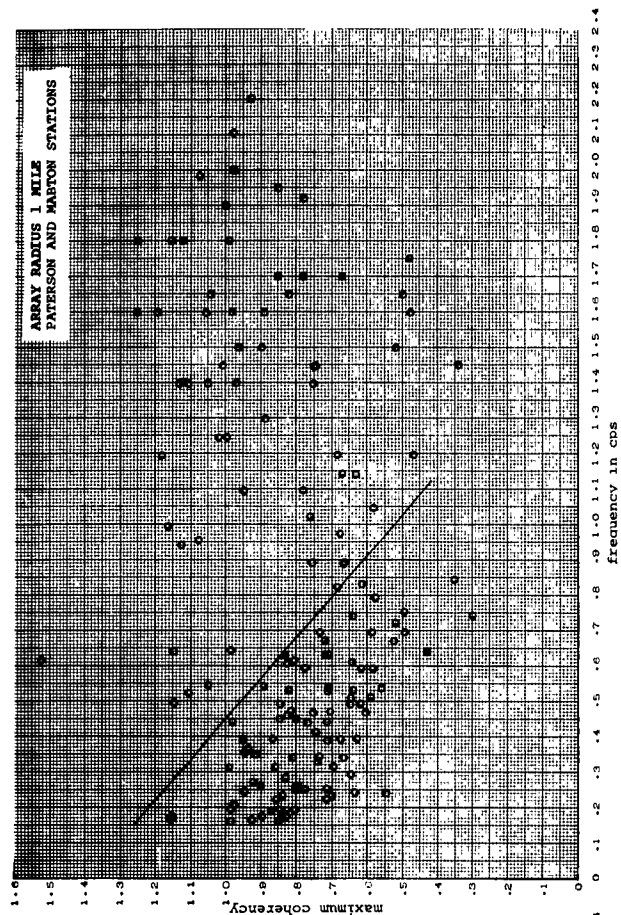
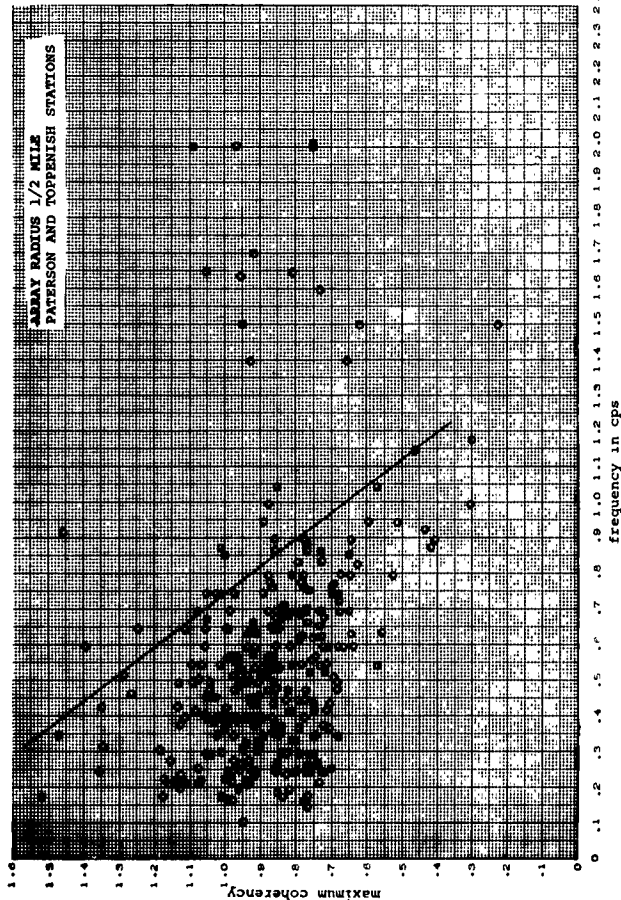
can vary between 1.0 for perfectly coherent waves, and zero, when seismometer outputs are unrelated (See Section 4.1.3).

Coherency values in the Pacific Northwest averaged between 0.5 for the lowest values and 0.9 for the highest values, with individual measurements varying widely. Scatter was too large to allow distinction of clear relationships between coherency and noise frequency or distance between seismometers, but results suggest that coherency decreases with increase in frequency and with increased seismometer spacing. For example, at 5 cps maximum coherency values average about 0.9 for  $\frac{1}{2}$  mile arrays and about 0.75 for 1 mile arrays, while minimum average values are about 0.7 for  $\frac{1}{2}$  mile arrays and 0.5 for 1 mile arrays (Figure 1.1.2.16). For frequencies below 1 cps there is a suggestion of decreased coherency with increased noise frequency, but no relationship is apparent for frequencies above 1 cps.

Degradation of noise coherency with increase in seismometer spacing and noise frequency is clearly visible on film recordings (Figure 1.1.2.17). At 1 second periods or less there is usually a noticeable decrease in trace similarity as array radius increases from  $\frac{1}{4}$  to 1 mile, while at frequencies above 2 cps there is little correlation between traces even for arrays of only  $\frac{1}{4}$  mile. Coherency of noise in the 2 second band is little affected by change in array radius from  $\frac{1}{4}$  to 1 mile, except at coastal stations, where phase shift is often hard to determine between seismometers less than  $\frac{1}{2}$  mile apart.

### 1.1.3 Relative Signal Strength Variations with Environment

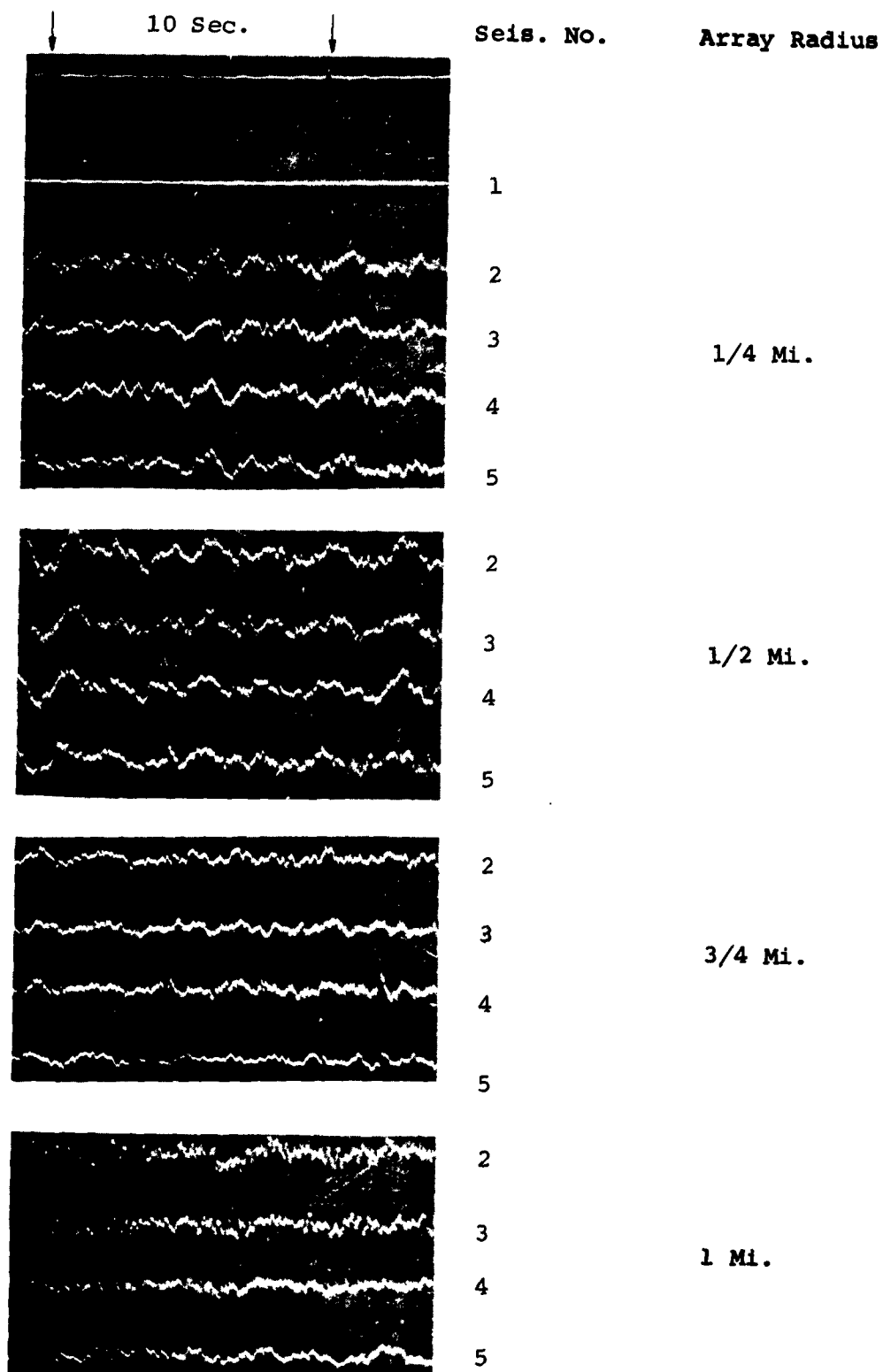
In order to show how geologic conditions influence the strength with which teleseisms are recorded, slave station recordings of teleseisms were compared with recordings of the same teleseism at the fixed master station. Trace amplitudes of matched phases of the same teleseism at both master and slave stations were measured from film records, corrected for attenuation differences and combined to give a



# NOISE COHERENCY VALUES BETWEEN PERIPHERAL SEISMOMETERS OF 1/2 and 1 MILE RADIUS ARRAYS

Maximum and minimum values of coherency between three pairs of peripheral seismometers, computed for seismic noise from .2 to 2 cps. PACIFIC NORTHWEST PROFILE

Figure 1.1.2.16



CHANGE IN COHERENCY OF SEISMIC NOISE  
WITH INCREASING SEISMOMETER SEPARATION  
Pacific Northwest Profile  
Gibbon Slave Station  
All seismometers recording at -20 db

Fig. 1.1.2.17

ratio of slave-to-master trace amplitude. Variations in this ratio at different stations reflected variations in recording conditions. Only teleseisms from long-distance earthquakes were used in these studies so that differences in travel paths would be minimal from focus to master and slave recording locations.

Because the objective was to observe relative differences in signal strength among slave stations at different locations, the same slave and master seismometer channel (SS #2 and MS #3), corrected for differences in recording attenuation, was always used when taking the ratio. No correction was made for gain differences, on the assumption that changes in relative gain between these two channels would be less than the random error involved in calibrating each channel and calculating its gain correction.

One of the more serious difficulties in analyzing signal strength from film recordings was the lack of dynamic range in film recordings. If noise was recorded at the high level required for easy visual monitoring, so much of the available film width was taken up that teleseism first motion of more than about 10 times noise amplitude was not clearly visible, and often could not be measured. For this reason, signal strength studies were based almost entirely on teleseisms where S/N ratio was less than 10, and averaged about 4.

To draw conclusions about change of signal strength with environment it must be assumed that signal strength ratios are distributed more or less normally around their true mean value and that their average value at any station is an indication of true relative signal strength at that station. Data were so sparse that average values are not easily defined, since scatter was of the same order of magnitude as the apparent differences in average level between stations (Figure 1.1.3.3.3). No conclusions can be safely drawn about relative signal strength at stations where too few teleseisms were recorded to define the distribution of signal strength ratios.

#### 1.1.3.1      Signal Strength Variations with Regional Geologic Environment

Signal strength ratios of teleseisms vary widely because of the relatively high background noise through which they are recorded, but their average values indicate that teleseisms are recorded more strongly in sedimentary than in crystalline provinces. Average signal strength ratios from California are all higher for stations on thick Tertiary sediments than for stations on granite, sometimes four or five times as high. There is little difference in relative signal strength between stations on massive granite and those on Paleozoic sediments.

Figure 1.1.3.3.1 summarizes signal strength data for the SS #2 and MS #3 seismometers on the California and Pacific Northwest profiles. For each station is shown first motion amplitude ratio, period of the first cycle of first motion, and background noise level through which the teleseisms were measured. The California master station at Round Mountain and the slave stations at Cedar Creek, Panamint and Darwin were all located either on massive granite or on well-indurated Paleozoic sediments and all show average signal strength ratios of 1.0 to 1.3. California stations at Death Valley, Mannot Creek, Carrizo and Huasna, all on relatively thick Tertiary sediments, gave average signal strength ratios varying from 1.4 to 5.0.

Variations in signal strength ratios among stations in the Pacific Northwest were smaller, probably because geologic conditions were less varied on this profile than in California. The master station at Toppenish Ridge was located on a thick section of successive basalt flows, and all other stations at which measurable teleseisms were recorded were also located on lava of various thickness and structural complexity. This probably accounts for the fact that average signal strength ratios differ by a factor of two, at most, among the stations of the Pacific Northwest.

No signal strength data are available from Pacific Northwest stations located in truly sedimentary or granitic environments, although such stations were occupied. Markham, on the coast, was on Tertiary sediments, but no teleseisms could be found because of the high noise level dominated by frequencies close to that of teleseism first motion. The Armin station on the opposite end of the profile was in essentially granitic environment but no usable data were found in recordings there.

Signal strength ratios out of accord with the regional environment, at least as reflected by other California stations, were obtained at Carrizo and Big Meadow. Regionally, Big Meadow was in granitic environment, but the seismometers were located in a bog-filled basin when teleseisms were recorded there, and response is the bog is apparently abnormally high. Although Carrizo was in a general environment of Tertiary sediments similar to that of Mannot Creek, signal strength ratio was lower than for any other station located on young sediments. The reason for this is not clear, but it was noted that sediments in the Carrizo area were contorted and sometimes on end, whereas sediments at other stations were more nearly flat-lying, even though contorted.

There is some indication that relatively high values of Bouguer gravity are associated with relatively high signal-strength ratios on both profiles (Figure 1.1.3.2.1) but neither gravity nor signal strength

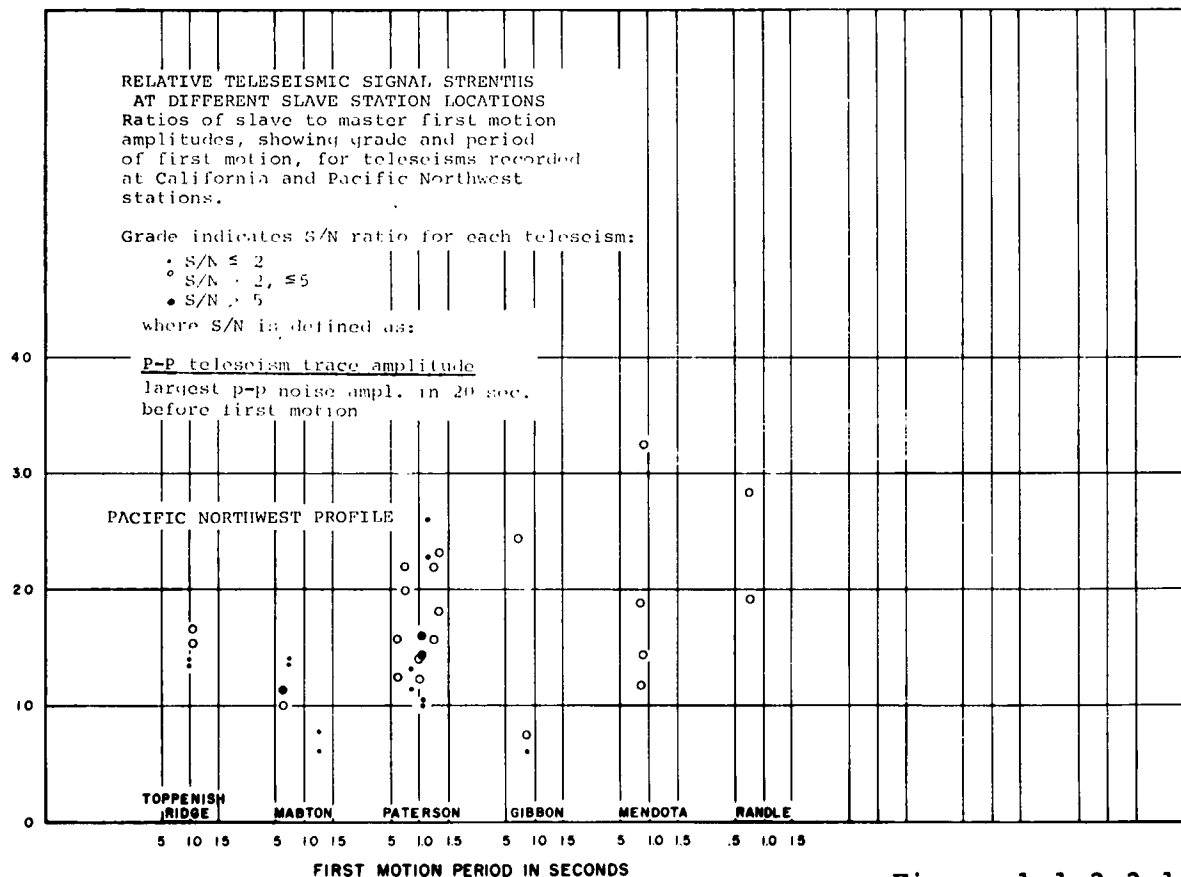
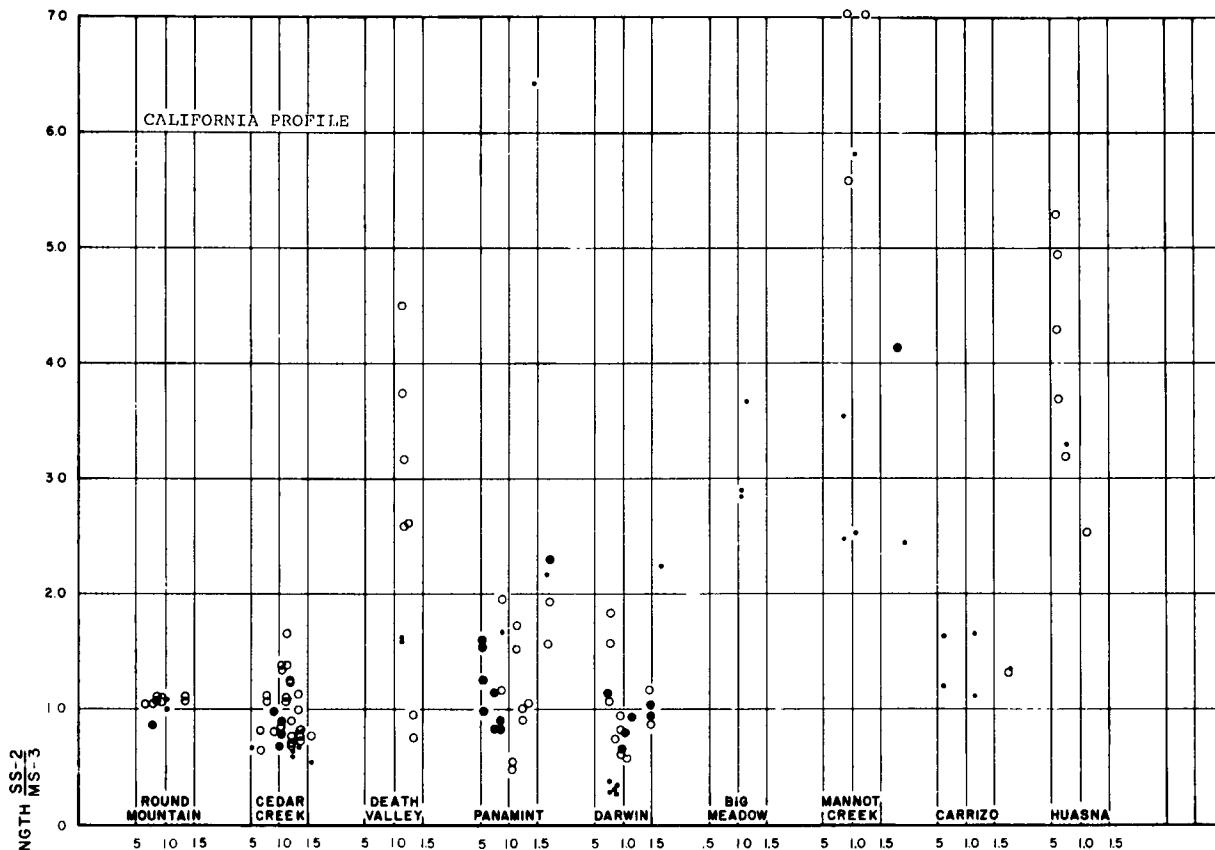


Figure 1.1.3.3.1



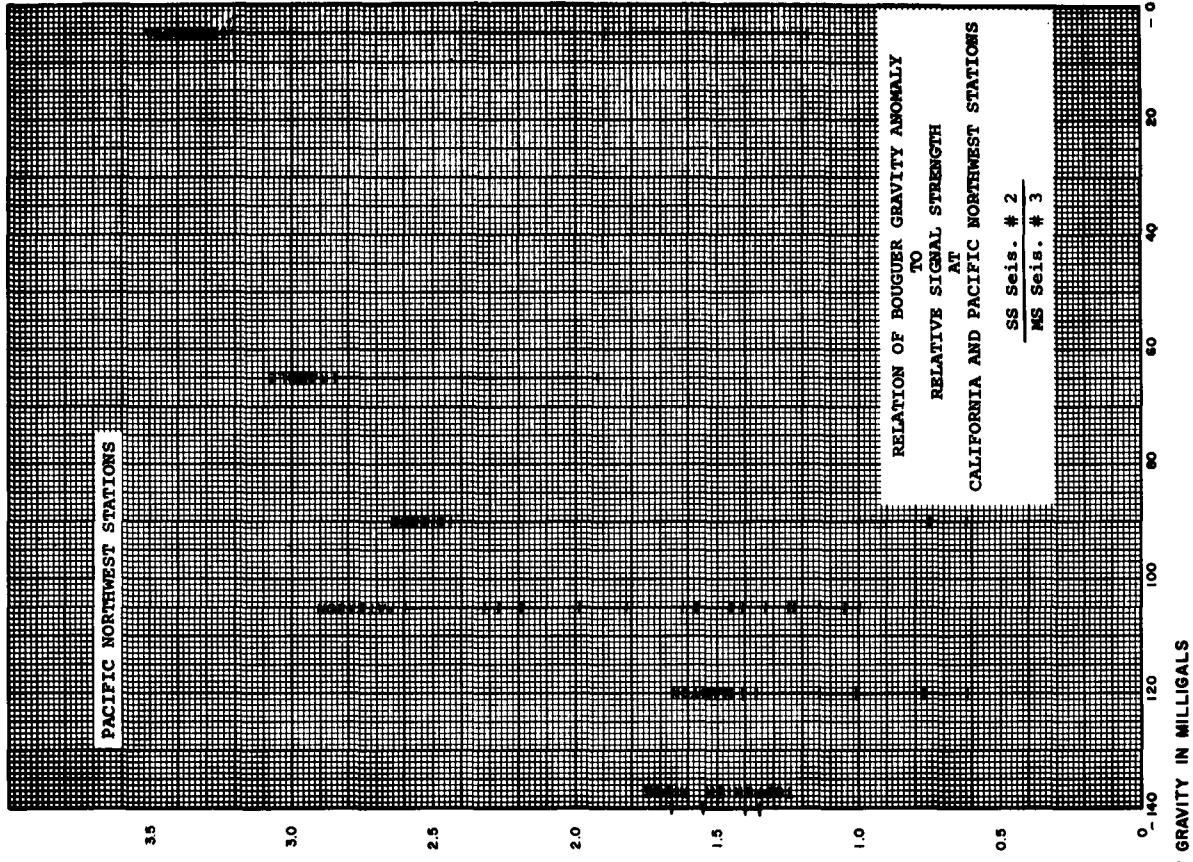
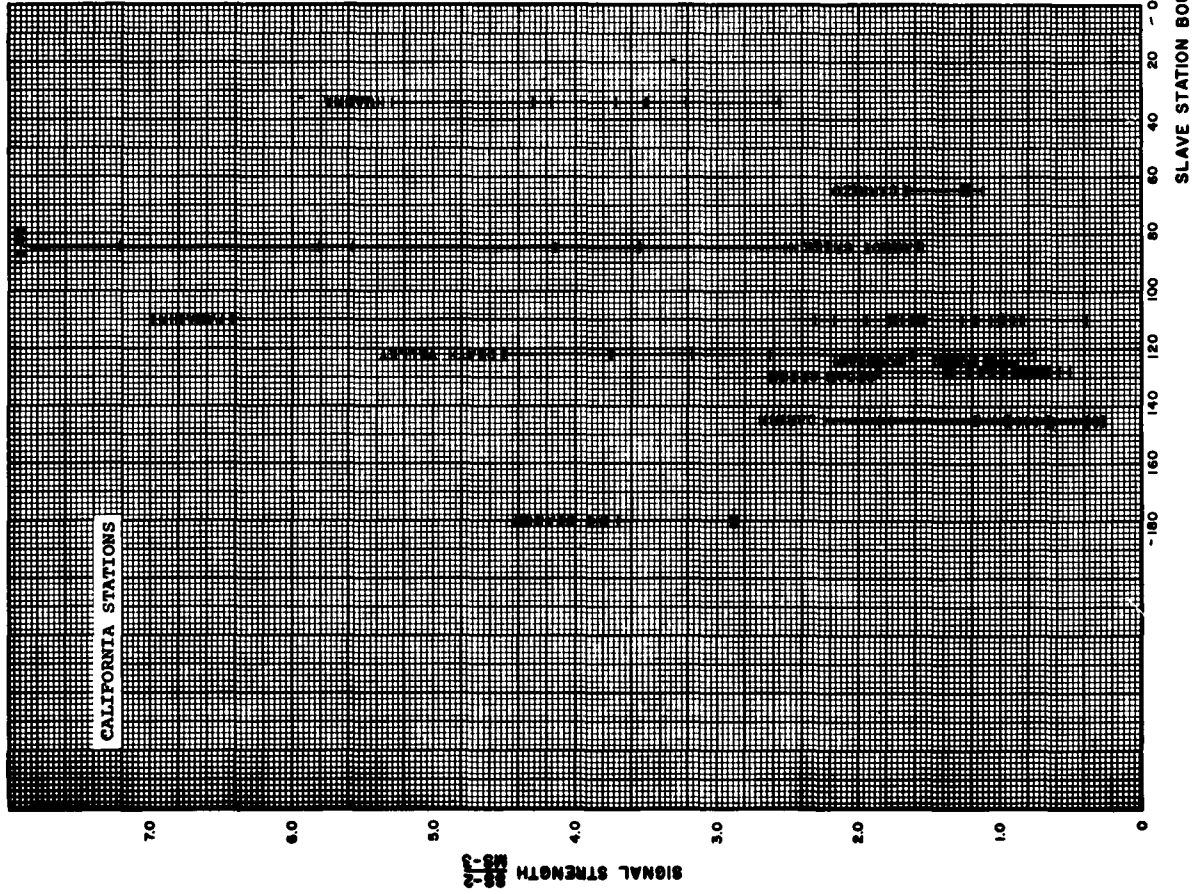


Figure 1.1.3.2.1

values are known to the degree required to test correlation between the two. The relation between observed gravity anomalies and geologic structure is quite complicated along the California and Pacific Northwest profiles, since both areas are geologically young and unstable, without general isostatic equilibrium. Because much of the terrain is mountainous, determination of terrain and elevation corrections is more difficult. The thick fill of dense basalt in Pacific Northwest basins reduces density contrast of underlying basement rock, obscuring definition of basin limits. Gravity data were taken largely from work by G. P. Woollard (24 b).

#### 1.1.3.2      Signal Strength Variation with Local Seismometer Environment

Although average signal strength ratios at adjacent stations differed by as much as a factor of five, variations between seismometers of each array were much less significant, usually about 20% of the mean signal strength ratio for the array.

At several locations there were differences in signal response between seismometers located on hardrock and those located on alluvium or other soil types, but signal response and local seismometer environment were not consistently related. At Panamint, Big Meadow and Carrizo, signal strength from some seismometers on hardrock (limestone, granite and sandstone) was lower than for seismometers in alluvium or topsoil. However, another seismometer at Panamint and one at Huasna located on hardrock showed stronger signal reception than those not on hardrock (Figure 1.1.3.1). Average signal strengths for Pacific Northwest seismometer positions varied in apparent independence of the observable local environment. For example, seismometers at Toppenish Ridge, Mabton and Paterson were all in essentially identical rock type within each array, yet average signal strengths at each seismometer position were not equal.

A multiple regression program was used in an attempt to relate relative signal strength within each array to alluvial depth, type of rock, and topography at each seismometer position on the California profile, but results were inconclusive. (See table following Figure 1.1.3.1).

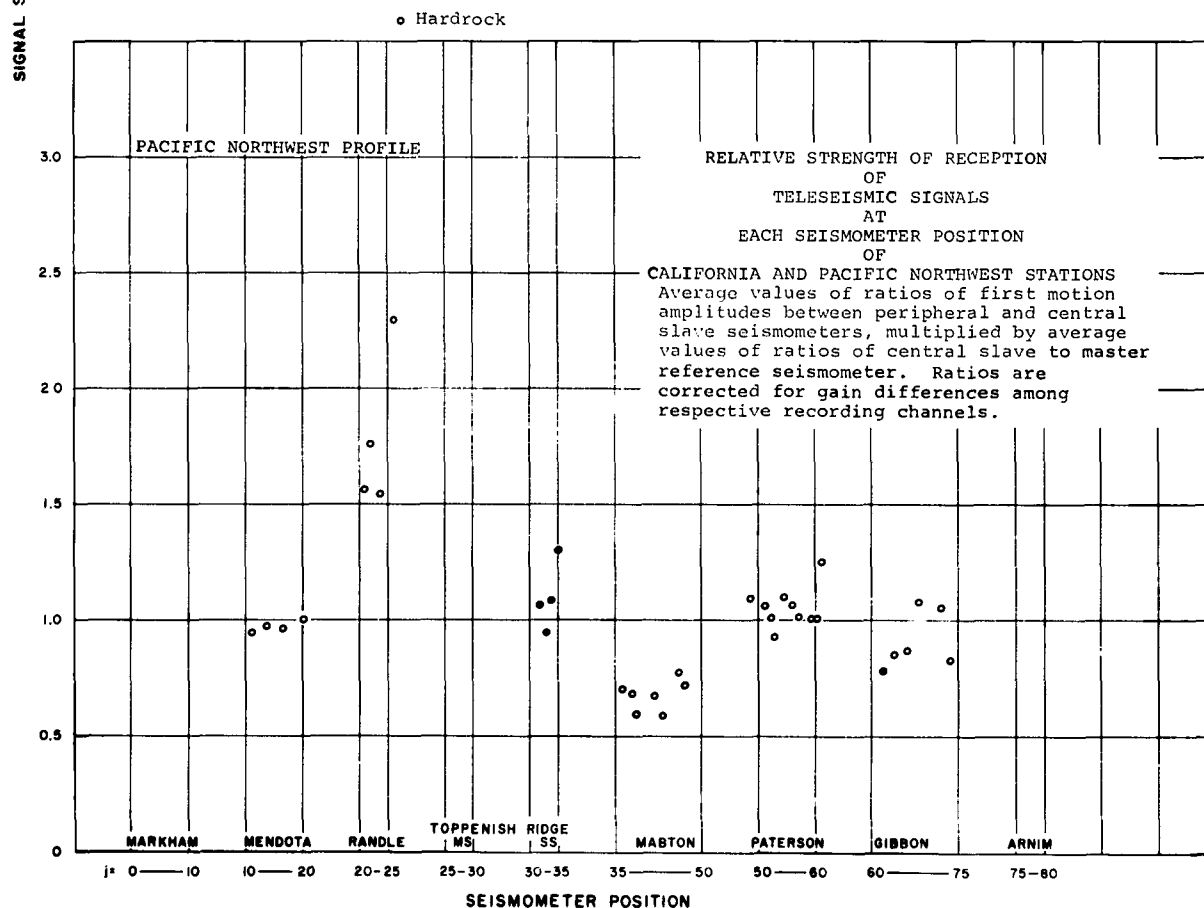
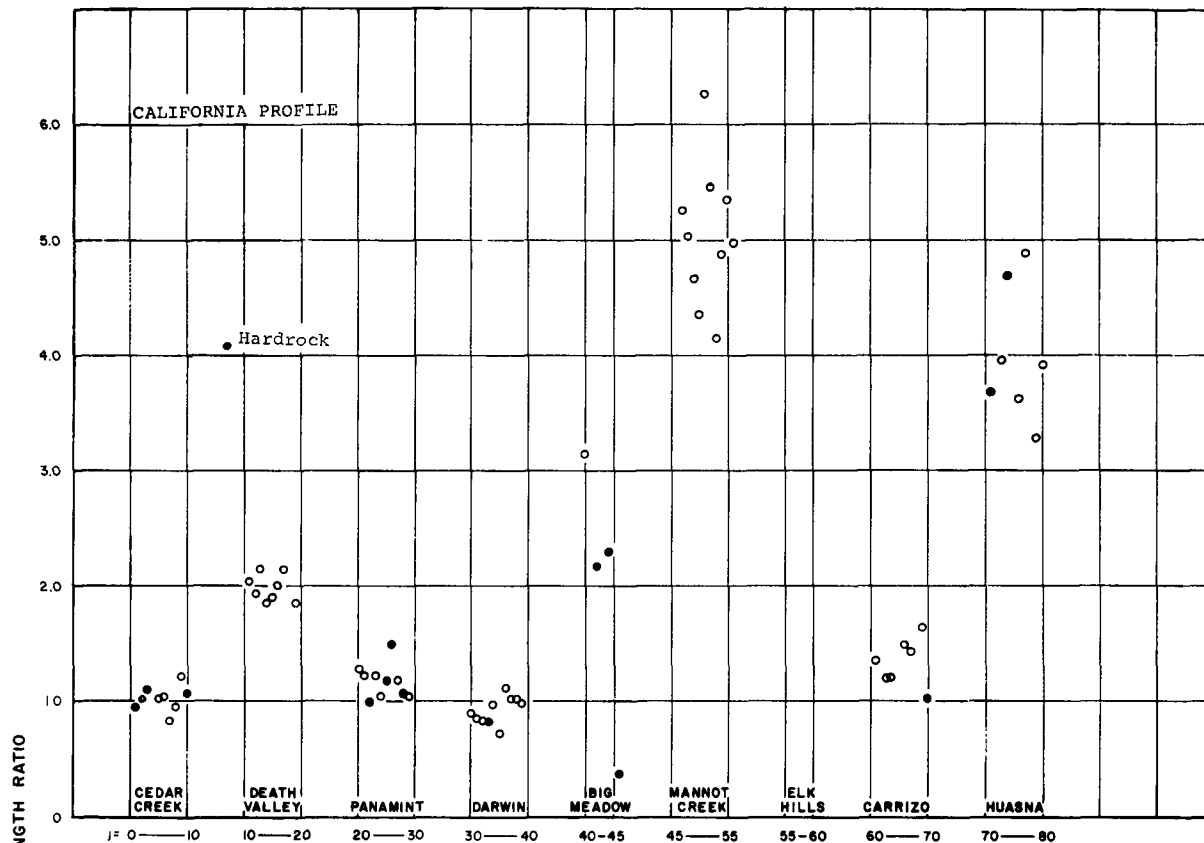


Figure 1.1.3.1

### Correlation Statistics from Studies of Local Signal Strength and S/W Ratio Variations

[illegible]

(1) 3d = Normalized residual S/N ratio about mean for station.  
3f = Normalized residual Sig. Strength about mean for station.  
3e = Normalized S/N ratio about mean for station.  
3c = Residual Signal Strength about mean for station  
3g = Normalized Residual .4 - .5 Second Noise Amplitude, about mean for each station.

#### 1.1.3.3 Effect of Background Noise on Signal Strength Measurements

Correlation of signal strength with the geology of recording stations was greatly complicated by scatter in values of signal strength ratios for different teleseisms recorded by the same fixed pair of master and slave seismometers. There was no apparent relation between the scatter and period of first motion or area of origin of teleseisms, but examination of distribution functions of signal and noise amplitudes showed that most of the observed scatter of signal strength ratios could be attributed to distortion of teleseism signal by background noise at the recording stations. Although there was noticeable scatter in ratios among seismometers of a single array, it was not so troublesome as the scatter between seismometers of different stations, probably because noise affects seismometers of a single array in less random fashion than it does seismometers separated by several noise wave-lengths.

A rough estimate of the effect of background noise on signal strength ratios can be made from data of Figure 1.1.3.3.3c. The California stations of Cedar Creek, Panamint, and Darwin had similar noise amplitudes at 1 second period, and similar signal strength ratios with respect to the master station at Round Mountain. Recordings at all four stations were made at the same gain, so that trace amplitudes could be compared directly. Measurements were made of trace amplitudes of maximum p-p noise in the 10 or 15 seconds preceding each teleseism, trace amplitudes of matched phases of the teleseism signal at master and slave station, and the ratio of trace amplitudes of each teleseism. These data were plotted in Figure 1.1.3.3.3c as cumulative frequency distributions, which show that trace amplitudes of signal and noise, as well as signal strength ratio, had log-normal distribution. Average signal amplitude was 24 mm at both master and slave stations. Maximum noise amplitude averaged 6 mm at both sites, but it should not be expected that noise maxima would distort signal frequently enough to account for the observed signal strength ratio dispersion. However, some lesser noise amplitude (assume an average of one-half maximum) is always affecting signal measurements. Assuming that effective average noise amplitude was about 3 mm and that both noise and signal could be expected to vary randomly through one standard deviation between successive events, then "true" signal strength ratio of 1.0 could be expected to show many values between 0.4 and 2.4, because of noise distortion of true signal. One standard deviation from the means of observed signal strength ratios included ratios from 0.65 to 1.5. The similarity of the observed and the possible ranges of variation suggest that most of the observed scatter was due to the effect of background noise.

SEISMIC BACKGROUND NOISE  
IN SIGNAL STRENGTH MEASUREMENTS

Cumulative log-normal distributions of master and slave signal amplitudes, slave/master signal amplitude ratios, and background noise amplitudes, showing for each:

means ( $\bar{x}$ ) and logs ( $\ln \bar{x}$ ) of means, standard deviations ( $s$ ) of  $\ln x$ , and values ( $x'$ ) corresponding to one standard deviation on either side of  $\ln \bar{x}$ .

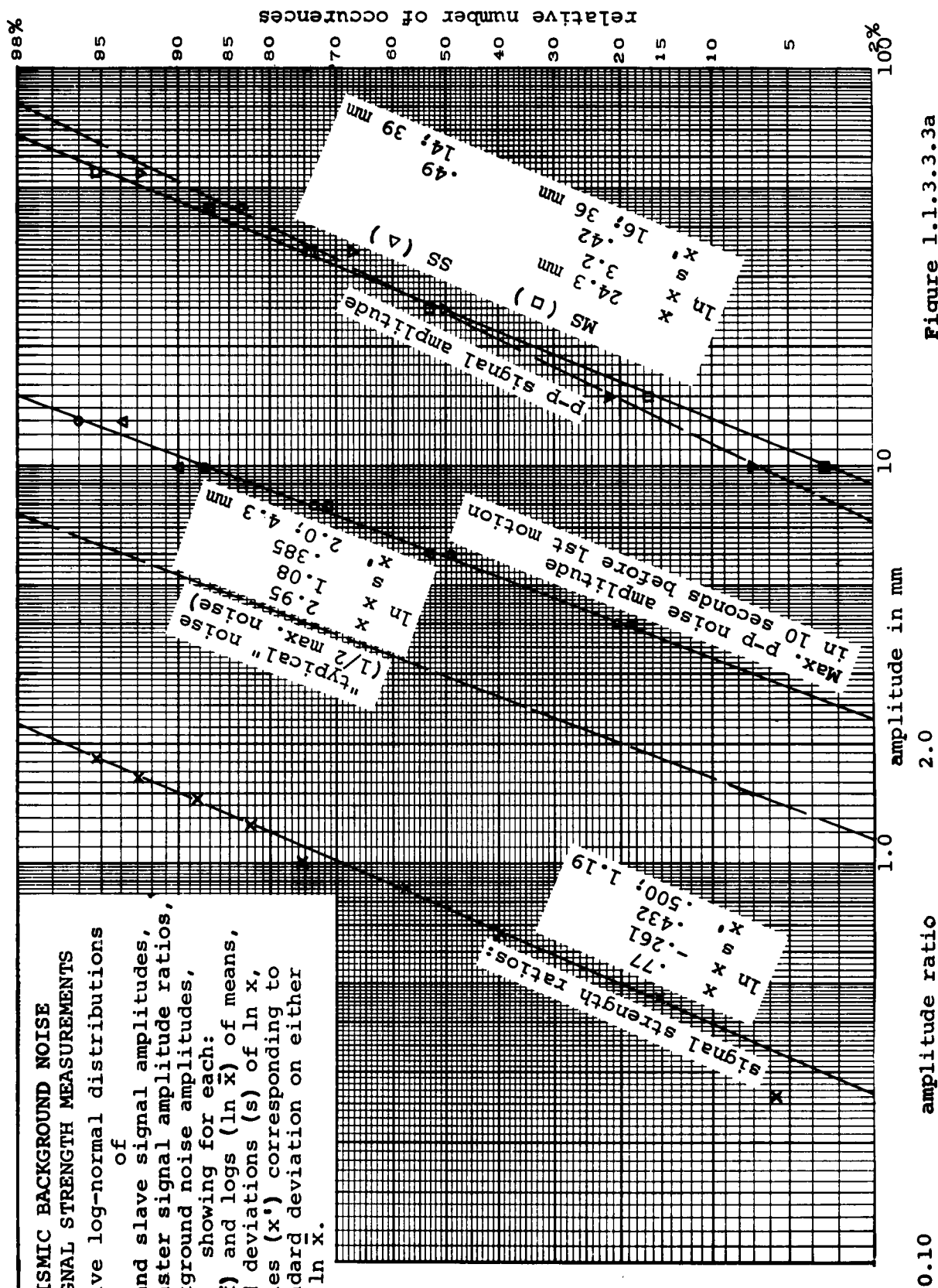


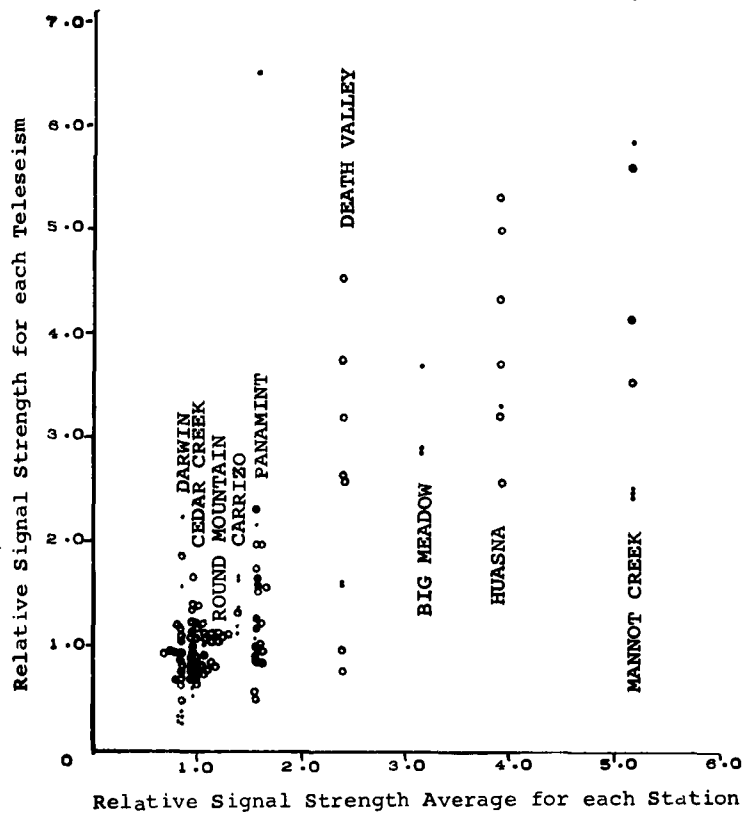
Figure 1.1.3.3.3a

Another way of testing possible influence of background noise is to express signal strength ratio as a Taylor's series expansion about the mean signal strength ratio. The square of the difference between the mean and the Taylor's series can be roughly interpreted as the expected variance of signal strength ratio, expressed in terms of mean and variance of signal and noise data at the two recording stations. Second-order approximation by this method gives a value of 0.26 for the expected deviation in signal strength ratio due to background noise, to be compared with a standard deviation of 0.43 for observed signal strength ratio. The implication again is that noise plays a large role in signal strength ratio scatter, provided that application of this method is valid. When signal-to-noise ratio is 1, signal strength ratios could conceivably have infinite values, in which case expression as a Taylor's series would be invalid. This condition is unlikely, since studies were made only of teleseisms whose phases of first motion could be correlated at both stations. A more serious question of validity concerns the assumption that cross-products sum to zero in squaring the expansion, which implies that all noise and signal measurements at both recording positions are randomly related. This is not true for two signal measurements on the same teleseism at different locations.

Some variation in observed values might be related to epicenter location, first motion period or some other mechanism, but these influences would probably not be identifiable through the larger effect of noise.

Scatter in signal strength ratios remained fairly constant when the distance between recording and reference seismometers was more than about five kilometers. The scatter decreased when the distance between seismometers was a noise wave-length or less, apparently because the same noise phase often affected both seismometers almost simultaneously when the distance between them was small. The observed scatter of ratios for teleseisms recorded in the Pacific Northwest area at varying distances from the reference station is illustrated in Figure 1.1.3.3.3b.

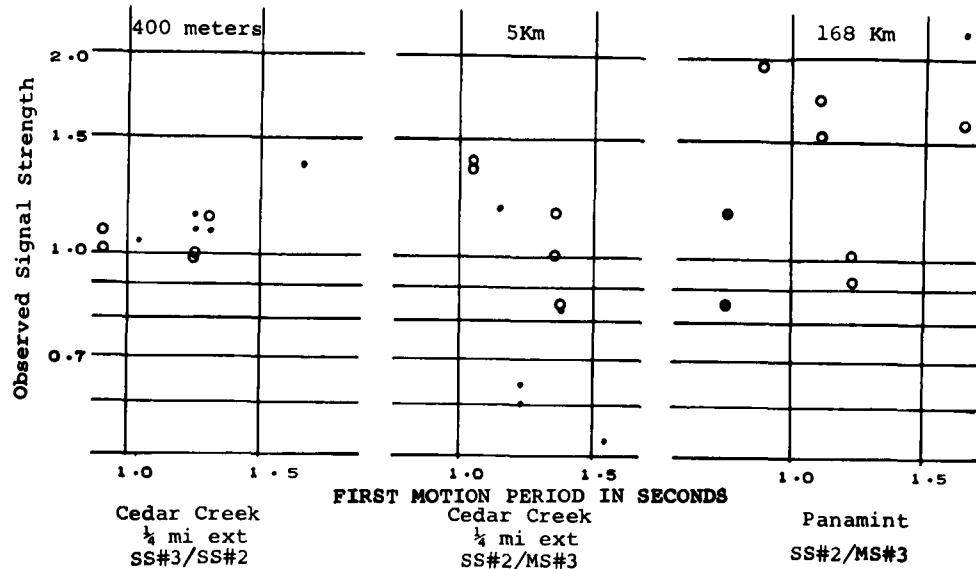
In this study, signal-to-noise ratios averaged about 4, for which signal strength ratio scatter was substantial, sometimes 5 to 1. Because of the effect of background noise, effective correlation of average signal strength ratios with any but the most general characteristics of station geology would probably require signal-to-noise ratios of 10 or more.



EFFECT OF DISPERSION OF SIGNAL STRENGTH RATIOS  
ON DETERMINATION OF AN AVERAGE VALUE FOR  
EACH SLAVE STATION

Fig 1.1.3.3.3a

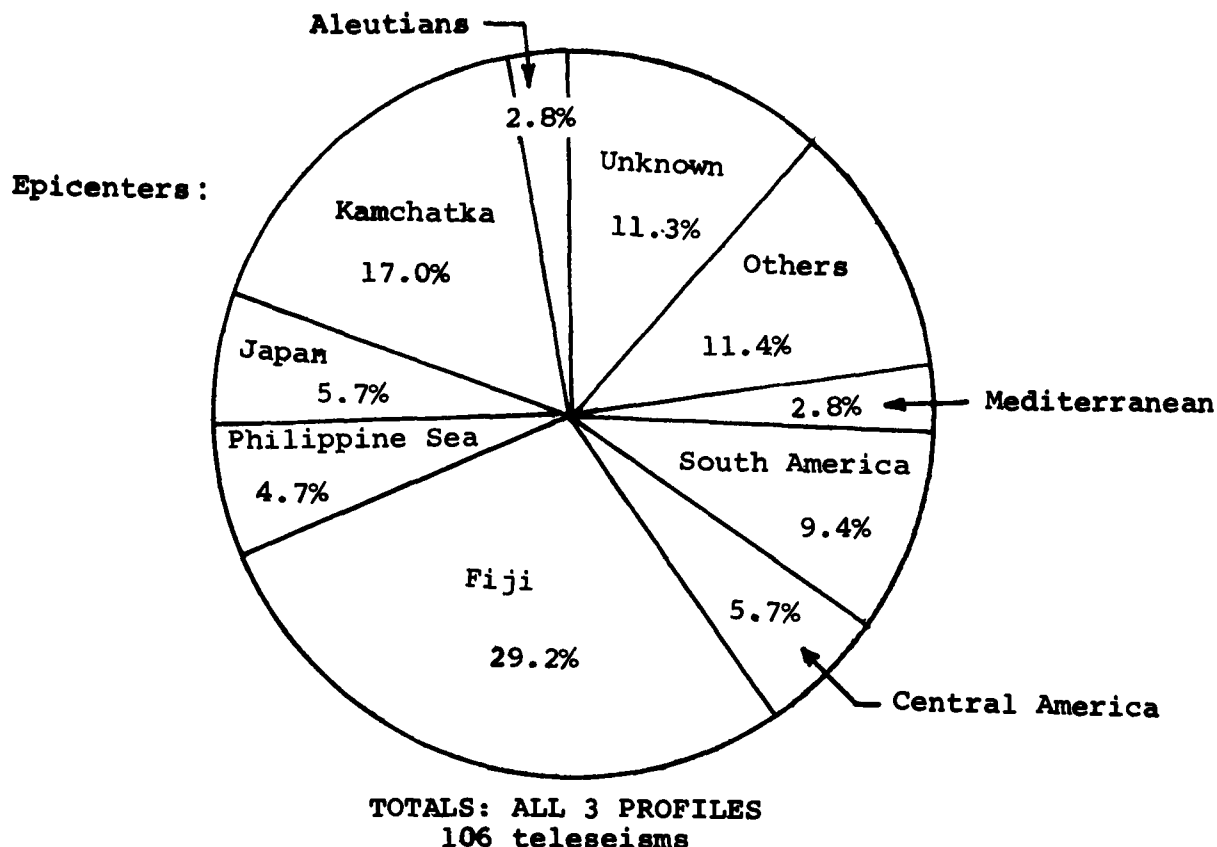
Separation between Recording and Reference Seismometers



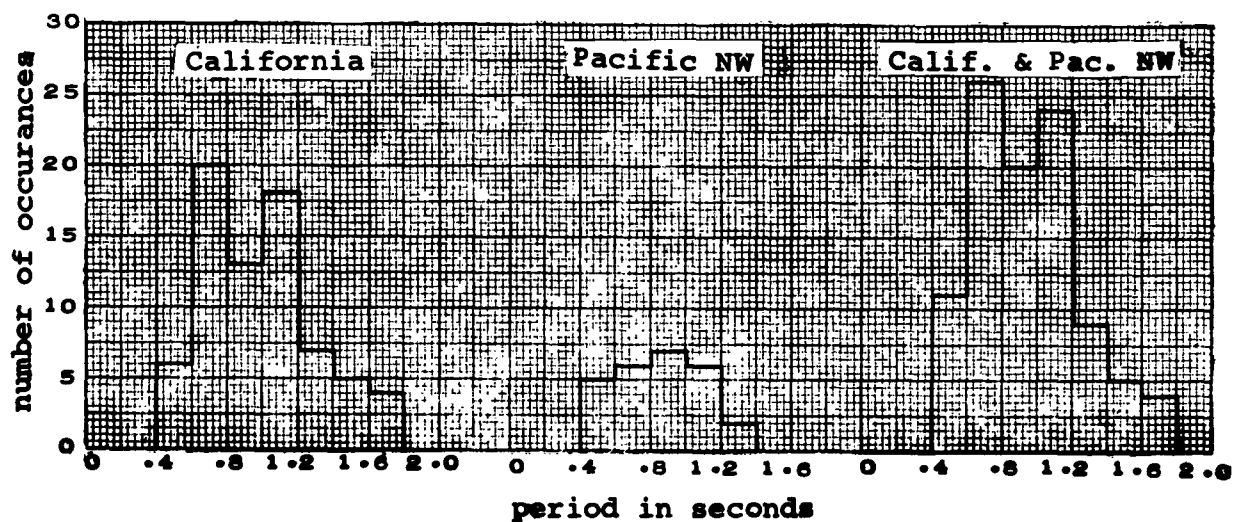
EFFECT OF SEISMIC NOISE ON SIGNAL STRENGTH RATIOS  
Scatter in ratios of signal strength for successive  
teleseisms, each recorded by two seismometers  
separated by various distances.

Fig 1.1.3.3.3b





**PERIOD OF FIRST MOTION :**



**EPICENTERS AND FIRST MOTION PERIODS  
OF TELESEISMS STUDIED ON VT/078**

**Figure 1.1.3.4**

#### 1.1.4 Variation of Signal-to-Noise Ratio with Environment

In general, data from California and Pacific Northwest profiles indicate that signal-to-noise ratio deteriorates rapidly as distance to the ocean decreases.

Relative signal-to-noise ratios for individual seismometer positions of the California and Pacific Northwest profiles are shown in Figure 1.1.4.1. Differences in signal-to-noise ratios among recording stations in this study were determined much more by relative noise level in the band being considered than by relative signal strength, because variation in noise level among these stations, all relatively near to the ocean, was often several times as large as the variation in signal strength. At stations farther inland than those studied here, however, signal strength is probably of equal or greater importance than noise level.

In California, signal strength was from one to five times as high at stations on Cenozoic sediments as it was at stations on granite or Paleozoic sediments. The inland station of Death Valley, on Cenozoic sediments, showed high relative signal strength which, combined with relatively low noise level in the 1.25 to 1.20 second band, gave this station the highest signal-to-noise ratio of any California station. Although signal strengths at stations on Cenozoic sediments between the ocean and the Sierra Nevada were sometimes higher than those at Death Valley, the higher noise levels at these stations gave them the poorest signal-to-noise ratios of the profile. Panamint and Darwin stations, on Paleozoic sediments, were well inland from the ocean and had the second best signal-to-noise ratios. Cedar Creek was a station on massive granite but was closer to the ocean than Darwin and had a lower signal-to-noise ratio.

Among Pacific Northwest stations, variation in signal strength was almost negligible compared to variation in noise level, and the signal-to-noise ratio increased almost uniformly as the distance from the ocean increased.

The relatively small variations in S/N ratio among individual seismometer positions were tested for correlation with ground environment at each seismometer (rock type, alluvial thickness, etc.) but results were inconclusive. Regression and correlation coefficients are listed in the table following Figure 1.1.3.1 of Section 1.1.3.2. The correlation program is described in Section 4.3.

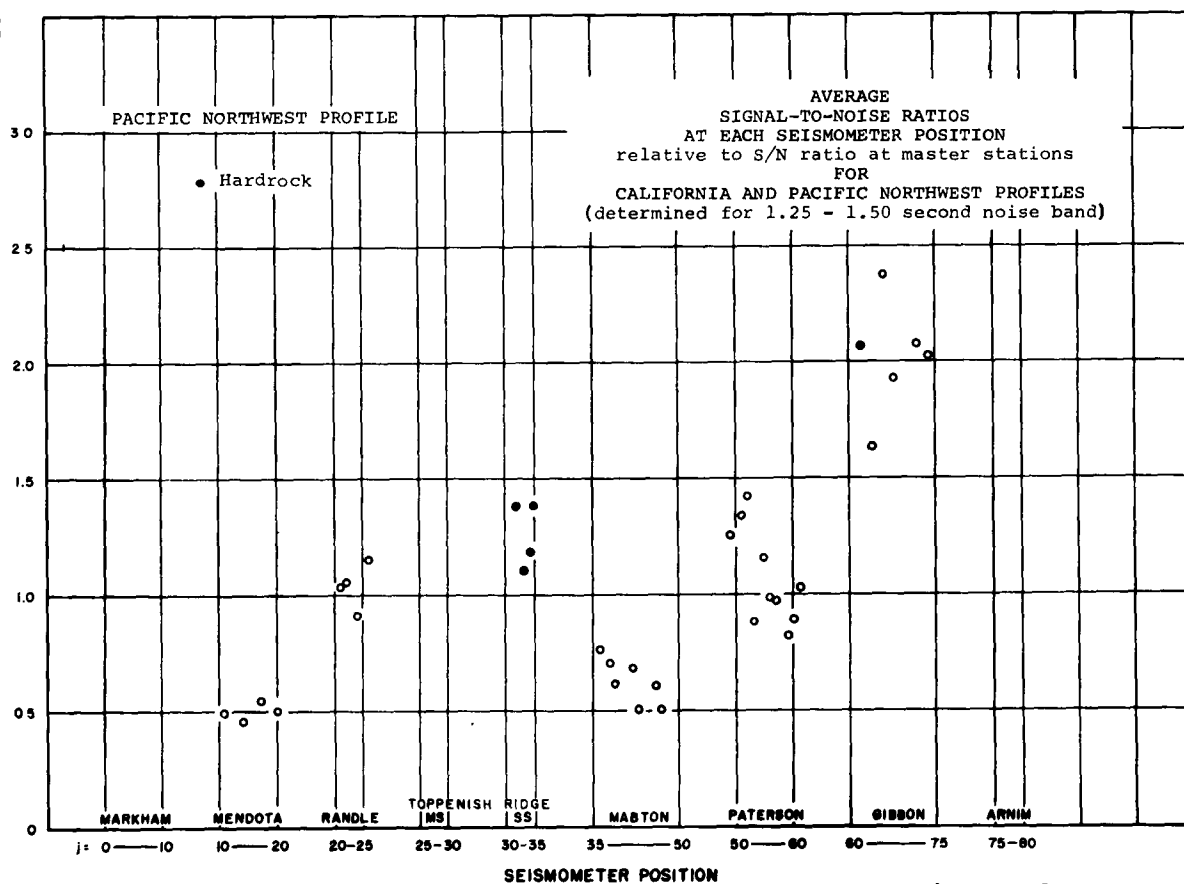
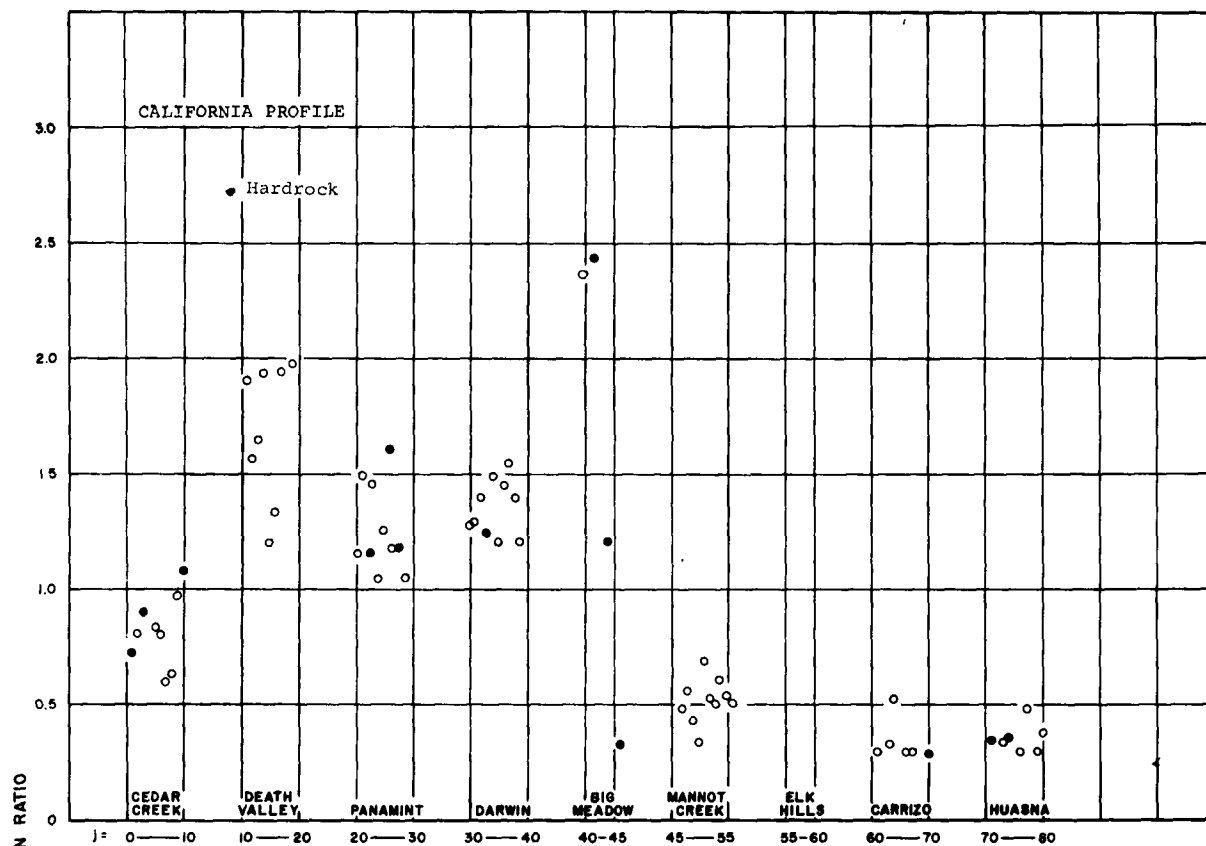


Figure 1.1.4.1

## 2. Areas Surveyed

This section describes the most important features along each of the three profiles studied. Detailed descriptions of individual stations are given in Appendix 6.1, 6.2 and 6.3.

### 2.1 The California Profile

#### 2.1.1 General Description

The California profile consisted of ten stations, at intervals of about 30 km, running in a line South 63° West from Death Valley to a point just north of Point Arguello on the Pacific Coast (Figure 2.1.1). The profile was perpendicular to the coastline and to all major structural trends in the area. Geologic and topographic conditions at California stations were generally more varied (9b) than those found at stations on the Pacific Northwest and Appalachian profiles, but weather conditions were generally much more stable than in the latter two areas of study.

The western limit of the Sierra Nevada mountains separated the stations of the California profile into two broad categories (Figures 2.1.2, 2.1.3 and 2.1.4). Stations west of this limit were all located on relatively thick sections of Mesozoic and Tertiary sediments (9b, 26b); the topography was flat to moderate, depending on structural complexity. Main geographic features were the broad San Joaquin Valley and the Coast Range mountains, with a major active fault zone, the San Andreas, running between the two. At these stations seismic noise level and signal reception strength were high and S/N ratios low.

Stations located in and east of the Sierra Nevada were in an older, mountainous region of batholithic granite and relatively thin Paleozoic sediments (18b). The mountains of the Sierra Nevada themselves are granitic and increase in both elevation and ruggedness eastward from the San Joaquin Valley. The eastern slope of the range is a large steep escarpment beyond which lie block-faulted Paleozoic sediments of the Basin and Range province, where the profile ends. At these eastern California stations seismic signal reception strength was low, noise level even lower, while S/N ratios were relatively higher than at the stations in thick young sediments west of the Sierra Nevada.

Bouguer gravity along the California profile (20b) is shown in Figure 2.1.5. When the negative eastward trend is removed, the locations of relative maxima correspond roughly to locations of stations where signal strength reception is relatively high. Mannot Creek station where signal strength is highest of all, is located over a relative maximum which runs the full length of the Great Valley (14b, 19b, 33b).

### 2.1.2 Selection of Locations for Signal and Noise Recording

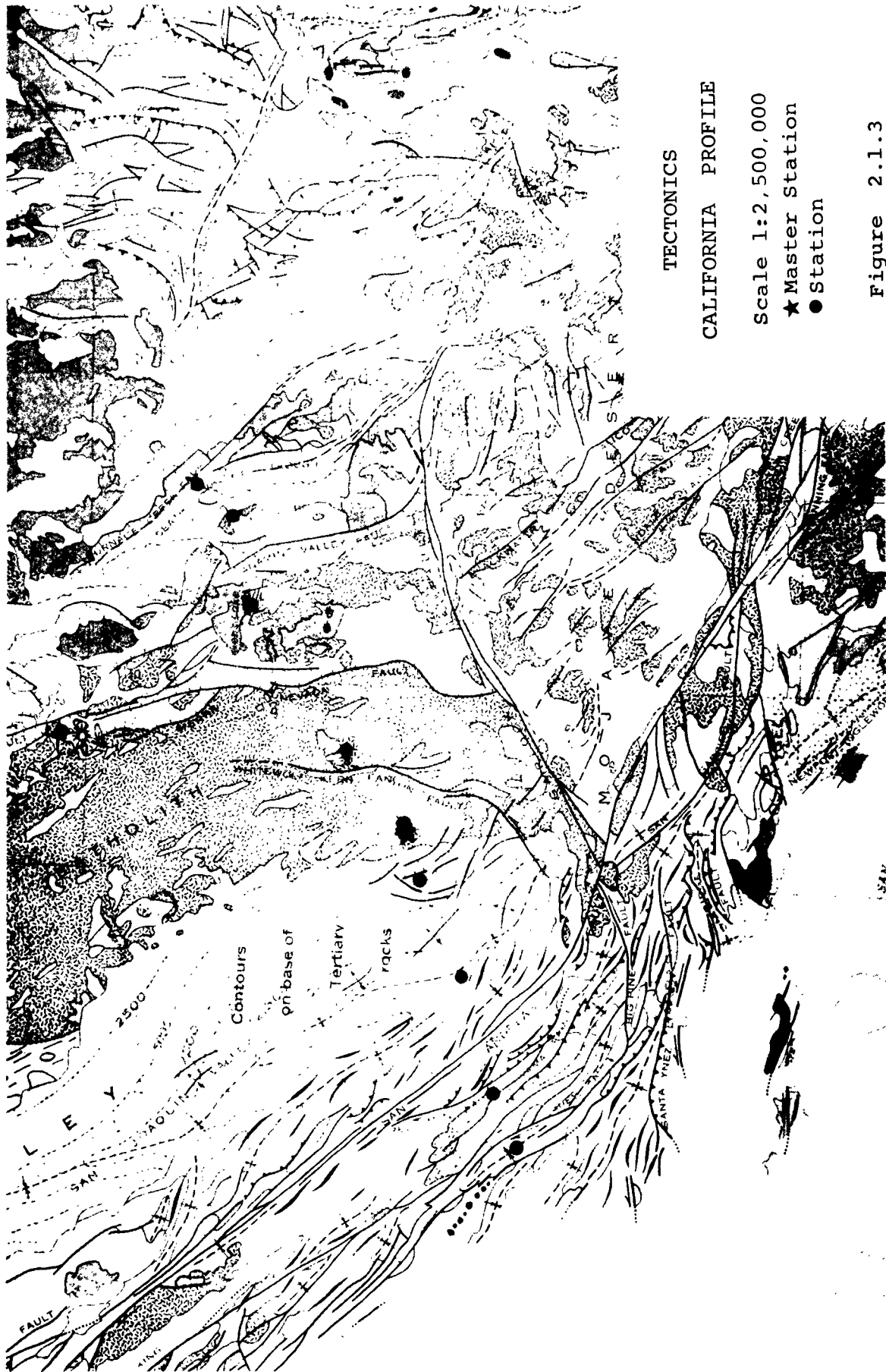
The master station was located on the granite of the western slope of the Sierra Nevada, in order to provide reference-level noise and signal recording in a quiet area within reasonable distance of the field analysis center in Bakersfield. Specific slave station locations were selected for representative geology and maximum possible remoteness from cultural noise sources. All the stations in the mountainous eastern part of the state were located at long distances from cultural noise, but those in the more densely populated western part of the state were more susceptible to contamination by noise from cities, railroads and oilfields. Indeed, one station in the San Joaquin Valley, Elk Hills, was occupied only briefly and abandoned because of large amplitude, high frequency noise, probably due to nearby oilfield operations.

At least one station was located in each geologic-topographic province. Huasna and Carrizo stations were in the Coast Range province of complexly folded and faulted Cretaceous and Tertiary sediments. The Elk Hills and Mannot Creek stations were in the deep, asymmetric Tertiary basin of the San Joaquin Valley, Elk Hills near its deepest part and Mannot Creek near its eastern border. The Round Mountain master station and the Cedar Creek and Big meadow slave stations were located on the Jurassic granite of the Sierra Nevada batholith, while the Darwin, Panamint and Death Valley stations were in the complex horst and graben structure of the Basin and Range province.



Figure 2.1.1





# TECTONICS

## CALIFORNIA PROFILE

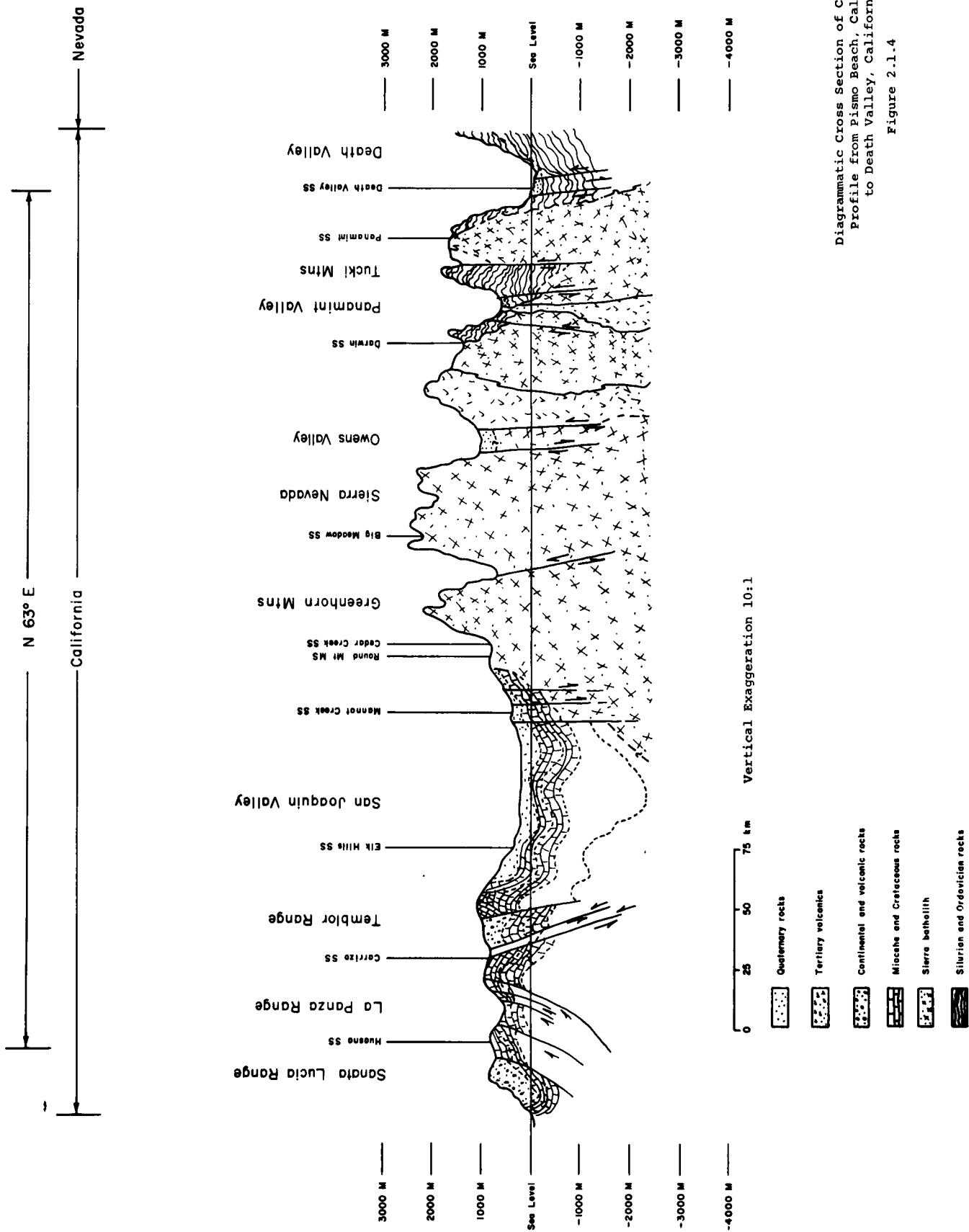
Scale 1:2,500,000

★ Master Station

● Station

Figure 2.1.3





Diagrammatic Cross Section of California  
Profile from Pismo Beach, California  
to Death Valley, California.

Figure 2.1.4

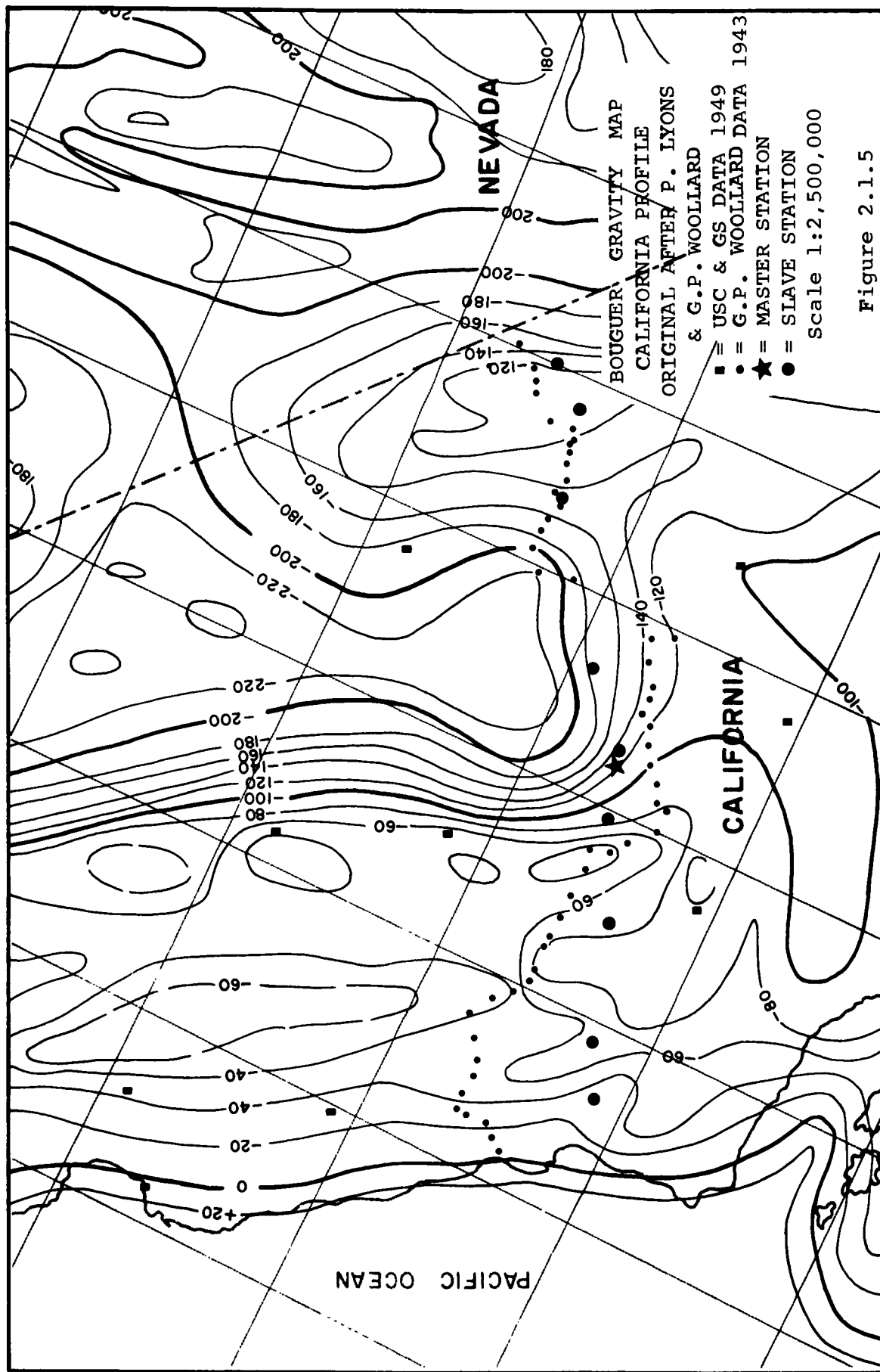


Figure 2.1.5

CALIFORNIA LINE STATION LOCATIONS

<u>STATION &amp; ELEVATION</u>	<u>INCLUSIVE REEL TIME</u>	<u>INCLUSIVE DATES</u>	<u>GEOGRAPHIC COORDINATES</u>	<u>TOPOGRAPHIC SHEETS</u>
Cedar Creek 2630'	SS 61 107 2140- 124 1600	4/17/61 5/15/61	35°40.5'N. 118°44.0'W.	Glennville, 1956
Death Valley -260'	SS 61 135 1752- 153 1900	5/24/61 6/2/61	36°34.0'N. 116°59.0'W.	Cloride Cliff, 1952
Panamint 5280'	SS 61 163 1803- 188 1900	6/12/61 7/7/61	36°24.25'N. 117°08.25'W.	Emigrant Canyon, 1952
Darwin 5120'	SS 61 194 1830- 213 1800	7/13/61 8/1/61	36°19.0'N. 117°37.0'W.	Darwin, 1950
Big Meadow 7750'	SS 61 222 1643- 233 2034	8/10/61 8/21/61	35°53.0'N. 118°20.25'W.	Kernville, 1956
Mannot Creek 1050'	SS 61 243 0030- 264 1730	8/31/61 9/21/61	35°35.5'N. 119°00.42'W.	Slater, 1942
Elk Hills 295'	SS 61 270 2130- 277 1545	9/27/61 10/4/61	35°22.0'N. 119°30.33'W.	West Elk Hills, 1937
Carrizo 1830'	SS 61 283 1632- 298 1730	10/10/61 10/25/61	35°14.08'N. 120°03.42'W.	Branch Mountain, 1952
Huasna River 1090'	SS 61 300 1919- 314 1700	10/28/61 11/10/61	35°08.0'N. 120°22.6'W.	Nipomo, 1952
Round Mountain Master Station 3280'	SS 61 107 2100- 314 1700	4/17/61 11/10/61	35°39.37'N. 118°46.0'W.	Woody, 1952

## 2.2 The Pacific Northwest Profile

### 2.2.1 General Description

The second profile selected for signal and noise studies was across the Pacific Northwest, where thick basaltic plateaus of central Oregon and Washington are flanked on the east by rugged inland granitic mountains and on the west by complex mountains of the Cascade and Coast Ranges (21 b, 36 b). The profile line of eight stations extended from Gray's Harbor on the Pacific Coast of Washington southeasterly to the Blue Mountains in northeastern Oregon.

Variations in meteorological conditions here are much more pronounced than on the California profile. In the Columbia basin, temperatures vary from -20°F in winter to the 90's in summer, and wind speeds of 25 knots are common in winter. Increases in wind speed are accompanied by large increases in noise level, much more than was noticed during recording in the milder and relatively unvarying weather along the California profile.

Geologic structure in the Pacific Northwest is generally less well known than that of California where commercial petroleum and mining development has contributed much to geologic literature. Thick lava flows in basins and heavy rainfall and dense forests in the mountains combine to make detailed geologic studies difficult in the Pacific Northwest (11 b). Although a number of relatively shallow wells have been drilled in Washington, only one provided information about sediments or rock under the basalt. A 1960 well about 160 km north of Paterson encountered sedimentary rocks below 1500 meters. Closer to the profile, a 1957 well near Paterson was stopped at 3000 meters while still drilling in basalt (32 b).

The relation of the Pacific Northwest profile to the regional geology of the Pacific Northwest is illustrated in Figures 2.2.1 through 2.2.5. The Pacific Northwest profile extended from the Tertiary sediments across the Puget Sound-Willamette trough, through the Cascade Mountains south of Mount Rainier, and across the Columbia basaltic plateau into the granite outcrop area in the Blue and Wallowa Mountains of Oregon.

### 2.2.2 Selection of Locations for Signal and Noise Recording

Station sites were selected along the profile line in each of the geomorphic provinces. From west to east these provinces are the coastal Tertiary province, the Puget Sound-Willamette trough (which is both a structural trough and the axis line of late Tertiary and Quaternary volcanism), the Columbia River Basin (22 b), the basaltic Blue Mountains, and the granitoid Wallowa Mountains (Figure 2.2.1).

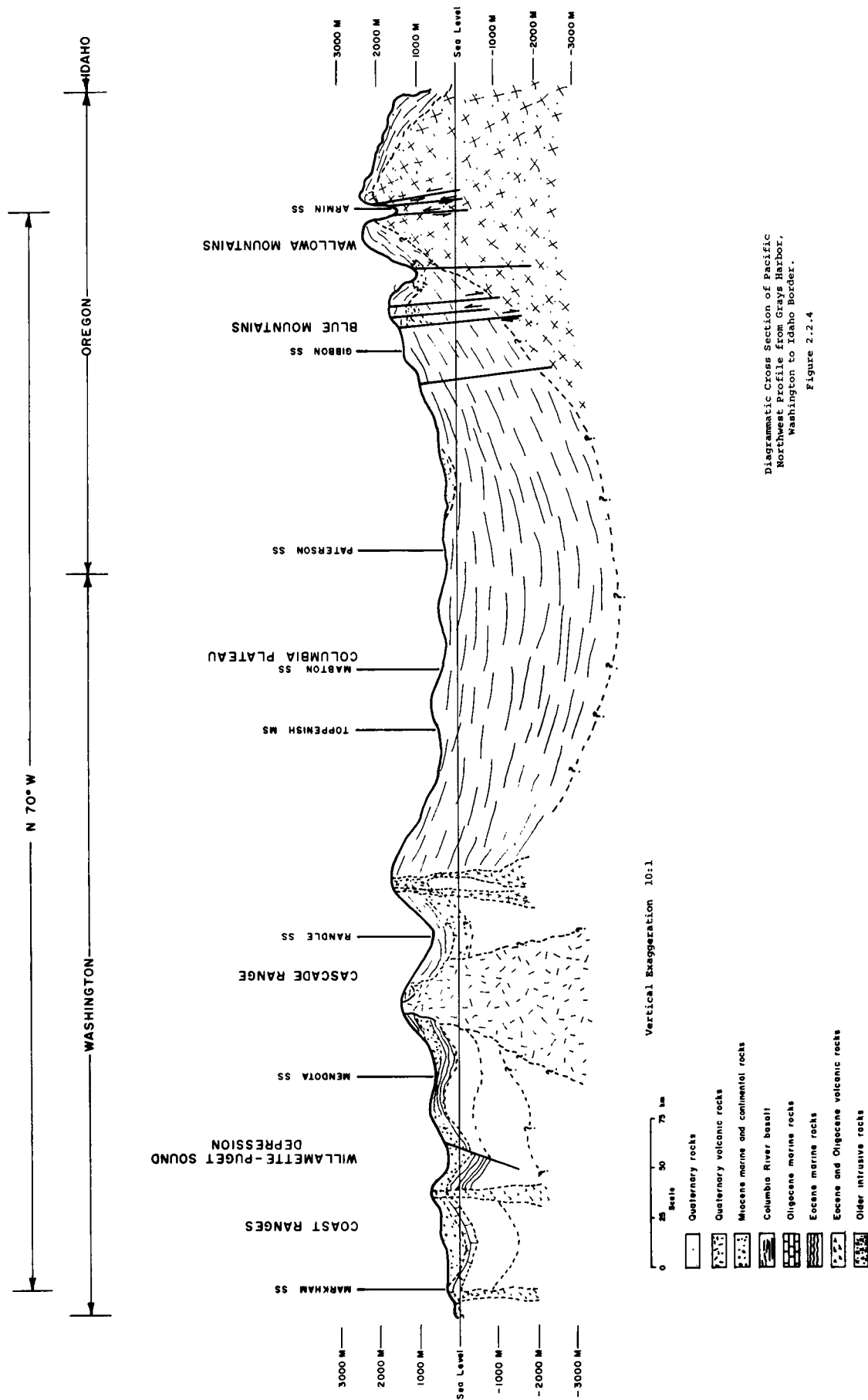
Markham slave station was on Tertiary marine sediments surrounded by Quaternary terraces of unconsolidated sand and glacial till. Mendota (29 b) and Randle (7 b) were located in the western and central Cascade Range, respectively, in Tertiary volcanics. The master station at Toppenish Ridge was on the topographic east slope of the Cascades about 65 kilometers west of the topographic axis of the Columbia River basin. Toppenish Ridge, Mabton and Paterson station sites were located to occupy the apex, the steep north flank and the south slope, respectively, of the easterly-trending ridge topography of south-central Washington. The Gibbon and Arnim slave station sites were both in the Blue Mountains; Gibbon in an area of loess and basaltic layers on top of granite, and Arnim as the only station in the profile on granite.











Diagrammatic Cross Section of Pacific Northwest Profile from Grays Harbor, Washington to Idaho Border.

Figure 2.2.4

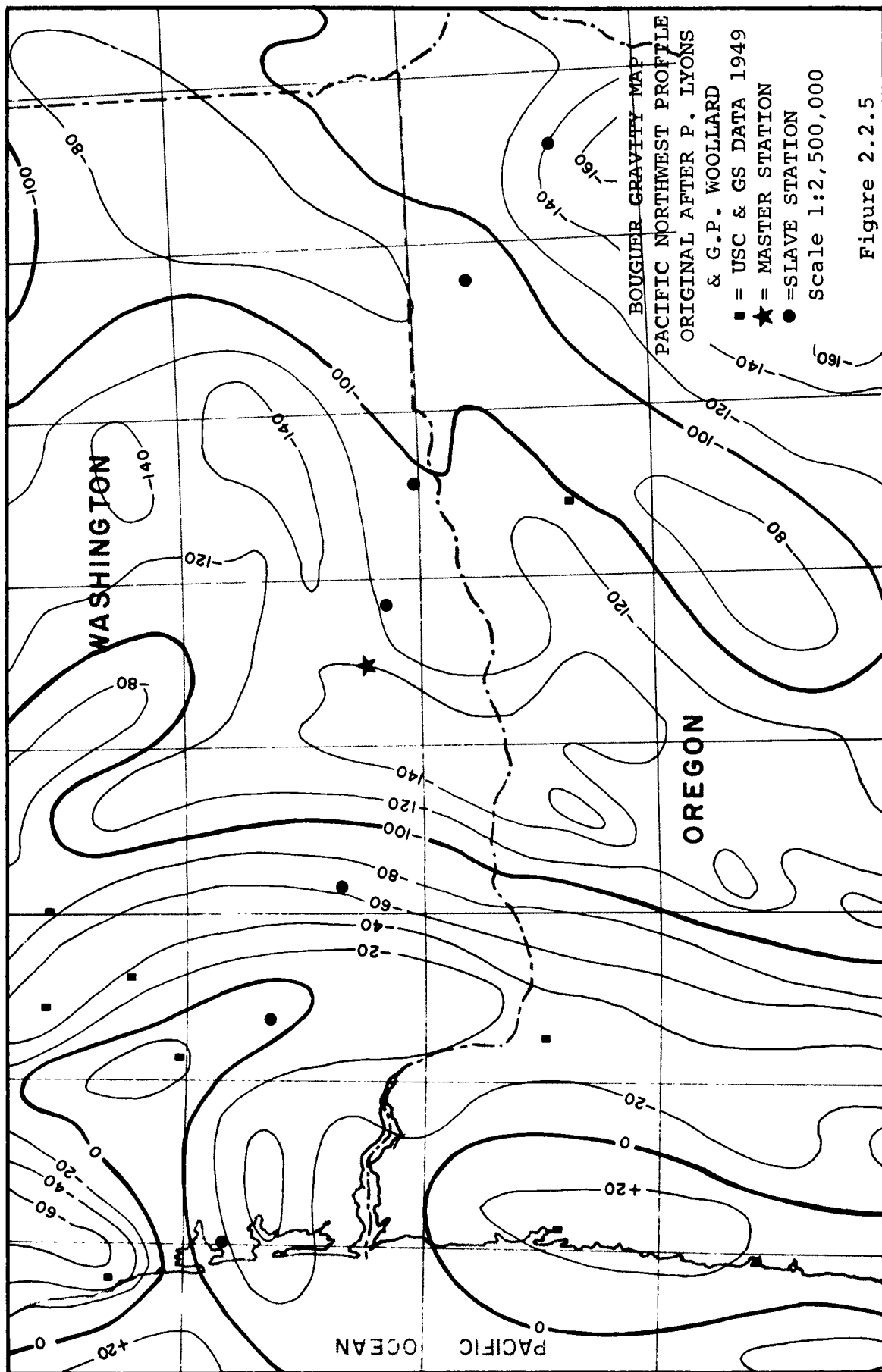


Figure 2.2.5

PACIFIC NORTHWEST LINE STATION LOCATIONS

<u>STATION &amp; ELEVATION</u>	<u>INCLUSIVE REEL TIME</u>	<u>INCLUSIVE DATES</u>	<u>GEOGRAPHIC COORDINATES</u>	<u>TOPOGRAPHIC SHEETS</u>
Toppenish Ridge 1680'	SS 61 333 1856- 338 1720	11/29/61 12/2/61	46°15.8'N. 120°31.0'W.	White Swan, Wash. 1937
Mabton 1060'	SS 61 341 2105- 357 1830	12/7/61 12/22/61	46°09.2'N. 120°09.7'W.	Zillah, Wash. 1910
Paterson 1070'	SS 62 008 1940- 031 1800	1/8/62 1/31/62	46°01.9'N. 119°26.2'W.	Pasco, Wash. 1917
Gibbon 4220'	SS 62 039 0505- 058 1800	2/8/62 2/27/62	45°48.3'N. 118°10.7'W.	Pendleton, Ore. 1:250,000
Markham 265'	SS 62 067 0917- 082 1800	3/8/62 3/23/62	46°51.1'N. 123°58.3'W.	Aberdeen, Wash. 1937
Mendota 1800'	SS 62 087 1700- 101 1800	3/29/62 4/6/62	46°39.7'N. 122°38.0'W.	Onalaska, Wash. 1954
Randle 2600'	SS 62 108 1800- 121 1700	4/18/62 5/1/62	46°21.0'N. 121°51.1'W.	Steamboat Mtn., Wash. - 1926
Armin 4300'	SS 62 129 1830- 135 1800	5/9/62 5/15/62	45°23.8'N. 117°25.7'W.	Enterprise, Ore. - 1957
Toppenish Ridge Master Station 1680'	MS 61 333 2350 62 135 2040	11/24/62 5/15/62	46°15.8'N. 120°31.0'W.	White Swan, Wash. 1937

## 2.3 The Appalachian Profile

### 2.3.1 General Description

The Appalachian Mountains system in the area of the profile may be divided into six major tectonic-geomorphic divisions. From the interior to the coast, these regions are the Appalachian Plateau, New Appalachian Mountains, Blue Ridge Mountains, Triassic Low Lands, Piedmont (16 b), and Coastal Plains (17 b). These provinces in West Virginia and Virginia constitute an old disturbed boundary zone separating relatively undisturbed sediments west of the Appalachian Mountains from younger coastal marine sediments (15 b).

The Appalachian Plateau is divided into two major provinces with an arbitrary boundary separating the Allegheny Plateau to the north from the Cumberland Plateau to the south. The synclinal, broad, and gentle basin has Permian Dunkard rocks at the surface with the edges exposing progressively younger formations north to Pottsville, Pennsylvania, where the youngest formation of the Allegheny area is found. The Cumberland Plateau to the south is an area of nearly flat-lying, less dissected sediments.

Folded and thrust-faulted Paleozoic strata are identified with the New Appalachian Mountains, characterized by parallel ridges and valleys. The Paleozoic rocks are thicker in this area, but thin out to the west as the interior of the continent is approached.

Cambrian and late and early Pre-Cambrian metamorphic and igneous rocks are folded and thrust-faulted toward the Appalachians to form the Blue Ridge Mountains. This major element forms a province of conspicuous relief east of the Great Valley and west of the crystalline Piedmont.

A broad, low-relief area of metamorphic Pre-Cambrian and Paleozoic crystalline rocks and volcanics comprises the Piedmont province. The contact of the Piedmont is sharply defined along the Blue Ridge Mountains and adjacent to the Appalachian Mountains in Pennsylvania.

Within this Piedmont province is a major rift zone, where the down-faulted blocks have formed traps for the sandstones and shales of Triassic age. These sediments, cut by dikes and sills of the same age, rest unconformably on older rocks of the Piedmont, Blue Ridge Mountains and the Appalachian Mountains.

The last major geomorphic province is the Coastal Plain (17 b), where Cretaceous and Tertiary sediments rest unconformably on the older Paleozoic and Pre-Cambrian rocks of the Piedmont, thickening as they extend toward the continental margin. Thickness of Coastal Plain sediments exceeds 3000 meters at Bodie Island Station.

### 2.3.2 Selection of Locations for Signal and Noise Recording

Locations along the Appalachian profile were selected to put one station in the Allegheny Plateau province (Birch River), one in the Appalachian Mountains (Warm Springs), one in the Blue Ridge Mountains (Buena Vista), and two in the Piedmont province (Farmville and Rawlings). Four stations were located in the Atlantic Coastal Plain (Franklin, Belvidere, Weeksville and Bodie Island) because of the progressive seaward thickening of sediments.

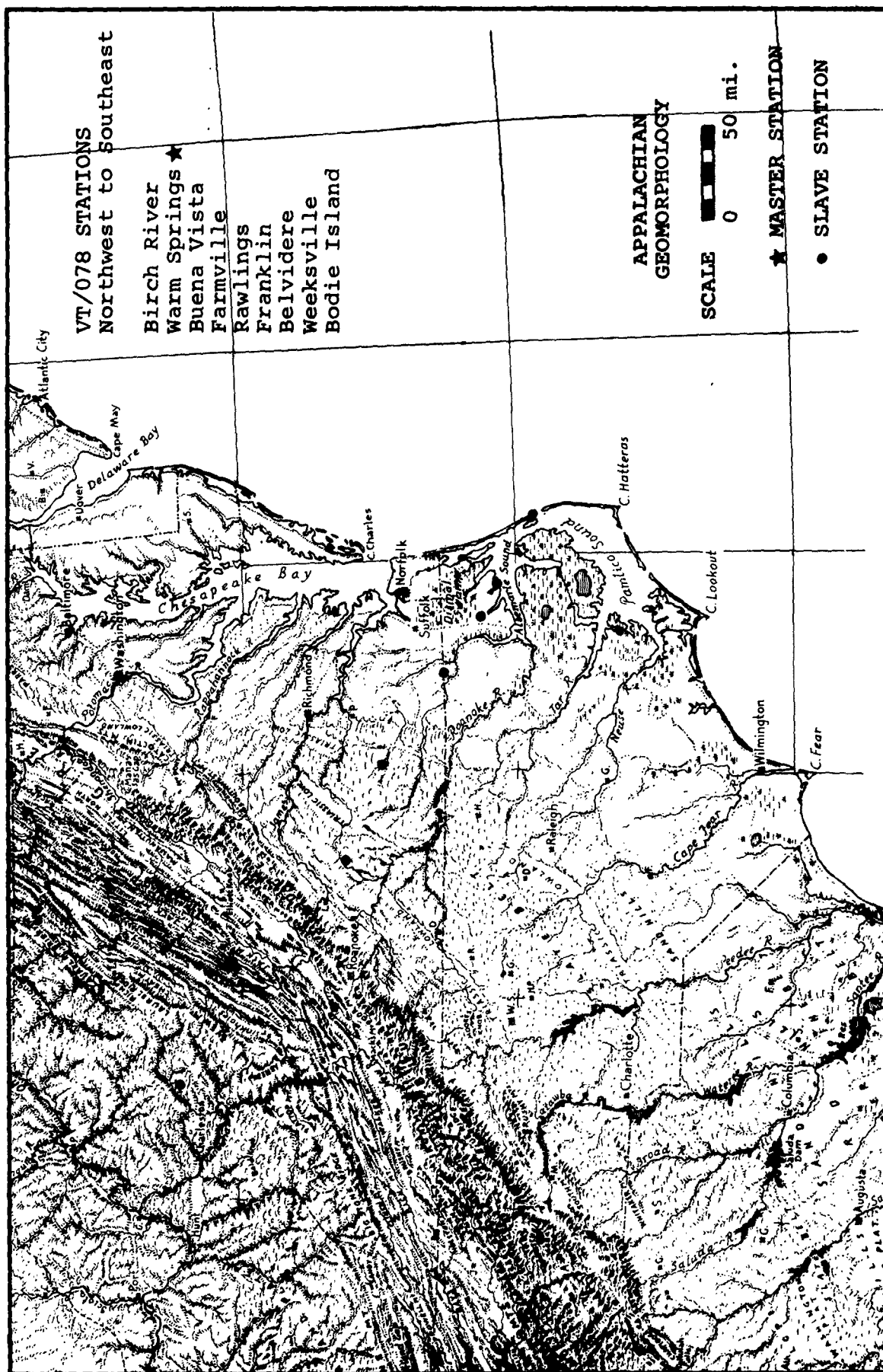
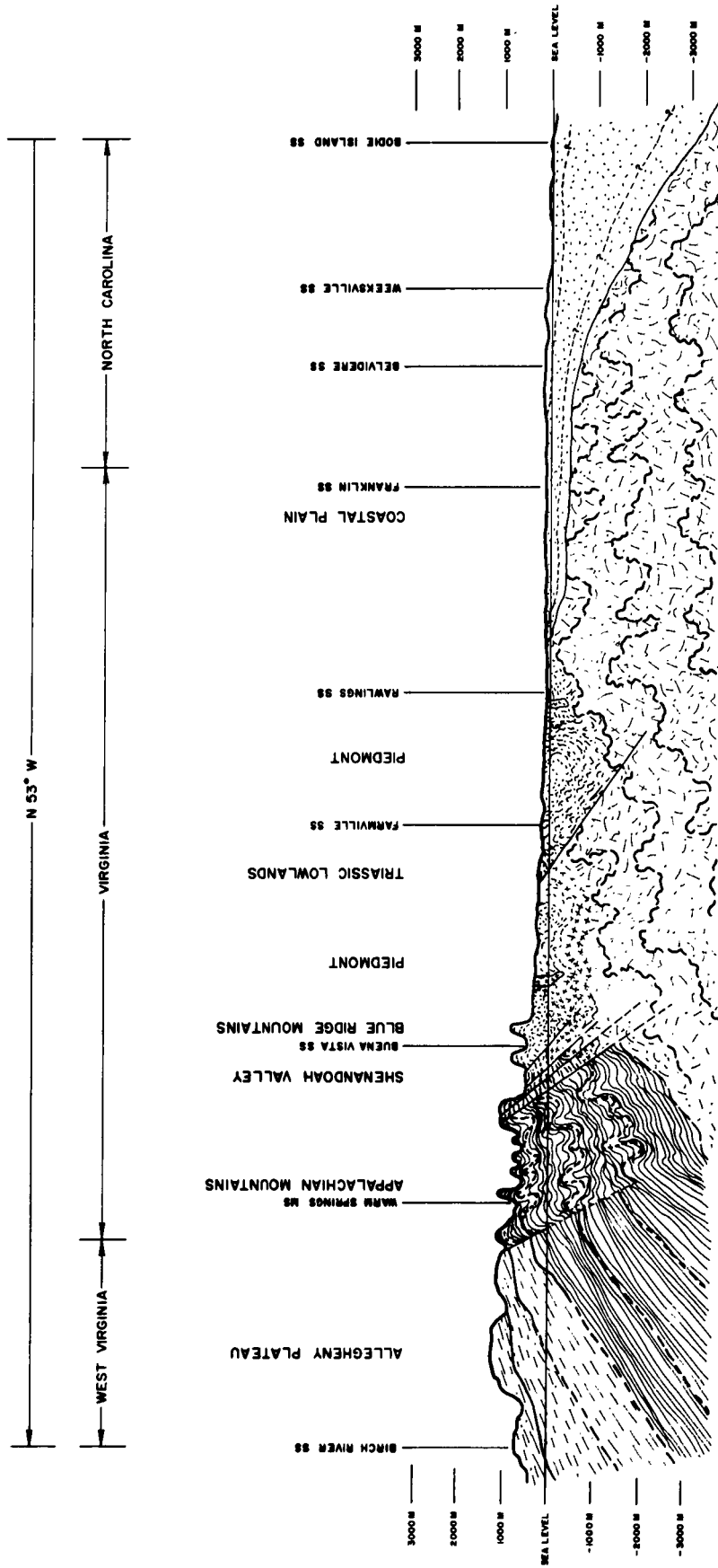


Figure 2.3.1









Diagrammatic Cross Section of Appalachian Profile from Birch River, West Virginia to Bodie Island, North Carolina.

Figure 2.3.4

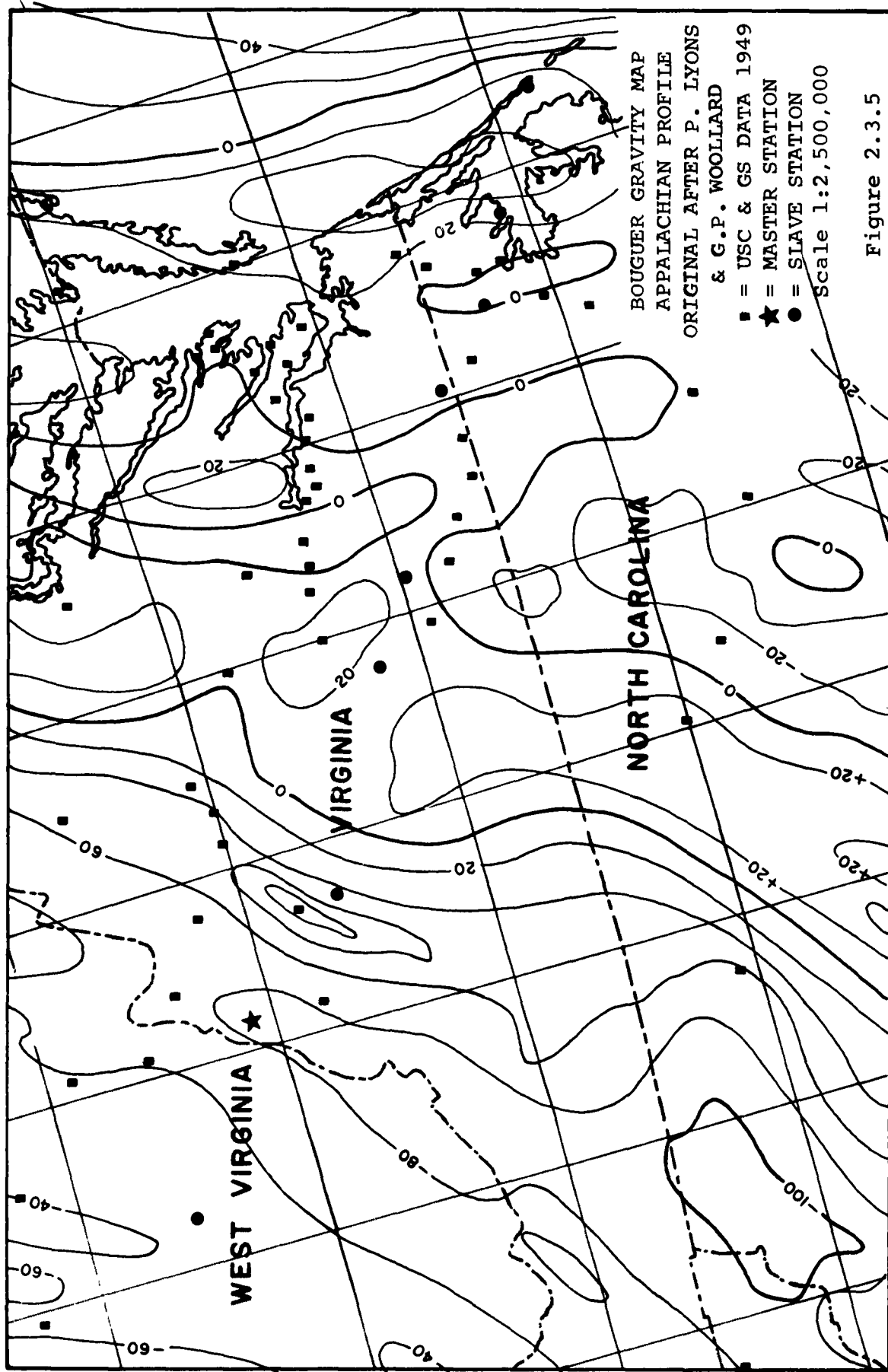


Figure 2.3.5

# APPALACHIAN LINE STATION LOCATIONS

<u>STATION &amp; ELEVATION</u>	<u>INCLUSIVE REEL TIME</u>	<u>INCLUSIVE DATES</u>	<u>GEOGRAPHIC COORDINATES</u>	<u>TOPOGRAPHIC SHEETS</u>
Birch River 1500'	SS 62 211 2024 214 1600	7/30/62 8/2/62	38°31.6'N. 80°46.3'W.	Gassaway, W. Va. 1910-51
Warm Springs 1800'	MS 62 164 1835 264 1700	6/13/62 9/21/62	38°06.5'N. 79°48.7'W.	Warm Springs, Va. 1923-45
Buena Vista 1000'	SS 62 198 1545 205 1410	7/17/62 7/24/62	37°36.7'N. 79°18.9'W.	Buena Vista, Va. 1935-50
Farmville 400'	SS 62 187 1540 191 1800	7/6/62 7/10/62	37°11.5'N. 78°23.7'W.	Keysville, Va. 1958
Rawlings 300'	SS 62 162 2000 173 1320	6/11/62 6/22/62	36°58' N. 77°49.5'W.	Lawrenceville, Va. - 1918
Franklin 20'	SS 62 225 1610 229 1600	8/13/62 8/17/62	36°35.3'N. 76°57.3'W.	Holland, Va. 1918-57
Belvidere 10'	SS 62 235 1640 240 1600	8/23/62 8/28/62	36°18.3'N. 76°31.6'W.	Beckford, N.C. 1906-40
Weeksville 0	SS 62 247 2134 249 1800	9/4/62 9/6/62	36°07.9'N. 76°10.5'W.	Wade Point, N.C. 1940
Bodie Island - 0	SS 62 260 1620 264 1700	9/17/62 9/21/62	35°49.8'N. 75°33.7'W.	Oregon Inlet, N.C. - 1953

### 3. Field Operations

Field operations were centered on controlled recording of seismic signal and noise at selected locations on each profile under study. The fixed master array was set up in a central location and temporary slave arrays were consecutively occupied on a line across the study area. Slave station locations were chosen to represent various geologic-geographic conditions typical of the regions. Because recordings at the slave stations were made simultaneously with recordings at the fixed master station, the latter recordings provided a standard for measuring changes in seismic characteristics among slave stations.

#### 3.1 Field Instruments and Equipment

Master and slave station equipment were essentially identical (Figure 3.1.0). At both stations it included long and short-period vertical seismometers, weather recording gear, recording systems for both magnetic tape and film; and support equipment. General views of recording equipment are shown in Figures 3.1.1 and 3.1.2. One man operated the master station, while two were assigned to the mobile slave station.

##### 3.1.1 Short Period Instrumentation

###### 3.1.1.1 Seismometers

Short period noise from 0.2 to 20 cps was recorded at each station by a tripartite array of four Johnson-Matheson Model 6480 vertical-component, moving-coil seismometers. This seismometer is a hermetically sealed, rugged and stable instrument, weighing about 80 pounds (Figure 3.1.3). Its free period is 1.25 seconds. Its response to constant driving velocity is nearly flat above 2 cps, falling off at about 14 db per octave below 1 cps (Figure 3.1.2.2.1). All eight of these seismometers maintained essentially identical performance throughout the study, except for a short period of operation in Death Valley, when No. 5 seismometer behaved abnormally because of a small piece of lint lodged inside the case between mass and frame. The flat velocity response of this seismometer enables it to record much of the noise velocity spectrum with little distortion. Its ability to operate for long periods without frequent adjustment makes it ideal for temporary field recordings where the seismometer is inaccessible for long periods because of its burial.

###### 3.1.1.2 Short Period Amplifiers

The seismometer was operated with a UED, Model CJ-40, solid-state amplifier (Figure 3.1.4), having voltage gain of about  $1 \times 10^6$  at 0 db attenuation. Choice of this amplifier over





Figure 3.1.1 Master Station Instrument Van, Pickup, and Generator



Figure 3.1.2 General View of the Field Recording System  
Calibration and timing equipment at left, tape  
recorder in center, develocorder at right.

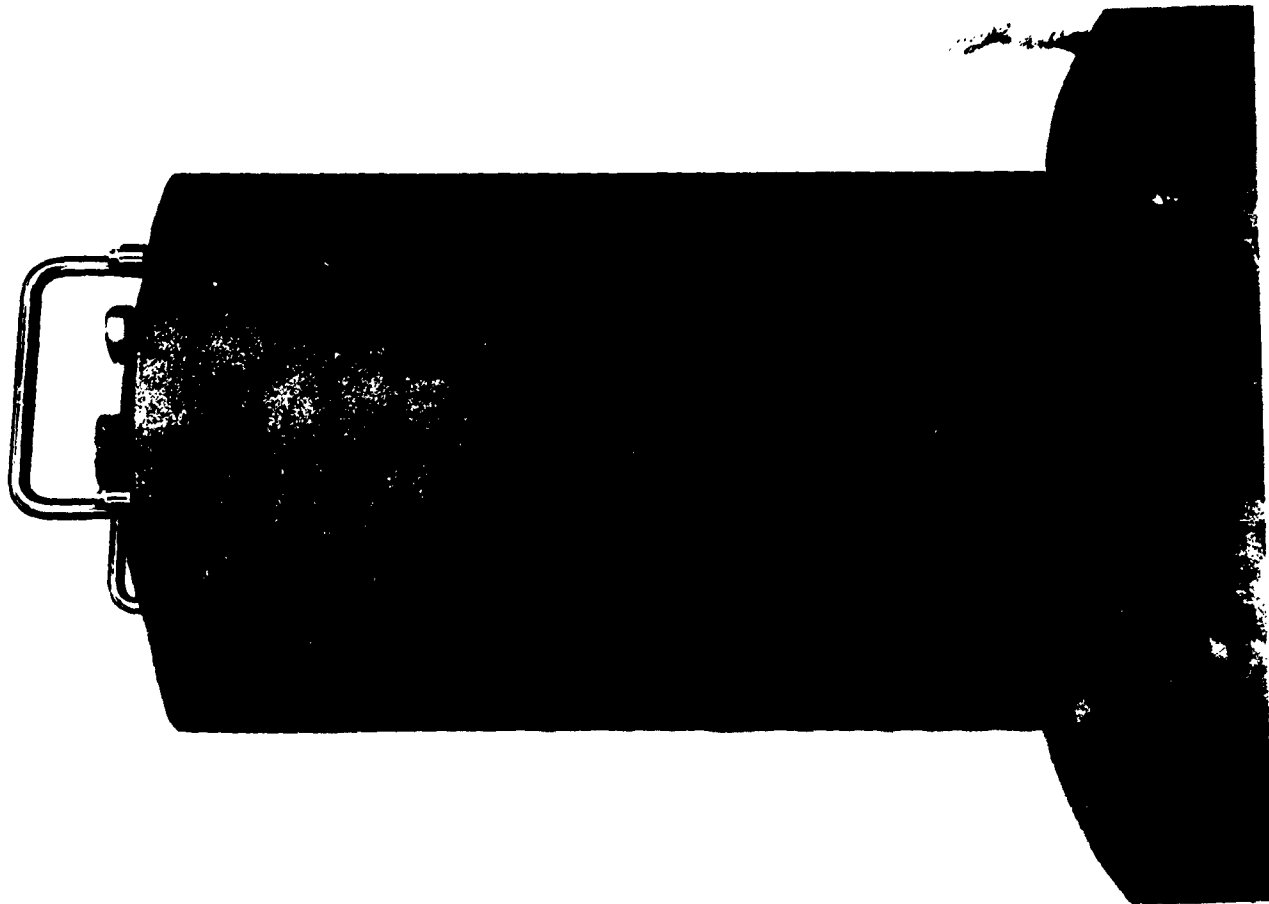


Figure 3.1.3 J-M Short Period Seismometer With and Without Case



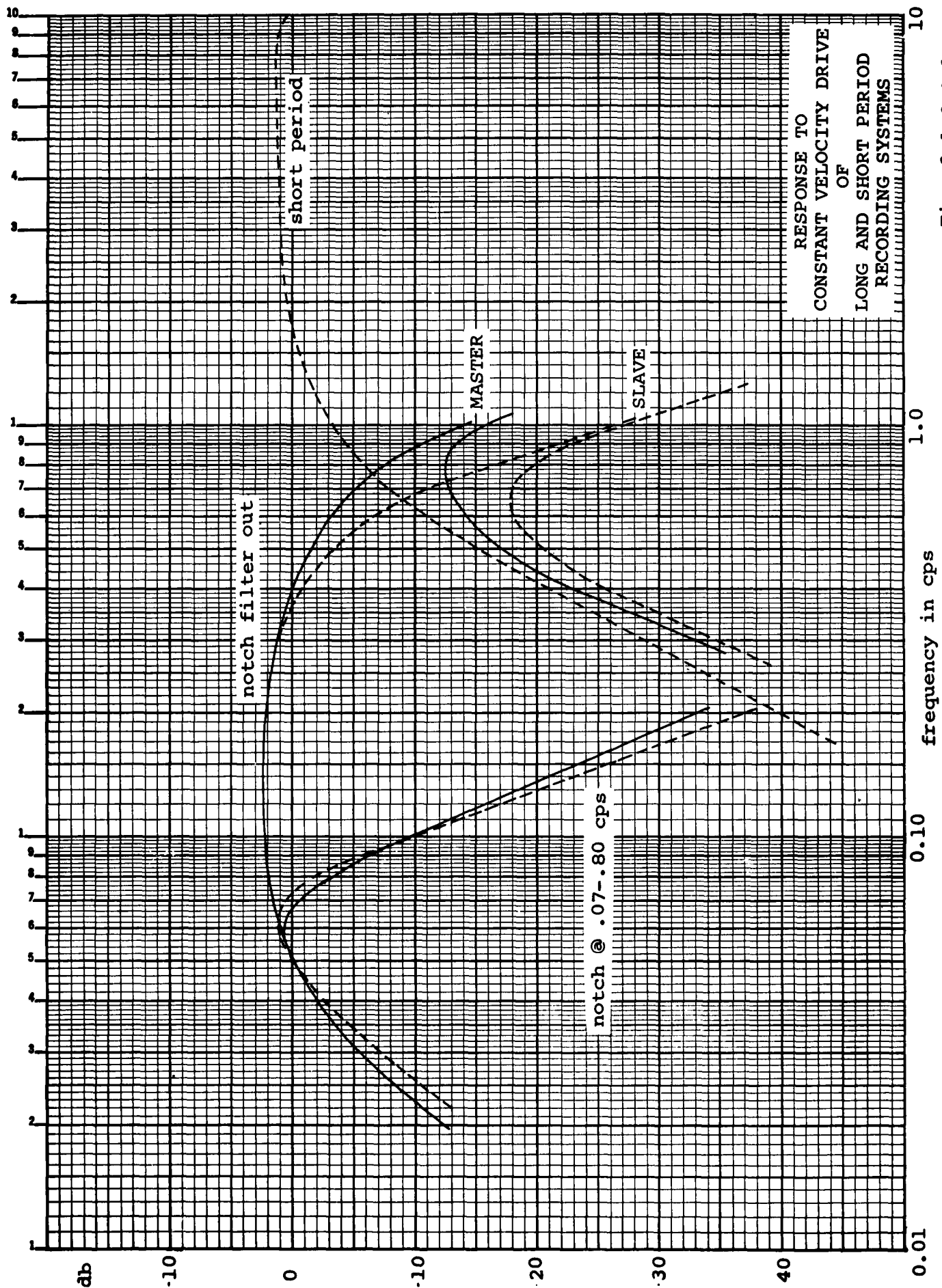
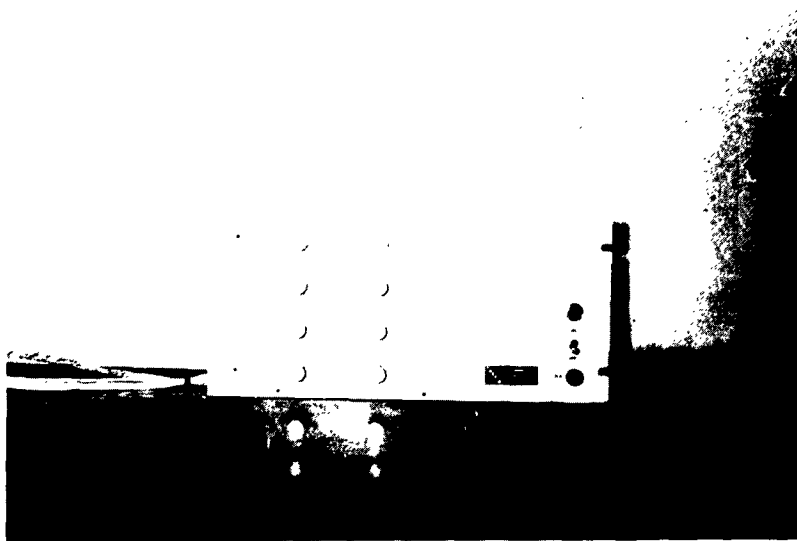


Fig. 3.1.2.2.1



Front View of Short-Period Solid-State Amplifiers



Rear View of Short-Period Amplifiers

Figure 3.1.4

photo-tube types was based on gain requirements as well as need for an amplifier which would operate effectively at frequently changed locations and various recording conditions. Sensitivity of the Johnson-Matheson seismometer is about 0.19 mv p-p per micron/sec at 1.0 cps and 0.675 critical damping (18a). Its output in response to minimal Brune and Oliver earth velocities of  $2.5 \times 10^{-3}$  microns/sec would be  $0.475 \times 10^{-3}$  mv p-p, or  $0.17 \times 10^{-3}$  mv rms. It was sought to center this expected minimal signal in the 55 db dynamic range of the tape system, whose full-scale-deflection input is 1 v rms, and whose "center" at -14 db corresponds to about 0.2 v rms input. To get this input from a  $0.17 \times 10^{-3}$  mv rms seismometer output requires an amplifier with voltage gain of about  $1.2 \times 10^6$ . The nominal gain of the Geotech Model 4300 Photo-tube Amplifier is  $0.25 \times 10^6$ .

Laboratory findings that use of an input transformer would substantially reduce amplifier noise were confirmed by field tests conducted in July 1961. Accordingly, master station channels Nos. 4 and 5 were modified at that time, but no change was made in the other two master station short-period channels or in the slave system until the end of recording on the California profile. All short period amplifiers were modified by the addition of input transformers for recording in the Pacific Northwest, beginning 29 November, 1961. System noise is shown on the same scale as seismic noise in figure 3.1.1.2.1.

#### 3.1.1.3 Tape Recording System

An FM tape system is required for effective analysis of seismic noise and signal. This is the only recording format which allows signal to be played back for analysis and which has sufficient range to record with fidelity over the wide area of amplitudes and frequencies of seismic noise and signal. Primary recording of all data in this report was made by the Minneapolis-Honeywell Model 3173 tape recording system (Figure 3.1.5). Dynamic range, from system noise to full-scale deflection, of the system is 55 db; this encompasses 30 db of seismic noise velocity variation indicated by Brune and Oliver data, plus another 25 db for signal. Flutter compensation was provided by recording a crystal-controlled standard frequency on one channel. Variations in this standard frequency, caused by flutter in the transport system, provided a compensation signal which was subtracted from the flutter-distorted data signals during play-back.

Normal data recording speed was 0.6 inches per second, with other speeds available. This speed allowed 24 hours of continuous recording on a single 5000 foot reel of tape. By playing back these reels at one hundred times real time, or 60 inches per second, low frequency data was shifted into higher frequency range, where it could be processed by

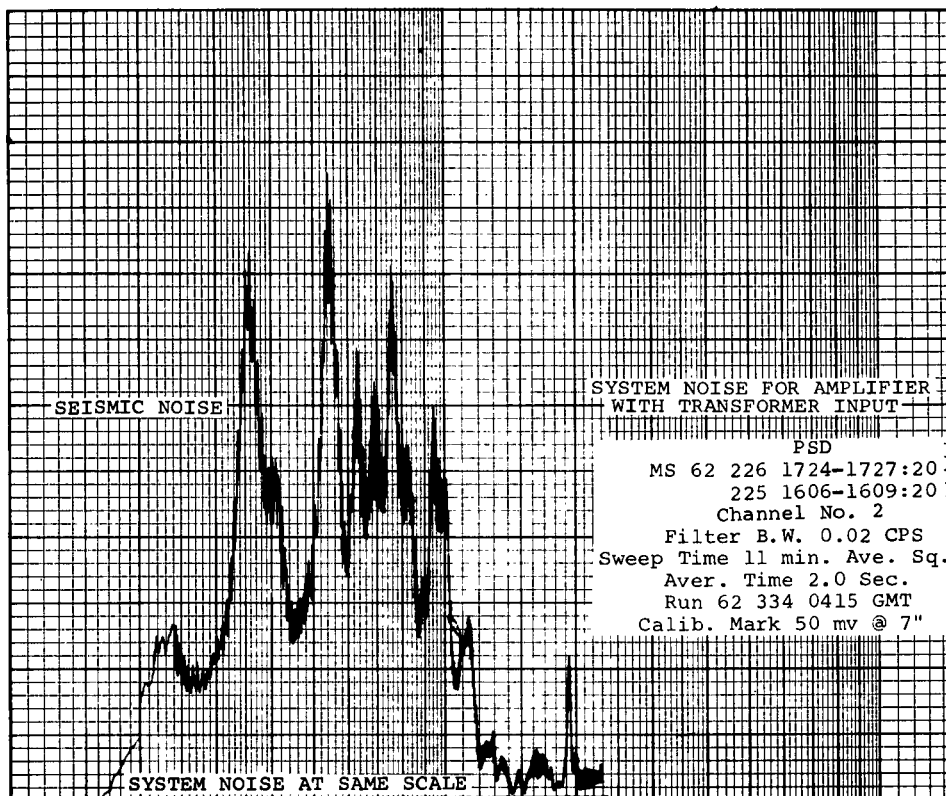


Figure 3.1.1.2.1a

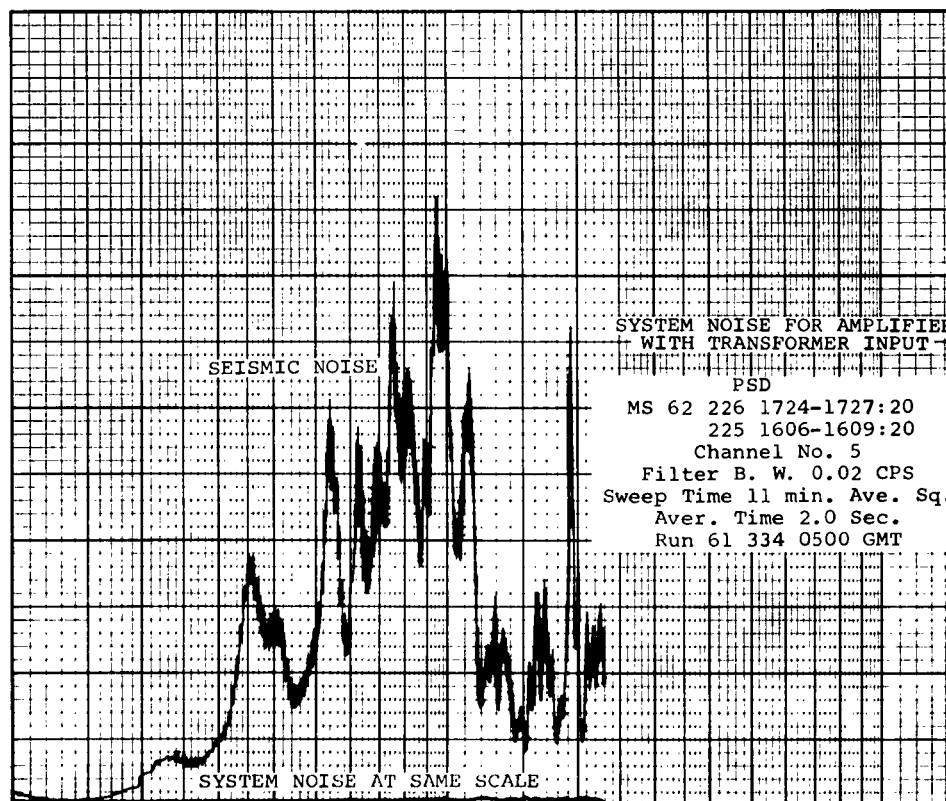


Fig. 3.1.1.2.1b

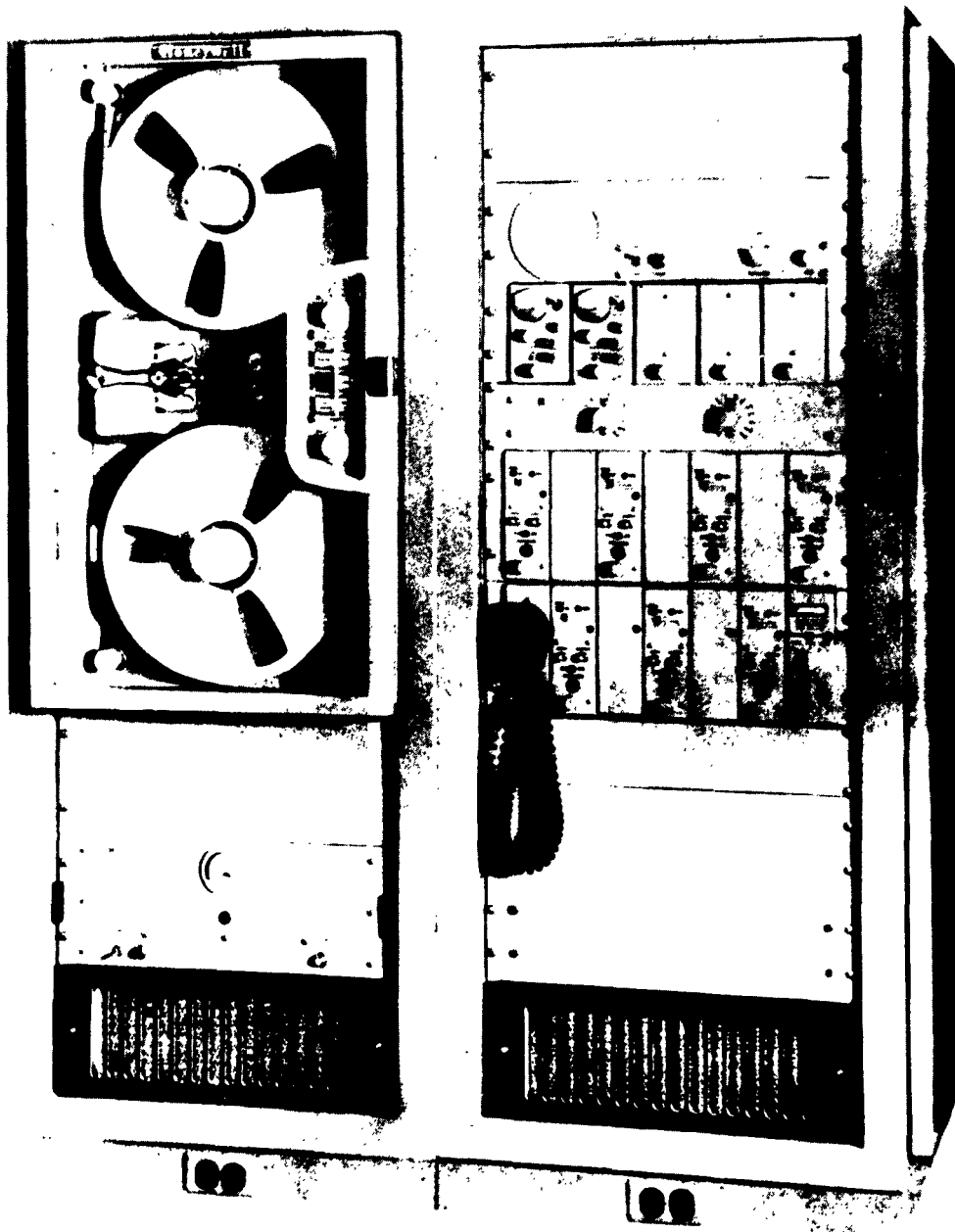


Figure 3.1.5 Tape Recording System, Master and Slave Station  
Minneapolis-Honeywell model 3173 tape  
recorder used in field recording systems.

spectrum analyzers not intended to handle data below 2 cps. The 100:1 increase in playback speed also reduced processing time.

Recording and playback heads conformed to IRIG specifications, with 14 tracks per inch. Nine of these were used in data recording.

Reeves Soundcraft magnetic tape, Type ITM 50 - 1.5, was selected for use on the project. This is 1 inch, 1.5 mil base, type A oxide tape, in 5000 foot reels of 14 inch diameter. Two other brands of the same price were tried and tested for relative signal-to-noise ratios, but the Reeves product proved slightly better than the other two. The 1.5 mil base was selected over 1 mil because of its greater strength. Type A oxide (standard grain) was chosen over type B (fine grain) because it provided essentially equivalent playback output at seismic frequencies, at lower cost.

#### 3.1.1.4 Film Recording System

Calibration and seismic data were recorded on 16mm film, as well as on magnetic tape, to permit immediate monitoring and quality control of data, preliminary data analysis, and sample selection without use of special FM equipment. The film recording was done on a Geotech Model 4000 Develocorder, using 16 cps galvanometers. This instrument provided continuous display at 10x magnification, of data being recorded on all channels, although the automatic developing and fixing process caused a delay of 11 minutes between recording and display. The character of data on film is essentially identical to that on tape for all frequencies below the 16 cps natural frequency of the recording galvanometers.

#### 3.1.1.5 Calibration and Timing

Daily calibration of both long and short-period seismometers was accomplished by remote sinusoidal drive. For each recording unit a calibration panel was built, by means of which each seismometer could be driven through its calibration coil by a known current, and at known frequencies chosen to outline the response curve of each instrument. This procedure allowed absolute as well as relative calibration. A switching circuit in the panel permitted easy separation of transducer, amplifier and recording systems; by-pass of the amplifiers only; or connection of transducers, amplifiers and recorders for normal operation.

Calibration current was supplied by a rack-mounted Hewlett-Packard Model 202A function generator. Voltage and current monitoring were done on a rack-mounted Hewlett-Packard Model 150A oscilloscope and a modified Triplet Model 420 d.c. milliammeter.

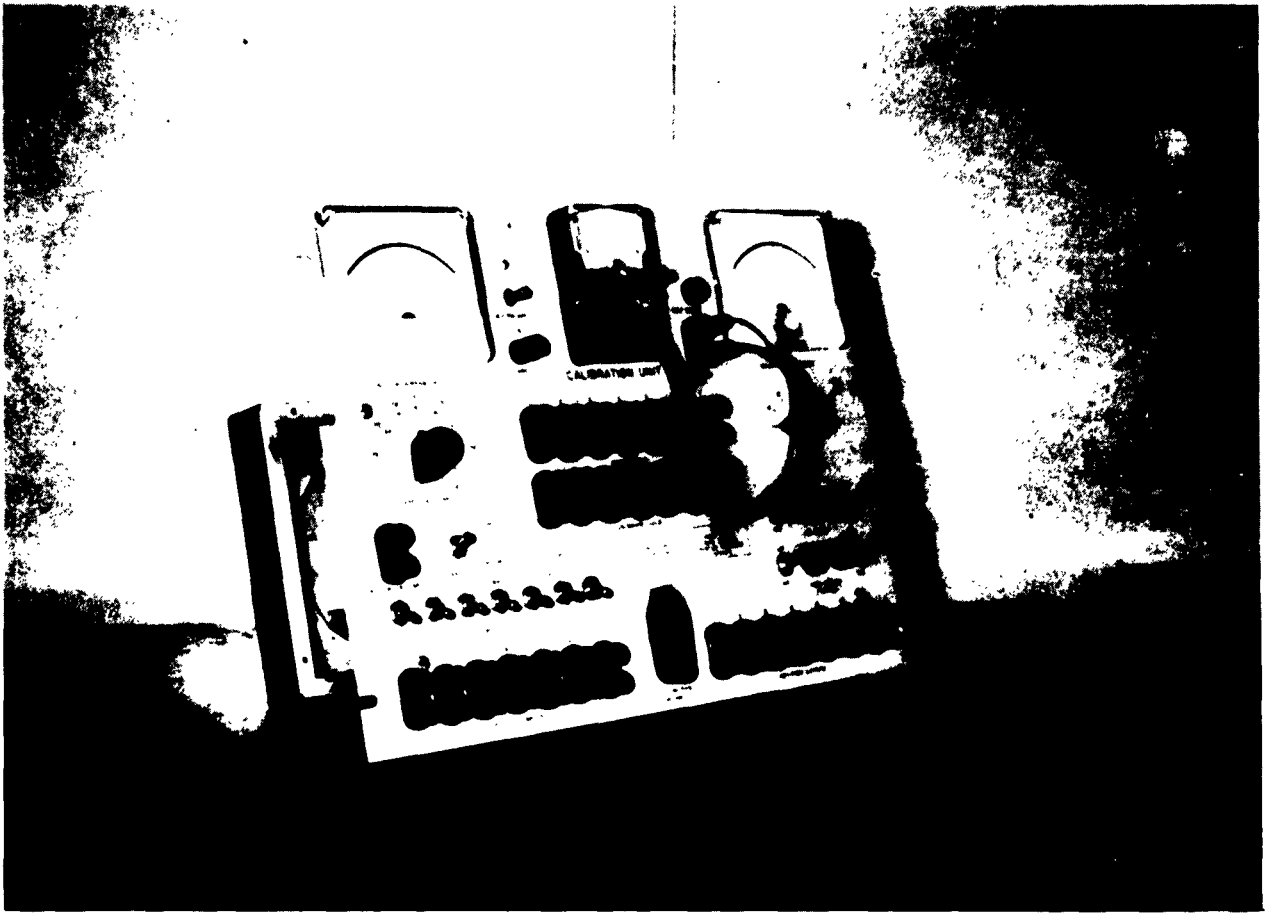


Figure 3.1.6 Front View of Calibration Panel

Timing for normal recording was provided from three sources. For basic continuous timing, a UED-built time pulse unit was used. This unit, built around three timers manufactured by the Industrial Timer Corporation, was driven by fork-controlled current from the tape units and recorded its output on two develocorder traces and one tape channel. The timer signal modulates a 60 cycle signal for recording on magnetic tape in order to preserve d.c. offsets at 5-minute and 1-hour marks. Verbal descriptions of calibrations and similar data were also recorded on this timing channel. Exact time was recorded from WWV, whenever reception conditions permitted, by means of a Specific Product Model SR7R WWV receiver. The third source of time, used as a security measure, was an auxiliary time code from a Ulysses Nardin chronometer.

### 3.1.2 Long-Period Instrumentation

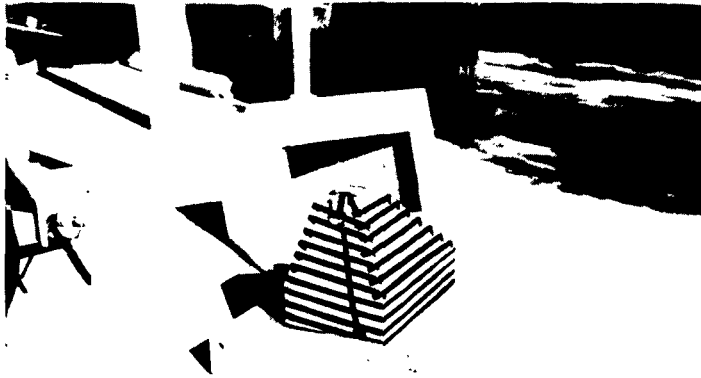
#### 3.1.2.1 Seismometers

For recording seismic events of over 1 second period at each station, a single verticle component long-period seismometer was used. This instrument was a Press-Ewing Model 1800-P seismometer with a natural period of 25 seconds, a high-impedance version of the standard Press-Ewing long-period seismometer. Each of its two transducer coils has 140,000 turns of wire, producing considerably greater output than the low-impedance model. For periods between 2 and 20 seconds, velocity response of the instrument is within about 6 db of being flat.

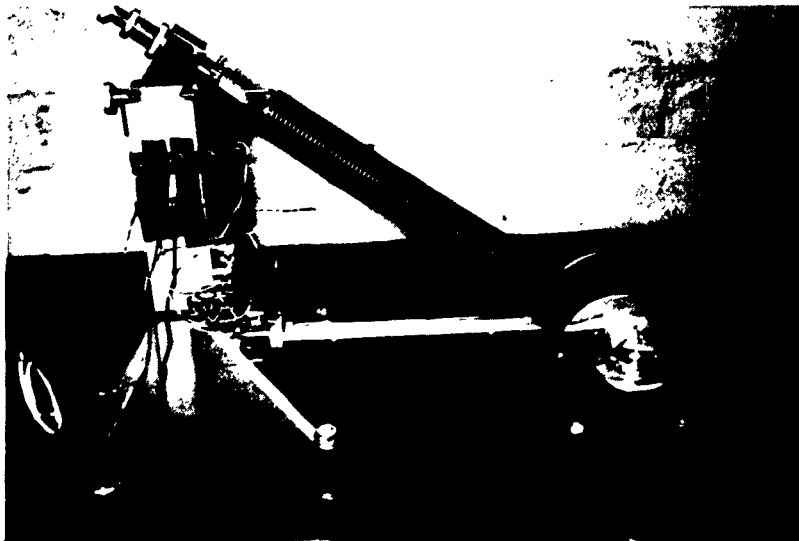
The seismometer was operated inside an insulated oven (Figure 3.1.7). This procedure allowed control of operating temperature to within 1° F of a previously selected temperature about 15° above maximum ambient temperature. Because there was no provision for cooling the oven except by natural heat transfer, the operating temperature was chosen to exceed the maximum expected ambient temperature. Controlled oven temperature also permitted remote control of the seismometer mass position. A variation of 10° F inside the oven caused a shift in mass position of about 3mm. By driving the seismometer through its calibration coil until the pendulum bounced slightly on the nearest stop, as indicated by the polarity of the resulting step in seismometer output, off-centering of the mass position could be checked. Oven temperature was then adjusted until the mass was centered.

The oven consisted of a one-eighth inch aluminum inner shell, a five-inch insulating layer of cork and a three-quarter inch outer plywood box. Heat was provided by a coil taped to the outside of the aluminum shell and by a "quick-heat" coil in the baseplate for getting the oven temperature into operating range.





Long-Period seismometer oven with cover removed,  
showing aluminum inner shell, heater wires and thermostat.



Press-Ewing Long-Period Seismometer Without Case

Figure 3.1.7

### 3.1.2.2 Long-Period Amplifier Filter Recording System

The d.c. amplifier selected for use with the Press-Ewing seismometer was the Hewlett-Packard Model 412A. Two of these were used in cascade, with a Krohn-Hite Model 350A rejection filter between them to prevent saturation of the recording system by 6-second microseisms. The combination of a long-period, high-impedance seismometer and an electronic d.c. amplifier was chosen for recording long-period noise because of the higher magnifications than would be possible with a combination of a short-period seismometer and long-period phototube amplifier (or vice versa). A Benioff-PTA combination would have flat velocity response for periods between 2 and 20 seconds, but operation in this zone would require sacrificing about 55 db of gain.

Peak velocity response of the Press-Ewing seismometer includes the 6-second band, in which large-amplitude microseisms could saturate the recording system. During the first month of recording, the Krohn-Hite "notch" filter, used as a pre-whitening filter in the 6-second band, was set to attenuate response from 0.07 to 0.28 cps. This proved insufficient to allow good recording at 10 seconds or longer period, so the notch was widened to reject (at 24 db per octave) the 0.07 to 0.80 band. All subsequent recording was done using this rejection band (Figure 3.1.2.2.1).

Long-period data was recorded on Develocorder and magnetic tape by the same recording system described above for short-period recording.

### 3.1.3 Weather Recording Instruments

Wind speed and rate of change of barometric pressure were measured continuously and recorded on tape and film at all stations. For barometric pressure variations a Model T-21-B microbarograph, manufactured by the Naval Electronics Laboratory, was used. This instrument consists of a microphone unit, housed in an insulated wooden box to minimize temperature effects, and an amplifier. The microphone is essentially a thin membrane between two air chambers; the membrane forms one plate of a variable capacitor, the other plate of which is a fixed metal disk. A controllable air leak connects the two chambers, while another controllable leak feeds pressure from the outside atmosphere to the front chamber. Signal is produced when the pressure in the front chamber changes faster than the leakage between chambers can compensate for. The two leak rates determine the band pass of the microphone.

Wind speed was measured with a Beckman-Whitley Model K100A anemometer, which determines wind speed in terms of the rotation rate of the anemometer rotor. Two perforated disks are mounted face to face, one fixed, the other revolving with the rotor. As the perforations are aligned in rotation, a beam of light passes through which activates a phototube, generating a pulse which is recorded on tape and film. Wind speed is proportional to the number of pulses per second.

### 3.1.4 Support Equipment

#### 3.1.4.1 Diesel Generators

Power plants at master and slave stations consisted of Kohler 7.5 KW generators driven by Lister Diesel engines (Figure 3.1.8), supplying basic 110 volt, 60 cycle a.c. power. These power plants provided very good service.

#### 3.1.4.2 Vehicles and Trailers

Ford F250 3/4-ton pick-up trucks, 1961 models, provided transportation at each station. The slave station truck was equipped with 4-wheel drive and a front-end winch for reliable transportation during frequent moves in all kinds of terrain, but 2-wheel drive was sufficient for the master station truck. These vehicles performed well and were in generally good condition after 50,000 miles, when the field work ended. When the field analysis center was located in Bakersfield, a 1960 Chevrolet station wagon was used as transportation for site selection and field inspection.

Master station recording equipment was housed in a motor-driven GMC van which had been used on the deep well project in 1960. Its lack of design for use in rough terrain was not a problem once the master station was set up, since there was no need to move the van until recording on the profile was completed. Slave station recording equipment was housed in a specially designed 8' x 16' trailer, manufactured to UED specifications. (Figure 3.1.11). It was well insulated, with interior heating and ventilation for temperature control under various highly different recording conditions.

#### 3.1.4.3 Signal Cables

Seismometers were connected to recording instruments by 1/4-mile lengths of 4-conductor, shielded, rubber-sheathed, "spiral four" cable, wound on metal reels. Two conductors comprised the signal circuit, the other two the calibration circuit.

#### 3.1.4.4 Lightning Arrestors

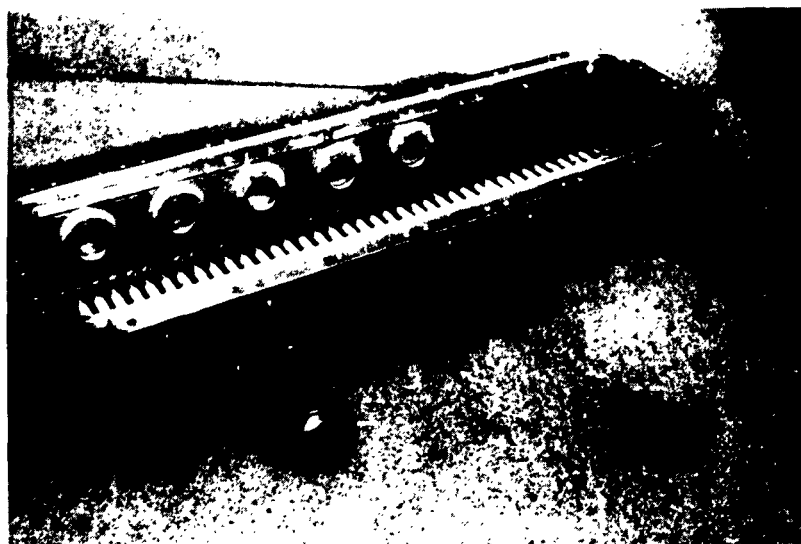
At each end of the signal cable lightning protection was provided by lightning arrestors, consisting of fuses, carbon blocks for high voltage arc-over path to ground, and diodes to bleed off accumulated static charge. This circuitry was mounted inside stake-mounted metal boxes near each seismometer position and the recording trailer (Figure 3.1.9). At seismometer positions the boxes also contained damping resistors for the seismometers and plug-in sockets for field telephones to allow communication with the instrument operator in the



Figure 3.1.8 7.5 Kilowatt Diesel Powered Generator  
Used to Supply 110 Volt AC Power to Recording Station



Inside and Outside Views of Lightning Arresters  
Installed at Each Seismometer Position



Central Lightning Arrester  
Installed at Instrument Trailer

Figure 3.1.9



Figure 3.1.10 Short-Period Vault Liners with Covers  
Motor Generator in Background.

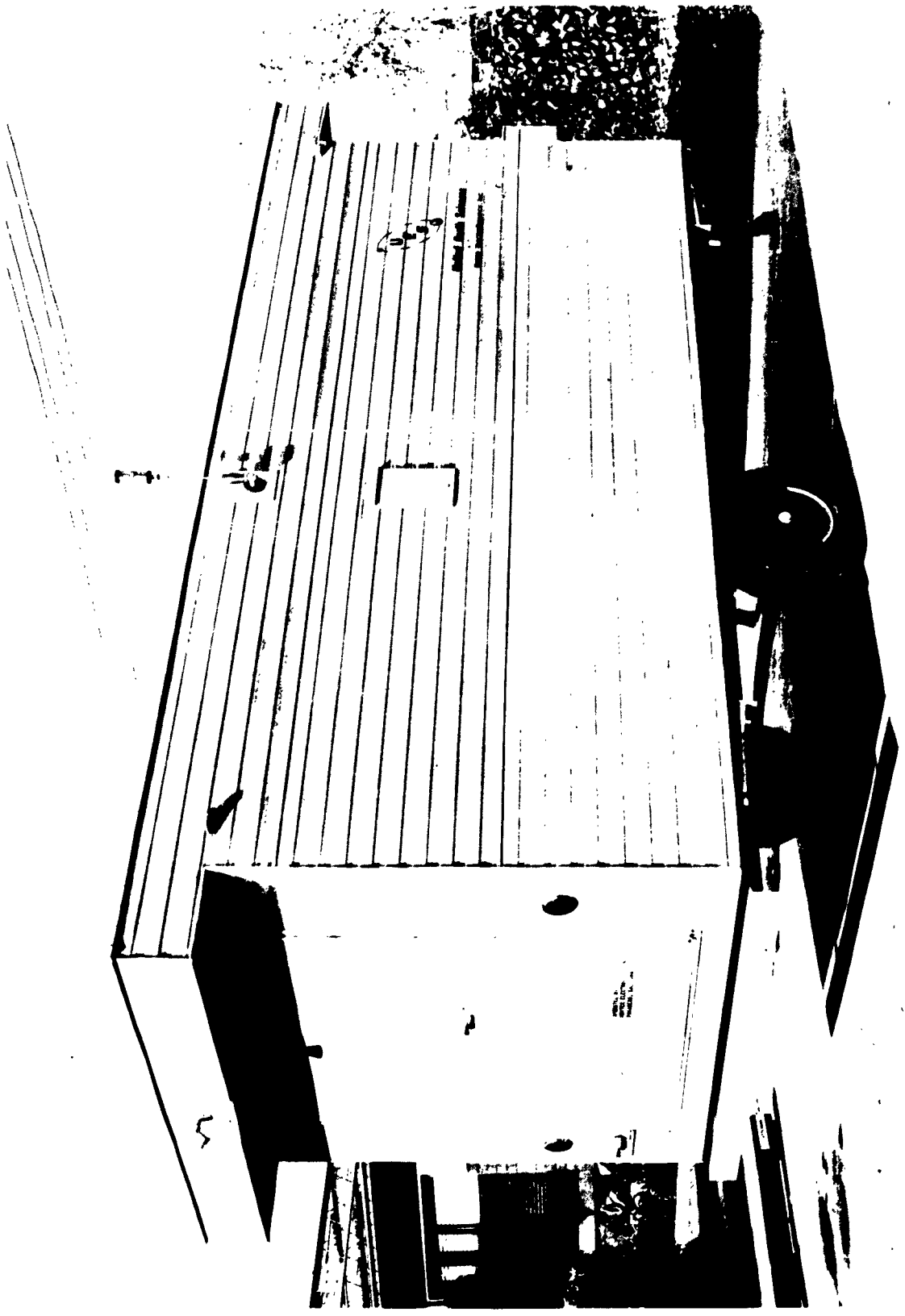


Figure 3.1.11 Slave Station Instrument Trailer.

recording trailer. Damping resistors were by-passed by means of a switch on the lightning arrestor box when free period checks were being made on the seismometers.

#### 3.1.4.5 Seismometer Vault Liners

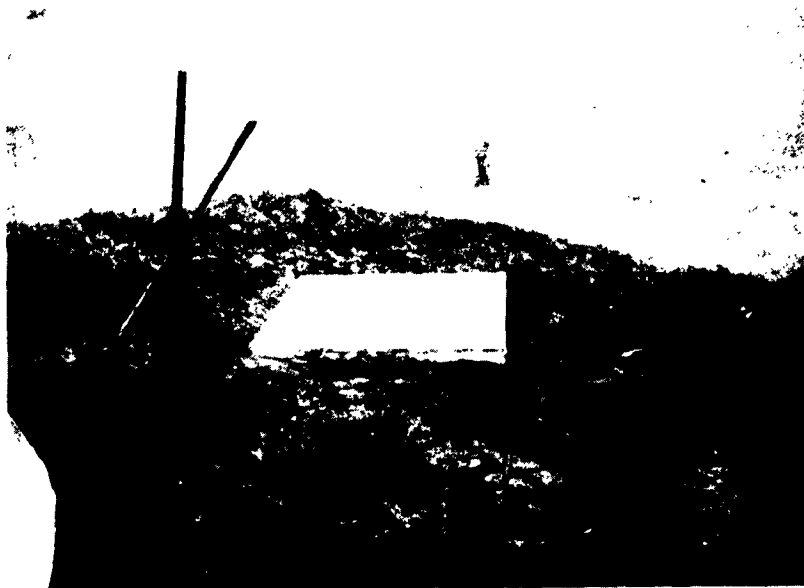
For normal recording the short period seismometers were buried in holes about three feet deep. To protect the seismometers from direct contact with dirt, steel vault-liners were made from short sections of well casing and provided with metal covers (Figure 3.1.10). After the pit was dug and its concrete floor hardened, the vault-liner was put down and the seismometer installed inside. The pit was then filled and packed down around the liner. When the recording was completed at the site, the seismometer was removed and the liner was pulled out of the hole by the two small steel horns welded near its top.

Long-period seismometers were similarly buried in larger pits, lined and covered by sections of heavy marine plywood, cross-braced by two-by-fours.





Digging Pit for the Long-Period Seismometer.



Short-Period Seismometer Vault Liner in Place.  
Liner is covered with metal lid for burial after installation of seismometer. Long-Period vault in background.

Figure 3.2.2.0

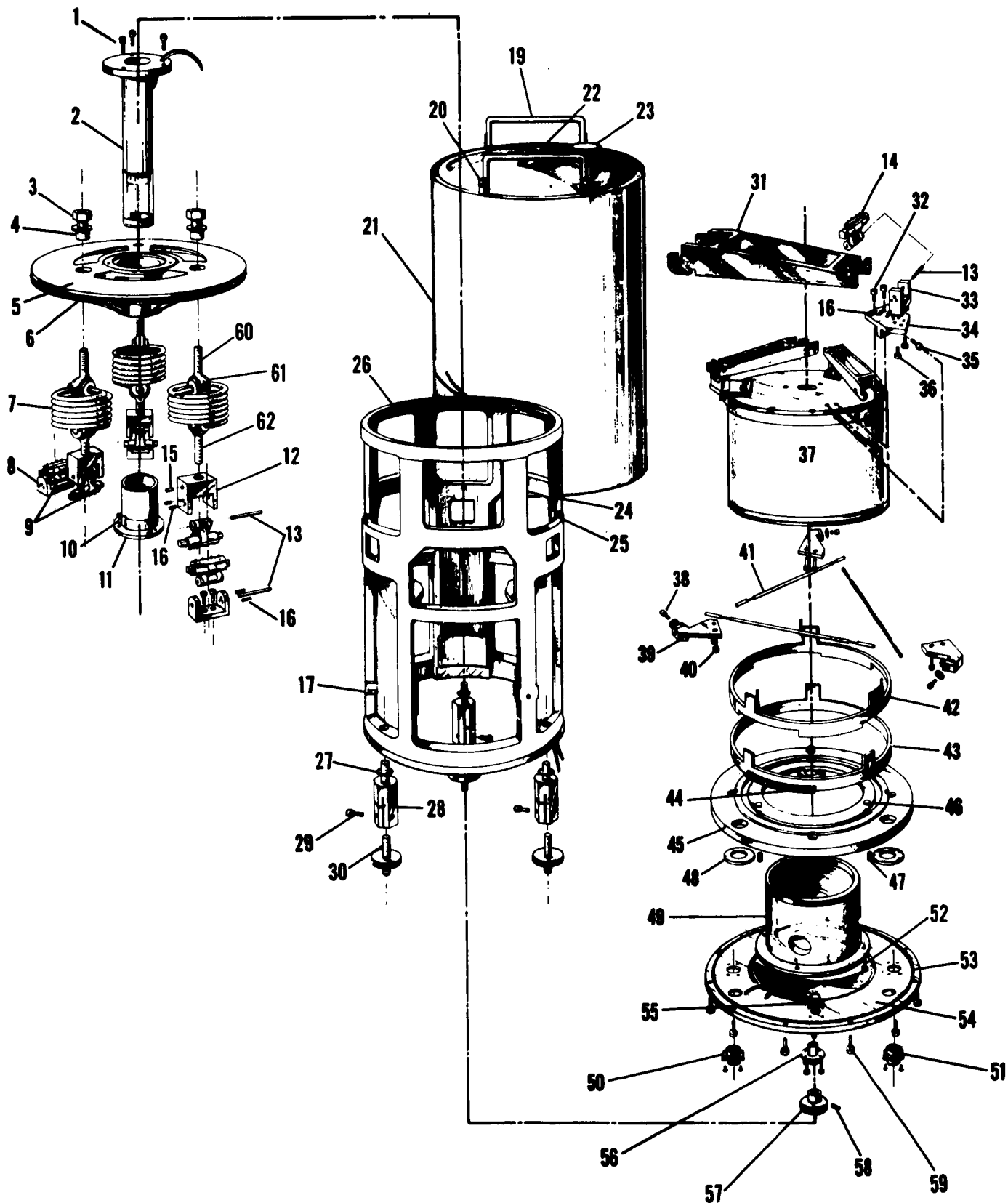


Figure 3.1.12 Exploded View, Johnson Matheson Seismometer, Model 6480

### PARTS LIST

Table below, lists the major replaceable parts of the Johnson-Matheson Seismometer, Model 6480.

<u>Replaceable Parts</u>		
<u>Item</u>	<u>Description</u>	<u>Quantity</u>
1	Socket-head cap screw, #3-40 x 1/2", stainless steel	3
2	Calibration coil assembly, Geotech No. 7055	1
3	Spring nut, Geotech No. 6519	3
4	Bushing, bronze, Boston Gear No. FB-1012-4	3
5	Cap, Geotech No. 7011	1
6	O-ring, National No. 623051	1
7	Spring assembly, Geotech No. 6481	3
8	Connector, Geotech No. 6927	3
9	Flexure pivot assembly, Geotech No. 7140	6
10	Socket-head cap screw, #4-40x3/8, stainless steel	3
11	Calibration coil pole piece assembly, Geotech No. 6935	1
12	Connector, Geotech No. 6521	3
13	Shaft, Geotech No. 6693	9
14	Flexure pivot assembly, Geotech No. 7141	3
15	Socket-head setscrew, #4-40x1/4", No-Mar	3
16	Socket-head setscrew, #2-56 x 1/8", stainless steel	18
17	Socket-head setscrew, #4-40 x 1/4"	6
18	Socket-head cap screw #4-40 x 3/8"	12
19	Handle assembly, Geotech No. 8246	2
20	Cap screw, 1/4-20 x 3/4", hex head, stainless steel	4

Model 6480

PARTS LIST (Continued)

<u>Item</u>	<u>Description</u>	<u>Quantity</u>
21	Cover assembly, Geotech No. 6670	1
22	Level, W.H. Curtin #12865	1
23	Plug, Geotech No. 8316	1
24	Wire duct, Geotech No. 8197	1
25	Tube clamp, Birnbeck No. 51	4
26	Housing, Geotech No. 6671	1
27	O-ring, National No. 622712	3
28	Leg, Geotech No. 6711	3
29	Socket-head cap screw, #8-32 x 1/2"	3
30	Leveling screw, Geotech No. 6842	3
31	Cantilever, Geotech No. 6728	3
32	Socket-head cap screw #8-32 x 3/8", stainless steel	6
33	Mass Connector, Geotech No. 6691	3
34	Upper arm, Geotech No. 6923	3
35	Socket-head cap screw, #10-32 x 1/2"	3
36	Socket-head cap screw #6-32 x 5/8"	6
37	Mass assembly, Geotech No. 7413	1
38	Socket-head cap screw, #4-40 x 5/8", stainless steel	3
39	Lower arm, Geotech No. 6920	3
40	Socket-head cap screw #8-32 x 7/16", stainless steel	6
41	Cantilever rod, Geotech No. 6524 (various stiffness, color coded)	3
42	Ring, Geotech No. 6718	1
43	Cam, Geotech No. 6714	1
44	Rack, Geotech No. 6855	1
45	Base, Geotech No. 6720	1

Model 6480

PARTS LIST (Continued)

<u>Item</u>	<u>Description</u>	<u>Quantity</u>
46	Disc, Geotech No. 6852	3
47	Setscrew, #3/8 - 24 x 5/16"	3
48	Washer, Geotech No. 6851	3
49	Main coil assembly, Geotech No. 6821	1
50	Receptacle, MS-3102C-10SL-3P	1
51	Receptacle, MS-3102C-10SL-4P	1
52	Socket-head cap screw, #4-40 x 3/8"	4
53	O-ring, National No. 623052	1
54	Base shield assembly, Geotech No. 6672	1
55	Shaft pinion, Geotech No. 6846	1
56	Bushing, Geotech No. 6850	1
57	Knob, Geotech No. 6849	1
58	Socket-head setscrew #6-32 x 3/16"	1
59	Socket-head cap screw, #10-32 x 1/2"	12

Model 6480

### 3.2 Field Measurements

Field recordings included seismic signals and noise, wind speed, changes in barometric pressure, and instrument calibrations. Observations were made and recorded of the daily range of temperature variations, local and regional surface geology, and the type of rock or soil at the bottom of each seismometer vault. Coordinates, dimensions, and orientation of each seismometer array were measured and recorded.

#### 3.2.1 Noise and Signal Recording Routine

##### 3.2.1.1 Seismometer Array Configuration

At both master and slave stations, short period seismometers were set out in tripartite arrays, with a long-period and a short-period seismometer at the array center (Figure 3.2.1). Array configurations at each station are given in Appendix 6.8.

At master stations, the seismometers were fixed for the duration of profile recording at 1/4 mile from array center on the California profile, and at 1/2 mile radius on the Pacific Northwest and Appalachian profiles. Slave station arrays were similar to those at the profile master station, except that the array diameter was not normally kept fixed throughout station recording. In the Pacific Northwest, peripheral seismometers were initially set out at 1/4 mile radius, which was then expanded to 1/2, 3/4, and 1 mile successively, at approximately weekly intervals. In California the same procedure was followed, except that the maximum array radius was 3/4 mile. No extensions were made at stations on the Appalachian line, where recordings were taken only from a single fixed array at a radius of 1/2 mile.

The use of slave station arrays of variable size at the same site increased the variety of geologic environments which could be tested, gave improved information on noise source direction, and permitted recording of variations in noise coherency with increased distance between seismometers. However, in the Appalachian area, the extensions were sacrificed in order to gather the maximum possible data from all planned station sites by 30 September 1962, when recording was scheduled to end.

##### 3.2.1.2 Recording Channel Assignments

Except for minor differences in voice annotation and program time, channels assignments were the same for film as they were for tape, and data channels followed the same sequence on both recording media. The following tabulation shows the channel assignments for recording in California and the Pacific Northwest:

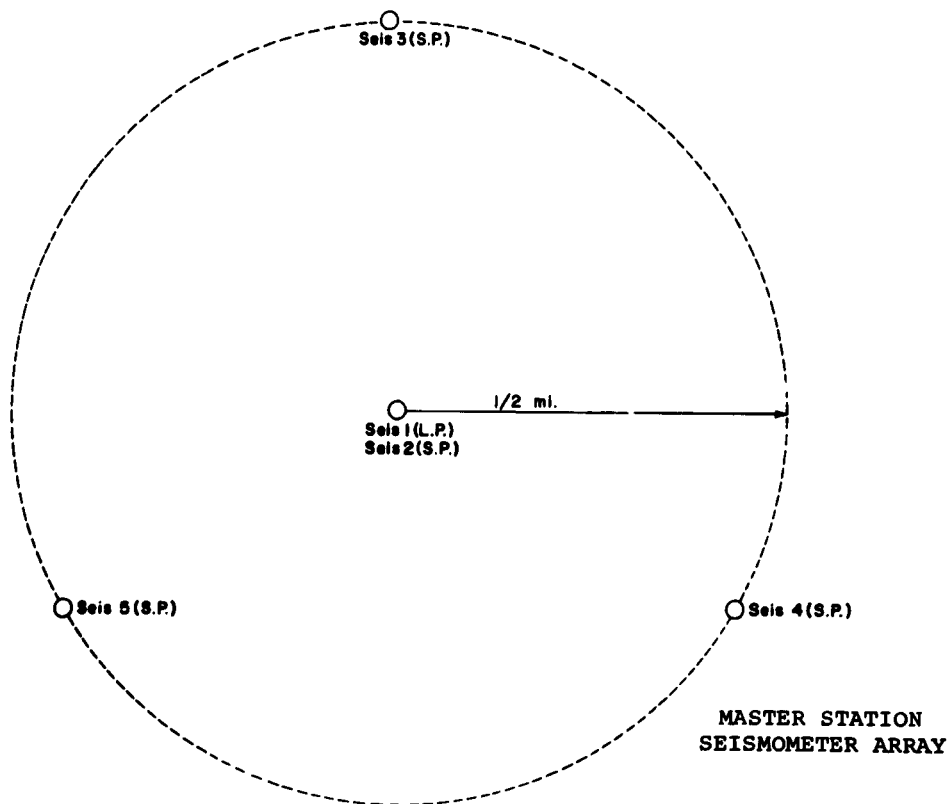
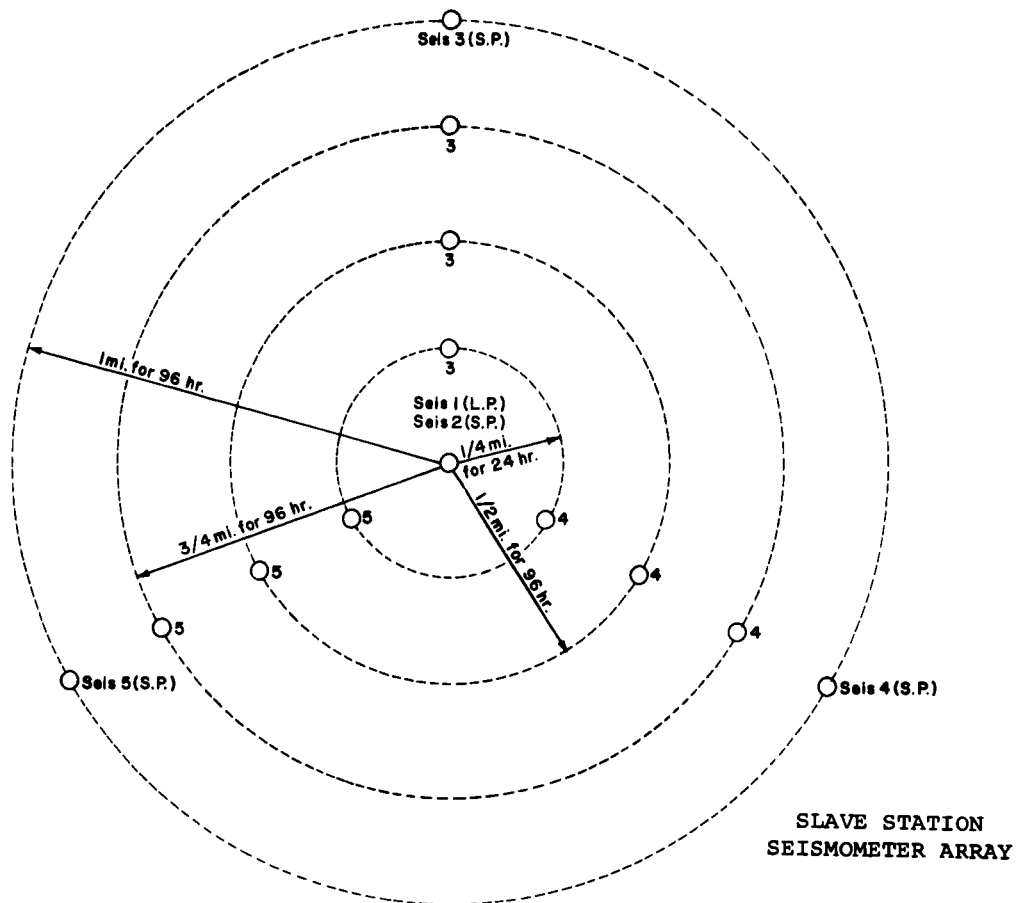


Figure 3.2.1 Array Configuration

TAPE CHANNEL OR DEVELOCORDER TRACE NUMBER	TAPE	ASSIGNMENT	DEVELOCORDER
(0)	----		Program Timer
1		Long period Seismometer (array center)	
2		#2 Short period Seismometer (array center)	
3		#3 Short period Seismometer (north)	
4		#4 Short period Seismometer (southeast)	
5		#5 Short period Seismometer (southwest)	
6		Anemometer	
7		Microbaragraph	
8		Voice; Program	Program Timer
		Timer; WWV	
9		Compensation	WWV
10	----		Chronometer

For Appalachian profile operations minor changes were made, consisting of assigning to tape channels 14 and 7 the data originally assigned to tape channels 8 and 9, respectively.

### 3.2.1.3 Daily Recording Routine

Work schedules were established so that daily recording could begin on each new 24-hour tape reel at approximately the same time of day (1800 GMT) at both master and slave stations. The first hour of recording on each reel was used for daily calibrations, while normal signal and noise recording filled the remaining 23 hours of the reel.

At each recording station, attenuators were set in such manner that seismic noise could be recorded at a high enough level to be clearly visible without saturating the recording equipment. More often than not, the noise level variation at a particular station was small enough so that the attenuators needed to be set only once and required no further adjustment during recording at that station. This was not the case in areas of high variable winds or at stations very near coastlines, where noise level changed widely from day to day. Infrequent attenuation changes, whenever feasible, helped to simplify and speed up data analysis.

### 3.2.2 Calibrations and Tests

Calibrations and testing of recording equipment were performed in detail once a month and in outline form daily. The tests were designed to indicate absolute calibration of the recording system as well as to show operating changes occurring in any stage of the system. System response and test data are included in the Appendix.



### 3.2.2.1 Monthly Detailed Calibration

The monthly calibration and testing, requiring several hours for completion, included outlining frequency response of each of the five seismometer channels, checking seismometer free periods, damping ratios and cable resistances, and checking frequency response and discriminator gain of the recording systems. The tests performed are described below.

Tape Discriminator Sensitivity. FM discriminator output should be zero volts dc for the center frequency signal of 540 cps and  $\pm 1.4$  volts dc for frequencies deviating 40% above and below the center. These three frequencies were fed to the discriminators from a function generator and the discriminator gain and zero adjusting controls were set as required until the output of the discriminator met these criteria.

Tape Recording Oscillator Sensitivity. The FM recording oscillator output frequency should be 540 cps for zero input and should deviate 40% from center frequency when input is 1.4 volts dc. Deviation in frequency was tested with a calibrated discriminator and the oscillator center frequency and 40% deviation frequencies were adjusted as required.

Seismometer Coil Resistance and Leakage. Resistances to ground through signal and calibration cables, as well as resistances of signal and calibration circuits, were measured and recorded for comparison with known nominal values for each resistance.

Seismometer Free Period. When damping resistances had been taken out of signal circuits, the seismometers were pulsed through calibration coils and the resulting free oscillations were recorded for measurement of the natural frequency of each seismometer.

Seismometer Damping Ratio. Short period seismometer damping ratio was checked by 1 gram manual weight lifts, with the seismometer output monitored on an oscilloscope. For correct damping, the voltage ratio out of the seismometer between first swing and overshoot should be about 16 to 1, with a corresponding voltage ratio of 6 to 1 at input to the short period amplifiers, the difference between the two ratios being due mostly to the effect of the amplifier input transformers. Tests with five different weights, varying from 0.2 gm to 5 gm showed that first peak and overshoot voltages both increase directly in proportion to the size of the weight used in the test, when measured either directly out of the seismometer or at the short period amplifier output.

Long period seismometer damping ratio was tested by applying a small dc voltage through the long period calibration coil, allowing the mass to stabilize in a new position of equilibrium, and then removing the dc voltage. The output of the seismometer as it returned to normal equilibrium was recorded on tape, film and oscilloscope.

Develocorder and Tape Calibration. Develocorder galvanometer displacement and tape discriminator output in response to the same calibrating signal were measured and recorded for two calibrating signals, 1 cps and 15 cps.

Detailed System Frequency Response. The response of both the long period and the short period systems was recorded on tape and film for a constant current (2 ma p-p) drive at enough frequencies to define completely the response curves. Long period response was measured both with the notch filter at normal recording setting and with the notch well removed from the range of normal recording frequencies.

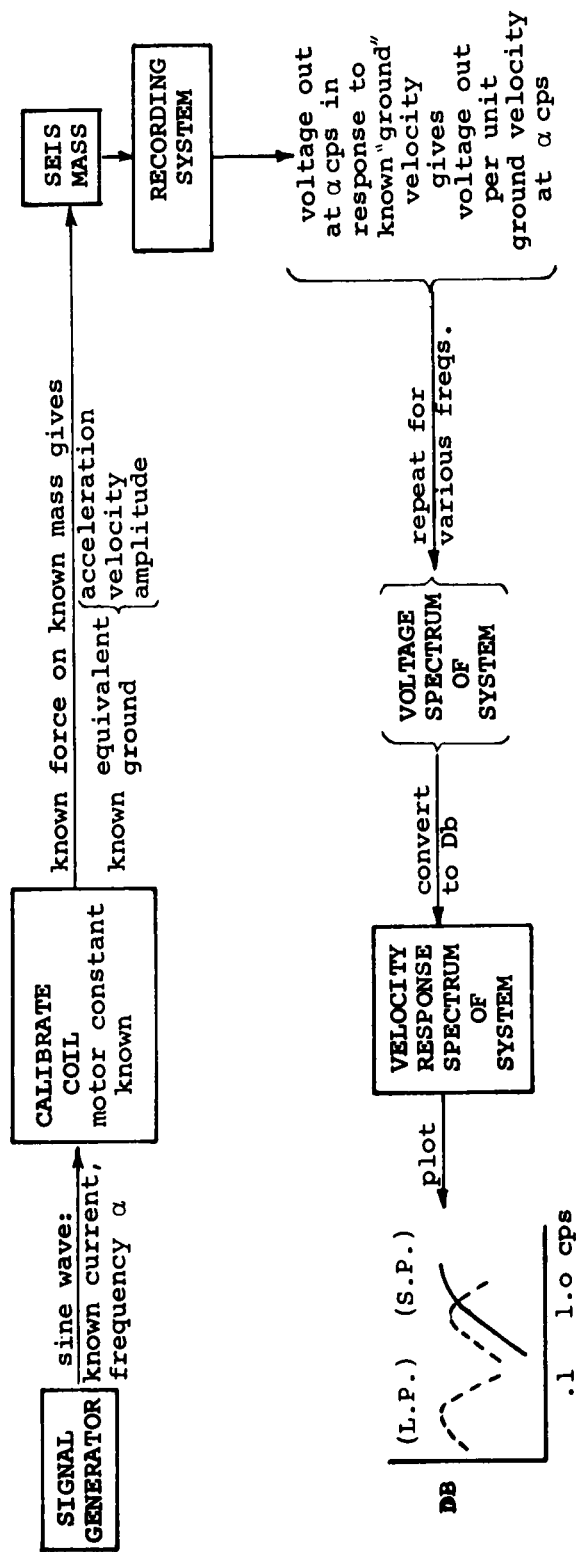
#### 3.2.2.2 Daily Calibrations

Each day at the beginning of a new tape, before normal noise and signal recording began, a short calibration was run on both tape and film. The daily series included a three-frequency outline of the short period system response and a six-frequency outline of the long period one, system noise at zero attenuation and at normal recording attenuation, and a 2 cps bridle test for comparison of amplifier gains. For the short period system response tests, the currents used for each seismometer were those which had been predetermined to drive the seismometer with equivalent velocities of 1.0, 0.5, and 0.1 micron/sec p-p at 0.5, 2.0 and 8.0 cps, respectively. Long period response tests were run with constant 2 ma p-p drive at 0.025, 0.05, 0.10, 0.50, 0.80 and 1.0 cps. During California recording, the daily long period system response tests were run with the notch filter out of range, but the notch filter was left at its normal setting of 0.07 - 0.80 cps rejection for daily calibrations on the Pacific Northwest and Appalachian profiles.

#### 3.2.2.3 Calibration of Weather Recording Equipment

Anemometer. Calibration data provided by the manufacturer permits anemometer output in pulses per second to be converted to wind speed in kilometers per hour by the following relation:  
$$\text{Wind speed (km/hr)} = 1 + (5.48) \cdot (\text{No. pulses per second})$$

Microbarograph. Sensitivity and bandpass of this instrument can be determined approximately by suddenly raising the microphone a known distance and measuring a few points of time and amplitude to outline the rise and decay response to this "step" function input. The microbarograph was calibrated about once a month by suddenly raising the microphone 38 inches. However, the calibration constants were not determined since the microbarograph trace was used only for qualitative correlation with noise level.



Daily Calibration Frequencies  $\alpha$  are  
 .5, 2.0, 8.0 cps for S.P. System,  
 .025, .05, .1, .5, .8, 1.0 cps for L.P. System

VT/078  
 SYSTEM RESPONSE  
 CALIBRATION

Figure 3.2.2

#### 3.2.2.4 Absolute Calibration of the Long-Period Seismometer

Absolute calibration of the long-period seismometers was based mainly on comparing their outputs with those of calibrated short-period seismometers in response to identical inputs of seismic noise.

All short-period seismometers were calibrated absolutely by the manufacturer, presumably by "shake-table" tests. In these tests, the output of a seismometer of known mass, driven at known amplitude and frequency, is measured. The amount of current required through the calibration coil to match that output at the same frequency determines the calibration coil motor constant. Knowledge of this constant and the seismometer mass allows determination of the current needed to make the seismometer respond exactly as though it were being driven by an equivalent earth motion of known amplitude and frequency.

This is essentially the same method used for calibration of the long-period seismometers. Long-period and short-period instruments, buried side by side in the ground at array center, were driven together by high-level noise in the 2 second band. High-level noise in this band is recorded strongly by both systems and PSDs taken from both systems are identical when effect of frequency response is considered (Figure 3.2.2.4.1). Equivalent amplitudes and frequencies of earth motion which drove the long-period instrument were determined from the short-period spectrum. Long-period response to this drive was compared with its response when the long-period mass was driven at known sinusoidal calibration currents and frequencies. These relationships allowed determination of the long-period calibration coil motor constant.

Long-period calibration was also checked in the manner described above, except that Develocorder trace response similarities between the long-period and the short-period systems were followed instead of PSD similarities. Impedance bridge tests (17a) for calculating calibration were performed by the results were not considered reliable because of difficulties in balancing the bridge and insufficiently accurate knowledge of bridge resistances.

From five PSDs at various stations, trace comparisons and bridge tests, 17 values were obtained for the motor constant, mostly agreeing within about 30%. The long-period motor constant was taken to be  $0.11 \pm .03$  newtons per amperes. Calibration coil motor constants for the short-period seismometers were all very close to 0.015 newtons per ampere.

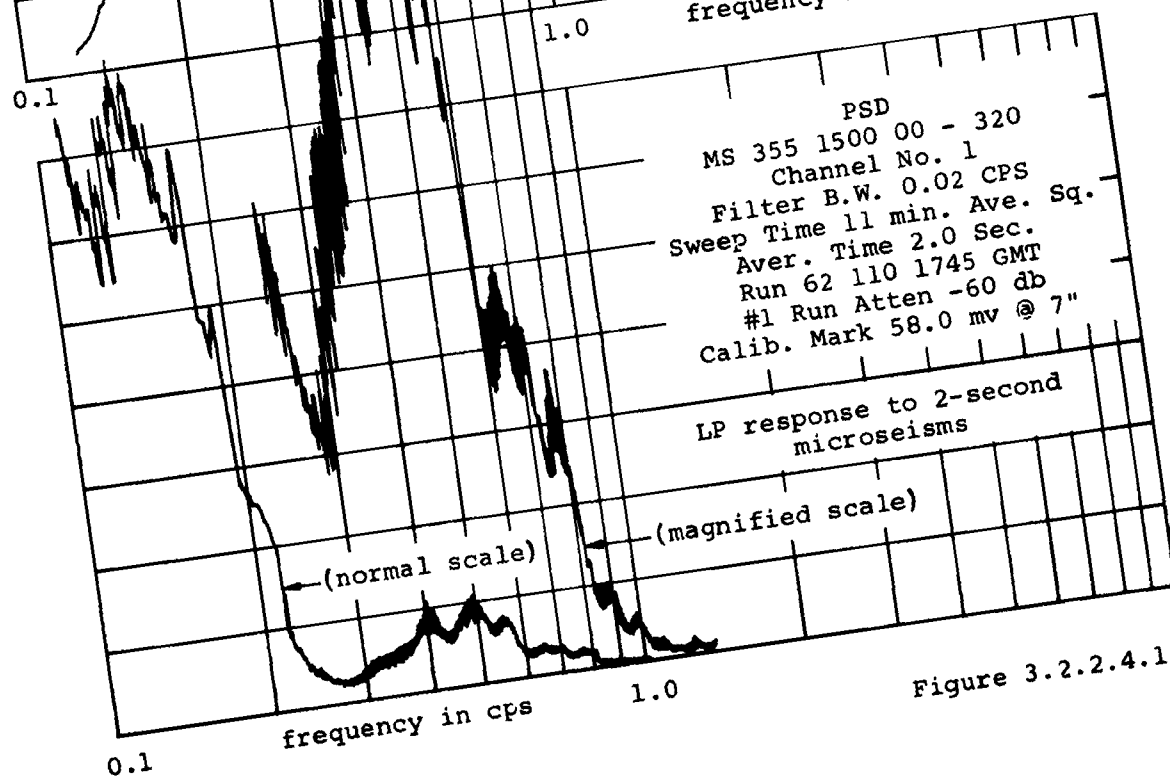
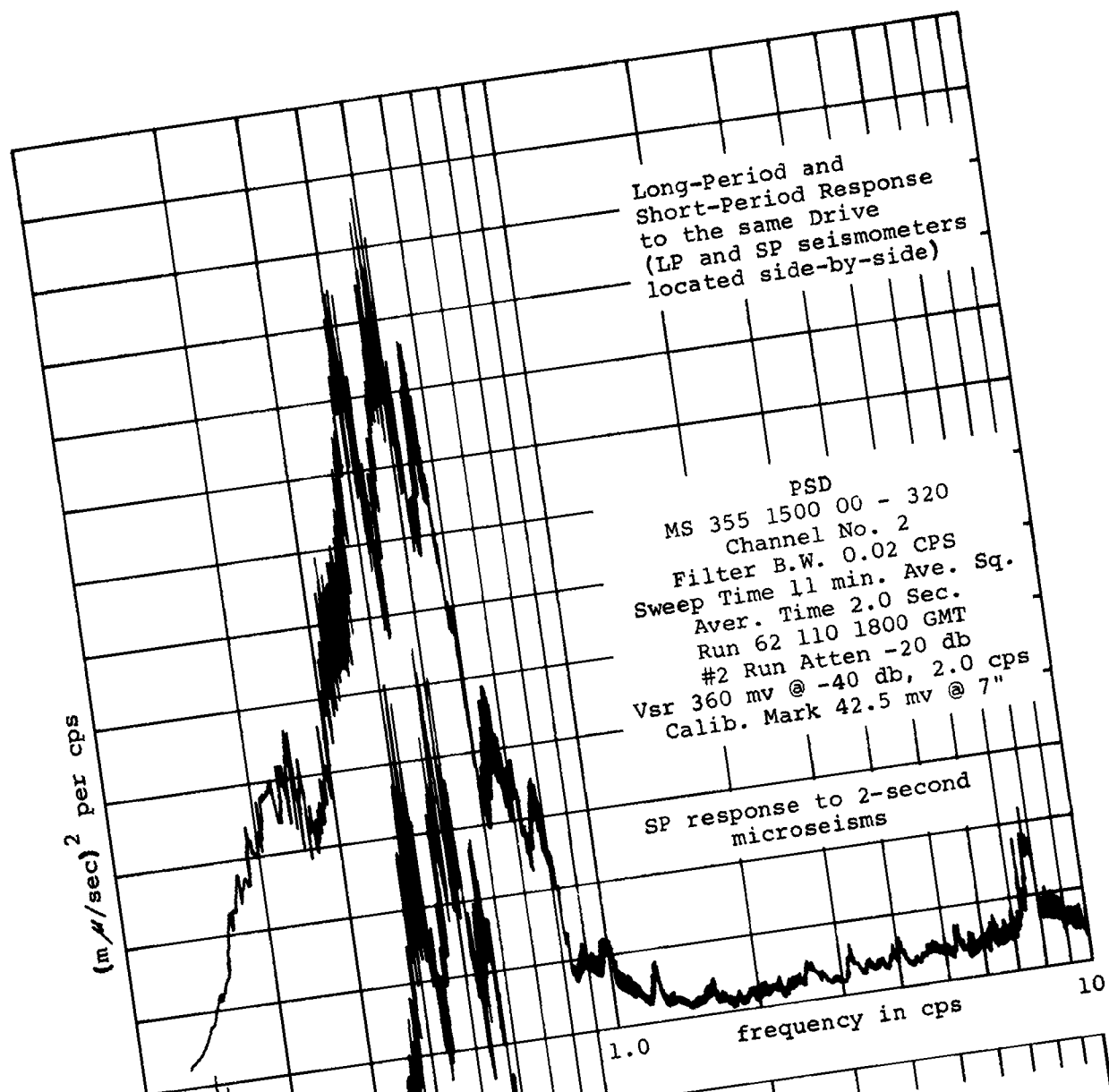


Figure 3.2.2.4.1

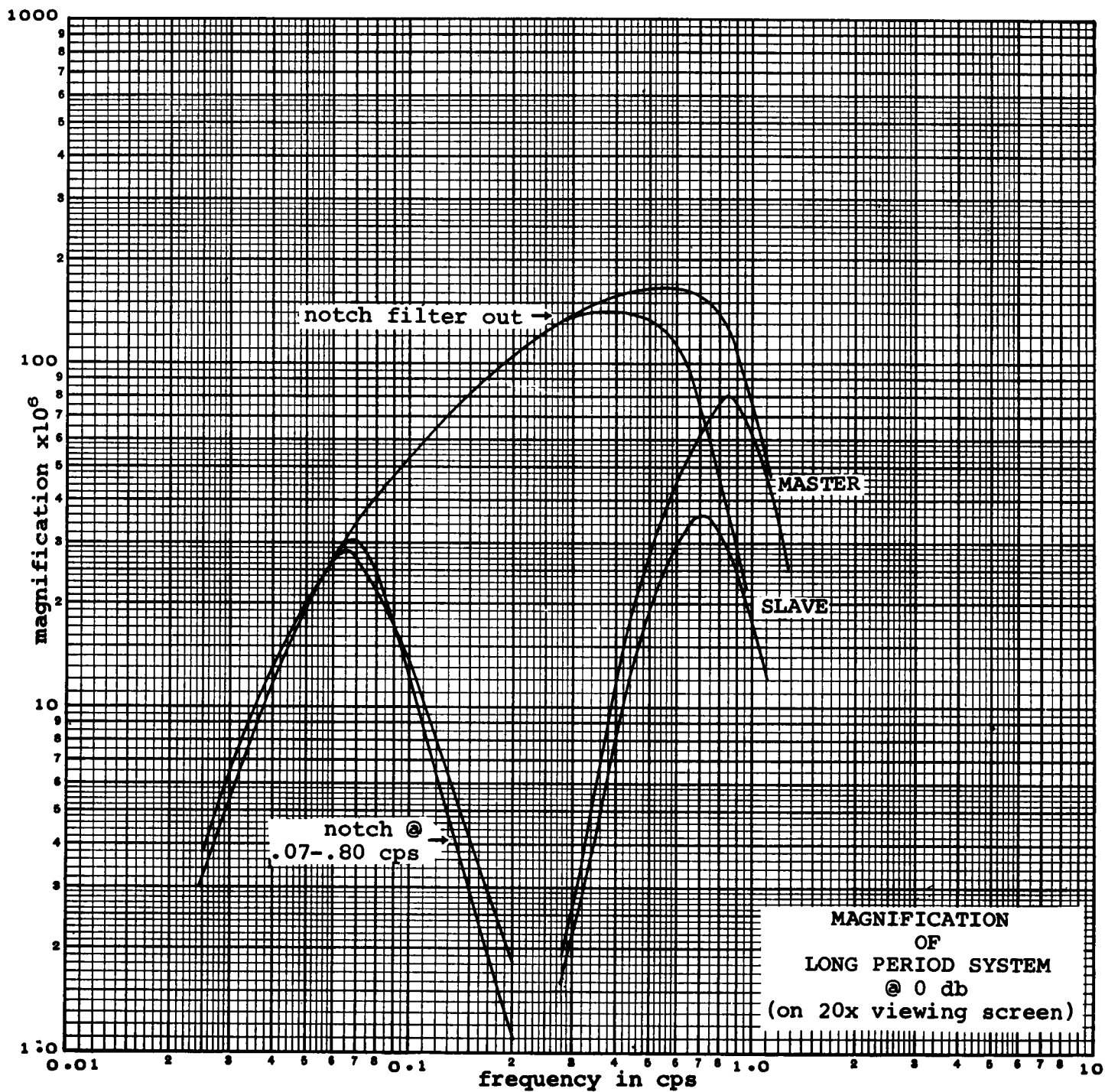


Fig. 3.2.2.5

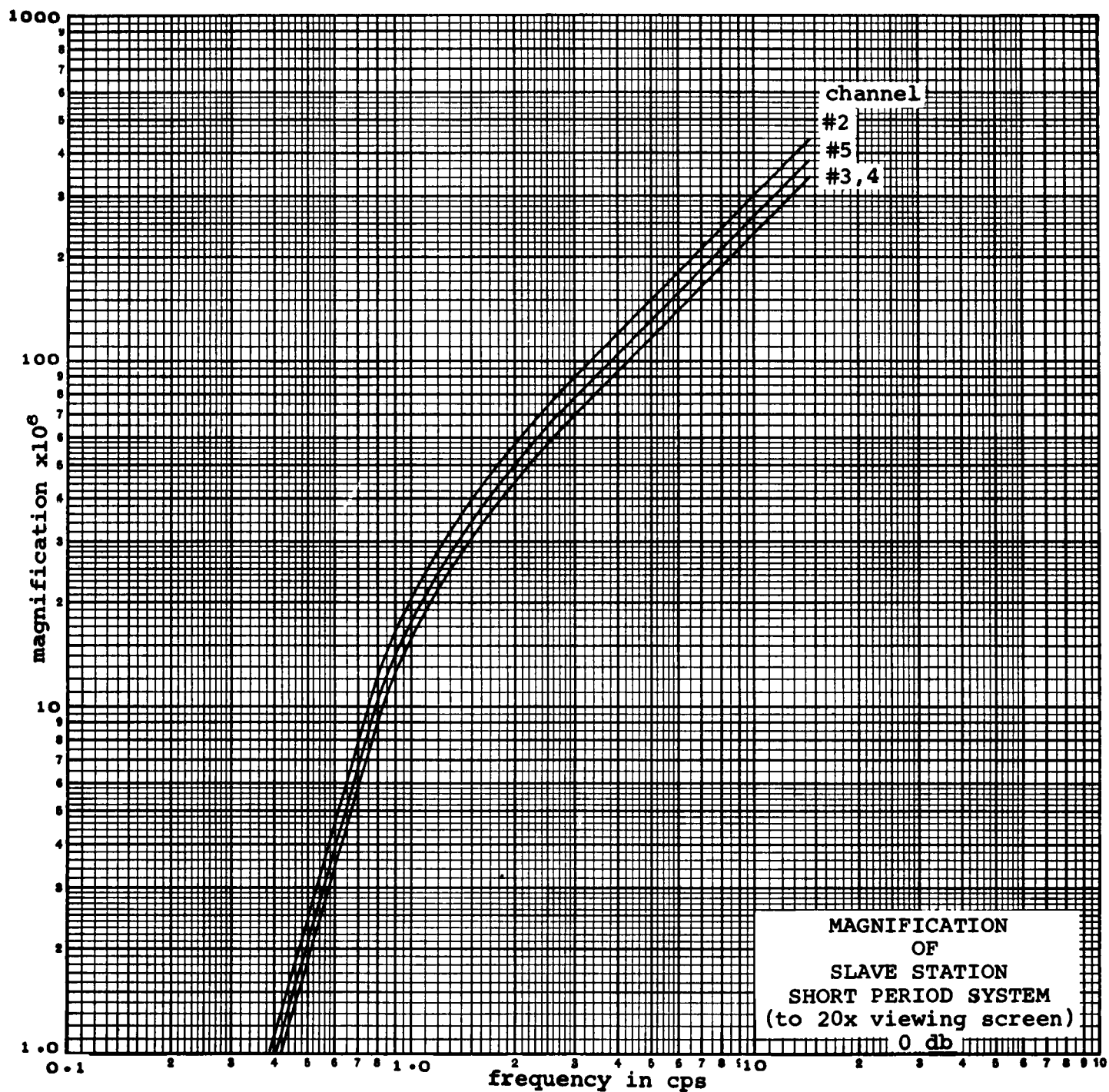


Fig. 3.2.2.6

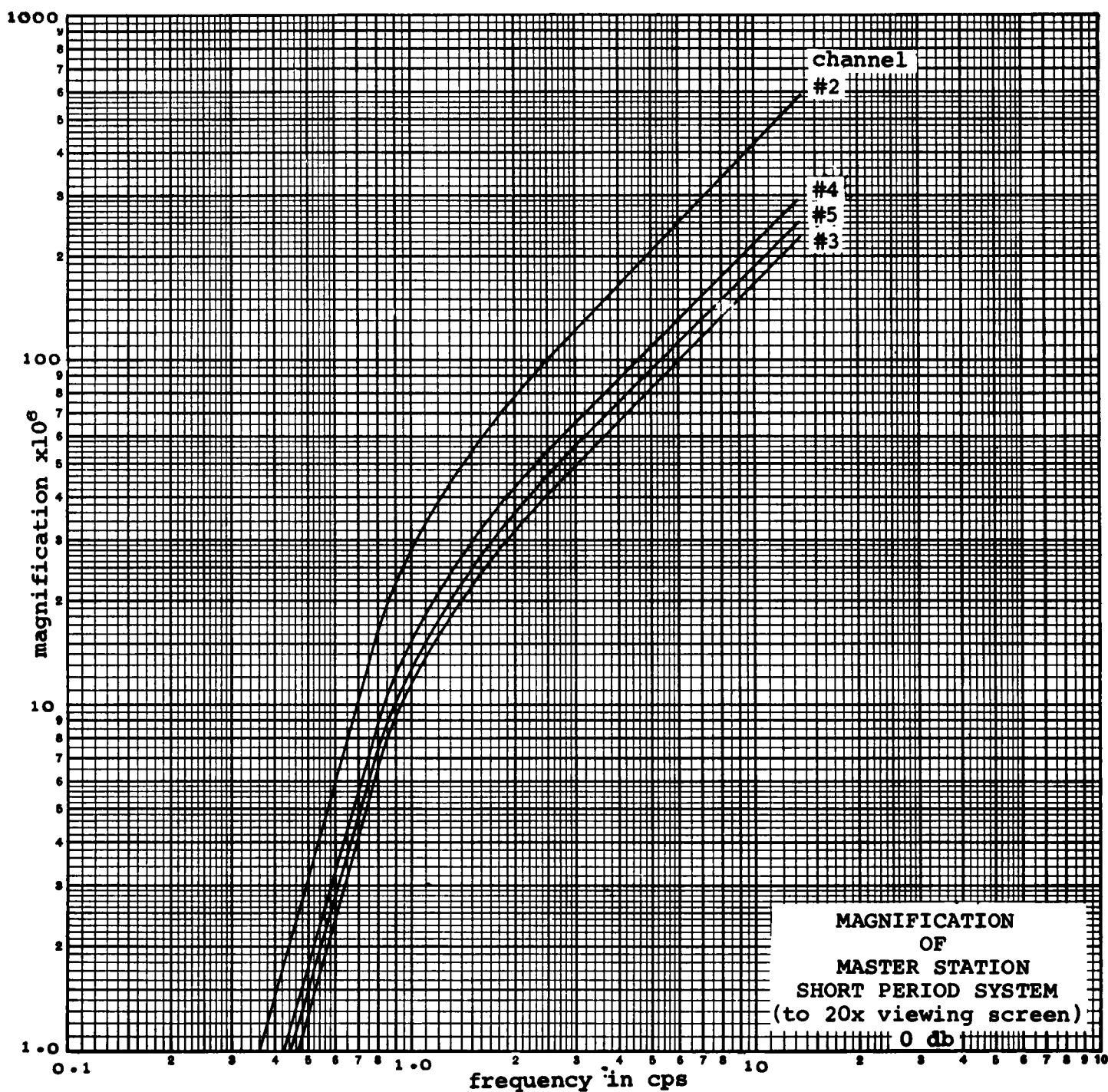


Fig. 3.2.2.7



Noise amplitude spectra computed for the entire range of periods from 0.1 to 50 seconds are based on PSD's from both long and short period seismometers. On these spectra, ground motion amplitudes computed from long period seismometers overlap those from short period seismometers in the range of periods from 1 to 3 seconds, but the long-period ground motion amplitudes computed in this range are greater than from short-period recordings of their common earth drive. This might be due to systematic error in determination of slope of the long period frequency response correction curve.

#### 4. Data Reduction and Analysis

This section describes the methods used in determining seismic noise amplitude, phase velocity and coherency, source direction, and teleseismic signal strength variations, as well as the methods used in correlating these factors with the geologic-geographic environment. General stages in data processing and analysis are shown in Figure 4.1.1.

Study of seismic noise was based largely on machine analysis of noise as recorded on magnetic tape. Analog plots of power, Co - and Quadrature spectral densities of seismometer output voltages provided data from which estimates were made of relative noise amplitudes and phase shifts between seismometer pairs, for narrow bands of frequency in the noise spectrum. Signal strength measurements were made directly from film recordings of teleseisms.

Correlation of noise and signal data with environment was done, where data was plentiful, by a multiple least squares method on a digital computer, and by general observation and comparison where data was sparse. Although signal-to-noise ratio was a primary target for correlation with environment, the approach used was first to find correlations with environment of seismic noise, and then of relative signal strength, independently, and to draw conclusions about signal-to-noise ratio as a final step, rather than to attempt direct correlation of signal strength with environment. Because teleseisms (high-velocity body waves) and noise (mostly low-velocity surface waves) are so fundamentally different, it was felt that they might correlate independently with geologic-geographic environment, while their ratio might not.

Some filter studies were made of teleseisms recorded through seismic background noise, and some spectra were run on teleseisms.

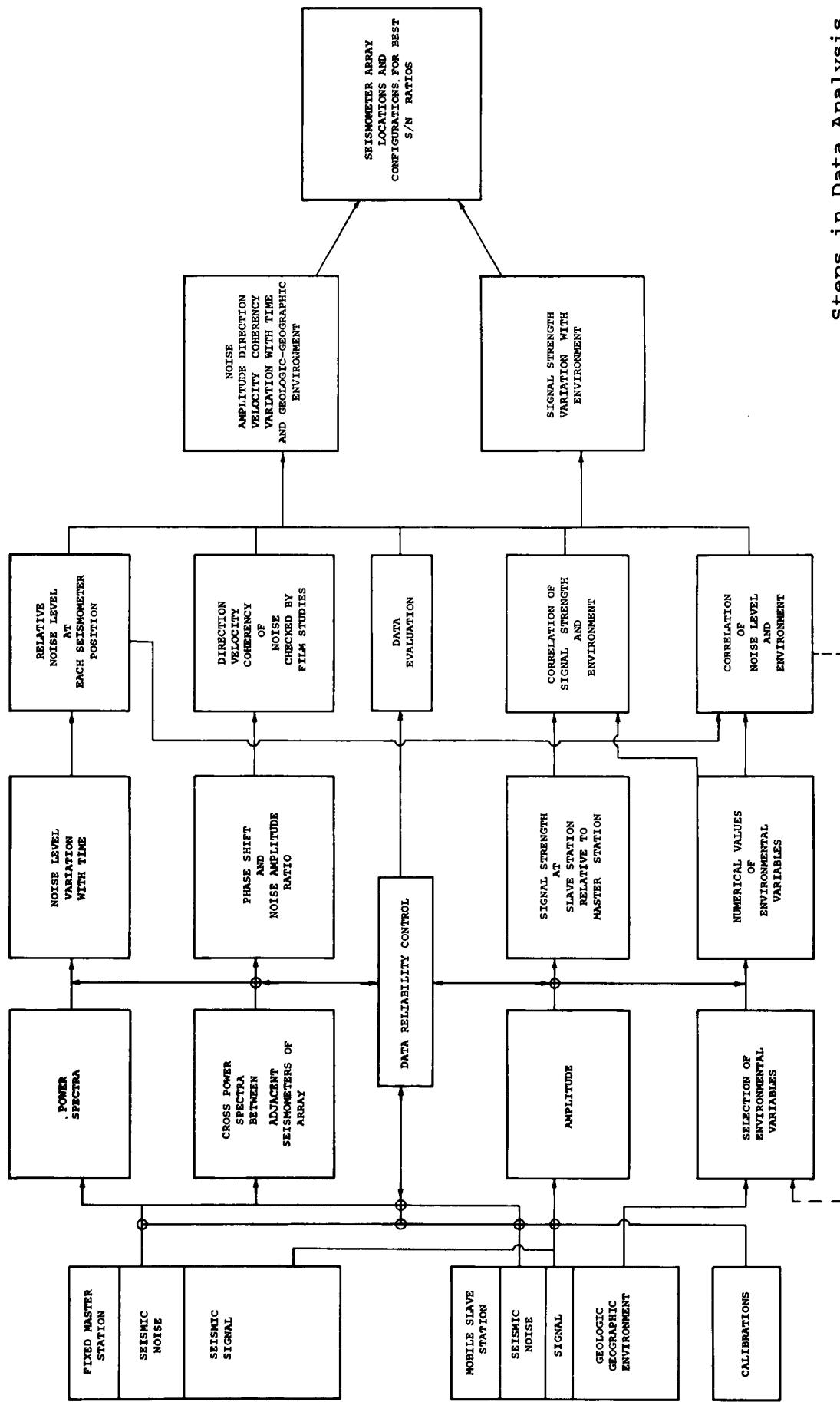
##### 4.1 Noise Analysis Methods

The seismic noise spectrum was studied in detail for periods from 0.25 to 2.5 seconds. Amplitude and some coherency studies were also made for long-period noise up to about 50 seconds period.

##### 4.1.1 Power Spectrum Analysis of Seismic Noise

##### 4.1.1.1 General Descriptions of Power and Cross-Power Density Spectra

The average power dissipated by an AC voltage (or current) in a circuit of unit resistance is equal to the mean squared deviation of that voltage about its average value (assumed to be zero). If the voltage is a random function having components at all frequencies and a continuous spectrum, then the average power dissipated by the random



Steps in Data Analysis

Figure 4.1.1

voltage can be expressed as the sum of average powers in each of a series and adjacent frequency bands covering the whole spectrum. Average power contributed by each band is proportional to the width of the band. If the spectrum is divided into narrower but more numerous bands, the contribution from each band will be smaller, but the total of all their contributions remains constant and independent of individual band-width. If the spectrum is divided into an infinite number of bands, each of zero band-width, then each "band" contributes a power density at a specific frequency, rather than average power in a finite band of frequencies. Power contributed by each zero-width band is infinitely small, but there are an infinity of bands, and the total of their contributions is still equal to the average power dissipated by the random voltage; that is, average power dissipated by the random voltage is equal to the total area under the power density spectrum curve. Units of true power spectral density are thus power per unit of frequency, so that integration of the power spectral density function over all of its frequency range gives an integral expressed in units of power.

Analytically, the power density spectrum of any stationary random time function can be expressed as a Fourier transformation of the autocorrelation function of the time series (7a). If  $f(t)$  is the time function, and

$$\phi(\tau) = \lim_{T \rightarrow \infty} \frac{1}{2T} \int_{-T}^T f(t) f(t+\tau) dt$$

is its autocorrelation function, then

$$\Phi(\omega) = \frac{1}{2\pi} \int_{-\infty}^{\infty} \phi(\tau) e^{-j\omega\tau} d\tau = \frac{1}{2\pi} \int_{-\infty}^{\infty} \phi(\tau) \cos \omega\tau d\tau$$

is its power spectral density function, where the variance of  $f(t)$  is equal to the area under its power density spectrum curve:

$$\lim_{T \rightarrow \infty} \frac{1}{2T} \int_{-T}^T f^2(t) dt = \int_{-\infty}^{\infty} \Phi(\omega) d\omega$$

Since the variance of each frequency component of  $f(t)$  is real, non-negative and independent of the variance in any other frequency component, it follows that the spectral density function is real, non-negative, and independent of relative phase of individual frequency components.

The complex cross-power spectral density function of two stationary random time functions can be expressed in similar fashion. If  $x(t)$  and  $y(t)$  are two time functions whose cross-correlation function is

$$\phi_{xy}(\tau) = \int_{-\infty}^{\infty} x(t) y(t+\tau) dt$$

and if the Fourier transformation of the cross-correlation function is

$$\Phi_{xy}(\omega) = \frac{1}{2\pi} \int_{-\infty}^{\infty} \phi_{xy}(\tau) e^{-j\omega\tau} d\tau$$

then the cross-power spectral density function of  $x(t)$  and  $y(t)$  is

$$\Phi_{xy}(\omega), \text{ of the form: } \Phi_{xy}(\omega) = A_{xy}(\omega) e^{-j(\phi_y(\omega) - \phi_x(\omega))}$$

whose real part,  $A_{xy}(\omega) \cos(\phi_y(\omega) - \phi_x(\omega))$ , is called the Co-spectrum, and

whose imaginary part,  $A_{xy}(\omega) \sin(\phi_y(\omega) - \phi_x(\omega))$ , is the Quadrature spectrum,

where  $(\phi_y(\omega) - \phi_x(\omega))$  is the phase shift between components of  $x(t)$  and

$y(t)$  at frequency  $\omega$ . When  $x(t) = y(t)$ , the Co-spectrum of  $x(t)$  and  $y(t)$

becomes the power density spectrum,  $\Phi(\omega)$ , of  $f(t)$ , and the Quadrature spectrum becomes zero. In other words, the complex cross-power spectral density of two identical time functions is the real power density spectrum of either one.

These relationships are strictly true only for stationary random functions, and their definitions, as given above, involve infinitely narrow filtering (Fourier transformations) and infinite integrals. These conditions are met only approximately by machine spectral analysis of seismic noise. Seismic noise is not a stationary random function, but is full of periodic components, which appear as "spikes" of finite power and infinite power density. Machine analysis requires finite filter band-widths, since infinitely narrow filters are impossible to manufacture. Because seismic noise is not analyzed over its entire past and future, but must be sampled for analysis, infinite integrals are replaced by integrals over very short time periods, relatively speaking.

These limitations mean that machine analysis of seismic noise can give no more than estimates of the true power density spectra. The wave analyzer plots analogs whose amplitudes at each frequency band are roughly proportional to average power spectral density across that band. Since filter band-width is finite, the wave analyzer plots average power in a band of frequencies, rather than power density at a specific frequency. The analog spectrum resembles the true power density spectrum in that over-all area under the spectrum can be made independent of filter band-width (by normalizing power through the finite filter to that for a 1 cps-wide filter), but the analog is measured in units of power per unit of filter band-width, rather than as power density.

Narrow filters give finer spectral detail than broader filters and thus would seem to represent the true spectrum better than broad filters. However, this is not true unless sample length is increased in proportion

to the reduction in filter band-width; narrowing filter band-width without increasing sample length provides no additional information about the shape of the spectrum.\*

Seismic noise can be sampled effectively in spite of such limitations and its machine analysis does reveal most of the important characteristics of relative amplitudes and phase shifts in the noise spectrum.

#### 4.1.1.2 Wave Analyzer Systems

The equipment used in noise and signal analysis consisted basically of a tape and loop transport system to handle noise data tapes, a wave analyzer system and plotters for spectrum analysis, a bank of band-pass filters for filter optimization studies, and a film viewer for monitoring noise data films (Figures 4.1.2, 4.1.3).

##### 4.1.1.2.1 Tape and Loop Transports

A Minneapolis-Honeywell 3173 tape transport, similar to that used in field recording, was used to search full 24-hour tapes. Samples chosen for analysis were located by monitoring time and verbal annotations on the voice track, and by means of a footage counter on the tape transport. The tape could be moved at 0.3, 0.6, 30 and 60 ips, the higher speeds allowing rapid access to the general location of interest.

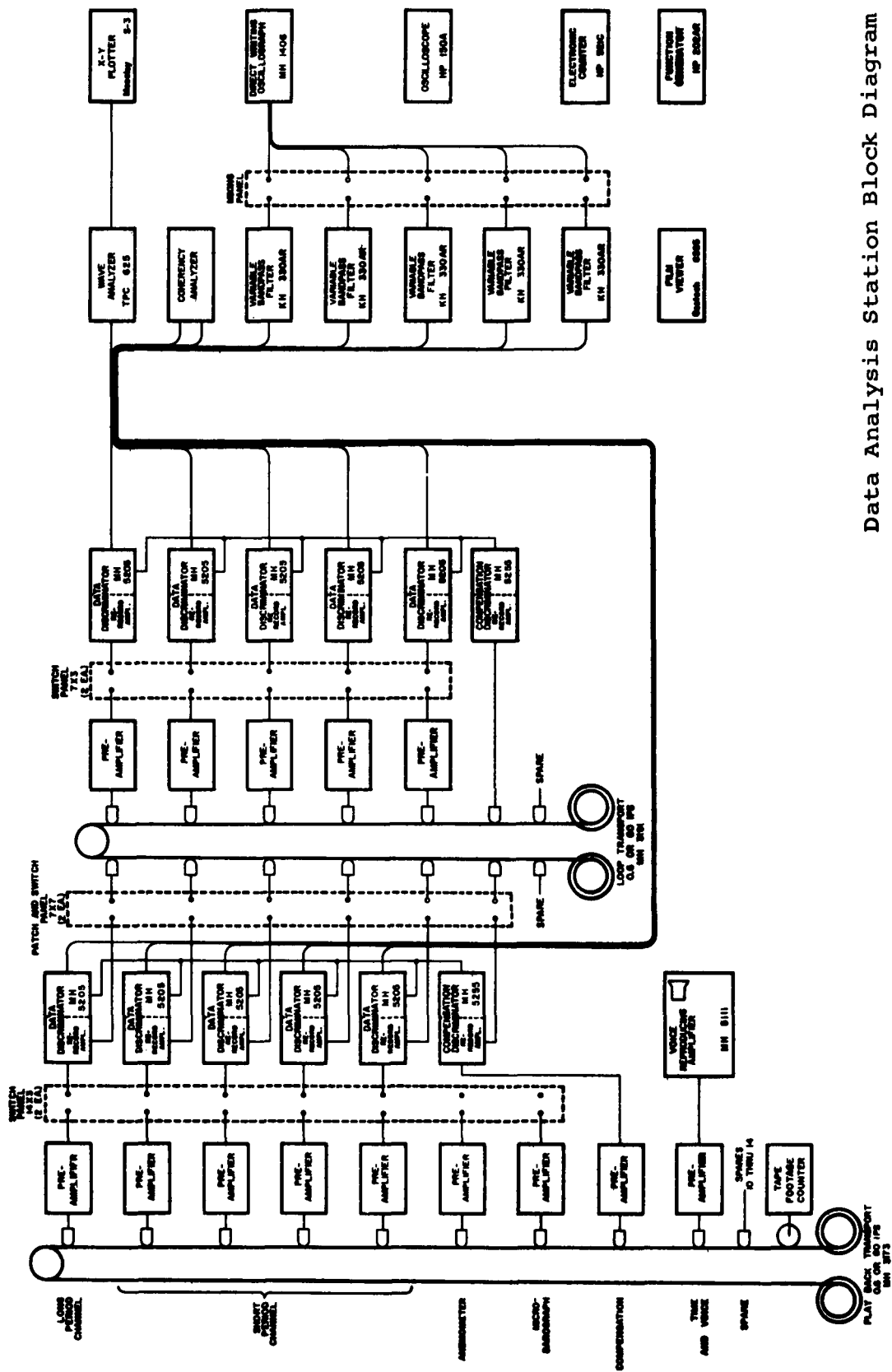
Analysis was not done directly on original data tapes. To avoid wearing out the originals, samples were first transferred to disposable loops of blank tape, which were transported and their data discriminated by means of an MH 3191 loop transport. After a 200-second noise sample had been chosen and located on the original tape, its data were transferred directly to a 10-foot loop of blank tape on the loop transport. The 10-foot loop was just long enough to take a 200-second sample of data recorded at 0.6 ips. Data on the loop was played back at 100 times recording speed to allow the spectrum analyzer to work at frequencies well above its lower frequency limit of 2 cps. Seismic noise with periods as long as 50 seconds could be processed by the spectrum analyzer with this speed-up. The increased loop speed also increased the number of samples that could be processed in a given time, since each 200-second sample was played back in only 2 seconds, and the short-period spectrum between 0.2 and 25 cps could be written in about 18 minutes.

##### 4.1.1.2.2 Power Spectrum Analyzer

Original wave analysis equipment consisted of the Technical Products, TP 633, Wave Analyzer, designed to show power spectral density in a single noise track. This system was composed of a TP 626 Oscillator, a TP 627 Analyzer, a TP 633 Power

---

\*Moody, R.C., Statistical Considerations in Power Spectral Density Analysis. Technical Products Company.



Data Analysis Station Block Diagram

Figure 4.1.2

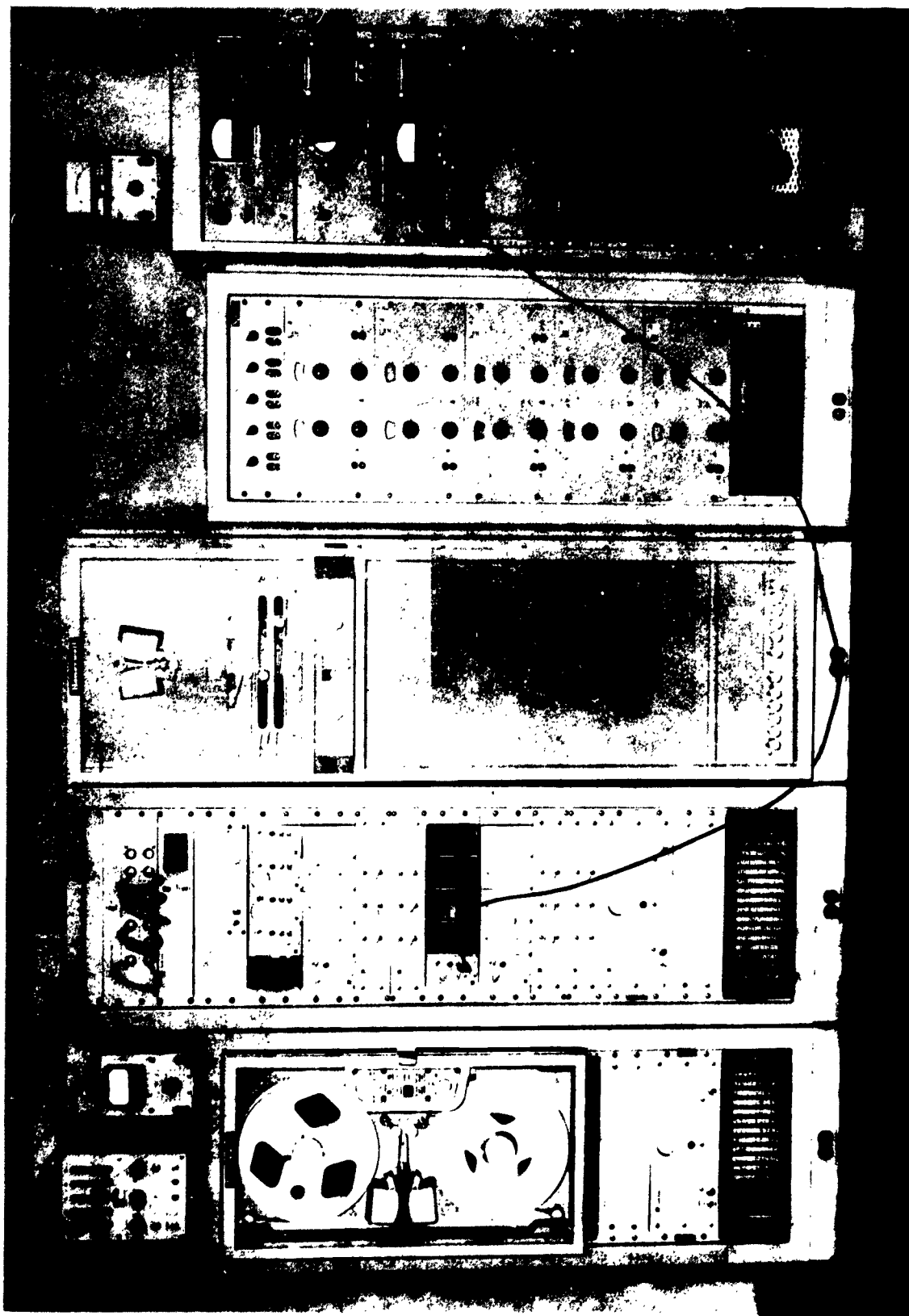


Figure 4.1.3 Data Analysis Center Equipment Tape Transport,  
FM Discriminators, Loop Transport, Band-Pass Filters,  
and Wave Analyze System, from Left to Right



Integrator, and a Moseley X-Y Plotter for graphing the power spectrum. Input to the system was a periodic noise function, repeating every 2 seconds, from the loop transport.

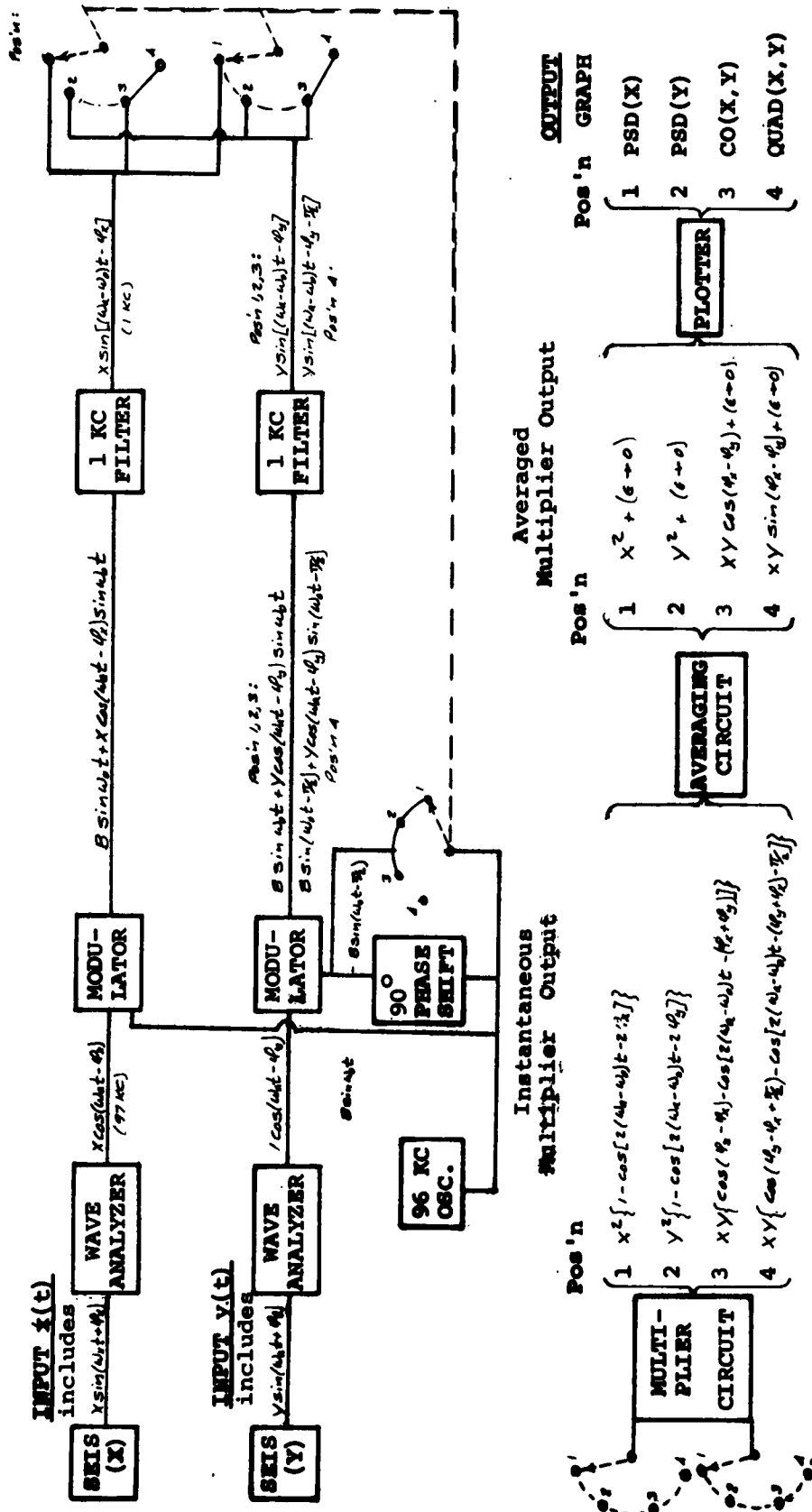
The oscillator produced a signal of known frequency equal to 97 kc plus any chosen frequency in the seismic range. Recorded seismic noise was used to modulate this oscillator signal in the analyzer. If the noise contained a component whose frequency was the "chosen" frequency, a 97 kc sideband was produced of amplitude and phase proportional to that of the component. No sideband was produced if the noise sample contained no significant component at the "chosen" frequency. The 97 kc sidebands were isolated in the analyzer by a narrow crystal filter centered at 97 kc and the filter output was fed to the integrator where it was squared and averaged. The output of the integrator, which was proportional to mean squared velocity (voltage) of seismic noise in a narrow band around the "chosen" frequency, was then fed to the plotter. This process was carried out automatically and continuously for each noise frequency, giving an analog plot of the whole spectrum.

#### 4.1.1.2.3 Cross-Spectrum Analyzer

Early in 1961, the wave analyzer system was augmented by a TP 645 Multiplier and another Analyzer. These additions allowed definition of the real and imaginary components of the cross-power spectrum between two distinct but simultaneously recorded noise channels. From these components, coherency and phase shift between the two noise channels could be estimated for each frequency band in the noise spectrum. A block diagram of operation of the TP 645 is given in Figure 4.1.4.

Input to the two channels of the cross-spectrum system was the output of the two TP 627 Analyzers for the seismic frequency being examined. Each input was a 97 kc signal of amplitude and phase proportional to a noise voltage component out of its respective seismometer for the chosen seismic frequency. Both 97 kc inputs were modulated by a common 96 kc signal from an oscillator in the TP 645 system, producing two 1 kc sidebands, each of amplitude and phase proportional to the output of its respective seismometer in the chosen frequency band. These 1 kc signals were isolated, then multiplied together and averaged by the TP 645, and plotted, producing the real component of the complex cross-power spectrum between the two noise channels (Co-spectrum).

The imaginary component of the cross-power spectrum (Quadrature spectrum) was produced in similar fashion, except that one side of the 96 kc modulating signal was phase-shifted  $90^\circ$  with respect to the other before reaching its noise channel. Modulation thus produced one 1 kc



GENERATION OF  
CROSS SPECTRUM ANALOGS  
TP 645  
Wave Analyzer System

Figure 4.1.4

sideband with amplitude and phase proportional to those of one noise channel, and another 1 kc sideband with amplitude and phase (shifted  $90^\circ$ ) proportional to those of the other noise channel.

Points for each frequency were generated and plotted continuously for Co- and Quad-spectra, just as for power spectra. All points on the power spectrum are positive, since it is essentially a plot of the mean squared noise voltage spectrum. Points on the Co- and Quad-spectra have both positive and negative values, determined by relative phase shift between the two noise signals at each frequency. Co- values are maxima or minima and Quad- values zero, when relative phase shift is zero or an even multiple of  $90^\circ$ . Quad- values are maxima or minima and Co- values zero, when relative phase shift is an odd multiple of  $90^\circ$ . When both noise channels are identical (i.e., a single noise signal is paralleled into both channels), the Co-spectrum should be identical with the power spectrum and the Quad-spectrum zero throughout. This fact provided a test of the system.

Co- and Quad- values for each frequency are proportional to the sine and cosine, respectively, of the phase shift between seismometer output voltages at that frequency. In many practical cases, this is enough to define the phase shift itself. In other cases, the problem is not simple and the solution for phase shift must be chosen after consideration of array geometry and expected noise velocity. This problem is discussed later.

#### 4.1.1.3 Instrument Constants and Sample Selection

The length and character of the sample and all instrument constants were chosen to give maximum spectral definition, without sacrificing too much spectral stability, and without making either the sampling process or the sample loops too cumbersome to handle efficiently.

It was found that reasonably stable spectra could be obtained from noise samples 200 seconds long, and with an effective filter band-width of 0.02 cps. At the analyzing speed of 100 times real time, this requires a filter band-width of 2 C.P.S. One test of the stability of spectra from such samples was provided by running spectra of an 800-second sample, then cutting the sample in half and running the two halves, and finally cutting these in half to run the four 200-second quarters of the original sample. When all resulting spectra were compared for similarity, the 200-second samples proved to be fairly good approximations of the 800-second sample (Figures 6.10.1 - 6.10.5).

Samples were selected to represent random seismic noise as much as possible. All films were monitored to avoid picking samples that might be contaminated by earthquake signals or extraneous noise, such as nearby automobiles or cattle near a seismometer position. In some California areas, it was difficult to find samples entirely free of noise from small earthquakes.

Averaging time was set at 2 seconds, so that each frequency component was averaged over its whole length of 200 seconds, when analyzed at 100 times real time. Even so, inequalities in time-distribution of energy at each frequency were often so large that the scribe "chattered" over a fairly large range with each pass of the loop.

The oscillator took 11 minutes to scan the seismic frequency range from 0.25 to 2.5 cps; in this time the loop passed about 330 times. Scanning rate was thus slow enough so that the frequency being analyzed remained practically constant during any one pass of the sample. Oscillator frequency shifted only about one-third of the filter band-width during one pass of the loop.

#### 4.1.1.4 Calibration of Power Spectra

Since seismic noise is more nearly random than sinusoidal for most frequencies, its spectrum is more nearly a continuous spectrum than a line spectrum. It was to be expected that the finite band-width filter would usually be filled by a continuous spectrum, the height of which would be directly proportional to the effective band-width of the filter in use. In order to make spectral height independent of filter band-width, a "band-width divisor" circuit at the analyzer input allowed attenuation of signal strength in proportion to the band-width of the filter being used. The effect of this proportional attenuation was to make the area under the spectrum the same for any one noise sample, regardless of the band-width of the filter being used to write the spectrum.

Calibration of spectra was accomplished by writing the mean squared voltage in a sinusoidal calibration of known equivalent earth velocity, for comparison with mean squared voltage (normalized to 1 cps BW) written by seismic noise. The recorded 2 cps calibration was played back, its voltage measured on an oscilloscope at the input to the wave analyzer, and this voltage recorded in a log book. Then, on the function generator, a 2 cps signal was set up whose voltage was the predetermined fraction of the measured calibration voltage required to make the PSD velocity scale a set of multiples of seven (since the scale was to fit a PSD plot 7 inches high). Sensitivity of the X-Y Plotter was set so that a sinusoidal input of the predetermined voltage would write exactly 7 inches on the plotter. The sinusoidal input was then replaced by the noise signal to be analyzed. The written noise spectrum thus had an integral velocity scale which fitted the spectrum at 2 cps, and which deviated from the spectrum at other frequencies in a manner determined by the shape of the velocity response curve of the recording system, which was known and could be corrected for.

A purely sinusoidal calibration voltage is a spike in the frequency domain, narrower than any of the filter band-widths of the analyzer system,

so its height on the PSD is not determined by filter band-width, as is the height of the continuous-frequency noise spectrum. For this reason, the band-width divisor attenuator was by-passed in writing the 7 inch mark by the calibration voltage. Before replacing the calibration voltage with the noise voltage to be analyzed, the band-width divisor for that filter was switched back into the analyzer circuitry. Since the calibration mark was not written through the band-width divisor while the noise spectrum was, any one noise sample had the same power density scale regardless of width of the filter used to write its spectrum. The general shape and smoothness of the spectrum was determined by the filter band-width, but total area under the spectrum was the same for all filters.

Calibration of the PSD was intended to compare finite mean squared velocity of the seismometer mass with respect to earth, moving at a single isolated frequency, with mean squared mass velocity due to the summed influence of infinitesimal earth velocities in a narrow continuous band of frequencies around some nominal frequency. Relative changes in average value of "true" power density across each band are reflected, more or less accurately, by changes in average power through the constant band-width filter. Relative changes of noise level can thus be measured, even though the actual numerical values of PSD-determined noise amplitudes cannot be easily compared with those obtained from observation of the noise trace itself.

In many cases, noise at some frequencies was so nearly sinusoidal that it probably did not fill the whole filter band-width. Noise of this type is written as a spike of constant height by filters of any band-width and therefore cannot go through the band-width divisor without distortion. For this reason, any scale based on the assumption of the random nature of seismic noise is probably not uniform at all frequencies.

#### 4.1.2 Noise Amplitude Measurements from Power Spectra

##### 4.1.2.1 Comparison of PSD-determined Noise Amplitudes with Trace-determined Noise Amplitudes

Direct comparison of the voltage out of a seismometer with the voltage obtained by writing its PSD is difficult. The calibrated PSD value at any frequency is determined by the variance of a narrow band of velocities centered at that frequency. This variance is not easily estimated from the seismometer output, unless that output happens to be largely restricted to the same band of frequencies. Longuet-Higgins (20 a) has shown that certain amplitude characteristics of Gaussian noise can be predicted from its power spectrum. This problem needs further investigation if visually determined noise amplitudes are to be related to spectrum-derived amplitudes.

Cumulative probability distributions were computed for samples of noise on which PSD's had been run, in order to compare PSD-determined amplitudes with those at the median point of the cumulative distribution curve. Samples included noise generally random in appearance, and again noise that was almost purely sinusoidal around 2-second period, the period where trace amplitudes were largest. In both types of noise, highest trace amplitudes and consequent PSD size were associated with fairly restricted bands, about 2 cps for the "random" noise sample and about 0.5 cps for the "sinusoidal" sample. Cumulative amplitude distributions in these frequency bands were compared with PSD-determined amplitudes in the same bands. Although PSD-determined amplitudes were smaller than median trace-determined amplitudes for both noise samples, the difference between the two amplitudes was less for sinusoidal noise than for the more random noise. In general, PSD-determined amplitudes are smaller than those determined from trace sampling methods, the amount of difference depending on the nature and dominant frequencies of the sample being analyzed. Trace amplitudes being sampled visually in a restricted period band (say 0.5 - 1.5 seconds) tend to show an association between large amplitude and long period in most noise samples. Cumulative probability distributions of noise in the 0.5 - 1.5 second band are usually determined by amplitude of the 1.5 second noise, so that amplitude variations observed in visual sampling will show up in the 1.5 second PSD band, but not necessarily in other PSD bands.

#### 4.1.2.2 Ground Motion Amplitude Computations from Analog PSD's

Calibrated PSD amplitude is proportional to the mean squared value of a narrow band of seismic velocities centered at some frequency. If this mean squared velocity is assumed to be caused by sinusoidal ground motion, the average amplitude of ground motion to which it corresponds can be found by taking the square root of the mean squared velocity to find its rms value, correcting this for system response difference from the response at calibration frequency, and dividing the corrected rms velocity by  $2\pi$  times its nominal frequency.

In order to allow fast hand processing of PSD's, a template was devised to divide the short period noise spectrum into 11 bands from 0.2 to 5 cps, and was laid over each spectrum. Average spectral values in each band were marked and recorded in the proper frequency column of a computation sheet, also divided into 11 bands. At the top of each column was written a factor combining system response correction with velocity-to-amplitude conversion for that band. The square root of the measured velocity-squared values was obtained and multiplied by the factor at the top of the column. The resulting value, proportional to ground motion amplitude at that frequency, was then recorded in red on the computation sheet. A similar procedure, using an appropriately prepared template, was followed for long period spectra.

### 4.1.3 Noise Source Direction, Phase Velocity and Coherency Determinations

#### 4.1.3.1 Phase Shift Measurements

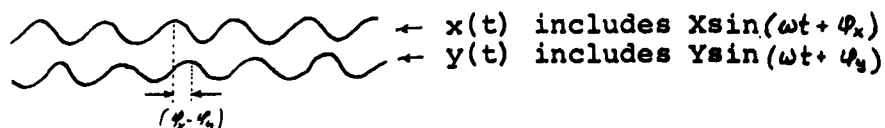
Determination of phase shift between outputs of two seismometers for a specified frequency is outlined in Figure 4.1.5. Co- and Quad-spectrum values at that frequency are proportional to the sine and cosine, respectively, of the phase shift between seismometer outputs, so that phase shift is given by the relation:

$$(\phi_x - \phi_y) = \tan^{-1} \frac{\text{Quad (xy)}}{\text{Co (xy)}} \text{ at frequency } \omega$$

Since this equation has an infinite number of possible solutions, it does not actually define phase shift, only its quadrant and position in it. The principal solution and the principal solution plus or minus any multiple of  $360^\circ$  are all possible solutions. Fortunately, knowledge of array dimensions and approximate expected phase velocity allows restriction of the possible solutions to one or a few. For example, allowing for plane surface wave phase velocity of about 4 km/sec and, assuming a symmetric tripartite array of 1 mile radius (i.e., 2.4 km between seismometers), the maximum phase shift to be expected between any of the three seismometer pairs, for 1 cps frequency, is about  $220^\circ$  (Figure 4.1.6). This value is for a wave front perpendicular to the line between a pair of seismometers. On the other hand, if the wave front is parallel to a pair of seismometers, there must be two phase shifts in the array with a magnitude no less than about  $220^\circ \cos 30^\circ$ , or  $190^\circ$ . This means that for the given array dimensions and noise phase velocity, there must always be at least one pair of seismometers in the array whose phase shift is about  $200^\circ$  at 1 cps,  $100^\circ$  at 0.5 cps, or  $400^\circ$  at 2 cps. Consequently, all solutions but the principal one can be discarded for frequencies much below 1 cps and, for frequencies below 2 cps, all solutions can be discarded but the principal one plus or minus  $360^\circ$ .

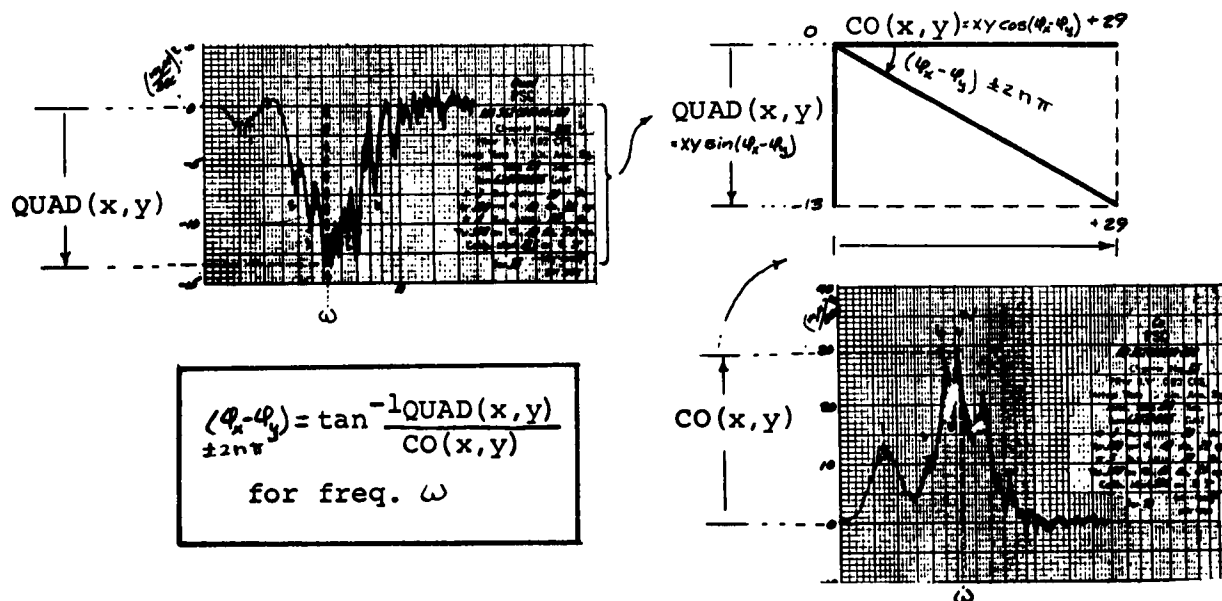
For frequencies above 1.5 or 2 cps, phase shift is often very difficult to determine from cross-spectra because of the multiplicity of solutions, several of which may often be equally possible. If phase shift is actually caused by plane coherent surface waves, then the sum of phase shifts around the array should add up to zero. This, in turn, defines limits within which phase shifts can vary, as shown in Figure 4.1.6. If the wave front is nearly perpendicular to the line between two seismometers, then phase shift between that pair must be near its maximum expected value for frequency and velocity, while each of the phase shifts between the other two pairs must be of opposite sign to, and about half the size of, the maximum phase shift. If the wave front is about parallel to the line

1. PHASE SHIFT BETWEEN SEISMOMETER OUTPUTS  $x(t)$  AND  $y(t)$  IS  $(\phi_x - \phi_y)$ :

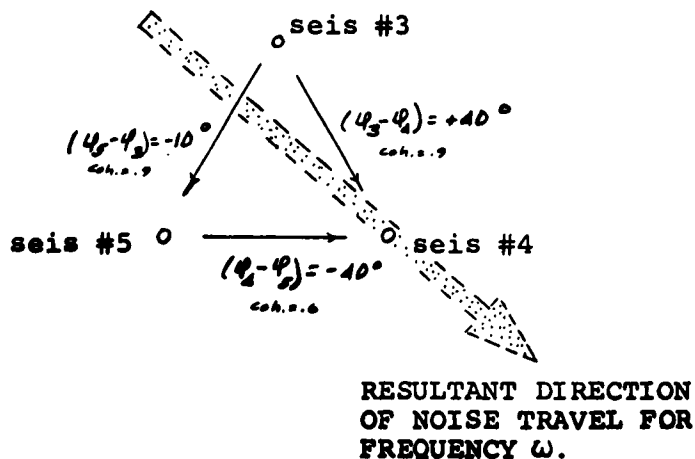


when  $\phi_x > \phi_y$ , noise travels from seis(x)  $\rightarrow$  seis(y).

2. CROSS SPECTRUM INDICATES PHASE SHIFT AT FREQUENCY  $\omega$ :



3. COMPUTE PHASE SHIFT BETWEEN EACH PAIR OF SEISMOMETERS AROUND ARRAY AND ESTIMATE RESULTANT DIRECTION OF NOISE TRAVEL.

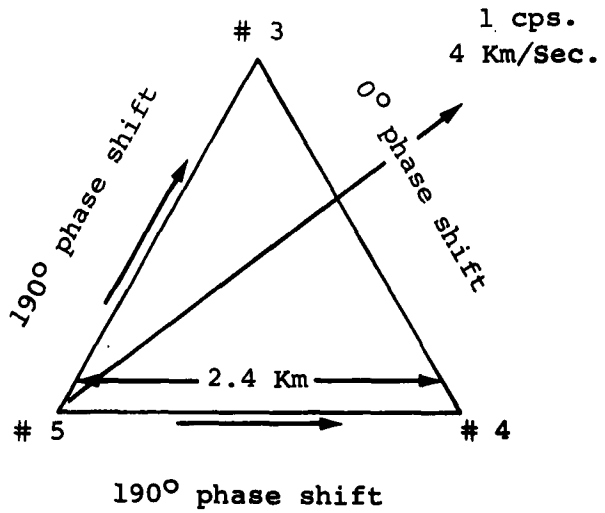
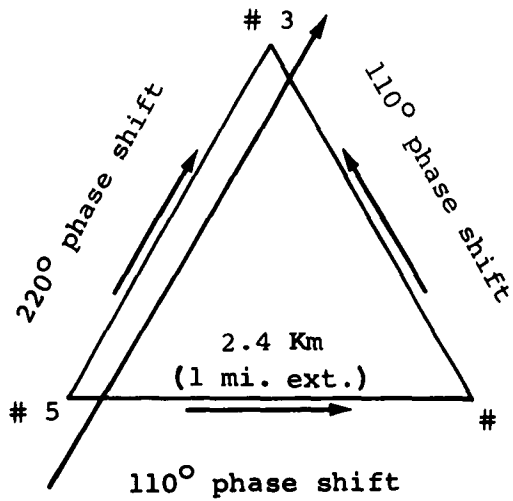


DETERMINATION OF  
 NOISE SOURCE DIRECTION  
 FROM  
 CROSS SPECTRA

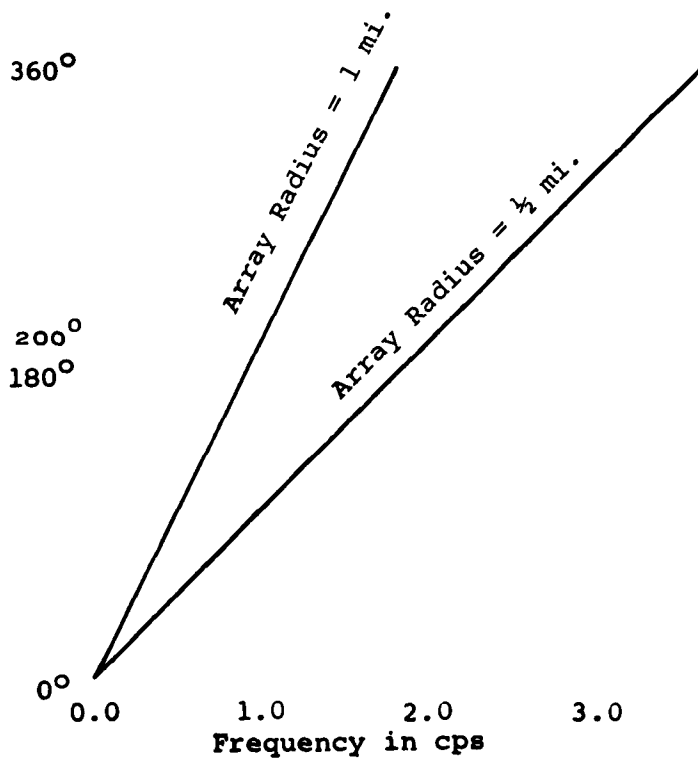
Figure 4.1.5



1 cps  
4 Km/Sec.



Most Probable Max. Phase Shift @ 4Km/Sec.



Determination of Maximum  
phase shifts to be expected  
around an array of known  
dimensions, for plane surface  
waves of 4 Km/Sec phase velocity

Figure 4.1.6

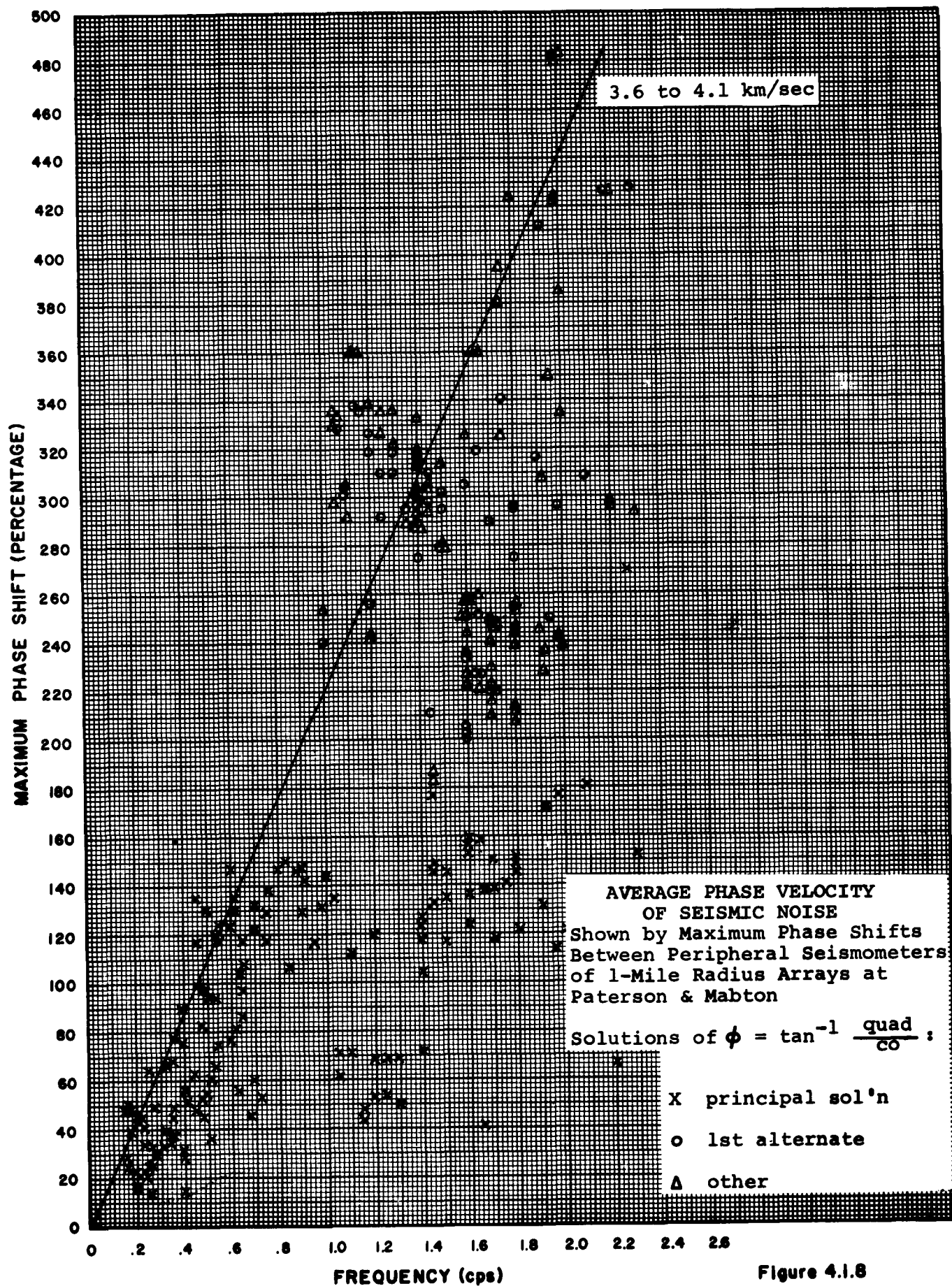


Figure 4.1.8

of one pair of seismometers, then phase shift between that pair will be small compared to phase shifts for the other two pairs of seismometers, each of which will be of opposite sign to, and about 85% of the magnitude of, the maximum possible phase shift for the pertinent frequency and phase velocity. When 2 cps noise was recorded across an array of 1 mile radius, there often appeared several combinations of phase shifts, all fitting the above criteria equally well, within available limits of accuracy. If the data were errorless, a single combination of phase shifts could probably have been found to fit the test criteria better than any other pair and could have been chosen as the true solution.

Many sets of phase shifts have been calculated for very small arrays and frequencies below 1 cps, where there can be no doubt of the maximum possible size of phase shift. In general, these phase shifts have somewhat lower values than would be expected for phase velocity of about 4 km/sec. There are several possible explanations. Errors in correlating peaks, and in calibrating cross-spectra are involved to some extent. Noise samples contaminated by earthquake energy would tend to show lower phase shifts than pure surface-noise samples. Possibly a better reason for consistently low values of phase shift is that noise of a single frequency sometimes crosses the array from more than one direction at once, the resultant interference pattern having a higher apparent velocity than its component waves.

Determination of phase shift from cross-spectra at frequencies above 1 cps involves two rather serious difficulties. One is that some sort of upper and lower limits on phase velocity must be assumed to solve the arc-tangent problem while the other arises from the nature of the spectra themselves. At each frequency, peaks from three pairs of spectra must all be picked consistently, in spite of often radical changes in the shape of the spectra around the array at higher frequencies. Small inconsistencies in initial settings of the X-Y plotter, or use of two different plotters within one set of spectra, can make exact readings of the frequency scale difficult, and the spectra must be picked partly on the basis of similarities in character to resolve this difficulty.

#### 4.1.3.2 Noise Source Direction Determination

Once the phase shifts between each of three seismometer pairs around the array had been decided upon, the direction of motion of the wave front assumed to have caused them could be decided from their relative magnitudes, keeping in mind the general limitations that determination of one phase shift imposes on the other two.

For small arrays, and for larger arrays at frequencies below about 1 cps, there is usually only one set of phase shifts possible at surface wave velocity, so that apparent source direction was not hard to determine.

uniquely. For higher frequencies, there are as many possible source directions as there are sets of phase shifts allowed by the array dimensions, assumed velocity, and accuracy of data.

Source direction determinations from cross spectra could be checked, for at least one frequency, by direct measurements from film recordings. Usually the trace showed a more or less coherent noise component in the 2-second band, of larger amplitude than other noise. By picking common peaks across the array for many cycles of this dominant frequency and taking the average peak time for each trace, the differences among these average times for the various traces gave a rough check on phase shifts and source direction. This was done with consistent results for several consecutive samples at Toppenish Ridge, which showed west or northwest sources, and phase velocity somewhere around 5 km/sec, in fairly good agreement with cross-spectrum data. Similar determinations of source direction for some California and Appalachian profile stations showed the source for 0.5 cps noise to be in the direction of the ocean.

#### 4.1.3.3 Determination of Apparent Phase Velocity

At first, average phase velocity across an array was figured for each source direction determination, but this procedure was abandoned as too cumbersome where phase shift (and consequently, source direction) was ambiguous. Probably more reliable over-all results were obtained by selecting the maximum phase shift observed among the three seismometer pairs for all reasonable solutions of the arctangent problem, and plotting this maximum against its corresponding frequency (Figure 4.1.8). The upper limit of the pattern formed by these plots lies along a line whose slope is determined by average phase velocity along the maximum "expected" distance between the pair of seismometers showing maximum phase shift. As shown in Figure 4.1.6, if seismometers are 2.4 km apart around a symmetric array, there is no direction from which a plane surface wave can approach without crossing a distance of at least 2.1 km ( $2.4 \text{ km} \times \cos 30^\circ$ ) between some pair of seismometers. Maximum phase shift thus would correspond to a maximum travel path of more than 2.1 km, but no more than 2.4 km, with the average maximum travel path probably at about 2.25 km. If phase velocity is more or less constant, the plot of maximum phase shifts vs. frequency should cluster around a line defined by average phase velocity over the maximum probable distance.

The upper limits of these plots tend to cluster along the slope for phase velocity of 3.5 to 4 km/sec, for the 1-mile radius arrays at Paterson and Mabton, and of 4.5 - 5.5 km/sec for the 1/2-mile arrays at Toppenish and Paterson. The higher velocity for the small arrays was almost entirely determined by relatively long period noise (1 to 5 seconds), whose plots scattered badly, while the lower velocity at the large arrays was determined by a much wider range (0.5 to 5 seconds) and is considered to be more reliable.

Points above 1 cps which fall far below the upper limit of the trend correspond to other solutions of the arctangent problem. In choosing the "correct" solution, one should probably be guided by which possibility shows the most reasonable velocity for surface waves. It should be noted that in some cases, possible solutions include phase shifts for velocities either around 8 km/sec or 4 km/sec. Such samples might have been contaminated by weak body waves from distant earthquakes. In such cases, the plane surface wave assumption would be invalid and what appeared to be the "correct" solution could be the wrong one.

#### 4.1.3.4 Phase Coherency Measurements

The term noise coherency here means phase coherency, a measure of the persistency of a phase shift between the outputs of two seismometers throughout the duration of a noise sample, for a specified frequency. It is easily measured by the cross-spectrum analyzer, as shown in Figure 4.1.9. Co- and Quad-spectra are proportional to the cosine and sine, respectively, of the average phase shift between two seismometer outputs at some frequency.

If the phase shift is random over the duration of the sample, Co- and Quad- values both approach zero, since the averages of random values of sine and cosine approach zero. When phase shift is constant over the sample, sine and cosine are constant, with a vector sum of one. The quantity,  $\sqrt{\frac{\text{Co}^2(x,y) - \text{Quad}^2(x,y)}{\text{PSD}(x) \cdot \text{PSD}(y)}}$ , thus can vary between zero, for completely incoherent noise, and one, for completely coherent noise.

#### 4.2 Signal Strength Determinations

When teleseisms were recorded both at the fixed master station and at variably located slave stations, observations were made of changes in relative strength of signal between the two sites, in order to obtain data for studying the effect of environment on signal strength.

##### 4.2.1 Measurements

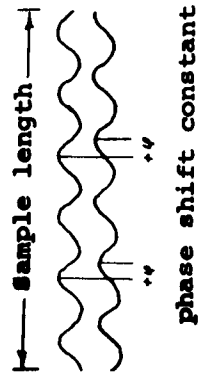
For every teleseism recorded at both stations, measurements were made of the calibration data for that day and of trace amplitude and period of first motion for the same phase of the teleseism. Measurements were not made if the same phase could not be identified at both stations.

The amplitude and half-period of the first and second halves of the first full cycle of motion were measured, when these clearly represented the same phase at both stations. First motion itself was not usually

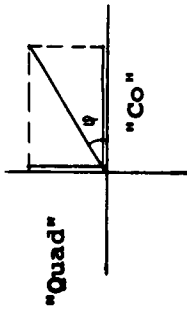
DEFINE "COHERENCY" BETWEEN TWO SEISMOMETER OUTPUTS, FOR SPECIFIED FREQUENCY, AS RELATIVE PERSISTENCE OF CROSS-SPECTRAL PHASE AND/OR MODULUS THROUGHOUT DURATION OF SAMPLE

DIAGRAMMATIC EXAMPLE:

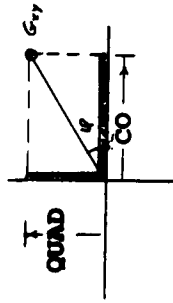
### COHERENT NOISE



instantaneous  
"Co" and "quad"  
values all equal

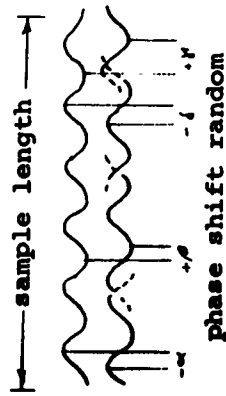


after averaging,  
co and quad values finite,  
and  $co^2 + quad^2 = PSD(x) \cdot PSD(y)$

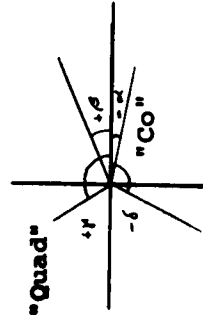


$$\text{"COHERENCY"} = \frac{CO^2 + QUAD^2}{PSD(x) \cdot PSD(y)} = 1.0$$

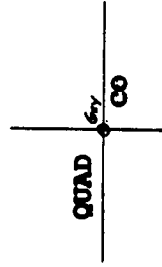
### INCOHERENT NOISE



instantaneous  
"Co" and "Quad"  
values random



after averaging,  
CO and QUAD values = 0  
and  $CO^2 + QUAD^2 \approx 0$



$$\text{"COHERENCY"} = \frac{CO^2 + QUAD^2}{PSD(x) \cdot PSD(y)} = 0$$

ILLUSTRATION OF HOW  
CROSS SPECTRUM PLOTS  
SHOW NOISE COHERENCY

Figure 4.1.9

measured, since it frequently was not clearly measurable at both stations. Peak noise amplitude during a short interval just prior to the teleseism was also measured at both stations.

For teleseisms recorded at Panamint and Cedar Creek slave stations, amplitudes were corrected for differences in recording attenuation, seismometer gain, and frequency response (based on measured period of first motion), in order to test the effect of these corrections on signal strength ratios between slave and master stations.

#### 4.2.2 Corrections

After correction for recording attenuation differences between master and slave stations, a ratio was made of signal strength at the center short period seismometer at the slave station to that at the same location at the master station. Because these ratios varied widely from one teleseism to the next, frequency response corrections, based on period of first motion, were also applied in an attempt to reduce the scatter of signal strength ratios. However, these latter corrections had practically no effect on the scatter, probably because first motion period was hard to measure accurately and was usually pretty much the same at both stations. Therefore, most signal strength studies were made by using always the same master and slave seismometers, corrected only for differences in recording attenuation. Gain for these two seismometers did not vary with time, so no gain correction was made.

Ratios of signal strength between peripheral seismometers and the central seismometer of each array were calculated also, again corrected only for recording attenuation.

#### 4.2.3 Investigation of "Scatter" in Signal Ratios

The ratio of recorded teleseism strength between fixed master and variable slave seismometers several kilometers apart was found to vary widely among individual teleseisms. In an attempt to explain this variation, ratios were plotted in a number of ways: with and without frequency response corrections against period of first motion; grouping teleseisms by general areas of origin and plotting ratios against period of first motion; and studying possible perturbations of the ratio by background noise. No functional relationship between signal strength ratio and first motion period was revealed by any of the methods, but much of the observed variation could be explained by the effect of background noise.

Signal-to-noise ratios of teleseisms which could be measured from the Develocorder film recordings varied from about 1, in poor samples, to about 15, in the strongest teleseisms whose amplitudes were still small

enough to stay on the film, with an average value of about 4 or 5. The measured signal-to-noise ratios consisted of the ratio between the teleseism phase film amplitude (whose signal ratio was to be found) and the film amplitude of the highest p-p noise cycle in the 15 or 20 seconds preceding the teleseism.

Signal strength ratios were observed to vary through 400% in some cases. This is probably explained by the wide variety of combinations through which noise can distort both the numerator and denominator of the signal strength ratios. For example, if the true (noiseless) signal strength ratio between two distant seismometers is always one, and if noise is then introduced at both stations so that S/N ratio is 5 at both stations, for all teleseisms, then p-p signal strength ratios measured through the noise can conceivably have values ranging from 0.67 to 1.6, due to noise distortion alone. If S/N ratio is allowed to decrease, the possible range of variations increases rapidly.

#### 4.3 Correlation of Seismic Signal and Noise with Geologic, Geographic and Time Variables

Noise and signal strength correlations with environment were intended to show how signal-to-noise ratio depends on geologic-geographic environment of the recording station. It was felt that any dependence could best be demonstrated by examining noise and signal separately, and then combining the independent observations to draw conclusions about relations between S/N ratios and environment.

##### 4.3.1 Methods Used in Correlating Noise Level with Environment

Observed noise levels at each seismometer position varied widely with time, but after the time variations were removed (by normalizing to noise level at a reference seismometer), the remaining noise levels fell into two distinct groups: relatively small variations among seismometer positions within each array, and much larger differences among averages over arrays at different stations.

Because of the complex way in which many different environmental factors might simultaneously influence noise level (or signal strength), it was decided to use multiple regression methods as much as possible in investigating the influence of seismometer environment on noise and signal level. For variations among individual seismometer positions, a relatively large amount of data was available for processing by multiple regression, (there were 80 seismometer positions on the California profile) but the more important differences among stations were determined by a much smaller amount of data, since only about 8 slave stations were occupied on each profile.



#### 4.3.1.1 Correction for Time Variations in Noise Level before Correlation

As each slave station seismometer on the array periphery was recording noise level under varying conditions of both time and environment, the fixed central seismometer was recording in a constant environment in which only time varied. The time-dependent part of noise level being recorded at peripheral seismometers could thus be removed by normalizing their outputs in any time period to that of the central seismometer for the same time period. Since the correlation in time between outputs of central and peripheral seismometers was usually very good, time variations could be removed effectively.

Similarly, when time variations in noise level correlated well over the relatively longer distances between master and slave stations, the time-dependent part of noise levels recorded at various slave stations could be removed by normalizing noise level at the central slave station seismometer to noise level at the master station for the same time interval.

The products of these two normalized sets of noise levels give relative noise levels at each seismometer position on the profile with respect to those at the master station. Multiplication of these products by the average noise level at the master station, taken over the whole period of operation of the master station, gives an approximation of what the long-time average noise level at each seismometer position would have been if each slave seismometer had operated at that fixed position for the whole period of operation of the master station. (Actually, peripheral slave seismometers moved about every two weeks, whereas master seismometers remained in one location for months.) The differences in resulting noise levels at the various slave seismometer positions thus reflect only the constant differences in their ground environments, not temporary changes in microseismic activity due to wind or storms.

Unfortunately, noise level changes between master and slave stations often correlate poorly when the stations are far apart, so that it is difficult to tell how much of the relatively large differences in noise levels at various slave stations is due to station location and how much depends on when the stations were occupied. In such cases, the value of normalization is questionable and probably gives no better correction for time variations in noise level than the simple assumption that average noise level at the central slave seismometer is a sufficient measure of long-time average noise level. In many cases this assumption is probably not unreasonable, since large temporary changes in noise level often have a period of about three or four days, while the central slave seismometer records at one location for several times that period.

The noise band chosen for correlation was for 1.25 to 1.50 seconds period. This is close enough to the 2-second microseism band to allow the hope that it would correlate over reasonably long distances, and is still close to the 1-second band occupied by most teleseisms.

#### 4.3.1.2 Correlation by Multiple Regression

In attempting to correlate noise levels with ground environments of each station and seismometer position, the assumption was made that noise level (for a particular period band and seismometer location) is a linear function of a variety of environmental influences, plus a base noise level essentially independent of environment. Noise level would then be of the form:

$$y_j = a_0 + \sum_{i=1}^N a_i x_{ij}, \quad j = 1, \dots, 80$$

where

$y_j$  = average noise amplitude in  $m\mu$  (p-p) typical of seismometer position  $j$  (there are 80 positions on the California profile).

$a_0$  = base noise level about which observed noise varies under influence of different environments.

$x_{ij}$  = numerical value of an environmental variable of type  $i$  at location  $j$  (i.e.:  $x_{ij}$ ,  $i=8$ ,  $j=20$  is the thickness in feet of alluvial fill under seismometer #2 at Panamint Slave Station)

$a_i$  = change in noise amplitude per unit change in environmental variable of type  $i$ .

$N$  = number of different types of environmental factors assumed to influence noise level. (Thirteen possible types were considered in the first test of California data.)

This system of equations is solved for least squares estimates of coefficients ( $a$ ) by a multiple regression method (UCLA BIMD 06) programmed for the CDC 1604 computer.

The coefficients ( $a$ ) are sought such that

$$(1) \sum_{j=1}^M \left[ y_j - a_0 - \sum_{i=1}^N a_i x_{ij} \right]^2 \text{ is minimized. This expression can}$$

be written (16 a)

$$(2) \quad u = \sum_{i=1}^N a_i p_i + \sum_{i=1}^N a_i \left[ \sum_{k=1}^N (a_k t_{ik} - p_i) \right] \text{ to be minimized,}$$

where

$$u = \sum_{j=1}^M (y_j - \bar{y})^2, \quad \bar{y} = \frac{1}{M} \sum_{j=1}^M y_j$$

$$p_i = \sum_{j=1}^M y_j (x_{ij} - \bar{x}_i), \quad \bar{x}_i = \frac{1}{M} \sum_{j=1}^M x_{ij}$$

$$t_{ii} = \sum_{j=1}^M (x_{ij} - \bar{x}_i)^2$$

$$t_{ik} = \sum_{j=1}^M (x_{ij} - \bar{x}_i) \cdot (x_{kj} - \bar{x}_k).$$

Differentiation of (2) with respect to  $a_i$  defines the normal equations

$$(3) \quad \sum_{k=1}^N a_k t_{ik} = p_i, \quad i = 1, \dots, N$$

where  $a_i$  are the estimates of  $a_i$  minimizing (2).

The normal equations (3) can be expressed in matrix form as

$$AT = P$$

$$\text{where } A = ((a_i)), \quad T = ((t_{ih})), \quad P = ((p_i)).$$

The matrix of estimates  $a_i$  of coefficients  $a_i$  is found through inversion of the matrix T, since

$$ATT^{-1} = A = PT^{-1}.$$

Estimates of  $a_i$  are then given by

$$a_i = \sum_{k=1}^N p_h t^{hi}.$$

This correlation method was actually applied in two separate stages. Large differences in noise level among stations were removed to allow correlation of the fairly large mass of data describing local noise level differences between seismometer positions. The sparse data describing large differences among stations were treated independently.

Local differences for the entire profile were correlated en masse. Data to be correlated in this fashion were first reduced to residual values about the means for the various stations. In later correlations, noise level residuals were also normalized so that their variance at each station was constant over the whole profile; this was done to avoid giving stations of very high noise variance more weight in determining regression coefficients than stations of low noise variance.

#### 4.3.1.3 Selection and Definition of Environmental Variables

Environmental variables for correlation with noise level were divided into three general categories:

a) Local ground environment, which varied over the 1/4 to 1 1/2 miles between seismometer positions within a station. These included estimated or known thickness of alluvium under the seismometer, solidity of the ground in which the seismometer was planted, ground slope at the seismometer, and similar variables.

b) Regional environment, which was essentially constant over the area of a single station, but which varied over the 30-odd kilometers between stations. These included thickness of the sedimentary column between ground surface and basement granite, geologic and topographic complexity in the general area of the station, and other regional factors.

c) Cumulative variables, which were intended to describe the cumulative attenuating effect on noise level of the travel path between the major source of noise (the ocean) and a recording station. These variables

included the total distance noise would travel across the conformable sediments of large open valleys, the total travel path through the complex geology of mountain areas, the total number of geomorphic interfaces in the travel path (fault zones, transition zones between mountain and valley terrains), total distance between station and coastline, and others.

Some of these variables could be measured directly and assigned their appropriate units, while others, such as the amount of forest cover, were assigned arbitrary relative values. Complete definitions and quantitative values for all variables are given in Appendix 6.4.

#### 4.3.1.4 Method of Evaluating Results of the Correlation Program

The basic criterion used in interpreting results of the correlation program was that of consistency of regression and correlation coefficients for different combinations of seismometers. The only conventional statistical test applied was observation of the F number (given as part of the program output), which is a measure of the ratio of mean variance due to regression to residual variance about the line of regression, and which can be an indication of how well the linear noise model fits observed variations in noise level. Small values of the ratio (below about 4.0) mean that the chosen set of environmental variables is not particularly influential in determining noise level. Large values can mean either that the set is influential, or simply that the noise observations are distributed in such a way that the effective number of variations in noise level is not much greater than the number of regression coefficients to be evaluated. To give reliable values of F and t statistics, noise level values should be normally distributed and have constant variance about the line of regression, and the values of each environmental variable should vary independently of the other variables and be determined without error. None of these conditions was strictly satisfied by noise level and environmental data available in this report. Noise levels could be given approximately normal distributions and constant variance by transformation, but little could be done about errors in determining environmental values or about the strong dependence among many of them. The amount of cross correlation between various types of environmental variables was revealed by the earliest runs, so that pairing of strongly dependent variables in a single regression could be avoided in later runs. Practically all local variables showed more interdependence than was desirable.

It was felt that inclusion of really significant environmental variables in the regression program would be revealed by the appearance of consistent values of their associated regression and correlation coefficients, regardless of the set of seismometers used to provide the data.

#### 4.3.2 Signal Strength Correlation

Correlation of signal strength variations with environment followed much the same path as for noise data. The same values of environmental variables were used, but the variables selected for use were restricted to those most probably affecting body waves approaching the recording station almost vertically. Environment not immediately related to the station itself was not considered.

## 5. Conclusions and Recommendations

### 5.1 Conclusions

A two-year study of seismic noise and signal, made under various geologic and geographic conditions in areas near the Atlantic and Pacific Coasts of the United States, leads to the following conclusions concerning the effect of recording environment on seismic signal and noise, and the importance of considering recording environment in planning the location and design of seismometer arrays.

#### 5.1.1 Signal-to-Noise Ratio

Relative signal-to-noise ratios, for noise periods near 1 second at stations less than 500 kilometers from the ocean, depend largely on distances of these stations from the ocean. The highest signal-to-noise ratios observed were for stations the farthest inland. Variation in S/N ratio between stations at different distances from the ocean is determined more by noise level than by signal strength, because of the greater range of variation in noise level than in relative signal strength.

#### 5.1.2 Seismic Noise Amplitude

Noise amplitudes between 0.4 and 5 seconds period at stations less than 500 kilometers from an ocean are determined largely by ocean distance and wind speed (for periods below 2 seconds). Amplitudes between 0.4 and 5 seconds period increase exponentially with period, in almost all recording environments.

Estimated long-term (6 months) average noise amplitudes increase approximately exponentially as recording stations approach the ocean. Deviations from the trend are treated as being dependent on geologic and topographic environment. Long-term noise levels in provinces of thick Cenozoic sediments, especially coastal provinces, appear to be two or more times higher than in granitic intrusive or Paleozoic sedimentary provinces, but simultaneous change in ocean distance and sequence of lithologic and topographic provinces makes it difficult to isolate the separate influence on noise level of ocean distance from that of topography and lithology. Average noise amplitudes more than 400 kilometers inland appear to continue to decrease with increasing ocean distance, although much less clearly than at stations closer to the coast.

Estimated long-term average noise amplitudes ranged from .01 m $\mu$ l (near 0.4 seconds period at inland stations) to almost 1 $\mu$ l (near 5 seconds period at coastal stations). Frequency-dependent increase of noise

amplitude with period averages about 500 to 1, and amplitude variation with change in recording environment ranges from about 50 to 1 for long periods to 100 to 1 for short periods. Short-term fluctuations, lasting from minutes to several days, of 5 to 1 about the long-term average were not uncommon.

Most long-term average amplitudes on each profile could be described within a factor of 3 by a function  $Y(f,x)$  of ocean distance and frequency alone, where  $(x)$  is distance in km to the nearest shoreline and  $(f)$  in cps is the center of the noiseband being considered:

$$Y(f,x) = Y_0(f) \left[ \frac{x}{x_0} \right]^{k(f)} ; x < 500 \text{ km}$$

where  $\ln Y_0(f) = a e^{-\beta (\ln f/\gamma)^2} - \ln 50 ; .25 < f < 2.2 \text{ cps}$

$$k(f) = a e^{-b (\ln f/c)^2}$$

and where  $x_0$ ,  $a$ ,  $\beta$ ,  $\gamma$ ,  $a$ ,  $b$ , and  $c$  are the constants given below:

Profile	$x_0$	$a$	$\beta$	$\gamma$	$a$	$b$	$c$
California	154 km	9.00	.275	.10	-.990	1.00	.73
Pacific Northwest	270 km	7.85	.365	.17	-1.094	.620	.90
Appalachian	350 km	7.61	.382	.20	-.878	.169	1.40

and where  $x_0$  is the distance from the master station to the nearest shoreline.

Use of distance to the nearest shoreline as a parameter was based only on the observation that its logarithm and that of average noise amplitude were related more or less linearly for most of the frequencies being studied; the shoreline itself is not assumed to be a source of any but local noise.

By adjusting these estimates at each station to account for the apparent correlations between noise level and certain geologic features, most long-term averages could be described within a factor of 2, and many within 30%. If a hypothetical noise amplitude spectrum is assumed for a station on massive intrusive granite, the average increase or decrease in amplitudes of noise between 0.4 and 5.0 seconds, due only to recording in a different lithologic or structural environment (that is, after correction for estimated effect of change in ocean distance),



can be roughly estimated by the factors below:

Recording Environment:	Regional Lithology			Structure Wedge-out of Tert. Sed Prov- ince	Local Lithology	
	granite	Paleozoic Sediments	Tertiary Sediments		Bog (deep, soft mud)	Swampland (packed sand)
California	1	1	2	2.5	3	-
Appalachian	1	1.4	2.1	2.	-	1.4
Pacific Northwest	-	-	-	-	-	-

The structural and lithologic correction factors appropriate to a slave station on a profile were selected and multiplied, and the resulting product was divided by the product for the master station. The ratio was then used as a factor for adjusting  $Y(f,x)$  for geologic variations between the slave and master stations. No corrections could be determined for the Pacific Northwest. The structural correction was based on observation of very high noise levels at two stations where thick wedges of seaward-digging Cenozoic sediments had thinned to thicknesses of less than 1500 meters; other explanations for the high noise levels cannot be excluded, however.

Local differences in long-term average noise levels within a small area (2 miles radius or less) are small below 1 cps, within about 20% of the mean for an area where all seismometers are planted in solid ground or rock of any sort, and not close to extraneous noise sources. Noise above 1 cps is usually of lower amplitude on solid rock than on sediment, but no finer distinction could be drawn from data used here. Differences in average noise level due to differences in average wind speed within each array might be as large as differences due to lithology alone, but these could not be determined because wind was measured only at one position in each array. Variation in local topography alone could not be related to noise level, except secondarily, due to more frequent occurrence of solid rock outcrops on hilltops than in valleys.

### 5.1.3 Signal Strength Ratio

Average signal strength is several times higher when recorded in Cenozoic sedimentary provinces than on granite intrusive or Paleozoic sedimentary provinces. No consistent local differences between recordings on hardrock and those on dry alluvial sediments could be noted in relative signal strength, although isolated differences of almost 2 to 1 were observed.

The background noise through which signal was measured was usually more than one-fifth the signal amplitude, and signal strength ratios scattered widely, complicating determination of an average value for each recording station.

### 5.1.4 Noise Source Directions, Phase Velocity and Coherency

Source direction studies were done in detail for two stations in the Columbia River basin and briefly checked in the California and Appalachian profiles.

About 40% of the noise above 1 second period studied at these two stations came from a 60° sector in the direction of the ocean and showed phase velocity of from 3.5 to 5.5 km/sec. Brief visual checks of 2-second noise in a few samples from four California stations and the Appalachian master station also showed noise source to be in the general direction of the ocean. About 30% showed erratic direction and phase velocity apparently over 6 km/sec, and is assumed to be from interference patterns.

Source direction for periods less than 1 second could not be determined uniquely.

Phase coherency over 200 seconds and between seismometers less than two miles apart was good for periods above 1.0 seconds at all except near-coastal stations.

### 5.1.5 Array Design Considerations

The relationship observed in this study between noise amplitude and ocean distance indicates that location of a seismometer array less than 400 kilometers from an ocean will probably cause some loss of S/N ratio relative to locations farther inland, about 40% of the noise between 1 and 2 seconds period, and possibly between .5 and 2 second period, will come consistently from a sector of about 60° in direction of the ocean, with about 4 km/sec phase velocity, at 300 kilometers from the ocean. About 30% of the noise in this period range will be essentially random, with uncertain velocity. The rest might be of either type. At distances less than 300 km a linear array designed to cancel ocean noise will probably provide

best S/N ratio; at more than 300 km cancellation of noise from random directions should probably be given most attention.

Location of the array on Cenozoic sediments will probably result in stronger recording of teleseisms as well as an unknown increase in noise level, so that improvement in S/N ratio would be questionable.

## 5.2 Recommendations

Noise and signal data from California shows that signal-to-noise ratio at seismic stations on massive granite is not necessarily higher than at stations in sedimentary provinces. Teleseisms were recorded more strongly at California stations on Cenozoic sediments than they were recorded on massive granite; the high signal strength and relatively low noise level on the thick sediments of Death Valley gave it the highest signal-to-noise ratio of any California station.

It is recommended that existing data be studied to show whether there is a consistent relationship between relative signal strength of teleseisms recorded both in sedimentary and in granitic provinces. The field teams of Project VT/074 could provide high-grade teleseismic signal strength data in a wide variety of geologic environments. Their recordings at two levels of attenuation will allow study of teleseisms of all sizes, so that distortion of signal by background noise can be minimized.

It is recommended further that existing VT/074 recordings of teleseisms be studied, using one (or more) VT/074 stations, in granitic environment, as control stations for the study of relative signal strengths of teleseisms recorded at other VT/074 stations which are located in both inland Paleozoic and coastal marine Cenozoic provinces.

It is also recommended that further study be made on existing signal strength data from VT/078 stations of the Appalachian and Pacific Northwest profiles, and that cross spectrum analysis be done on seismic noise from the inner-most stations of all three profiles, in order to determine better the source directions and phase velocity of seismic noise at stations far removed from high-level ocean noise.